Naval Command,
Control and Ocean
Surveillance Center RDT&E Division
San Diego, CA
92152-5001

Design and Structural Analysis of Alumina-Ceramic Housings for Deep Submer

Fifth Generation Housings

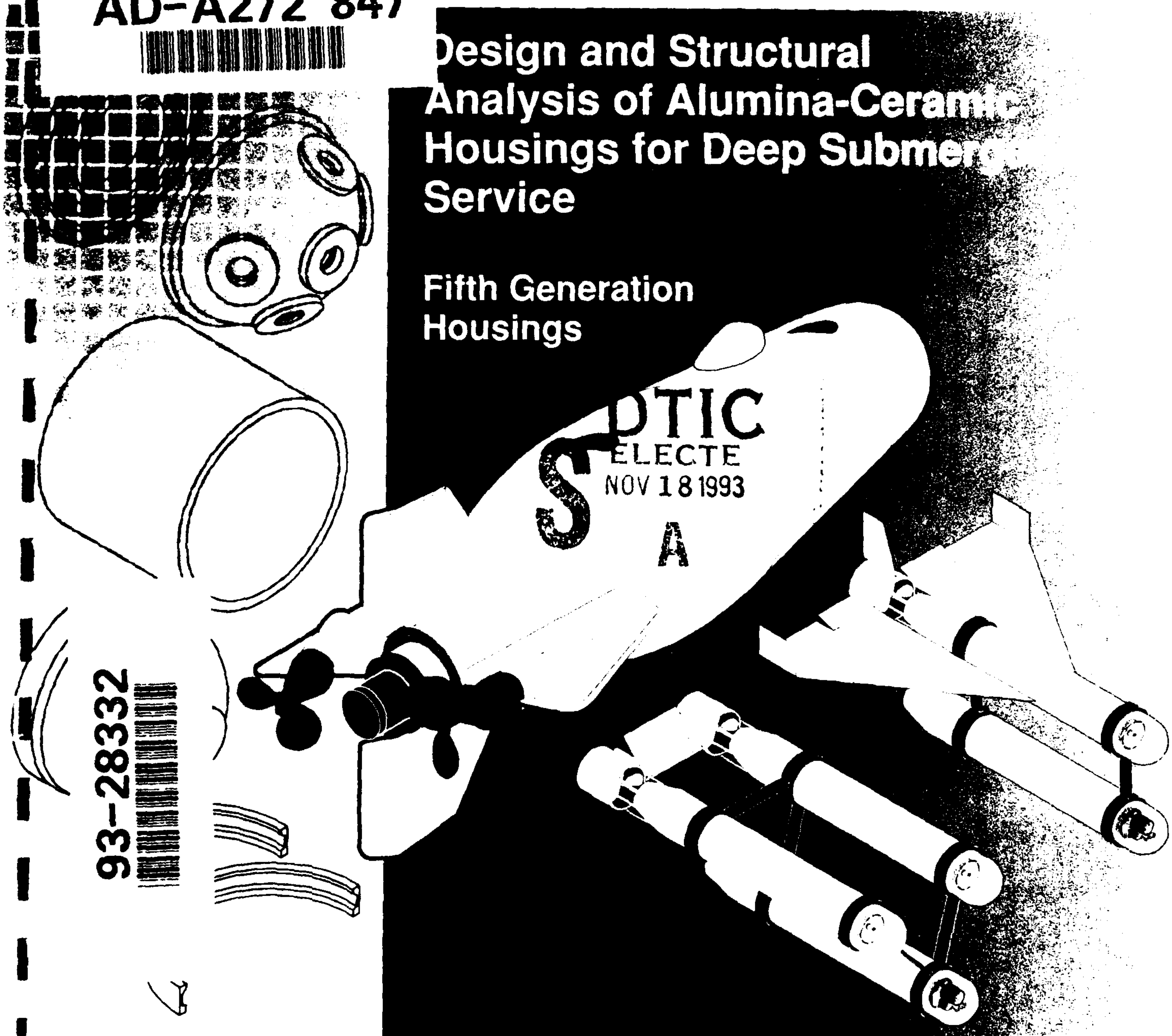

R. P. Johnson
R. R. Kurkchubasche
J. D. Stachiw

Technical Report 1583
March 1993

Technical Report 1583
March 1993

Design and Structural Analysis of Alumina-Ceramic Housings for Deep Submergence Service

Fifth Generation Housings

R. P. Johnson
R. R. Kurkchubasche
J. D. Stachiw

NAVAL COMMAND, CONTROL AND OCEAN SURVEILLANCE CENTER RDT&E DIVISION
San Diego, California 92152–5001

J. D. FONTANA, CAPT, USN
Commanding Officer

R. T. SHEARER
Executive Director

ADMINISTRATIVE INFORMATION

This work was performed by the Marine Materials Technical Staff, RDT&E Division of the Naval Command, Control and Ocean Surveillance Center, for the Naval Sea Systems Command, Washington, DC 20362.

Released by
J. D. Stachiw, Head
Marine Materials
Technical Staff

Under authority of
N. B. Estabrook, Head
Ocean Engineering
Division

ACKNOWLEDGMENT

Michael J. Plapp is acknowledged for his support with the finite element analysis (FEA) presented in this report.

ES

SUMMARY

The United States Navy has a requirement for unmanned underwater vehicles (UUVs) with depth capabilities of 20,000 feet. The environment at these depths necessitates structures capable of withstanding extreme pressure (9,030 psi external). Although materials such as steel and titanium can be utilized to build structures capable of withstanding these loads, their relatively low specific strength and modulus result in structures that are very heavy; having weight-to-displacement (W/D) ratios greater than 0.80.

Alumina ceramic, with its high specific strength and modulus, is ideally suited to the construction of pressure-resistant housings for a 20,000-foot service depth with W/D ratios of less than 0.60. Alumina's nonmagnetic characteristics, impermeability to water, corrosion resistance, and heat conductivity are additional advantages.

Two large housings were designed and structurally analyzed utilizing alumina ceramic as the primary hull material. The smaller of the two housings has 26.0-inch outer diameter (OD), 90.96-inch overall length, and has a calculated W/D ratio of 0.585, while the larger housing has a 33.0-inch OD, 112.87-inch overall length, and a calculated W/D ratio of 0.545.

The two housings incorporate a number of advanced design features such as skirted ceramic hemispheres, a minimum clear-bore diameter requirement allowing access to the entire payload from one end of the housing, an epoxy-bonded central joint, graphite fiber reinforced (GFR) PEEK composite gaskets to delay the onset of spalling, and an almost neutrally buoyant spectra composite fairing to protect against impact.

Both housing designs were analyzed for buckling stability using the computer program BOSOR4 and stress analyzed using ABAQUS.

The housings will be fabricated, assembled, and tested to a proof load of 10,000 psi external pressure. Subsequently, the housings will be cyclically tested at 9,000 psi external pressure. The results from these tests will be compared to results obtained from tests already performed on a half-scale model of the 26-inch OD housing to determine the effect of scaling on the housings' structural performance.

CONTENTS

FIGURES

TABLES

INTRODUCTION

The United States Navy has requirements for unmanned underwater vehicles (UUVs) with depth capabilities of 20,000 feet. Their complexity makes them heavy, such that UUVs must rely on their own displacement in water or the use of syntactic foam to achieve neutral buoyancy.

Two ways of increasing UUV buoyancy are enlarging the hull (thereby creating more displacement), or using syntactic foam. Both methods of increasing buoyancy are accompanied by a corresponding increase in structural weight. Although these methods increase the payload capacity, they also increase the vehicle's size and underwater drag. This results in increased energy requirements and decreased range, maneuverability, and speed.

A more advantageous approach to providing a UUV with more lift is to decrease the weight-to-displacement (W/D) ratio of the vehicle's pressure-resistant structure(s). Metallic pressure housings designed for 20,000-foot service pressure cannot achieve W/D ratios of less than 0.80. This means that a pressure housing that displaces 1,000 pounds of water when submerged requires 800 pounds of dry-weight structure. This leaves only 200 pounds for payload if the vehicle is to remain neutrally buoyant. If the W/D ratio of a hull can be decreased, considerable gains can be made in payload capacity.

For this reason, the Navy has chosen to further the development of lightweight pressure-resistant housings that provide a dry, one-atmosphere environment for a variety of payloads. The Naval Command Control and Ocean Surveillance Center (NCCOSC) RDT&E Division (NRaD) has an extensive history of evaluating the performance of lightweight ceramic materials used in the structures of external pressure-resistant housings.

Ceramic materials are ideally suited for application to the design of deep-submergence pressure housings. External pressure housings are predominantly loaded in compression. Therefore, materials having high specific compressive strength and high specific modulus are best suited for this application. Ceramic materials have these high specific properties and are also nonmagnetic, impervious to water, corrosion resistant, and heat conducive. Table 1* shows how the structural properties of ceramic materials compare with other structural materials, including metals, glasses, and graphite composite.

Dr. Stachiw has done extensive testing of cylindrical housings made from alumina ceramic since 1965. He has tested housings made from alumina-ceramic cylinders as large as 20-inches OD by 30-inches long (reference 3). Dr. Stachiw's work has demonstrated that the fabrication of large housings is not only possible, but that significantly lower W/D ratios can be achieved than are obtainable with traditional materials. W/D ratios as low as 0.5 have been obtained for housings with a 20,000-foot depth capability. For a housing which displaces 1,000 pounds of water, the payload capacity is increased from 200 pounds as provided by a typical titanium housing, to 500 pounds for an equivalent alumina-ceramic housing. This difference in payload capacity can be made up for by adding 300 pounds, approximately 9 cubic feet, of 32 pound/cubic foot syntactic foam to the titanium housing.

NRaD hopes to transition the use of alumina-ceramic material from the developmental stage to the operational environment by designing large alumina-ceramic pressure housings to operational constraints. Since Naval Sea Systems Command (NAVSEA) approval for the use of ceramic materials in Navy UUVs may at some point be sought, thorough analysis, design documentation, and quality assurance have been performed. This document serves as a record of this design and analysis effort.

OBJECTIVE

There are two main objectives to the development of 26-inch-OD and 33-inch-OD housings. First, to demonstrate that large housings utilizing alumina ceramic as the main structural material with W/D ratios less than 0.60 can be designed and

*Figures and tables are placed at the end of the text.

fabricated. Second, to determine what the effect scaling up in size has on the structural performance of alumina-ceramic pressure housings.

REQUIREMENTS

The following practical design requirements were selected for the two large housings. The housings were to be capable of service to a 20,000-foot ocean depth (9,030 psi external pressure) to be demonstrated by a proof test to 10,000 psi. The housings had to fit into an operationally useful dimensional envelope as shown in figure 3. To be of practical use, it was decided that the housings should be capable of having their entire payload loaded from one end. Previous NRaD designs made use of a large internal central ring stiffener which obstructed the vessel's interior and required that the payload be inserted and removed from both ends. The requirement of loading from one end motivated the minimum clear-bore diameter requirement shown in figure 3.

Temperature and transportation requirements listed below were also selected. Stresses induced on the large housings by these temperature and handling loads were found to be relatively insignificant. Consequently, the design of the major components of the large housing was driven entirely by their structural response to the depth loading requirement.

Temperature Range:	-40 F to +140 F
Storage and Transit:	3.0 g Longitudinal Forward
	1.5 g Longitudinal Aft
	1.5 g Transverse
	2.0 g Vertical Up
	4.5 g Vertical Down

APPROACH

MATERIAL SELECTION

Alumina ceramic was chosen as the structural material for the primary housing components, although other ceramic materials were considered. Table 1 reveals that stronger, stiffer, tougher, and lighter ceramic materials such as silicon nitride, boron carbide, and silicon carbide-reinforced alumina exist. Alumina was selected over other materials primarily because of its fabricability. The trade-off among these materials is addressed in reference 13 by Dr. Stachiw, who points out that alumina ceramic is the only material whose manufacturing technology is mature enough to fabricate large ceramic parts without requiring extensive development. Cylinders fabricated from silicon nitride, zirconia-toughened alumina, and silicon carbide-reinforced alumina are being procured by NRaD for test and evaluation, but their sizes are currently limited to a 12-inch OD by 18-inch length.

Titanium alloy 6Al-4V was selected for the majority of the metallic components used in the design of the housings based on its exceptional strength-to-weight ratio and resistance to corrosion. Furthermore, the coefficients of thermal expansion for titanium and alumina are closely matched, which minimizes stresses in the housing caused by thermal loads.

Polyurethane rubber was initially considered as impact protection for the housing. It was dismissed in favor of a hard-shell fairing made from spectra fiber-reinforced composite. Spectra was chosen for its low specific gravity, high specific strength, and impact toughness.

DESIGN

The design of the housings was driven by three basic requirements: the W/D ratio was to be minimized, stresses were to be kept below allowables, and the housing was to be resistant to buckling.

HOUSING CONFIGURATION

26-INCH OD HOUSING

Before going into the detailed analysis of the design of the large housings, the following is a description of the components which make up each assembly. The 26-inch OD housing consists of two alumina-ceramic cylinders joined by a central stiffener of which the inner- and outer-diameter dimensions meet the selected dimensional requirements shown in figure 3. The remaining exposed ceramic bearing surfaces at each end of the cylinder assembly are capped by channel-shaped titanium end caps. The cylinder assembly is closed off with alumina-ceramic hemispherical bulkheads.

The bearing surfaces of the ceramic hemispheres are capped with channel-shaped titanium end caps that mate with the ends of the cylinder assembly. These joints are made water tight with an O-ring face seal machined into the hemisphere end cap and are held together with a split aluminum clamp band. The Type 6 ceramic hemisphere used in the forward head assembly has two ports for pressure-relief valves and four ports for electrical connectors. The Type 4 ceramic hemisphere used in the aft head assembly contains no ports. The exterior of the entire assembly is protected from impact by a spectra composite fairing.

Cylinder Assembly

The cylinder assembly was the most technically challenging part of the entire assembly because it presented the designers with many choices and required an extensive trade-off study. Ten design options were evaluated. These options, A through J, are shown in figure 4, Sheets 1 through 5. Option J was chosen, but it is of interest to describe the other designs and explain why they were not chosen.

Initial sizing calculations for trade-off studies were simplified by assuming that the ends of the cylinder assembly were simply supported. Detailed design of the ceramic hemispheres was not considered at this point, as it has been shown that hemisphere stiffness has almost no effect on the overall buckling resistance of the housing due to failure by general instability (reference 9).

Option A presents itself as the most obvious choice since it consists of a single ceramic cylinder. The approximate dimensions of this cylinder would have been 25-inch OD, 64.5-inch length, and 1.0-inch-thick wall. Although this assembly appears to have advantages such as its simplicity, fewer bearing surfaces, fewer leak paths, and no need for a large titanium central stiffener, it also has some disadvantages. The design is not optimized because it is driven solely by buckling considerations. The high length/diameter (L/D) ratio necessitates a high thickness/diameter (t/D) ratio resulting in a wall that is thick and understressed. Therefore, the design does not take advantage of the alumina's high compressive strength. A more serious problem with this design is that cylinders of this length cannot be fabricated by currently available means. This is due to a number of reasons including the limitations of isopress and kiln size, handling difficulties, and green body self weight (a green body of this size may sag under its own self weight).

Option B is an attempt to make option A more fabricable by requiring two cylinders of half the assembly length joined with a coupling ring. At the time of design, it was not known whether this option would act like one long cylinder under load. The concept was later verified experimentally (reference 8). This concept still has the disadvantage of not using the material's compressive strength and, therefore, resulted in a high W/D ratio.

Option C is an elaboration of option B. This concept involves a thinner-walled cylinder supported by integral-rib stiffeners, resulting in a lighter-weight structure. Although calculated to have the lowest W/D ratio, the drawback to this design approach is that alumina-ceramic cylinders with integral ribs are very expensive to fabricate because of the extensive amount of grinding required. To make this cylinder, a very thick uniform wall would have to be pressed and fired, and then, the material between the ribs would have to be ground out. Less-expensive green machining of the ribs is not possible, as the differential in shrinkage of the thick- and thin-walled areas may lead to cracking during firing, or may cause unacceptable residual stress fields.

Option D attempts to lower the manufacturing costs of integral rib stiffeners by using alumina-ceramic rings that are epoxy-bonded into place. This makes it possible to manufacture a cylinder of uniform wall thickness, then reinforce it with rings. The idea was disqualified, because the tolerances required on the cylinder inner diameter (ID) and the ring's OD to ensure proper assembly would make this option prohibitively expensive. Furthermore, no previous test data of this design concept exists, making this a high-risk choice.

Option E is the same concept as option D, but instead of alumina-ceramic stiffeners, it incorporates metallic stiffeners which may be lightweight, but, at the same time, have a relatively low elastic modulus compared with alumina-ceramic.

Option F is the conventional NRaD design, which has been tested in the 6-, 12-, and 20-inch OD ceramic housing programs (references 11 and 14). The cylinder walls are thin enough to take advantage of alumina's high compressive strength. The titanium central stiffener is an optimized design, taking advantage of a small clear-bore to provide adequate stiffness which prevents general instability failures. This design was preferred because it was tested and, therefore, considered low risk. Unfortunately, the depth of the central stiffener interferes with the desired clear-bore requirements.

Option G is an attempt to make option F work, while obeying the minimum clear-bore diameter requirement. This results in an inefficient central-stiffener design. Inertia that was easily obtained in design option F through the depth of the stiffener has to be compensated for by increasing the stiffener width. This is an unsatisfactory way of providing additional buckling resistance, given weight constraints.

Option H is basically the same concept as option G, except that the stiffener is oriented outward from the cylinder wall, instead of inward. The cylinder has a reduced outer diameter and wall thickness. The excess space outside the cylinder is filled with syntactic foam, which provides buoyancy and protection from impact. The stiffener was found to be less effective in this configuration. Concentrating the mass of the central stiffener toward the inner diameter of the part results in a more-optimized stiffener design.

Option I incorporates a "composite" stiffener. The stiffener is constructed from both titanium and ceramic. This design takes advantage of alumina's greater specific modulus. The idea was dismissed as being too risky, since there is no experience with this design. Tolerances required for proper assembly would also make this option costly to manufacture.

Option J was a compromise solution between options B and G. It was discovered as a result of a trade-off study in which central stiffener size was reduced at the expense of thicker walls. The stiffener obeys the minimum clear-bore diameter, while the walls are still somewhat understressed. This actually may be advantageous, since there is reason to believe that the number of depth-loading cycles that a ceramic housing can withstand depends upon the stress to which the ceramic hull components are subjected (reference 11).

The final cylinder assembly design (drawing SK 9402-054) consists of two 96-percent alumina-ceramic cylinders (drawing 0126544) with a 25.0-inch OD, 31.90-inch length, and 0.90-inch-thick walls. These are joined at midbay with an epoxy-bonded titanium-alloy central stiffener (drawing SK9402-004) with a 26.0-inch OD, 20.50-inch ID, and an overall width of 5.0 inches. All bearing surfaces are protected with a 0.040-inch-thick GFR PEEK composite gasket (drawing 0128903). The remaining cylinder ends are capped with epoxy-bonded, two-inch-deep channel-shaped titanium-alloy end caps (drawing SK9402-002). Attachment ears for internal payload rails and tie rods are electron-beam welded to the ID of the cylinder end caps.

Four 0.25-inch-diameter tie rods (drawing SK 9402-012) are assembled in each bay of the cylinder assembly. Their primary function is to share in withstanding handling loads on the housing which would otherwise be exerted solely on the epoxy-bonded joint rings at the interface between hull components. More substantial tie rods to preload the cylinder assembly in compression to offset any tensile or flexural loads that may occur during transport were considered and determined to be unnecessary. Two aluminum rails (drawing SK9402-020) with lubricative anodic coatings act as guides and supports for loading payload into the interior of the housing. The center of each rail is notched to straddle the inner flange of the central stiffener. Dove-tail cutouts in the ears of the cylinder end caps provide radial support at the ends of the rails. This end-support configuration allows for relative sliding between the rails and the ears as the housing assembly shortens under hydrostatic loading.

Aft Head Assembly

The aft head assembly (drawing SK9402-053) contains a 96-percent alumina-ceramic Type 4 hemisphere (drawing 0127649) with a 2.50-inch-long, 25.0-inch OD by 0.90-inch thick wall cylindrical skirt that transitions into a tapered hemisphere with a minimum wall thickness of 0.375 inch at the pole. The skirted hemisphere design has two distinct design advantages over previous hemisphere designs (reference 14). First, the thickened bearing surface reduces the bearing stress by a factor of two, which may increase the cyclic fatigue life of the hemisphere. Second, the straight portion of the hemisphere allows an easier assembly with the titanium end cap. The bearing surface of the ceramic hemisphere is protected by a 0.040-inch-thick GFR PEEK composite gasket and epoxy bonded into a 2.5-inch-deep titanium-alloy end cap (drawing SK9402-001).

Forward Head Assembly

The forward head assembly (drawing SK9402-052) contains a 96-percent alumina-ceramic Type 6 hemisphere (drawing 0127755) with six off-axis through holes. The meridian of the Type 6 hemisphere transitions from a 2.50-inch-long, 25.0-inch OD by 0.90-inch-thick-wall cylindrical skirt into a uniformly 0.563-inch-thick walled hemisphere. The bearing surface of the ceramic hemisphere is protected with a GFR PEEK composite gasket and titanium-alloy end cap, of the same design used for the aft head assembly. All six penetration holes are on the lower half of the hemisphere. Tapped ports for electrical connectors and relief valves are provided at each through hole with titanium alloy penetration inserts. Four 1.500-12UNF-2B threaded ports are provided via electrical connector penetrations (drawing SK 9402-031) with O-ring surfaces for both radial and face seals. Military straight-thread tube-fitting boss per MS33649-08 are provided via two relief valve penetrations (drawing SK 9402-030).

Fairing

The entire ceramic housing is protected by a spectra composite fairing. Spectra consists of extended ultra-high molecular-weight polyethylene fibers woven into cloth and impregnated with epoxy resin. Spectra was selected for protecting the housing's ceramic components because of its low-specific gravity, high-specific strength, low water absorption, and excellent impact resistance.

The cylindrical hull assembly is covered with four semi-cylinders (drawing SK9402-92-001) made from this material. Integral ribs stiffen these semi-cylinders and serve as hard points on the housing assembly for handling with be' y bands or lifting slings. The ceramic hemispheres are protected with spectra hemispherical shells (drawing SK 9402-92-003). These fairings are attached to each hemisphere assembly with split-fiberglass clamp bands (drawing SK9402-051). Lift pads and lugs (drawing SK9402-029 and SK9402-027) are bolted to each hemisphere fairing to provide hard points for handling and assembling. Lift lugs, placed at the center of gravity of the hemisphere, enable the hemisphere assembly to hang vertically during assembly procedures. All spectra components contain through holes that allow the fairing to fill and drain with water when lowered into and raised out of the test chamber during pressure testing.

33-INCH OD HOUSING

The 33-inch OD housing consists of two alumina-ceramic cylinders joined with a titanium central stiffener. The joint configuration between the cylinder assembly and the hemispherical bulkheads is identical to that of the 26-inch OD housing, except that closure is maintained with four circumferential bolts, rather than a split aluminum clamp band. Type 4 ceramic hemispheres, with two pressure-relief valve ports, are used for both forward and aft head assemblies. The exterior of the entire assembly also is protected from impact by a spectra composite fairing.

Cylinder Assembly

The cylinder assembly (drawing SK9402-057) consists of two 96-percent alumina-ceramic cylinders (drawing 0127545) with a 32.0-inch OD, 39.53-inch length, and 1.15-inch-thick walls. These are joined at midbay by an epoxy-bonded titanium alloy central stiffener (drawing SK9402-011) with a 33.[illegible] inch OD, 26.0-inch ID, and 5.5-inch overall w[illegible]n. All bearing surfaces at each of the cylinder ends are protected with a 0.040-inch-thick GFR PEEK composite gasket (drawing 0128904). The remaining cylinder ends are capped with 2.5-inch-deep channel-shaped titanium-alloy end caps (drawing SK9402-009) which are epoxy bonded to the ceramic. Attachment ears for internal payload rails and tie rods are electron-beam welded to the ID of the cylinder end caps. Four 0.25-inch-diameter tie rods (drawing SK9402-023) are assembled in each bay of the cylinder assembly.

Two aluminum rails (drawing SK9402 022) with lubricative anodic coatings act as guides and supports for loading payload into the interior of the housing. The center of each rail is notched to straddle the inner flange of the central stiffener. Dove-tail cutouts in the ears of the cylinder end caps provide radial support at the ends of the rails. This end-support configuration allows for relative sliding between the rails and the ears as the housing assembly is axially shortened under hydrostatic loading.

Aft Head Assembly

The aft head assembly (drawing SK9402-056) contains a 96-percent alumina-ceramic Type 4 hemisphere (drawing 0127651) with a 3.0-inch-long, 32.0-inch OD by 1.15-inch-thick wall cylindrical skirt that transitions into a tapered hemisphere with a minimum wall thickness of 0.480 of an inch at the pole. The bearing surface of the ceramic hemisphere is protected by a 0.40-inch-thick GFR PEEK composite gasket and is epoxy bonded into a 3.0-inch-deep titanium-alloy end cap (drawing SK9402-008). Two off-axis 1.0-inch-diameter holes are for pressure-relief port valves.

Forward Head Assembly

The forward head assembly is identical to the aft head assembly.

Fairing

The entire ceramic housing is protected by a spectra composite fairing. The cylindrical hull assembly is covered by four semi-cylinders (drawing SK9402- 92-002) made from this material. Integral ribs stiffen these semi-cylinders and serve as hard points on the housing assembly for handling with belly bands. The ceramic hemispheres are protected with spectra hemispherical shells (drawing SK9402-92-004). These fairings are attached to each hemisphere assembly with split-fiberglass clamp bands (drawing SK9402-061). Lift pads and lugs are bolted to each hemisphere fairing to provide hard points for handling and assembly. Lift lugs, placed at the center of gravity of the hemisphere, enable the hemisphere assembly to hang vertically during assembly procedures. All spectra components contain through holes that allow the fairing to fill and drain with water when lowered into and raised out of the test chamber for testing.

ANALYSIS TOOLS

STABILITY ANALYSIS

Stability analysis of the 26- and 33-inch OD housings was performed using BOSOR4 developed by David Bushnell at Lockheed Missiles & Space Company, Inc. BOSOR4 is a structural-analysis program that can be used to predict the buckling behavior of complex shells of revolution. The code is written in FORTRAN IV. Predictions are based on a finite difference energy minimization with constraint conditions for the structure under study. The meridian of the shell of revolution is modeled using a number of segments with material, geometric, and boundary-condition properties representative of the real structure. BOSOR4 is currently run on a Sun SPARC station 2 through a personal computer workstation.

STRESS ANALYSIS

Final stress analysis of the 26- and 33-inch OD housings was performed using the finite-element method (FEM). All FEM models were created using the pre/post processing code PATRAN (version 2.5) developed by PDA Engineering. Analysis was performed using ABAQUS (version 4.9) developed by Hibbitt, Karlsson, and Sorensen, Inc. Translations between PATRAN and ABAQUS databases were made with the software PAT/ABA and ABA/PAT (version 3.1) provided by PDA. At NRaD, PATRAN is run on DEC VAX Station II GPX through a Tektronix 4236 graphics workstation.

ABAQUS is executed on NRaD's centrally operated Convex C-480 minisupercomputer.

To reduce computation time, all FEMs were developed for axisymmetric analysis. Although axisymmetry holds for the loading condition (hydrostatic external pressure), it is not strictly true for the housing geometry because of the off-axis penetrator holes in the hemispheres. However, Saint-Venant's Principle leads to the assumption that local stress concentrations around hemisphere through holes would not affect the overall structural response. To further reduce model size, half-symmetry was assumed at the midpoint of the central stiffener. Again, this is not strictly true because the hemispheres are not identical for the 26-inch OD housing; however, the effects of this geometry were considered minor.

Both linear four-noded (CAX4R) and quadratic eight-noded (CAX8R) axisymmetric-reduced integration solid elements were used in the models. In regions of expected uniform stresses, two CAX8R elements were used through the ceramic components' wall thickness. In regions requiring finer mesh detail, CAX4R elements were used with up to eight elements through the wall thickness. To model interface behavior at the cylinder and hemisphere joint, gap (INTER3A) elements were used in the joint contact region. These elements transmit pressure and shear stress between the contact surfaces, but allow normal separation and relative transverse displacements to occur. All finite-element analysis results presented here were calculated for an external pressure of 10,000 psi, which represents the proof load for both housing assemblies.

In modeling the joint designs it was assumed that the titanium end caps and central stiffener were rigidly bonded with epoxy to the ceramic component ends. Thus, boundary nodes were shared (i.e., rigidly linked) between the ceramic and epoxy and the epoxy and titanium. The modeling was done assuming that there was 0.040 of an inch of epoxy in the radial clearance and 0.010 of an inch of epoxy in the axial clearance between the ceramic component ends and their titanium joint rings. All materials were modeled assuming linear elastic-isotropic material properties. No attempt was made in the FEM to account for possible epoxy extrusion, fracture, separation, or any other nonlinear response in the bonded regions of the joint. All structural analysis was based on the following material properties:

96-percent Alumina-Ceramic:	Elastic Modulus = 44.0 Mpsi
	Poisson's Ratio = 0.21
	Flexural Strength = 53 Kpsi
	Compressive Strength = 300 Kpsi
Ti-6Al-4V Titanium:	Elastic Modulus = 16.4 Mpsi
	Poisson's Ratio = 0.31
	Yield Strength = 90 Kpsi (proportional limit)
Fabric-Reinforced Phenolic:	Elastic Modulus = 1.0 Mpsi
	Poisson's Ratio = 0.375
Epoxy:	Elastic Modulus = 130.0 Kpsi
	Poisson's Ratio = 0.457

ANALYSIS

Design stress allowables for structural analysis are shown in table 2. The Maximum-Normal-Stress-Theory is used as a failure criteria for stress analysis of the ceramic components in each housing. Minimum principle stresses are compared to the compressive strength of alumina, and tensile maximum-principle stresses are compared to the flexural strength of alumina. Flexural strength is used instead of tensile strength since the tensile stresses found in the ceramic components are bounded by compressive stresses as exists in flexural test specimens. In addition, the flexural-strength data for a ceramic composition is typically more available than tensile-strength data since tensile tests for ceramics tend to be unreliable. The von Mises Theory is the failure criteria for stress analysis of all metallic housing components.

BUCKLING ANALYSIS OF 26-INCH OD HOUSING

The buckling analysis was performed by first estimating the required alumina-ceramic cylinder wall thickness using hand calculations for the 26-inch OD and 64.5-inch length constraints. The cylinder wall thickness was calculated assuming that the hemispheres and central stiffener would act as rigid end constraints. Hemisphere wall thickness was determined by stress, not buckling, considerations. Because bearing surfaces are a source of crack initiators, axial stresses were lowered in these regions by thickening the walls, hence, the skirted hemisphere design. The wall thickness for the ceramic components, along with a first-order estimate of the central stiffener, was calculated with the computer code BOSOR4 to model the 26-inch OD housing. Iterations on stiffener size and wall thickness were then performed to come up with component dimensions, resulting in a minimum buckling pressure of 12,500 psi.

As the detailed design of the ceramic-hull components, titanium end caps, and central stiffener progressed, the BOSOR4 model of the entire assembly was updated to ensure that the desired safety margin was being maintained. The central stiffener design was based on BOSOR4 calculations of the required cylinder end support needed to meet the buckling criteria. The central stiffener is designed to minimize the weight of the part while meeting OD and ID constraints. In addition, the central stiffener required sufficient width to encapsulate the cylinder ends, as done with the end caps. Maximum cylinder-end support for minimum weight was achieved by concentrating the mass of the central stiffener at its inner flange. The ID of the inner flange was constrained by the 20.5-inch clear-bore requirement for packaging. Otherwise, a smaller ID would be desirable to further optimize the design of the central stiffener.

The final models constructed for the 26-inch and 33-inch OD assemblies utilized a total of 15 segments to define an axisymmetric model for each housing. Three segments are used to properly define the spherical, conical, and cylindrical regions of each ceramic hemisphere. Each ceramic cylinder is modeled using a single segment. Earlier models of the housings incorporated more detail in modeling both the cylinder and hemisphere end caps, but it was shown that their presence in the model has little effect on the general instability failure modes for the entire assembly. Seven discrete branched-shell segments were used to accurately model the central stiffener. BOSOR4 models allowed for meridional rotations at the interface between the cylinder and hemisphere ends. The calculated differences between modeling fixed or free rotations at the clyinder/hemisphere interface were shown to be minimal for the overall calculated buckling capacity of the assembly.

The results of the BOSOR4 model are shown in figures 5 and 6 for the first two critical buckling modes for N=2 and N=3. The N=2 buckled configuration (figure 5) indicates that a general instability is occurring at a critical pressure of 12,463 psi with two lobes forming (the cylinder cross section is becoming oval in shape). The N=3 buckled configuration (figure 6) indicates that three lobes are forming in each bay, and the lobes in the first bay are out of phase with the lobes in the second bay which results in twisting of the central stiffener. The N=3 mode occurs at much higher pressure (18,653 psi), so the collapse of the battery housing assembly would always occur in the N=2 mode. It is interesting to point out that it is primarily the cylinder wall thickness that defines the critical buckling pressure for the N=3 mode, and it is primarily the central stiffener design that drives the critical buckling pressure for the N=2 mode. This implies that the cylinder-wall thickness could be reduced further, until the N=3 critical buckling pressure is lowered to achieve equal critical buckling pressure for N=2 and N=3 modes, allowing for a more optimized design. This option was not pursued since the tradeoff for reducing cylinder wall thickness is higher stresses in the cylinder under depth loading. Local buckling of webs and flanges that comprise the central stiffener and end caps also were calculated using BOSOR4, but were not a factor at the operating pressures for which the housings were intended.

STRESS ANALYSIS OF 26-INCH OD HOUSING

The design criteria for evaluating the stress analysis results are shown in table 2. Figure 7 is a plot of the deformed and undeformed shape of the half-symmetry model of the 26-inch housing under 10,000 psi external load. The plot reveals that bending is occurring at both ends of the ceramic cylinder because of the higher relative radial stiffness of the hemisphere and central stiffener. The bending stresses could have been reduced by matching the radial deflection of the hemisphere to that of the cylinder. A hemisphere with approximately half the wall thickness of the cylinder would result in almost equal radial deflection. The idea of a thinner wall thickness at the bearing surface of the hemisphere was dropped in favor of a thicker wall which would lower stresses at the bearing surface, thereby delaying the onset of spalling in the hemisphere. The presence of encapsulating metallic end caps on the ceramic cylinders makes it difficult to completely design away bending stresses in the joint region. Figure 8 shows a view of the deformed and undeformed shapes of the hemisphere and cylinder end caps under external pressure. Deflections in this figure have been scaled-up 10 times for clarity.

Individual stress analysis results will be presented for each of the ceramic components first. Figure 9 shows the axisymmetric model of the original design of the Type 6 ceramic hemisphere. This hemisphere was to contain six off-axis through holes for pressure-relief valves and electrical connectors. These penetrations were to be located in a circumferential band of increased wall thickness to offset stress concentrations associated with the presence of the six through holes. The shell wall was then thinned at the pole and at the transition between the hemisphere end skirt and the circumferential band to minimize weight. This design was quickly rejected when it became clear that any gains associated with increased wall thickness for the penetrations were offset by high bending stresses that occurred in the transition regions.

The final design of the Type 6 hemisphere consisted of a cylindrical skirt originating at the equatorial bearing surface with a more-gentle transition into a hemisphere with uniform wall thickness. The thickness of the hemisphere was sized to handle stress-concentration effects of through holes with a margin of safety of 1.5. Figures 10 and 11 show the FEM minimum-principal stress results for the final Type 6 hemisphere design. Figure 10 shows stress contours with no through holes modeled. Figure 11 shows stress contours of a Type 6 hemisphere cross section with a single two-inch diameter through hole at the pole. This centerline location is not actually used on the Type 6 hemisphere, but calculations of the state of stress around this single hole can be inferred to be the identical stress state for the off-axis through holes that are actually present. Without any penetrations, the highest compressive stress of −162,590 psi occurs at the inner radius of the hemisphere at the transition point from the cylindrical skirt resulting in a safety factor of 2.04 at 9,030 psi. The highest compressive stress due to stress concentrations at the through holes equals −226,360 psi resulting in a safety factor of 1.47 at 9,030 psi. Comparison of the membrane stresses of figures 10 and 11 confirms that the presence of the two-inch diameter through hole results in a stress-concentration factor of approximately 2.0. This is a conservative calculation since the presence of a penetrator in the through hole will act to reduce the stress-concentration effects of the hole. The wall-thickness transition out of the cylindrical end skirt results in substantial stress gradients, but these are well within the design criteria selected for alumina. Figure 12 shows a close up of the minimum principal stresses in the region of the hemisphere/cylinder joint.

Figure 13 is a maximum principal stress plot for the Type 6 hemisphere. This plot is important because it indicates that localized tensile stresses as high as 18,910 psi are occurring at the bearing surfaces of the hemisphere. These tensile stresses can initiate cracks that may propagate under cyclic loading and eventually degrade the structural performance of the ceramic hull. Figure 14 offers a close-up view of the maximum principal stresses in the joint region, while figure 15 confirms that these tensile stresses are radially orientated. These radial stresses are primarily caused by the mismatch in radial expansion between the ceramic and titanium under axial load. The titanium will strain radially almost four times more than the alumina because of the difference in Poisson's ratio and elastic modulus of these two materials. The lack of relative displacement causes this tensile strain to be transferred directly into the ceramic-bearing surface, possibly opening up microcracks already on, or below, the surface. Intuitively, the amount of epoxy-filled space that exists between the titanium and ceramic bearing surface should affect the magnitude of the tensile stresses that occur in the ceramic. Modified FEMs that were run appear to show trends in the magnitude of ceramic tensile stresses as a function of epoxy thickness.

Figure 16 indicates the effect of axial clearance on the radial tensile stresses. Increasing the axial clearance between the ceramic end and the titanium end cap from 0.010 to 0.040 resulted in a 37.5-percent reduction in tensile stress level. However, no substantial design changes in axial clearance were made because of the lack of knowledge of the mechanical behavior of the epoxy at the high stress levels that were present in the joint region. Increased axial clearance between the ceramic and titanium bearing surfaces also had the drawback of increased localized stresses in the titanium end caps. Tests performed on 8-inch OD cylinders with 0.25 of an inch of epoxy at the bearing surface have shown that the increased localized stresses in the end caps can, indeed, lead to failure of the end cap.

Stress analysis of the 0.040-inch-thick GFR PEEK composite bonded to the ceramic component ends indicates that the presence of gaskets reduces tensile stresses that occur in the ceramic ends. The actual magnitude of reduction was difficult to determine because of the difficulties of modeling an orthotropic (0/90) laminate within an axisymmetric model. Three-dimensional models were not pursued since actual cyclic tests of alumina cylinders with GFR PEEK composite gaskets indicated that the gasket prolonged the cyclic life of the housing assemblies. A possible explanation for the benefits of GFR PEEK composite gaskets are the high- modulus carbon fibers used to reinforce the peek matrix. The modulus of the fibers is intermediate between the ceramic and the titanium which helps buffer the radial expansion mismatch previously described. This helps reduce the radial tensile stresses in the ceramic ends the same way that using a higher modulus material to fabricate the end caps would help. For example, steel end caps would result in lower tensile stresses in the ceramic, but at the expense of increased weight. Although the gaskets have relatively high in-plane stiffness, the peek matrix offers a more compliant material perpendicular to the fiber orientation which should act to buffer any stress concentrations caused by local imperfections in the ceramic bearing surface.

Figure 17 shows the minimum principal stress plot (principal stress 1) and figure 18 shows the maximum principal stress plot (principal stress 3) for the Type 4 ceramic hemisphere for the 26-inch housing. The highest compressive stress of −172,430 occurs at the tapered pole and at the inner radius of the transition region out of the cylindrical skirt. These stress levels result in a safety factor of 1.93 at a working pressure of 9,030 psi. The maximum principal stress plot indicates the presence of tensile stresses at the bearing surface of the Type 6 hemisphere. Since the Type 4 hemisphere was not to contain any through holes, the hemisphere wall was tapered by having offset centers of radii for the inner and outer radius. This tapering offered an optimized weight hemisphere while still incorporating the cylindrical skirt design.

Figure 19 shows the minimum principal stress contour plots and figure 20 shows the maximum principal stress contour plots for the ceramic cylinders used for the 26-inch housing assembly. The left side of these plots corresponds to the hemisphere end of the cylinder, while the right side represents the end that is bonded to the central stiffener. The highest compressive stress of −144,720 psi occurs at the inner radius of the cylinder towards midbay and corresponds to a safety factor of 2.30 at 9,030 psi. Reducing the wall thickness of the cylinders to allow for higher membrane stresses was not pursued because this would result in less bearing surface at the cylinder's ends. Figure 20 shows that radial tensile stresses are occurring at both ends of the cylinder with peak stresses of 19,935 psi at the hemisphere end and 18,803 psi at the central stiffener end. Figure 21 shows a close-up view of the maximum principal stress plot at the central stiffener end of the ceramic cylinder. These plots indicate that the bearing surfaces of the cylinder and hemisphere ends are equally loaded through the joint regions. Figures 22, 23, and 24 show radial, axial, and circumferential stress contour plots, respectively, for the ceramic cylinders to clarify the directionality of the stresses displayed in the minimum and maximum stress contour plots.

Figure 25 shows von Mises (Distortion-Energy Theory) stresses for a half-symmetric plot of the central stiffener. The maximum von Mises stress of 49,395 psi corresponds to a 2.02 safety factor at 9,030 psi. These stresses are low because the design of the central stiffener is driven by stability, not strength, requirements. Figure 26 shows von Mises stress contours for the hemisphere and cylinder end caps for 10,000 psi external load. The maximum von Mises stress of 71,930 psi occurs in the region adjacent to the O-ring gland on the hemisphere end cap. This peak stress corresponds to a 1.39 safety factor at 9,030 psi.

With the exception of the bearing surfaces around the O-ring seal, the hemisphere and cylinder end caps are relatively low-stressed parts. Like the central stiffener, the design of the end caps was driven by criteria other than strength requirements. The depth of the channel-shaped end cap that acts to encapsulate the ends of the ceramic components has relatively little effect on the stresses in the adjacent ceramic, or in the end cap itself. A depth of 2.50 inches for the hemisphere end cap and 2.0 inches for the cylinder end cap was chosen, based on the success of the 2.0-inch-deep design used in the 20-inch OD testing program. As mentioned previously, cracks that propagate from radial tensile stresses at the ceramic-bearing surfaces can degrade the structural performance of the housing assembly. The depth of the U-shaped end cap acts to contain the effects of cracks that may appear and, thus, prolongs the cyclic life of the pressure hull.

The inner lip of the hemisphere end cap provides a guide for centering the hemisphere assembly on the cylindrical hull assembly. Under hydrostatic load, the radial clearance in this lap joint closes and the hemisphere assembly acts to support the ends of the cylindrical hull assembly. The von Mises stress plot indicates that the stresses in this extended lip are low, given the strength of material used. However, reducing the wall thickness of the lip further was not pursued in order to avoid damage that could occur while handling and assembling the 26-inch OD housing components.

Figure 27 shows the element mesh used to model the electrical feedthrough penetrator assembled in the two-inch-diameter through holes of 26-inch housing Type 6 hemisphere. Stress analysis of the penetrator was performed using an axisymmetric model of the Type 6 hemisphere with the through hole located at the pole. Again, this is not an actual location of a Type 6 hemisphere through hole, but since the hemisphere wall is of uniform thickness and the stress concentration effects around the hole are localized, this was deemed an acceptable modeling approach. The penetrator design is based on earlier inserts designed by Stachiw (reference 3). The purpose of the penetrator is to provide a threaded metallic port that can accept bulkhead connectors and relief valves. The seal between the penetrator and the through hole in the ceramic is accomplished with a fabric-reinforced phenolic spacer. This spacer is sized so that when assembled with the titanium penetrator insert, an annular O-ring gland is formed to provide a face seal for the external hydrostatic load. The pressure load on the penetrator is assumed to act on the interior of the flange up to the location of the O-ring seal, as well as all external surfaces outside of the ceramic through hole. A disk of material was modeled at the tapped-through hole of the penetrator to simulate the force that would be exerted on the penetrator by the pressure that acts on the surface of an assembled electrical connector. This disk was given a low modulus value so that it would not act to stiffen the penetrator, but merely transfer load to it. To allow for relative displacements under load, gap elements were used at the boundaries between the ceramic hemisphere, phenolic spacer, and titanium penetrator.

Figure 28 shows the von Mises stress plot for the electrical feedthrough penetrator for 10,000 psi external load. The highest stresses occur in the region around the O-ring gland where the penetrator is essentially unsupported and at the inner radius of the penetrator as the diameter of the through hole is squeezed by the compressive membrane stresses in the ceramic hemisphere. This peak stress corresponds to a safety factor of 0.95 at 9,030 psi which was considered adequate because of the conservative nature of the modeling approach. Figure 29 shows the von Mises stress plot for the pressure-relief valve penetrators assembled into the one-inch-diameter through holes in the 26-inch housing Type 6 ceramic hemisphere. The modeling approach used for the one-inch penetrator was identical to that described above for the two-inch penetrator. The peak stress calculated for the one-inch penetrator was 97,835 psi for 10,000 psi external pressure. This corresponds to a safety factor of 1.02 at 9,030 psi. Stress analysis results for the 26-inch housing are summarized in table 3.

BUCKLING ANALYSIS OF 33-INCH OD HOUSING

The iterative process for designing the 33-inch OD housing proceeded in the same manner as that of the 26-inch OD housing. Because the design of the 26-inch OD housing parallels the design of the 33-inch OD housing, the buckling modes of failure for the larger housing are very similar to those shown for the 26-inch OD housing. Figure 30 shows the N=2 buckled configuration which occurs at a critical buckling pressure of 12,737 psi.

STRESS ANALYSIS OF 33-INCH OD HOUSING

The configuration of the 33-inch housings is a scaled-up version of the 26-inch OD housing. The modeling techniques and design philosophy used in the stress analysis of the 33-inch housings were similar to those used for the smaller housings. Figure 31 shows the deformed and undeformed shape of the half-symmetry model of the 33-inch OD housing. As with the 26-inch OD housing, bending is occurring at both ends of each cylinder. Figures 32 and 33 represent minimum and maximum principal stress plots, respectively, for the Type 4 hemisphere used to cap both ends of the 33-inch pressure hull. Figure 34 shows a close-up view of the maximum principal stress plot at the hemisphere/cylinder joint where localized tensile stresses are present. The highest compressive membrane stress that occurs in the hemisphere is -170,165 psi which corresponds to a safety factor of 1.95 at 9,030 psi external pressure. The peak tensile stress of 21,940 psi occurs toward the inner edge of the hemisphere bearing surface.

Minimum and maximum stress plots for the ceramic cylinders are shown in figures 35 and 36 respectively. The highest compressive stress of -145,255 psi results in a safety factor of 2.29 at 9,030 psi external pressure for the alumina cylinder. The peak tensile stress of 17,505 psi occurs at the bearing surface of the cylinders at the hemisphere/cylinder joint interface. Von Mises stress plots for the major titanium components of the 33-inch housing are shown in figures 37 and 38. The magnitudes and distribution of the stresses in these parts is again very similar to the equivalent parts designed for the 26-inch OD housing. The one-inch penetrators used for the 33-inch OD housing are identical to those described for the pressure relief ports on the 26-inch OD housing. Stress analysis results for the 33-inch OD housing are presented in table 3.

DISCUSSION

The buckling and stress analysis of the two large alumina-ceramic housings show that they are both designed with an adequate safety factor for utilization on unmanned vehicles for deep submergence applications. The component weight summary is shown below:

26-INCH OD HOUSING

Component	Component Weight in Pounds
Forward Ceramic Hemi (Type 6)	77.75
Aft Ceramic Hemi (Type 4)	74.17
Titanium Hemi End Cap (Qty:2)	36.90
Hemi Penetrator Inserts (Qty:6)	3.86
Ceramic Cylinder (Qty:2)	565.16
Titanium Cyl. End Cap (Qty:2)	25.20
Titanium Central Stiffener	85.24
Internal Tie-Rods (Qty:8)	1.76
Aluminum Clamp Bands (4 halves)	5.50
TOTAL WEIGHT	875.54
TOTAL DISPLACEMENT (in seawater)	1,495.67
WEIGHT-TO-DISPLACEMENT RATIO (in seawater)	0.585

33-INCH OD HOUSING

Component	Component Weight in Pounds
Forward Ceramic Hemi (Type 4)	154.17
Aft Ceramic Hemi (Type 4)	154.17
Titanium Hemi End Cap (Qty:2)	55.00
Hemi Penetrator Inserts (Qty:4)	0.42
Ceramic Cylinder (Qty:2)	1,145.52
Titanium Cyl. End Cap (Qty:2)	39.60
Titanium Central Stiffener	139.28
Internal Tie-Rods (Qty:8)	2.19
TOTAL WEIGHT	1,690.77
TOTAL DISPLACEMENT (in seawater)	3,038.82
WEIGHT-TO-DISPLACEMENT RATIO (in seawater)	0.556

As the summary shows, the W/D ratio of the two housings falls below 0.60. The 26-inch OD housing has a dry structural weight of 876 pounds and a displacement in seawater of 1,496 pounds (W/D = 0.585) which provides a payload capacity of 620 pounds for the housing to remain neutrally buoytant. As an exercise, a titanium pressure housing was designed to the same requirements as the 26-inch OD housing. The optimized design resulted in a housing that weighs 1,364 pounds, displaces 1,571 pounds of seawater, and has a W/D ratio of 0.868. It provides for a payload capacity of only 207 pounds while remaining neutrally buoyant. The ceramic housing provides 2.99 times the payload capacity of the optimized titanium housing.

Another interesting comparison is to determine how much syntactic foam it would take to make up for the difference in payload capacity between the alumina ceramic and titanium designs. To gain the additional 413 pounds in payload capacity the ceramic housing provides, the titanium housing would require that 413 pounds of syntactic foam be strapped to it. This raises the structural weight of the titanium housing to 1,777 pounds and adds 13 cubic feet of volume to the vehicle (using 32 pound/cubic feet foam). The cost of that amount of foam rated for a 20,000-foot service depth is approximately $23,400 at 1993 prices.

The 33-inch OD alumina ceramic housing has a calculated dry structural weight of 1,690 pounds and a displacement in seawater of 3,039 pounds. This provides a payload capacity of 1,348 pounds while the housing remains neutrally buoyant. An optimized titanium housing designed to the same constraints would weigh 2,720 pounds and have a displacement of 3,170 pounds in seawater, providing 450 pounds of payload capacity while remaining neutrally buoyant. The payload capacity of the ceramic housing is, again, three times that of the optimized titanium design.

In order to make up the difference in payload capacity between the two housing designs, the titanium design would require an additional 898 pounds (28 cubic feet) of 32 pound/cubic feet foam. Increasing the dry weight to 3,937 pounds at a cost of approximately $50,400 (1993 prices of syntactic foam rated for a 20,000-foot service depth).

CONCLUSION

Large pressure-resistant housings for a 20,000-foot service depth can be designed using alumina ceramic as the main structural material. Furthermore, these housings can be analyzed for buckling and stress using commercially available computer programs without modification. When alumina-ceramic housings are designed to the same safety factors as titanium housings, their high-specific strength and modulus allow them to provide up to three times the payload capacity of titanium housings, while the dry structural weight remains 35-percent lower than their titanium counterparts.

RECOMMENDATION

The analysis of the two large alumina-ceramic housing designs presented in this report shows that significant reductions in the W/D ratio are possible when alumina ceramic is utilized as the main structural material. It is recommended, therefore, that alumima-ceramic housings be seriously considered for all unmanned deep-submergence applications and that the two housings described in this report be built and tested to determine fabrication feasibility and structural performance.

Furthermore, it is recommended that before the 26-inch OD and 33-inch OD housings are fabricated, a half-scale model of the 26-inch OD housing be fabricated, instrumented with strain gages, and tested to validate the buckling and stress analysis presented in this report. The test plan for the model housing should call for a proof test to 10,000 psi, at least 500 cycles to 9,000 psi, and a final pressurization to destruction to determine the accuracy of the buckling prediction. Parts for the 26-inch OD and 33-inch OD housings should not go into final machining until the model has validated predicted results.

REFERENCES

1. Allied Signal. 1990."Spectra, High Performance Fibers," P. O. Box 31, Petersburg, VA 23804.

2. Bickell, M. B., and C. Ruiz."Pressure Vessel Design and Analysis," St. Martin's Press.

3. Brush. D. O., and B. O. Almroth. 1975."Buckling of Bars, Plates, and Shells," McGraw-Hill Company.

4. Bushnell, David."BOSOR4 User's Manual," Lockheed Missiles & Space Co., Inc.

5. Bushnell, David. 1981."Buckling of Shells-Pitfalls for Designers," AIAA Journal, Vol. 19, (Sep), pg. 1183.

6. Department of Defense. 1986."Metallic Materials and Elements for Aerospace Vehicle Structures," MIL-HDBK-5E, Washington, DC (Jun).

7. Hibbitt, Karlsson, and Sorensen, Inc. 1989."Abaqus User's Manual."

8. Johnson, R. P., R. R. Kurkchubasche, and J. D. Stachiw. 1993. "Exploratory Study of Joint Rings for Ceramic Underwater Pressure Housings," NRaD TR 1586 (May), NCCOSC RDT&E Division, San Diego, CA.

9. Kurkchubasche, R. R. 1992."Elastic Stability Considerations for Deep Submergence Ceramic Pressure Housings," Intervention '92, Marine Technology Society.

10. Kvitka, A. L., and Diachkov. 1983. "Stress Composition and Strength of Containers From Brittle Non-Metallic Materials," Ukrainian SSR Academy of Sciences, Kiev.

11. Stachiw, J. D. 1989."Exploratory Evaluation of Alumina Ceramic Housings for Deep Submergence Service—Third Generation Housings," NOSC TR 1314, Naval Ocean Systems Center, San Diego, CA.

12. Stachiw, J. D., R. P. Johnson, and R. R. Kurkchubasche. 1993."Evaluation of Scale-Model Ceramic Pressure Housing for Deep Submergence Service—Fifth Generation Housings," NRaD TR 1582 (Mar), NCCOSC RDT&E Division, San Diego, CA.

13. Stachiw, J. D. 1992."Engineering Criteria Used in the Selection of Ceramic Composition for External Pressure Housings," Intervention '92, Marine Technology Society.

14. Stachiw, J. D. 1990."Exploratory Evaluation of Alumina Ceramic Housings for Deep Submergence Service—Fourth Generation Housings," NOSC TR 1355 (Jun), Naval Ocean Systems Center, San Diego, CA.

15. Young, W. C. 1989."Roark's Formulas for Stress and Strains, Sixth Edition," McGraw-Hill Company.

16. Wesgo."Technical Ceramics and Metals," 477 Harbor Boulevard, Belmont, CA 94002.

GLOSSARY

AUTB	Advanced Ultrasonic Test Bed
FEA	finite element analysis
FEM	finite element model
GFRP	graphite fiber-reinforced peek
ID	inner diameter
IED	independent exploratory development
Kpsi	one thousand psi
L	length
L/D	length/diameter
MEK	methyl ethyl ketone
MOR	Modulus of rupture
ND	nondestructive
NDE	nondestructive evaluation
NDT	nondestructive test
NOSC	Naval Ocean Systems Center
OD	outside diameter
PEEK	poly-ether-ether-ketone
rms	root mean square
SAM	Scanning Acoustic Microscopy
S.F.	stress factor
t	ceramic shell thickness
t/D	thickness diameter
t/Ro	thickness external radius
W	width
W/D	weight-to-displacement

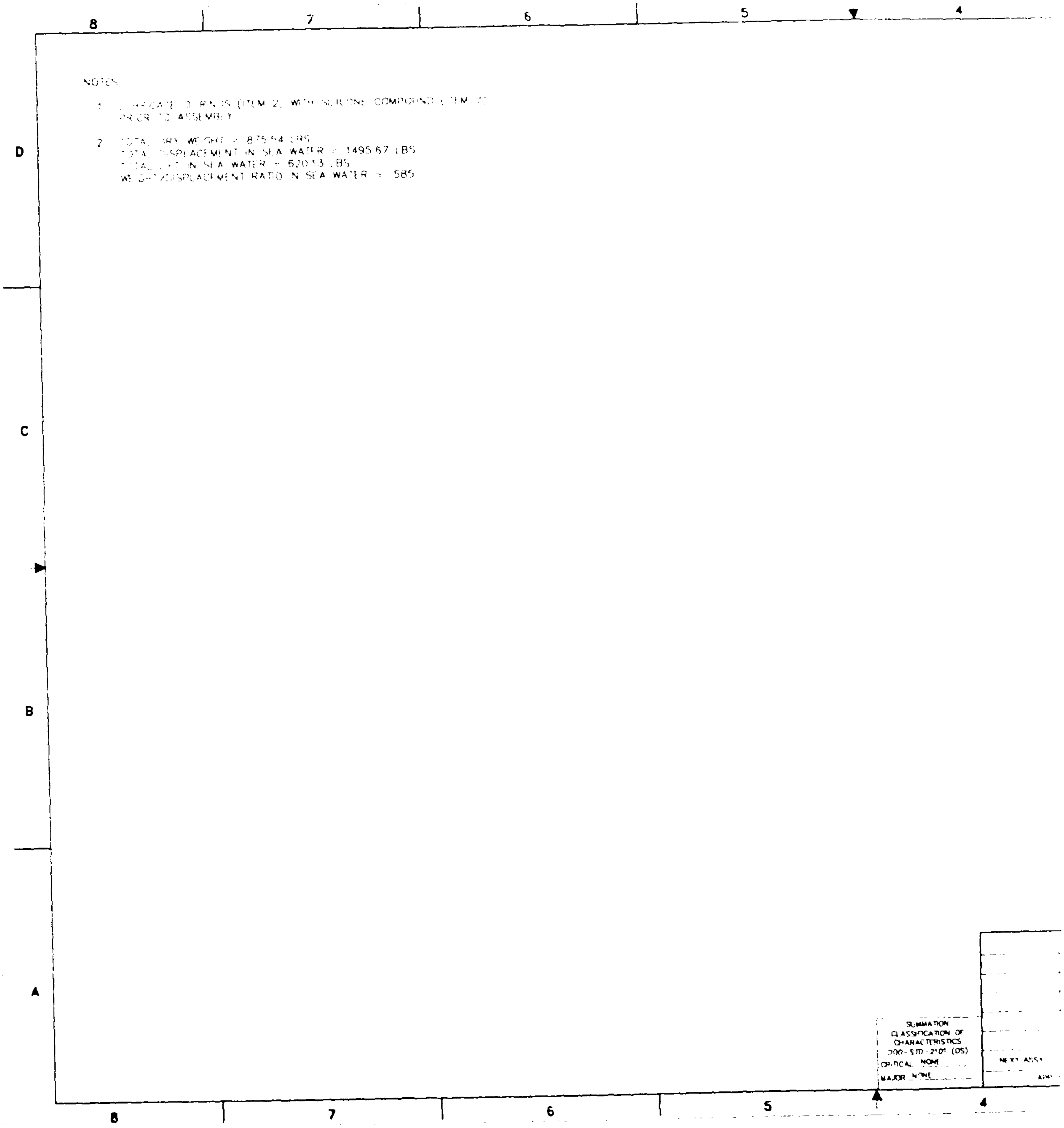

Figure 1. 26-inch housing assembly drawing, Sheet 1.

DWG NO SK9402-055

SHEET	2	1
REV	2	2

REV STATUS OF SHEETS

REVISIONS

ZONE	LTR	DESCRIPTION	DATE	APPROVAL
			[illegible]	
	1	ADD OVERALL DIMENSIONS TO SHEET 2	[illegible]	
	2	ADD WEIGHT/DISPLACEMENT NOTE	[illegible]	

PARTS LIST

QTY REQD	CAGE CODE	PART OR IDENTIFYING NUMBER	DESCRIPTION OR NOMENCLATURE	MATERIAL/SPEC/REF DESG	FIND NO
					10
					9
					8
AR			SILICONE COMPOUND	MIL-S-8660	7
8		MS16996-16	SCREW, CAP, SOCKET HD, HEX, CRES, .190-32UNF-3A X 1.50		6
1	55910	SK9402-054	HULL, 26 INCH HOUSING		5
1	55910	SK9402-053	ASSY, AFT HEAD, 26 INCH HOUS		4
1	55910	SK9402-052	ASSY, FOR HEAD, 26 INCH HOUS		3
2	55910	SK9402-033	O-RING, 26 INCH HOUSING		2
4	55910	SK9402-003	CLAMP BAND, 26 INCH HOUSING		1

SUMMATION CLASSIFICATION OF CHARACTERISTICS DOD-STD-2101 (OS)
CRITICAL NONE
MAJOR NONE

NEXT ASSY | USED ON
APPLICATION

INTERPRET DRAWING IN ACCORDANCE WITH DOD-STD-100

DO NOT SCALE THIS DRAWING

UNLESS OTHERWISE SPECIFIED
DIMENSIONS ARE IN INCHES
BREAK ALL EDGES MAX
REMOVE ALL BURRS
TOLERANCES ARE
.XX ± .XXX ±
ANGLES ±
FILLETS MAX
SURFACE ROUGHNESS √

RELEASED DATE

APPROVED	J. STACHIW
CHECKED	R. KURKCHUB
PREPARED	R. JOHNSON

PROJECT NUMBER
COGNIZANT CODE 9402
APPROVED FOR
BY DIRECTION

NAVAL COMMAND, CONTROL, AND OCEAN SURVEILLANCE CENTER
RESEARCH, DEVELOPMENT, TEST AND EVALUATION DIVISION
SAN DIEGO, CA 92152-5000

ASSEMBLY,
26 INCH HOUSING

SIZE D | CAGE CODE 55910 | DRAWING NUMBER SK9402-055

SCALE NONE | 94020551 | SHEET 1 OF 2

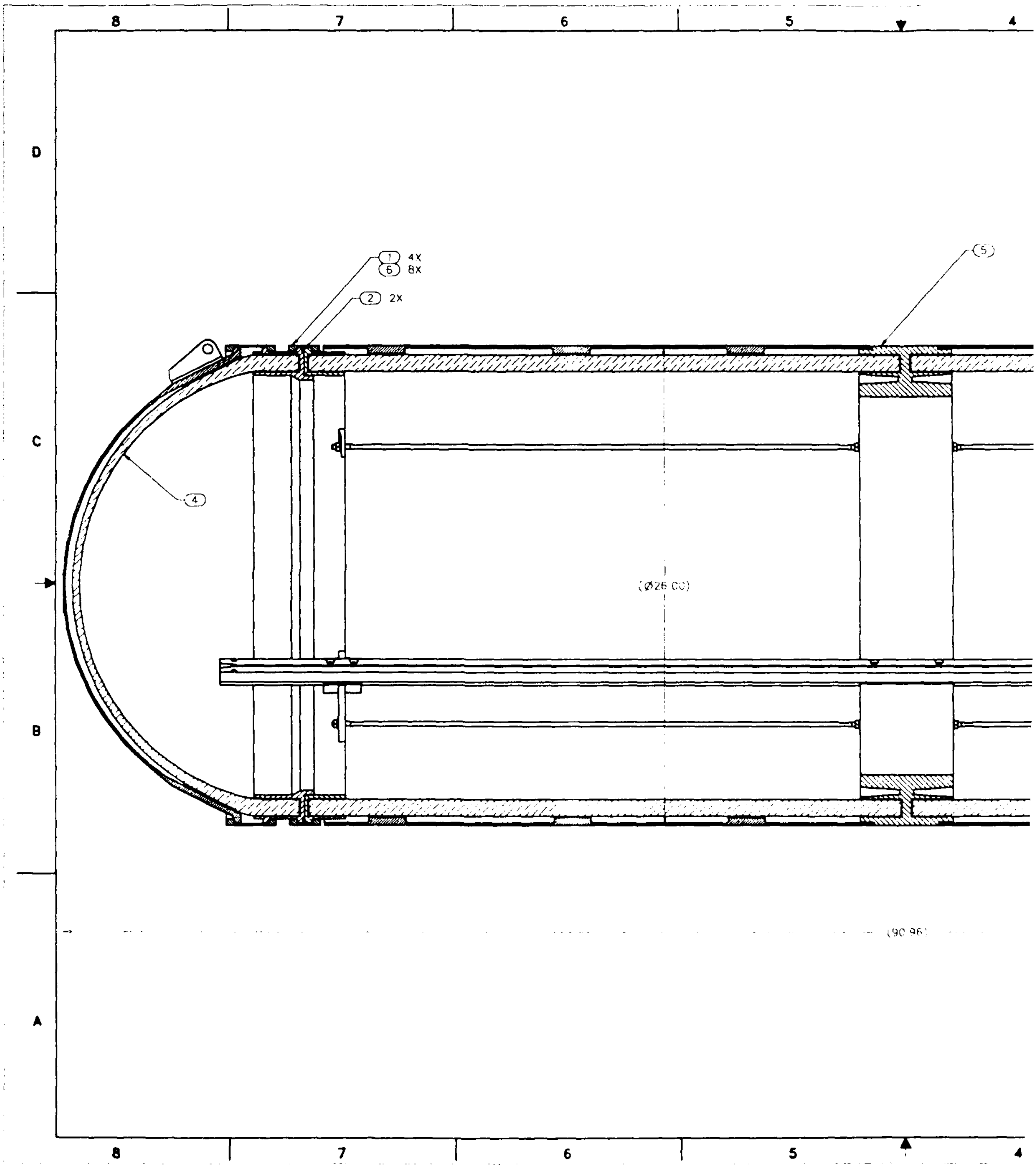

Figure 1. 26-inch housing assembly drawing, Sheet 2.

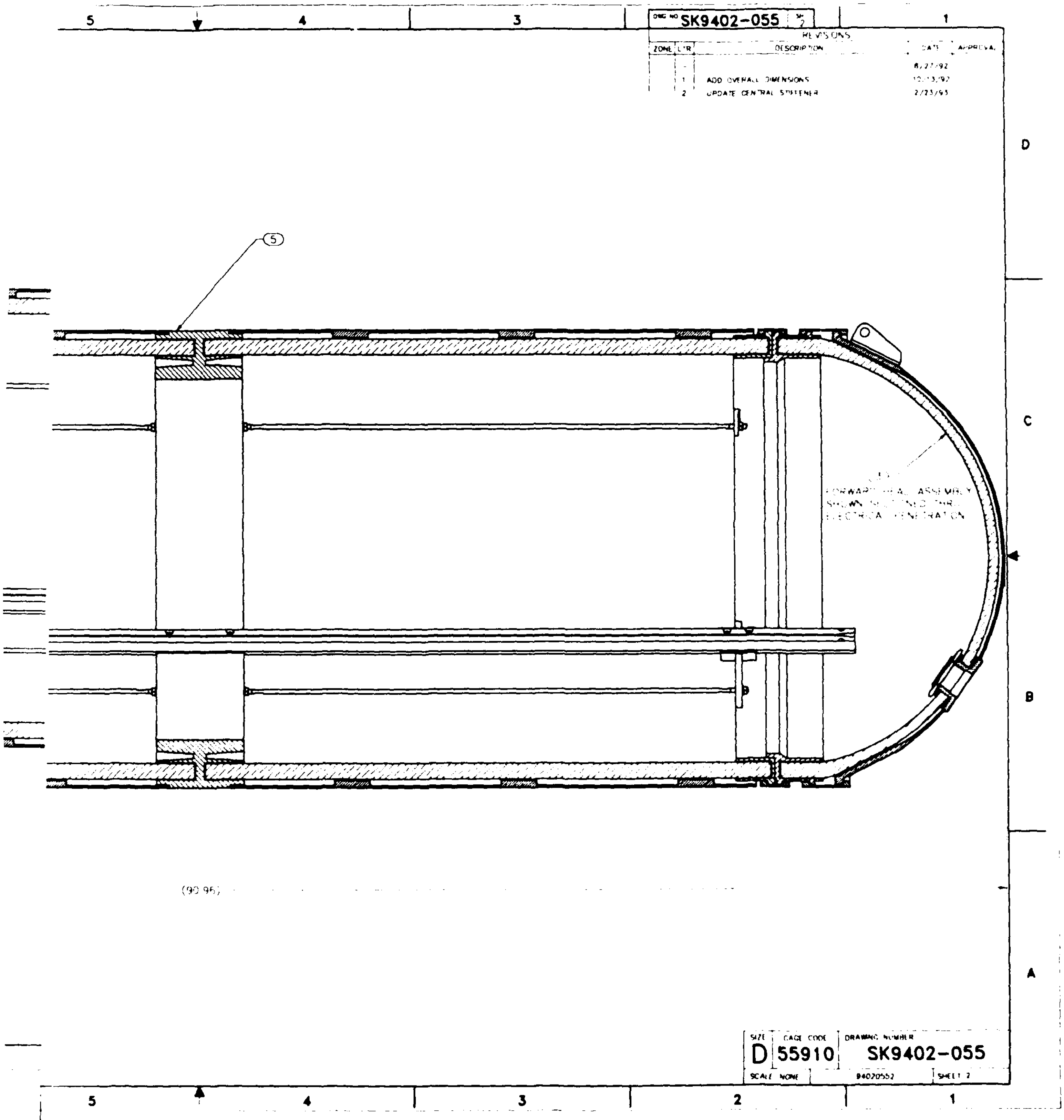
DWG NO SK9402-055 SH 2
REVISIONS
ZONE LTR DESCRIPTION DATE APPROVAL
- 6/27/92
1 ADD OVERALL DIMENSIONS 12/13/92
2 UPDATE CENTRAL STIFFENER 2/23/93
5
FORWARD HEAD ASSEMBLY
SHOWN SECTIONED THRU
ELECTRICAL PENETRATION
(90.96)
SIZE D
CAGE CODE 55910
DRAWING NUMBER SK9402-055
SCALE NONE
94020552
SHEET 2

NOTES:

1. LUBRICATE O-RINGS (ITEM 1) WITH SILICONE COMPOUND (ITEM 7) PRIOR TO ASSEMBLY.

2. TOTAL DRY WEIGHT = 1690.77 LBS.
TOTAL DISPLACEMENT IN SEA WATER = 3038.82 LBS.
TOTAL LIFT IN SEA WATER = 1384.05 LBS.
WEIGHT/DISPLACEMENT RATIO IN SEA WATER = .556

SUMMATION CLASSIFICATION OF CHARACTERISTICS DOD-STD-2101 (OS)
CRITICAL NONE
MAJOR NONE

NEXT

Figure 2. 33-inch housing assembly drawing, Sheet 1.

DWG NO SK9402-058

SHEET	3	2	1
REV	2	2	2

REV STATUS OF SHEETS

REVISIONS

ZONE	LTR	DESCRIPTION	DATE	APPROVAL
	–		8/31/92	
	1	ADD OVERALL DIMENSIONS TO SHEETS 2 & 3	10/13/92	
	2	ADD WEIGHT NOTE	2/23/93	

	QTY REQD	CAGE CODE	PART OR IDENTIFYING NUMBER	DESCRIPTION OR NOMENCLATURE	MATERIAL/SPEC/REF DESG	FIND NO
						10
						9
						8
	AR			SILICONE COMPOUND	MIL-S-8660	7
	8		MS35691-35	NUT, HEX, JAM, CRES, .500-13UNC-2B		6
	8		MS35338-143	WASHER, LOCK, CRES, 1/2 NOM		5
	8		MS35307-419	SCREW, CAP, HEX HEAD, CRES, .500-13UNC-2A X 3.00 L		4
	1	55910	SK9402-057	ASSEMBLY, HULL, 33 INCH HOUS		3
	1	55910	SK9402-056	ASSEMBLY, HEAD, 33 INCH HOUS		2
	2	55910	SK9402-034	O-RING, 33 INCH HOUSING		1
-1						

PARTS LIST

SUMMATION CLASSIFICATION OF CHARACTERISTICS DOD-STD-2101 (OS)
CRITICAL NONE
MAJOR NONE

NEXT ASSY | USED ON
APPLICATION

INTERPRET DRAWING IN ACCORDANCE WITH DOD-STD-100

DO NOT SCALE THIS DRAWING

UNLESS OTHERWISE SPECIFIED
DIMENSIONS ARE IN INCHES
BREAK ALL EDGES MAX
REMOVE ALL BURRS
TOLERANCES ARE
XX ± XXX ±
ANGLES ±
FILLETS MAX
SURFACE ROUGHNESS ✓

RELEASED DATE

APPROVED	J. STACHIW
CHECKED	R. KURKCHUB.
PREPARED	R. JOHNSON

PROJECT NUMBER
COGNIZANT CODE 9402
APPROVED FOR

BY DIRECTION

NAVAL COMMAND, CONTROL, AND OCEAN SURVEILLANCE CENTER
RESEARCH, DEVELOPMENT, TEST AND EVALUATION DIVISION
SAN DIEGO, CA 92152-5000

ASSEMBLY, 33 INCH HOUSING

SIZE	CAGE CODE	DRAWING NUMBER
D	55910	SK9402-058

SCALE NONE | 94020581 | SHEET 1 OF 3

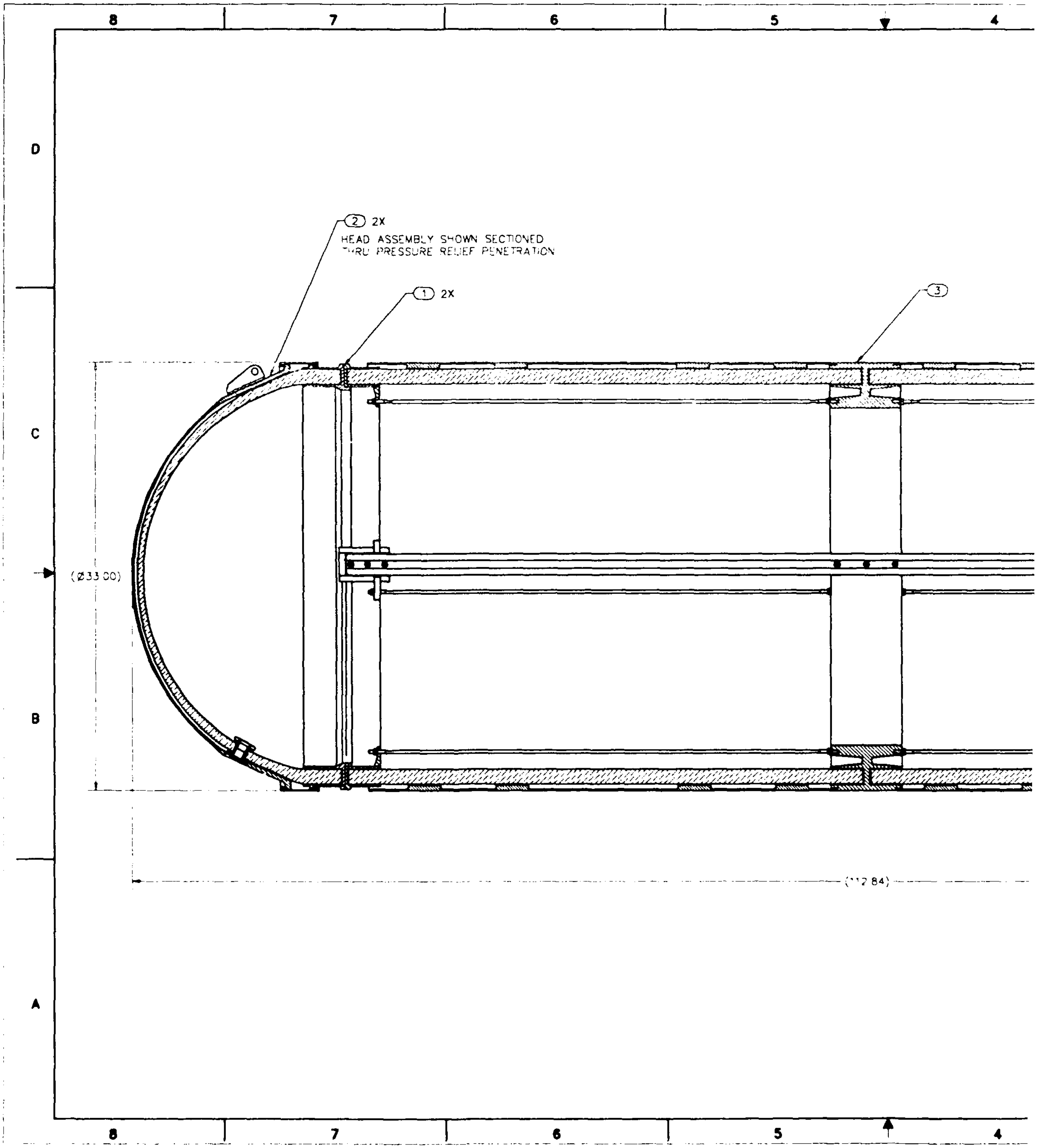

Figure 2. 33-inch housing assembly drawing, Sheet 2.

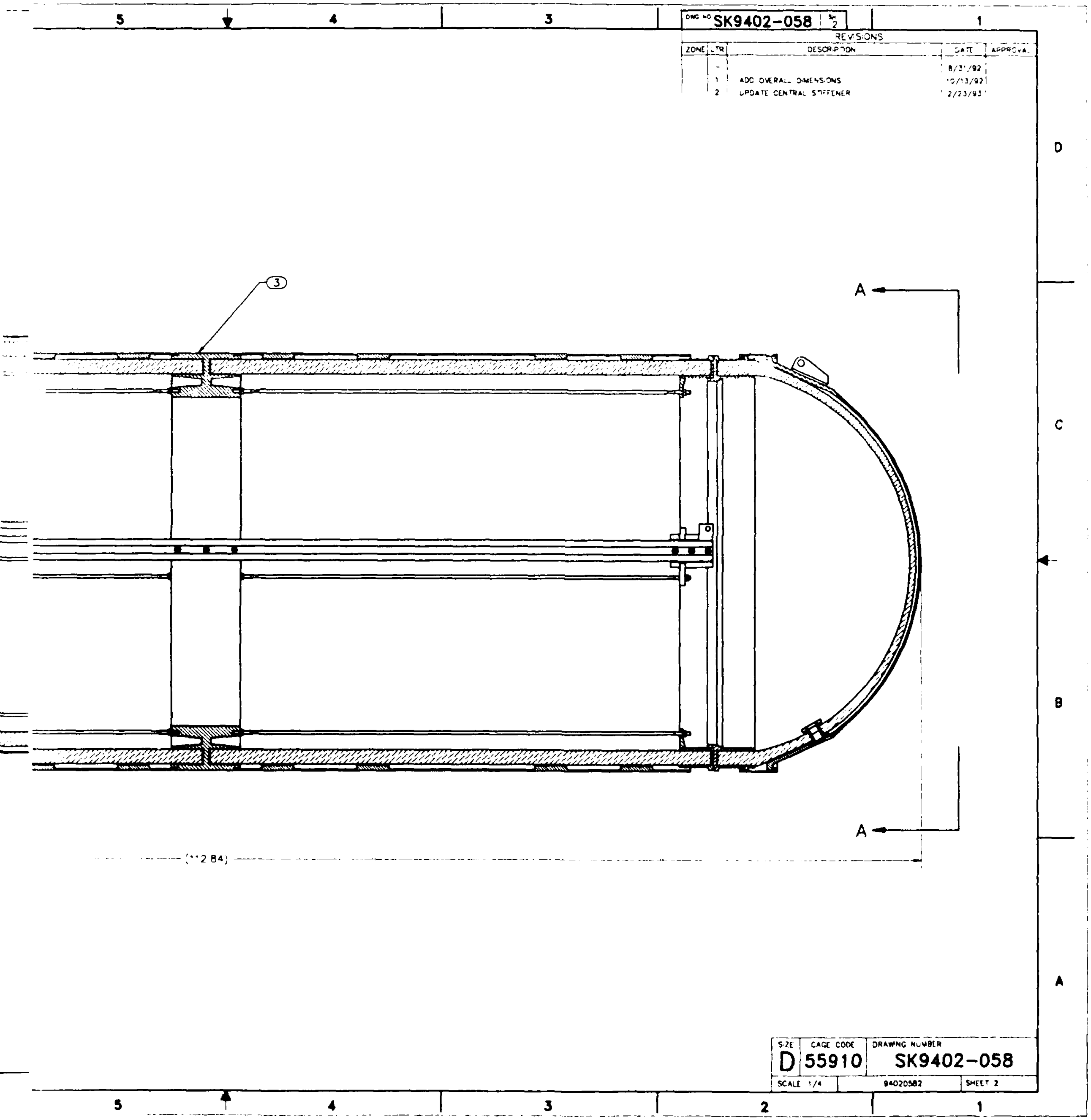
DWG NO SK9402-058 SH 2
REVISIONS
ZONE LTR DESCRIPTION DATE APPROVAL
- 8/31/92
1 ADD OVERALL DIMENSIONS 10/13/92
2 UPDATE CENTRAL STIFFENER 2/23/93
3
A
A
(112.84)
SIZE D
CAGE CODE 55910
DRAWING NUMBER SK9402-058
SCALE 1/4
94020582
SHEET 2
5 4 3 2 1
D C B A

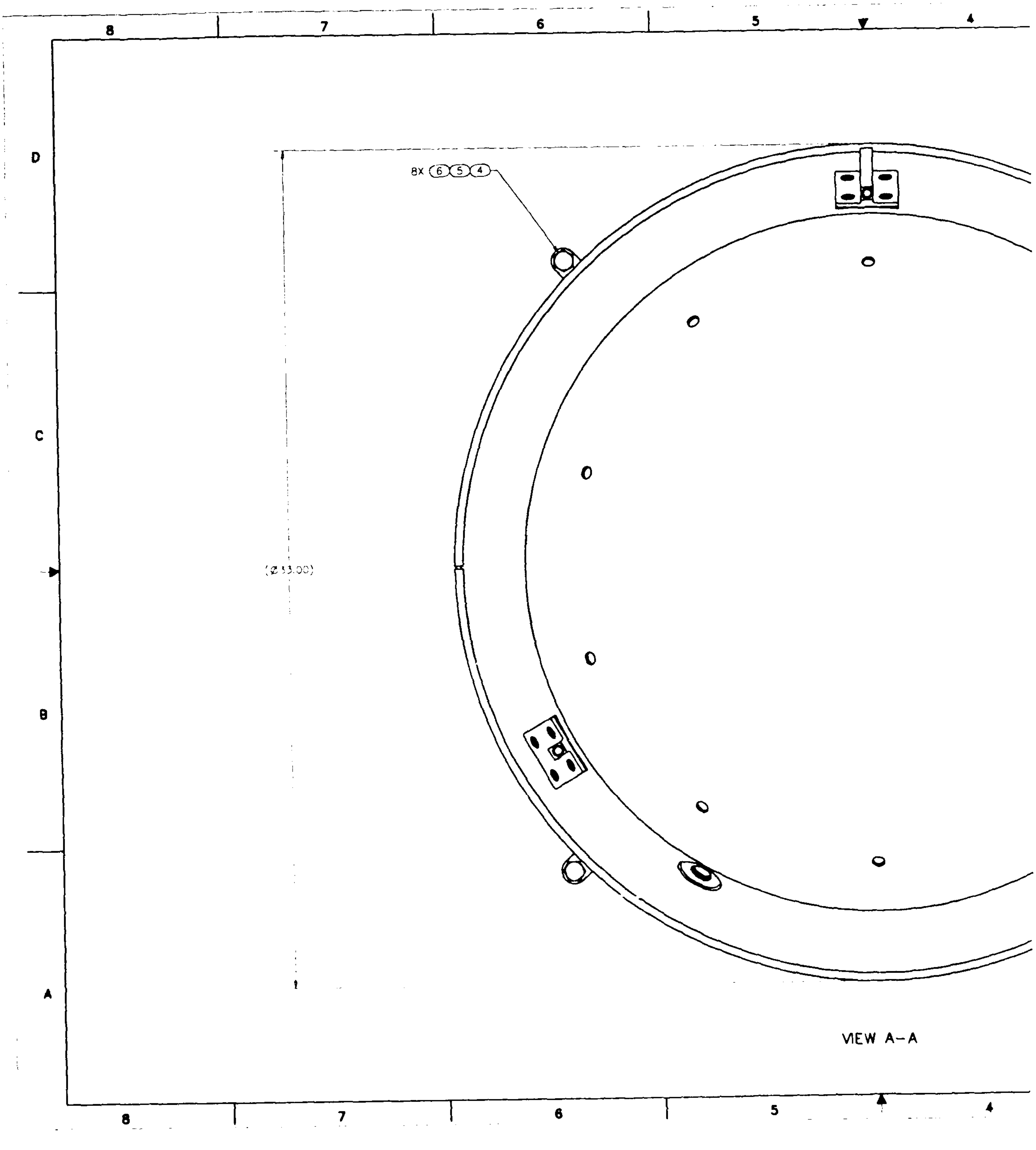

Figure 2. 33-inch housing assembly drawing, Sheet 3.

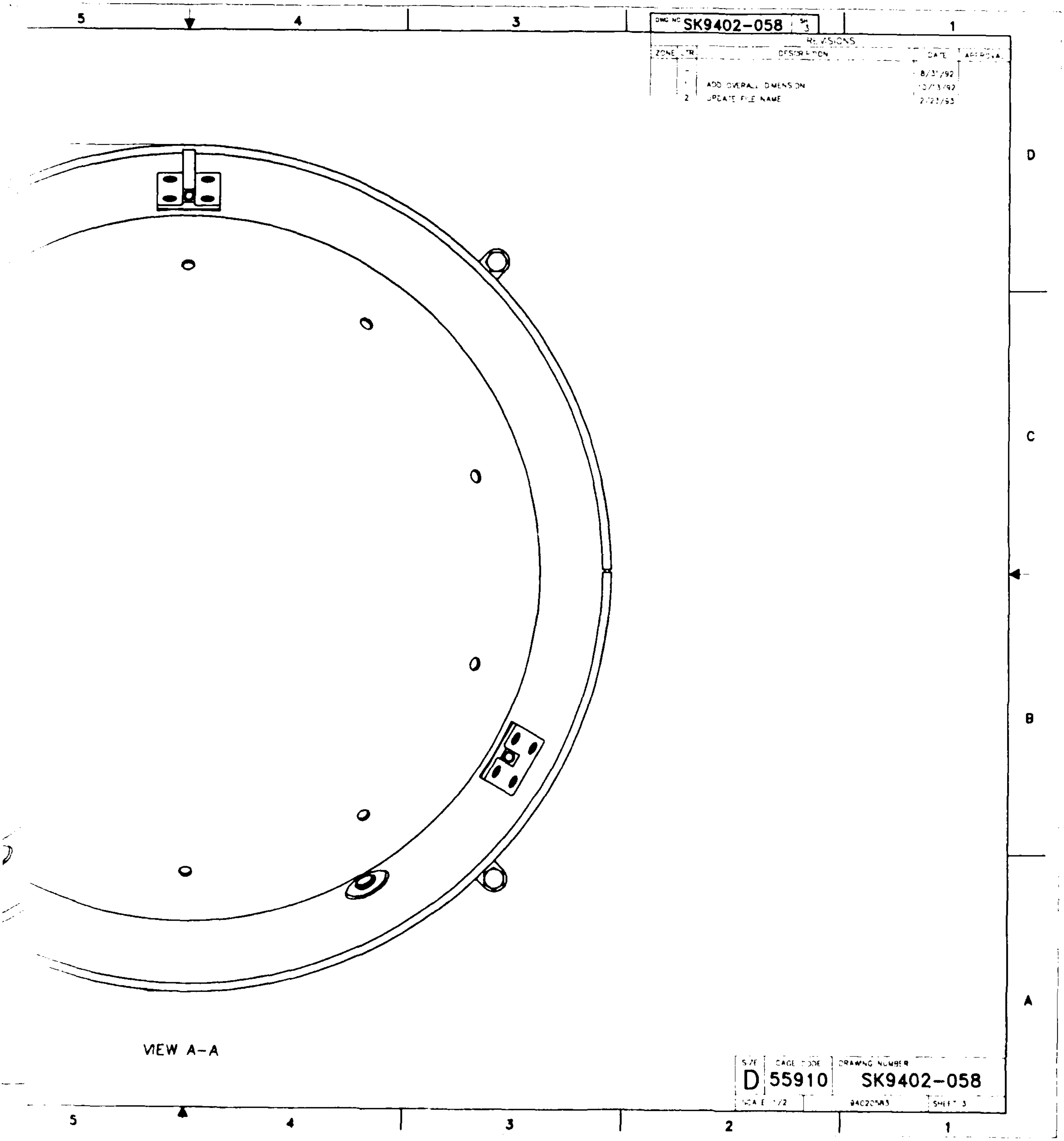
SK9402-058
REVISIONS
ZONE
LTR
DESCRIPTION
DATE
ADD OVERALL DIMENSION
UPDATE FILE NAME
8/31/92
VIEW A-A
SIZE
D
CAGE CODE
55910
DRAWING NUMBER
SK9402-058
SCALE 1/2
SHEET 3

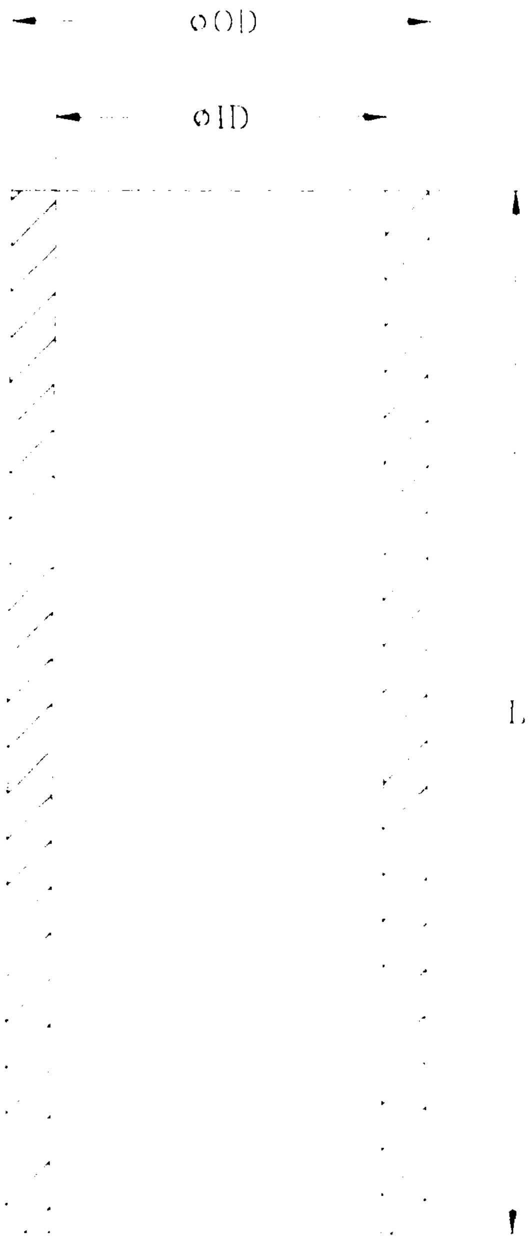

	26 INCH HSG	33 INCH HSG
ID	20.50"	26.0"
OD	26.0"	33.0"
L	64.5"	80.0"

Figure 3. Dimensional envelope for 26-inch and 33-inch housing assemblies.

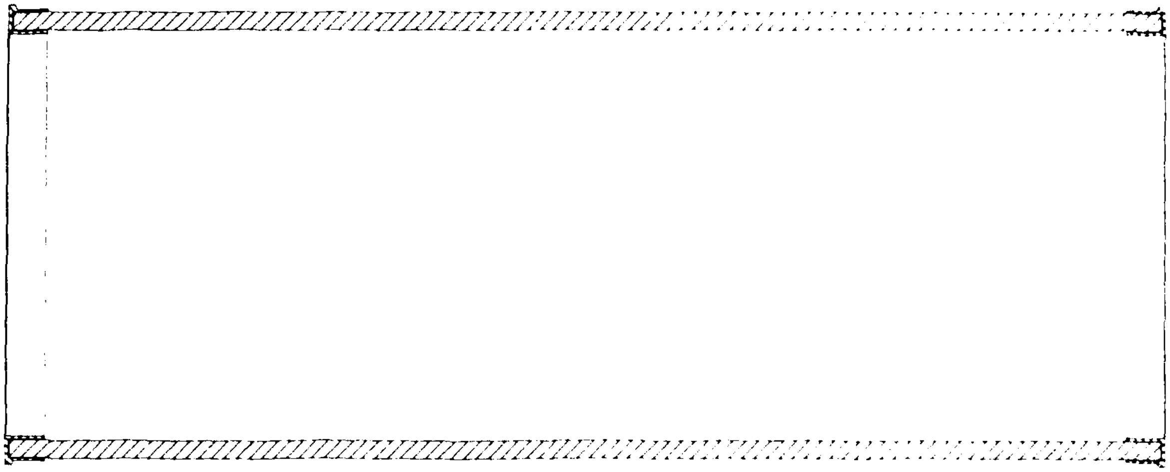

4A

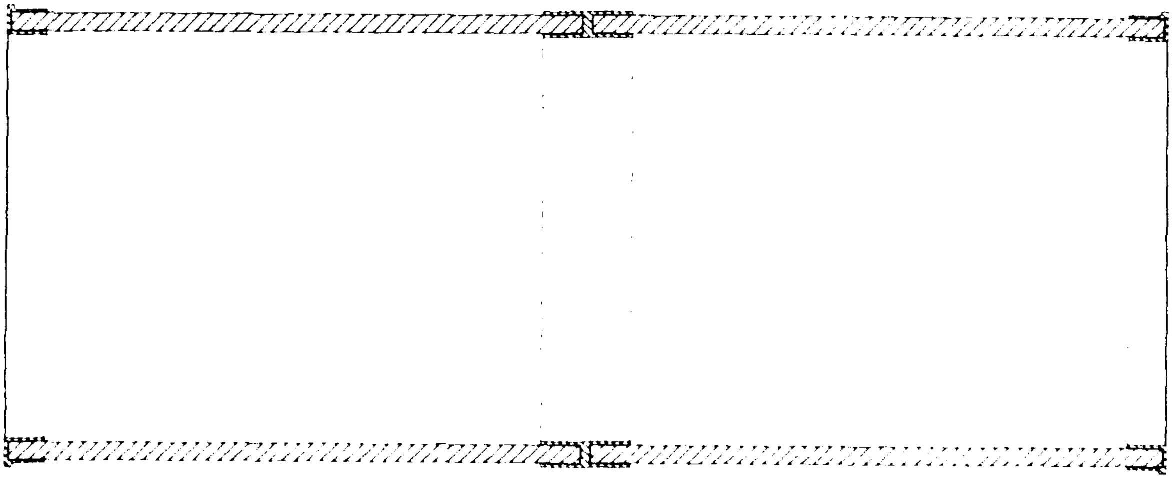

4B

Figure 4. Cylindrical hull design options A and B for 26-inch and 33-inch housings, Sheet 1.

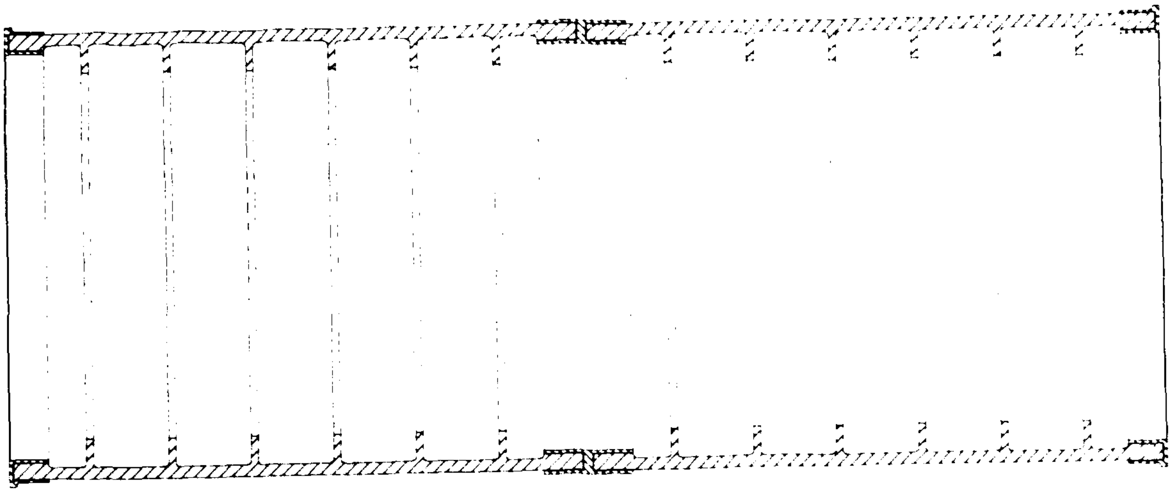

4C

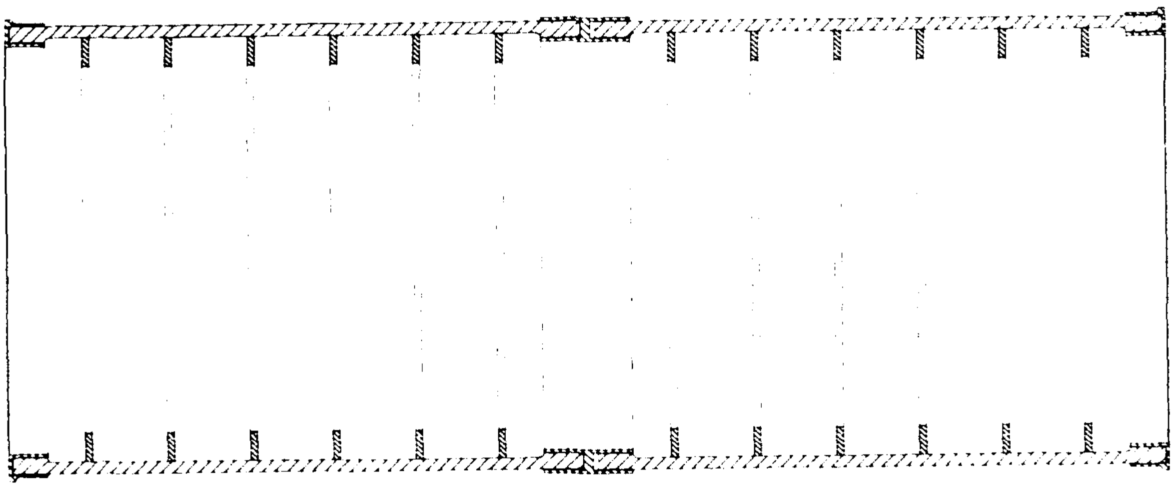

4D

Figure 4. Cylindrical hull design options C and D for 26-inch and 33-inch housings, Sheet 2.

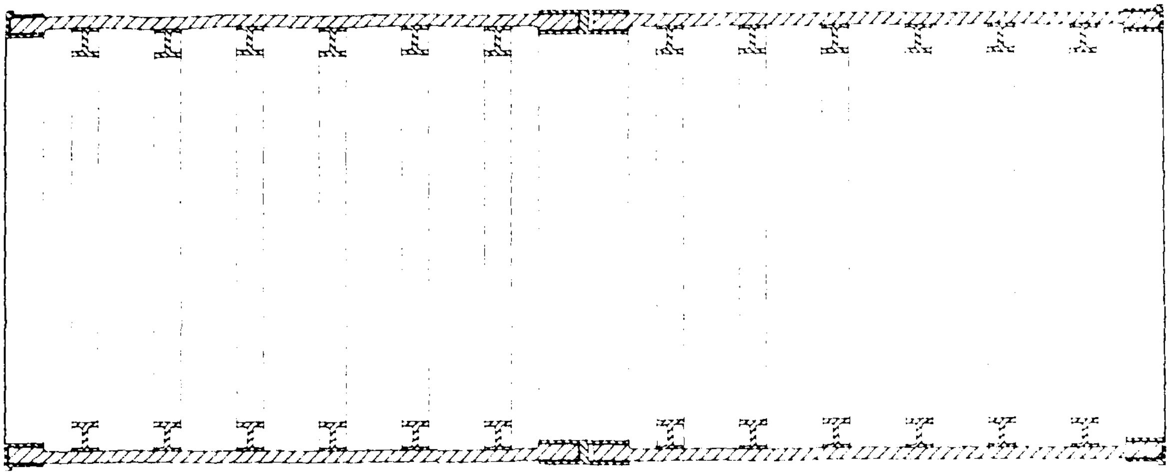

4E

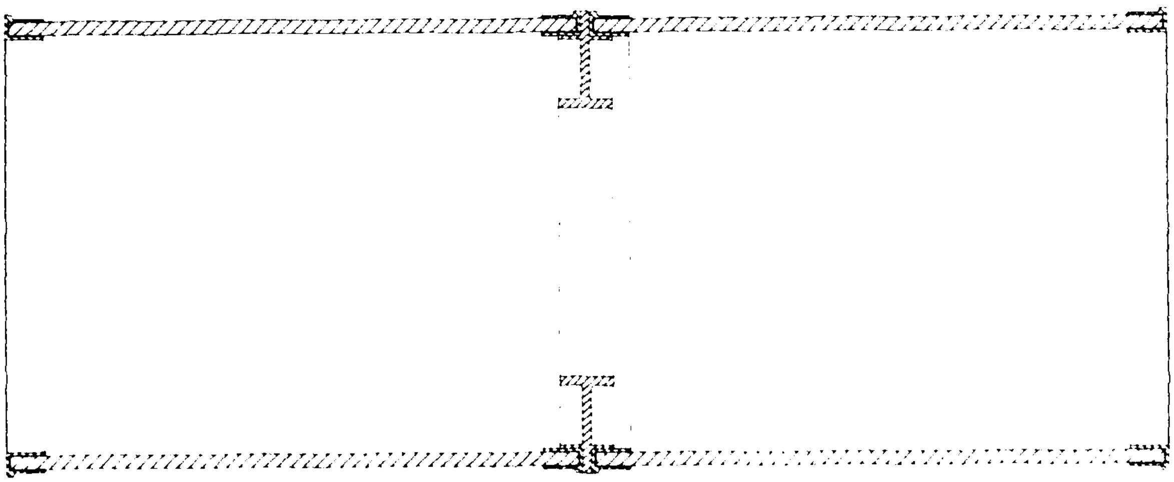

4F

Figure 4. Cylindrical hull design options E and F for 26-inch and 33-inch housings, Sheet 3.

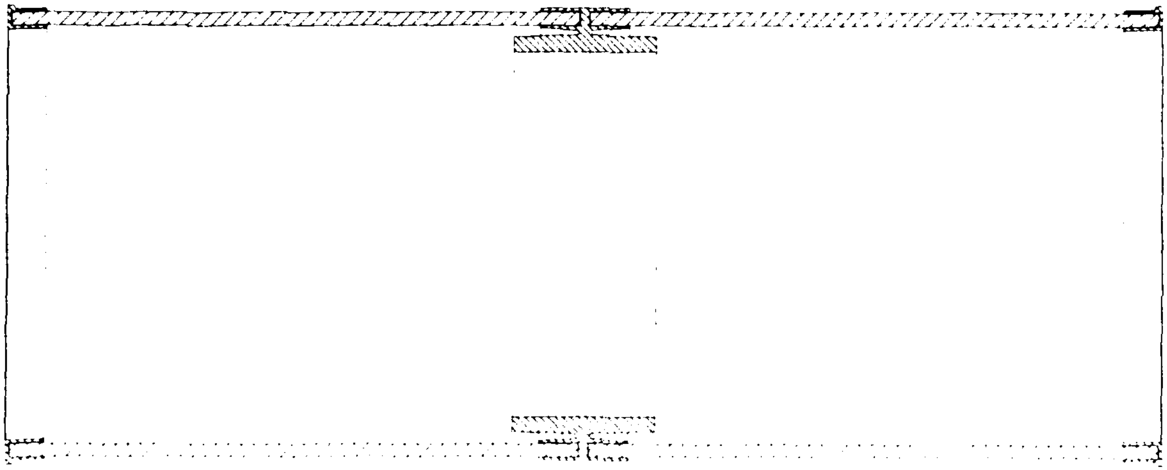

4G

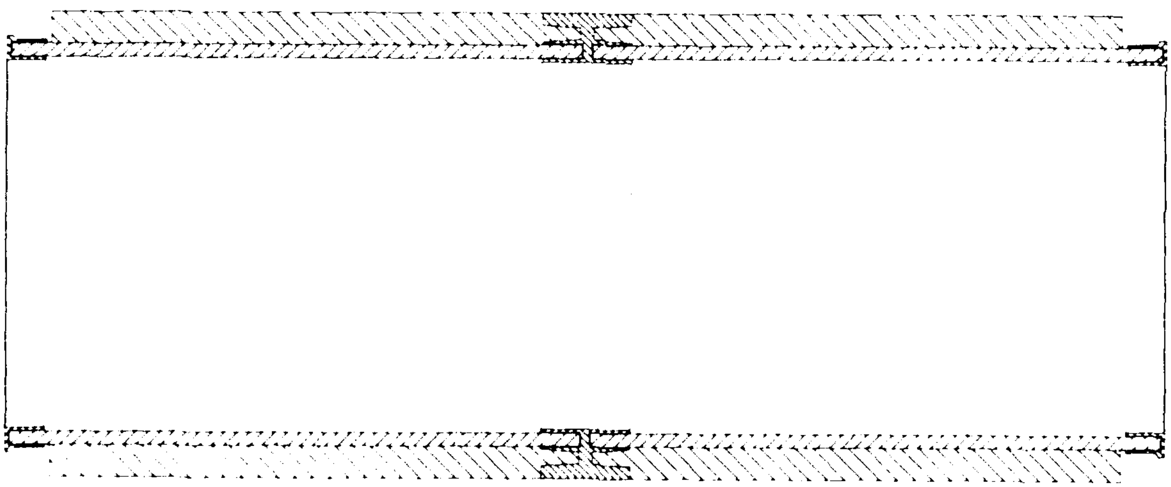

4H

Figure 4. Cylindrical hull design options G and H for 26-inch and 33-inch housings, Sheet 4.

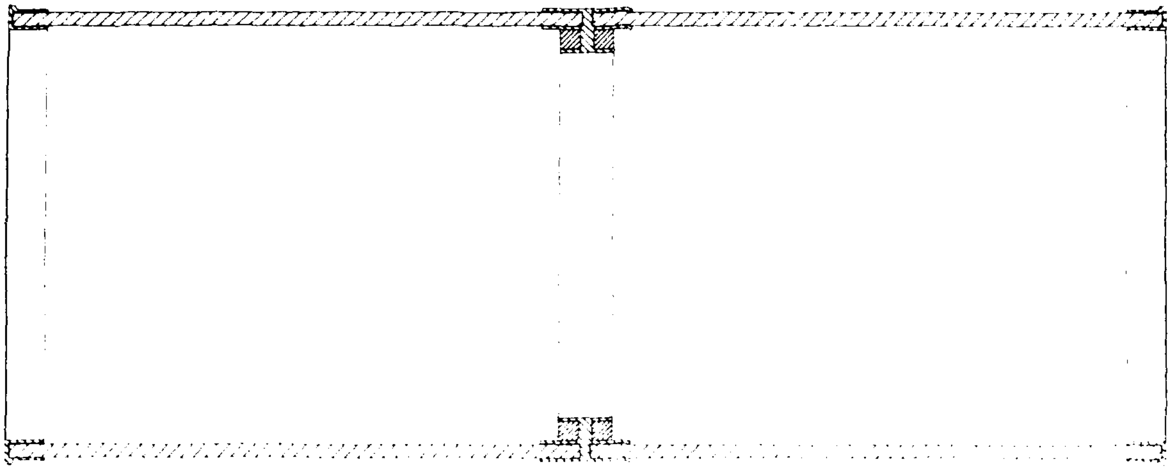

4I

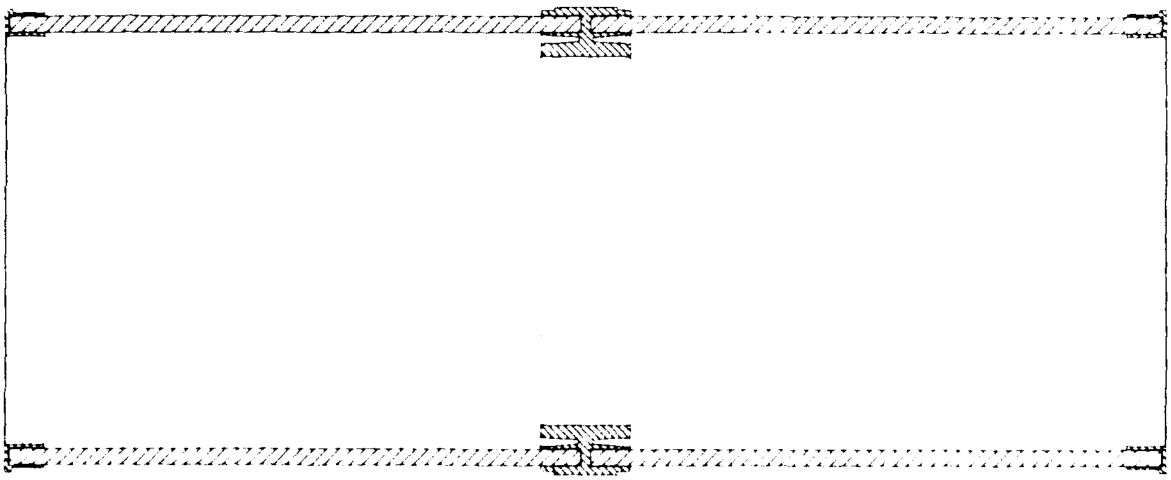

4J

Figure 4. Cylindrical hull design options I and J for 26-inch and 33-inch housings, Sheet 5.

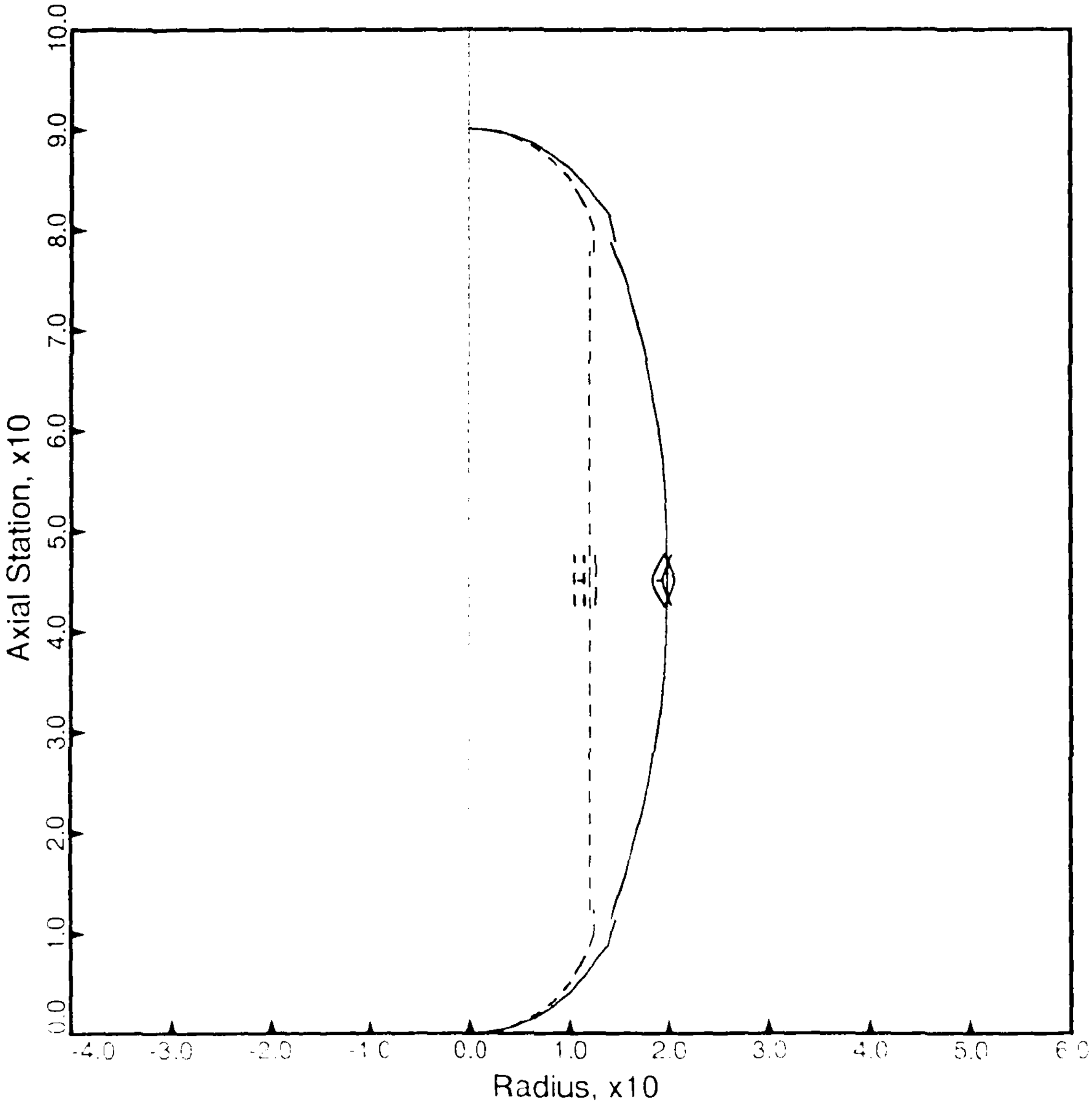

Figure 5. N=2 buckled configuration for 26-inch housing.

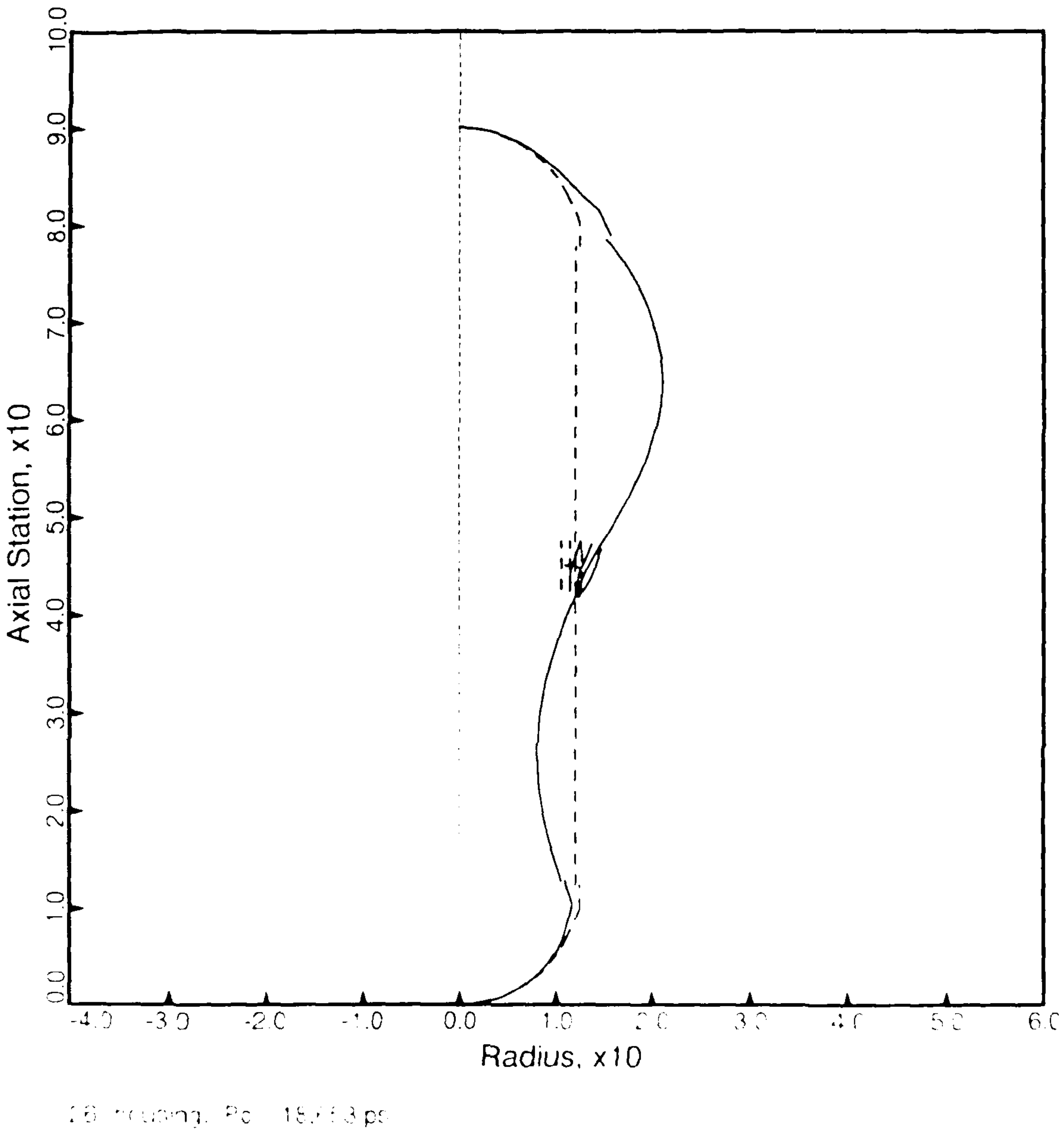

Figure 6. N=3 buckled configuration for 33-inch housing

Figure 7. Comparison of undeformed and deformed shapes of the 26-inch housing under external hydrostatic pressure.

Figure 8. Comparison of undeformed and deformed shapes of the hemisphere/cylinder interface under external hydrostatic pressure.

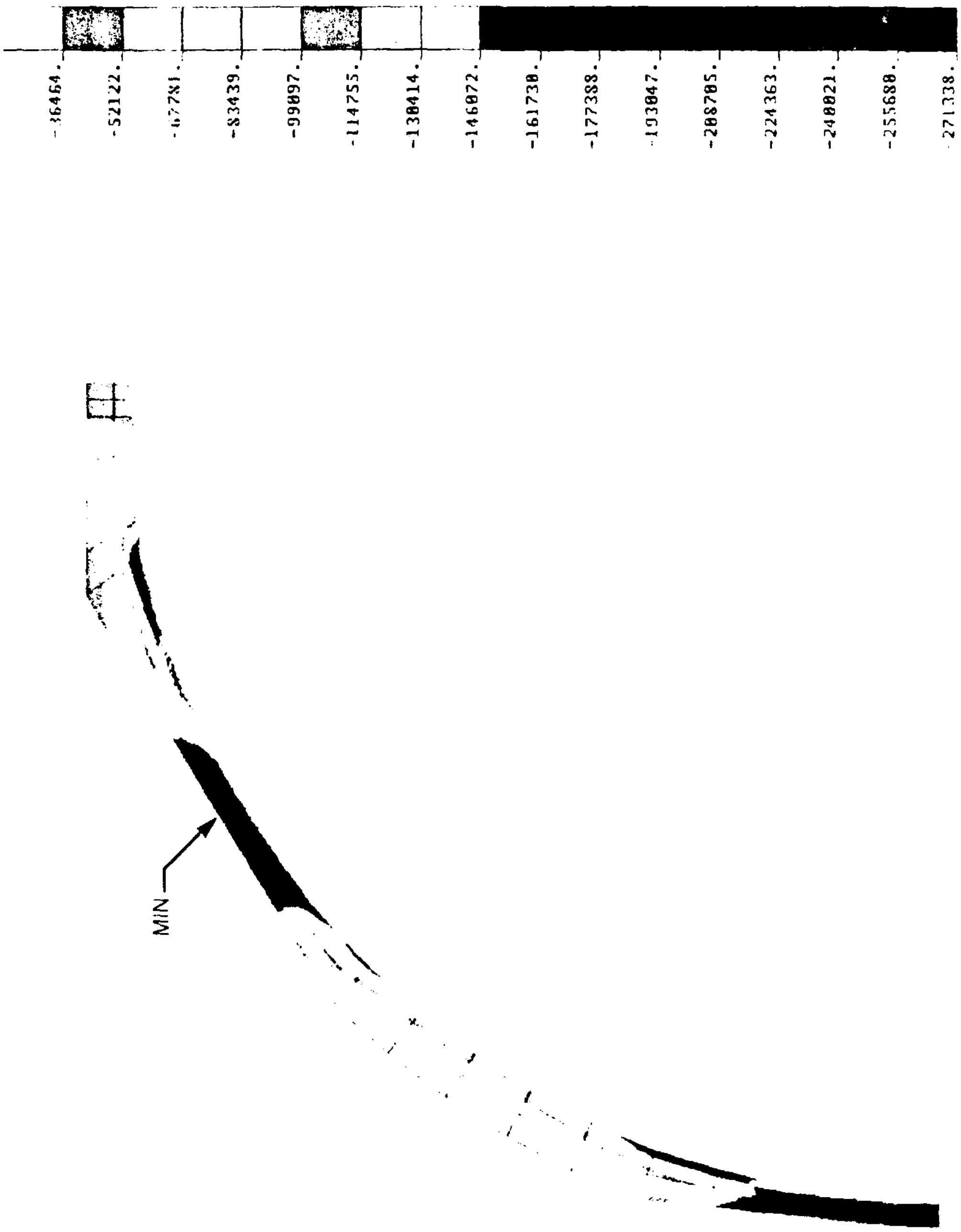

Figure 9. Minimum principal stress plot of *original* Type 6 hemisphere design for 26-inch housing.

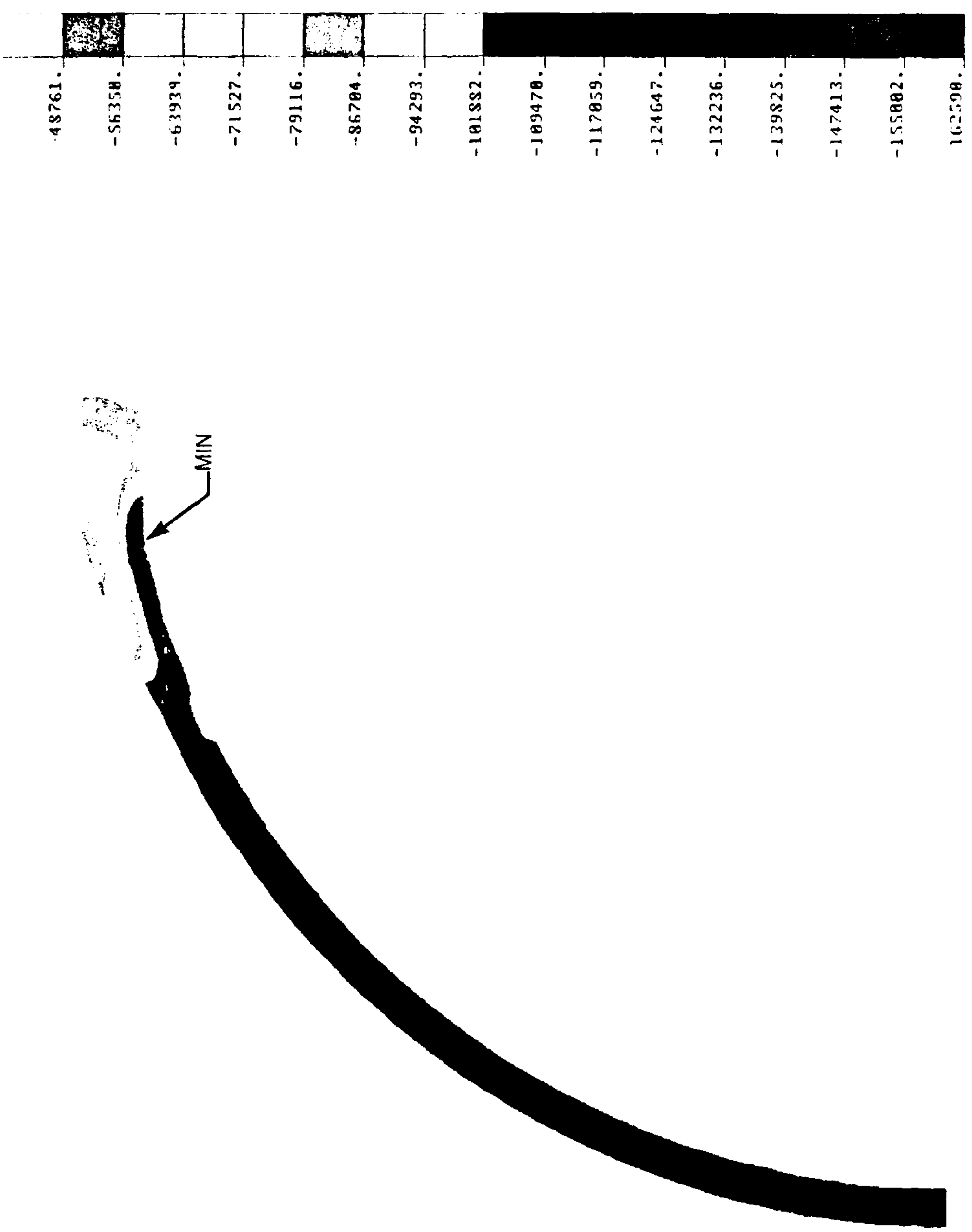

Figure 10. Minimum principal stress plot of Type 6 hemisphere design for 26-inch housing without penetrations.

Figure 11. Minimum principal stress plot of Type 6 hemisphere design for 26-inch housing with polar penetration.

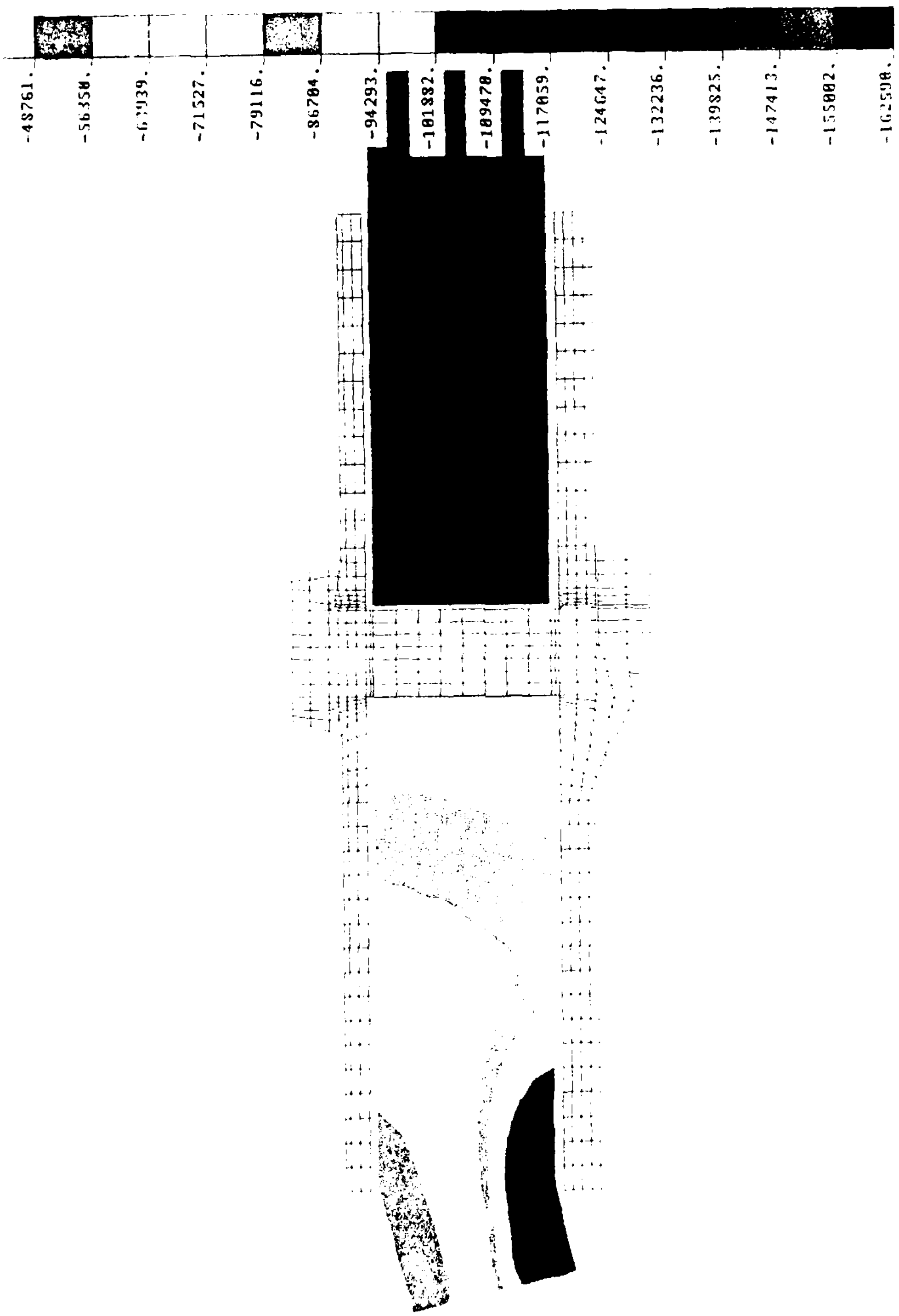

Figure 12. Detail of minimum principal stress plot of Type 6 hemisphere/cylinder interface for 26-inch housing.

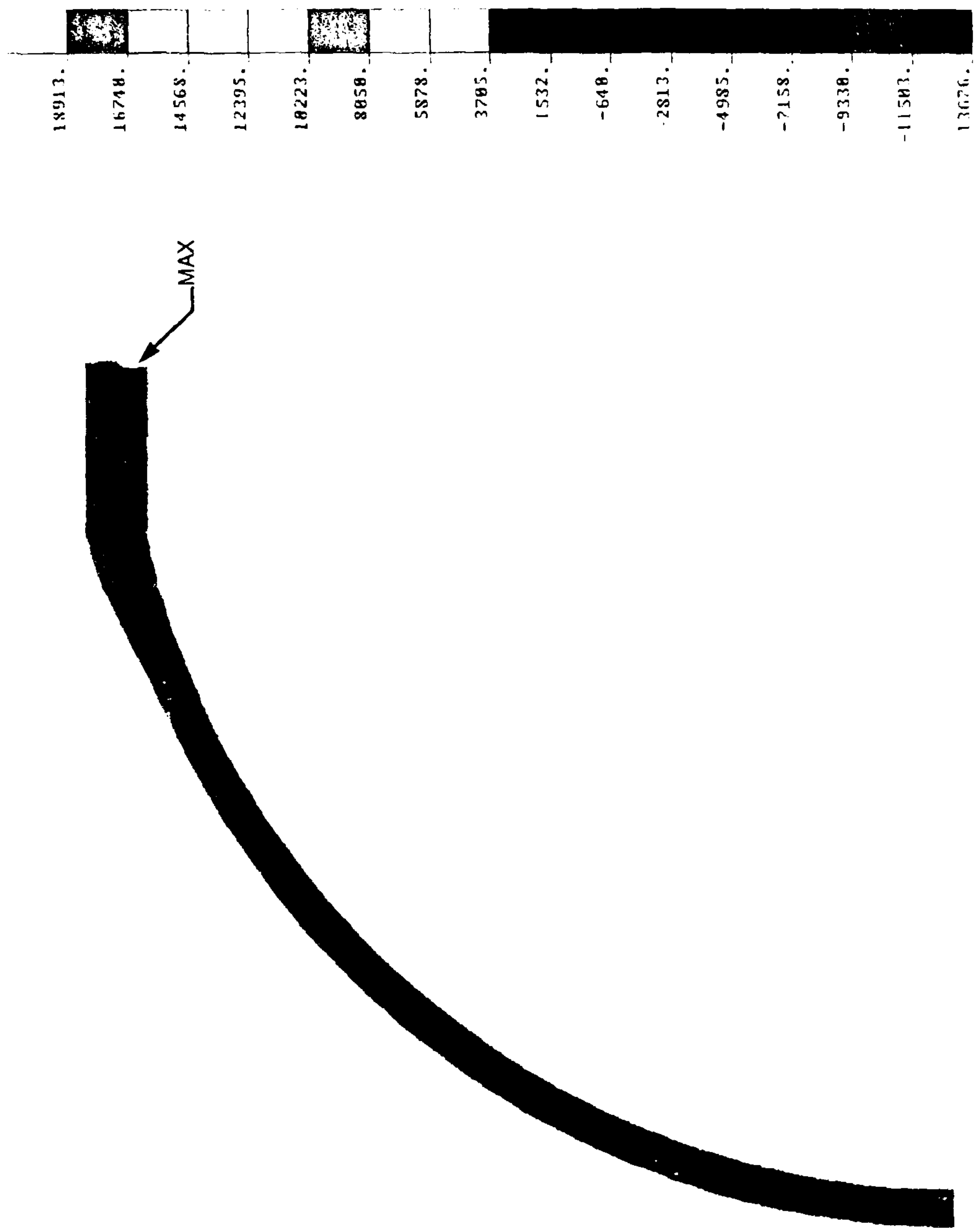

Figure 13. Maximum principal stress plot of Type 6 hemisphere for 26-inch housing.

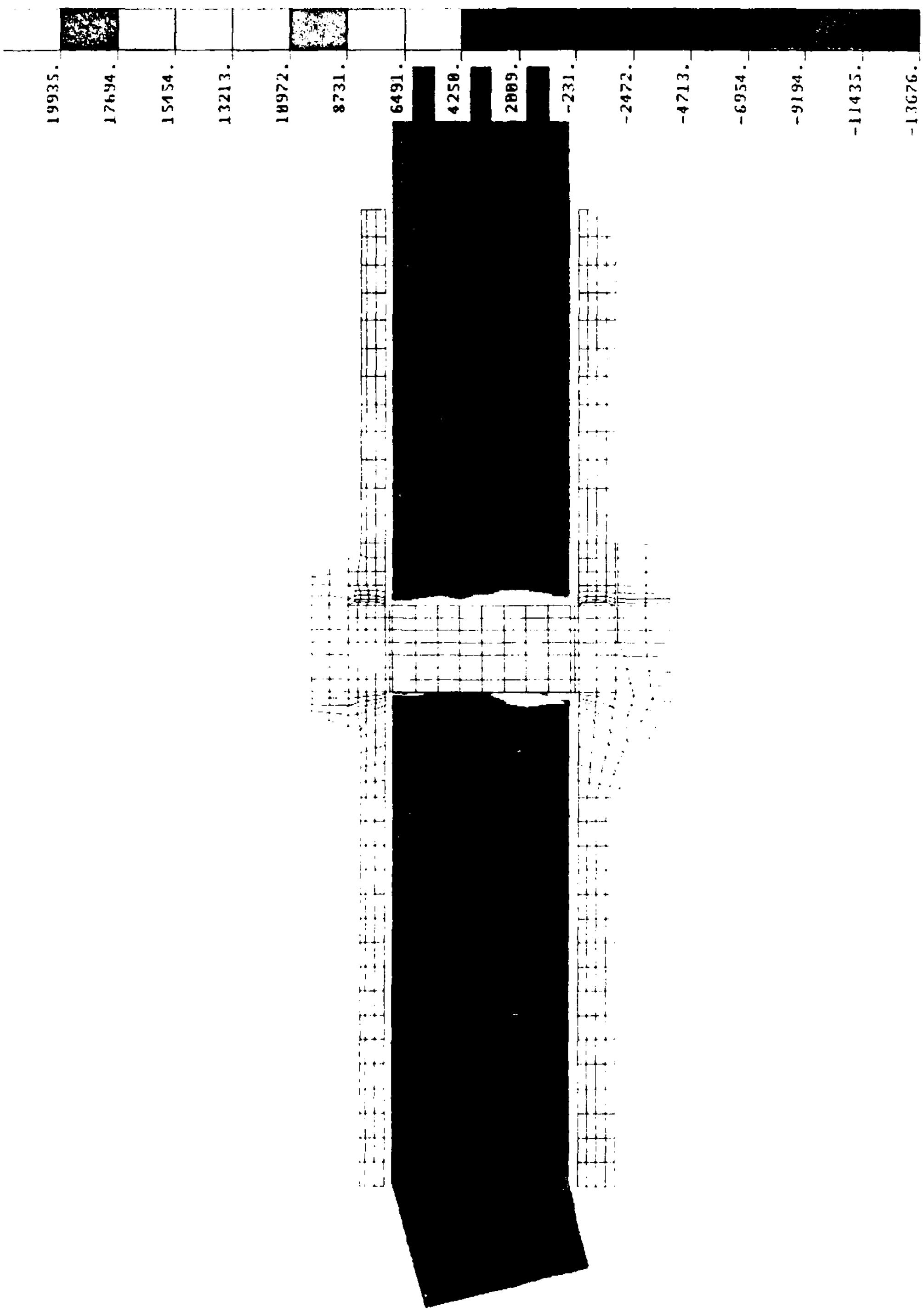

Figure 14. Detail of maximum principal stress plot of Type 6 hemisphere/cylinder interface for 26-inch housing.

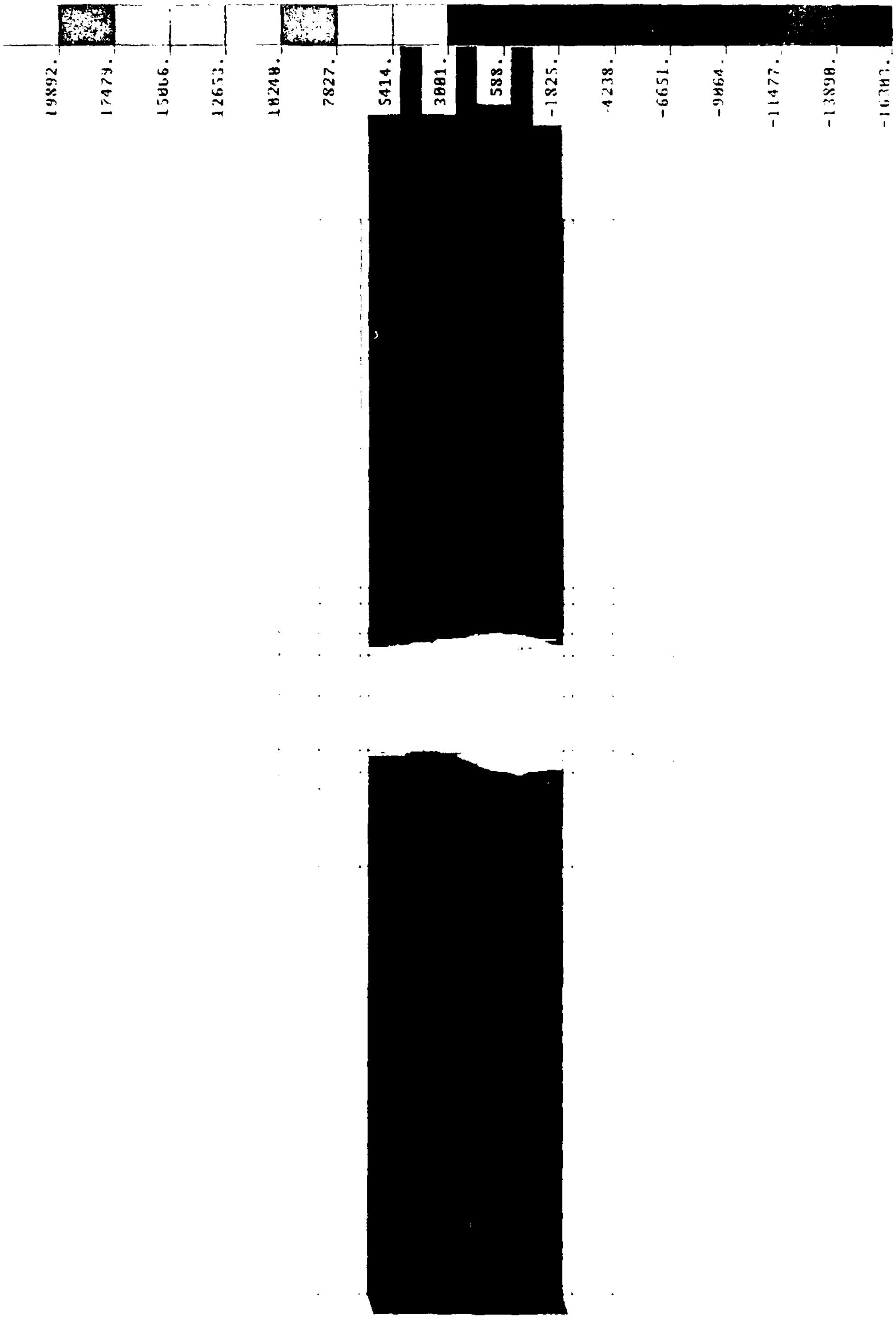

Figure 15. Detail of radial stress plot of Type 6 hemisphere/cylinder interface for 26-inch housing.

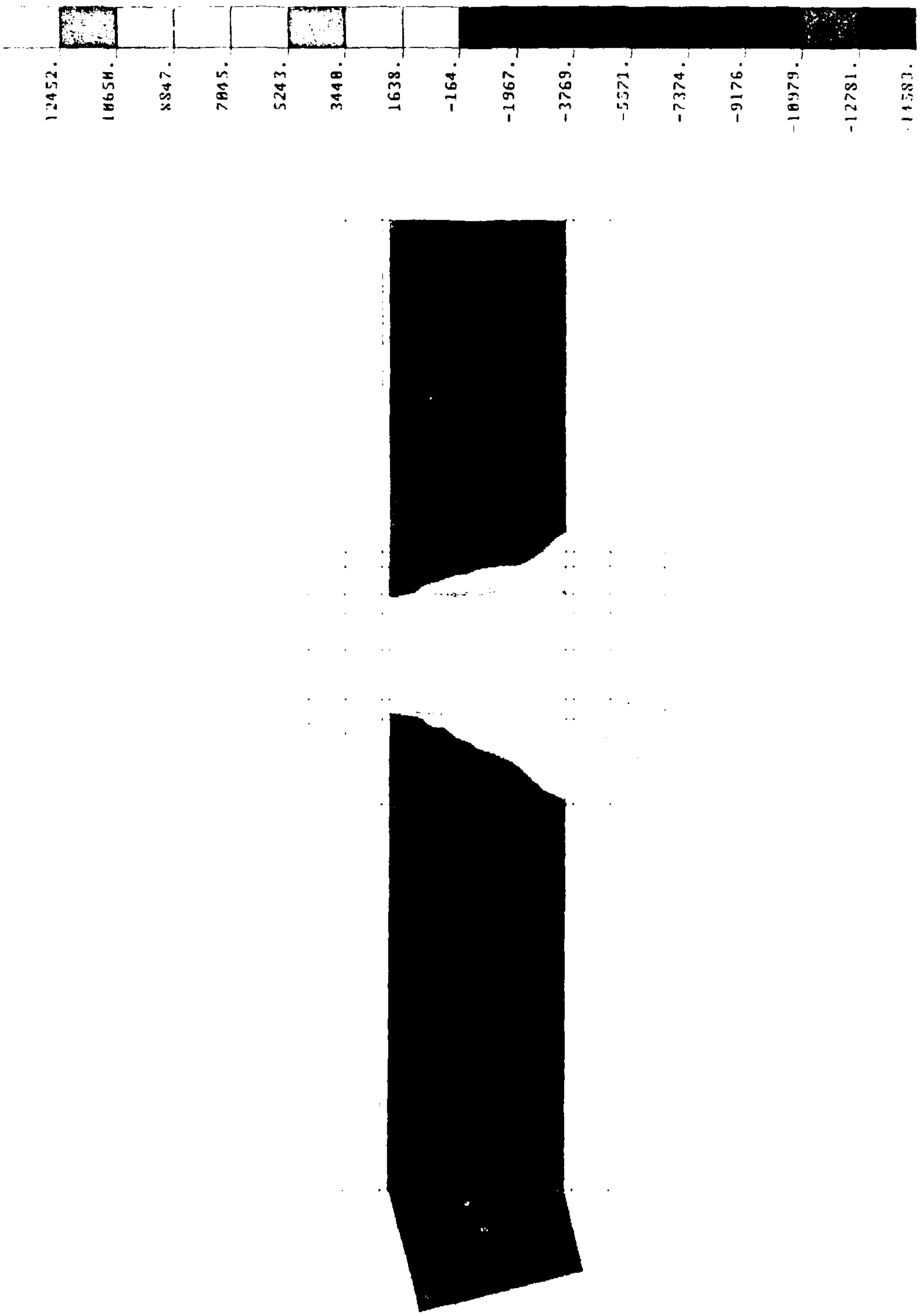

Figure 16. Detail of maximum principal stress plot of Type 6 hemisphere/cylinder interface for 26-inch housing with 0.040 inch of axial clearance.

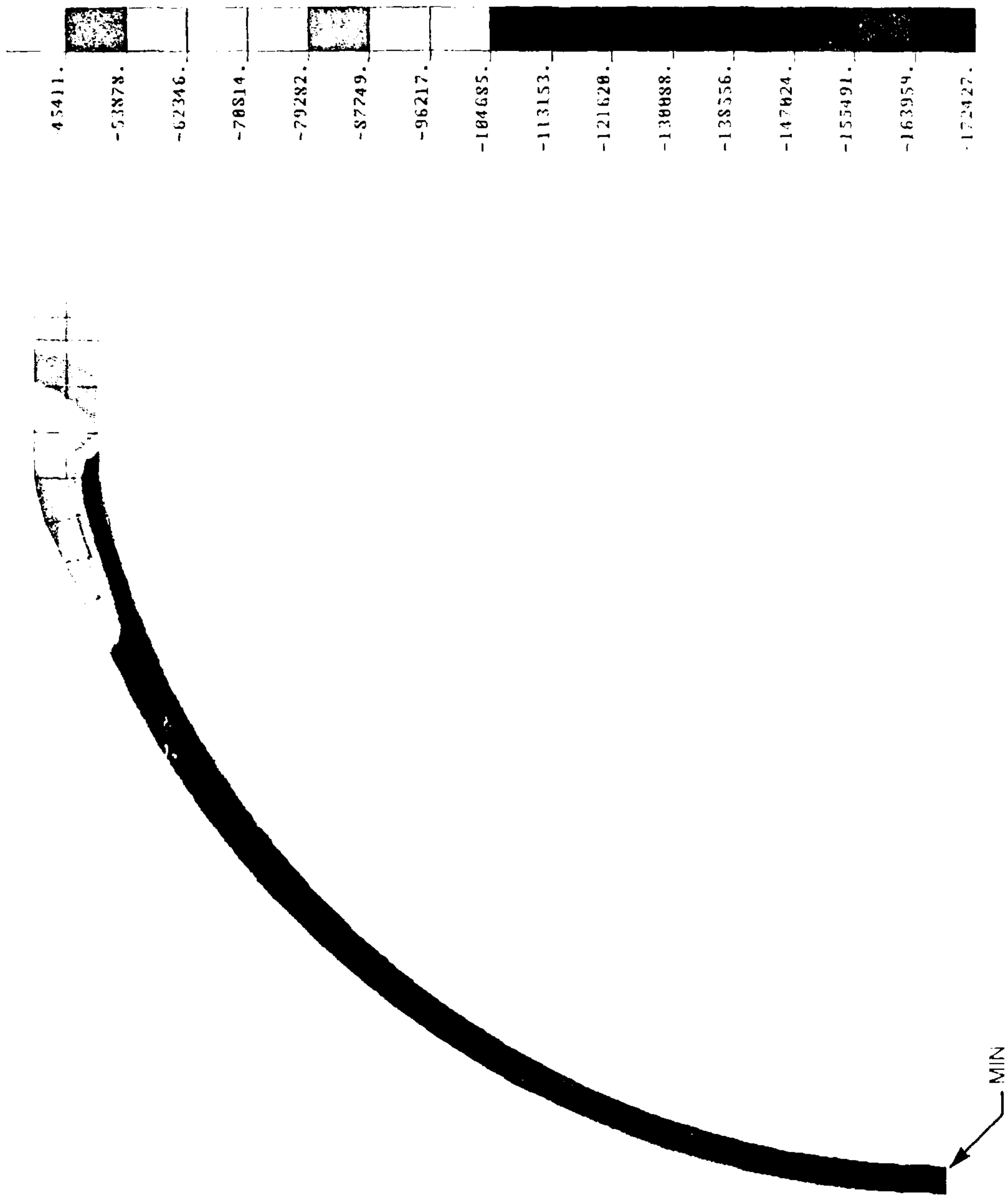

Figure 17. Minimum principal stress plot of Type 4 hemisphere for 26-inch housing.

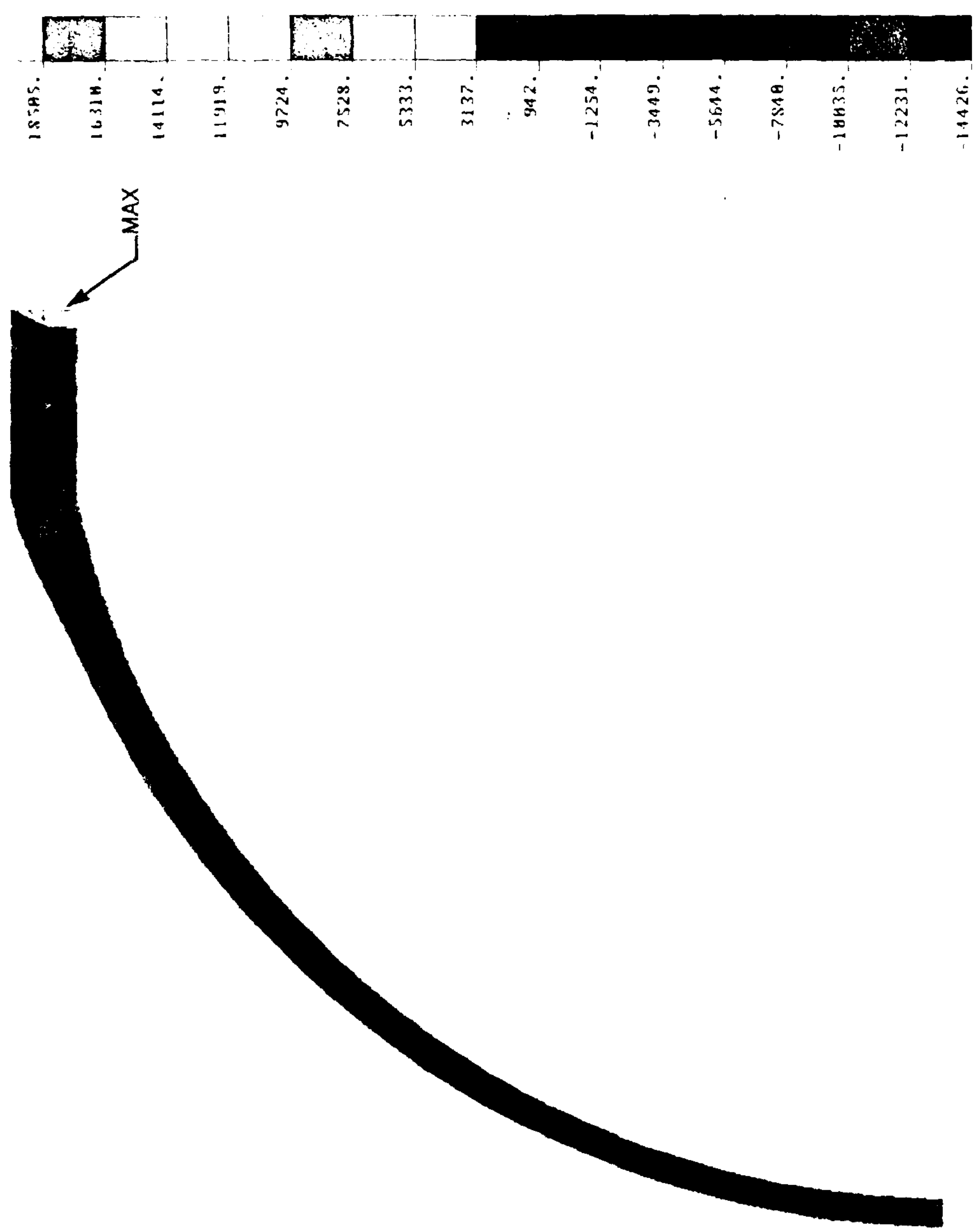

Figure 18. Maximum principal stress plot of Type 4 hemisphere for 26-inch housing.

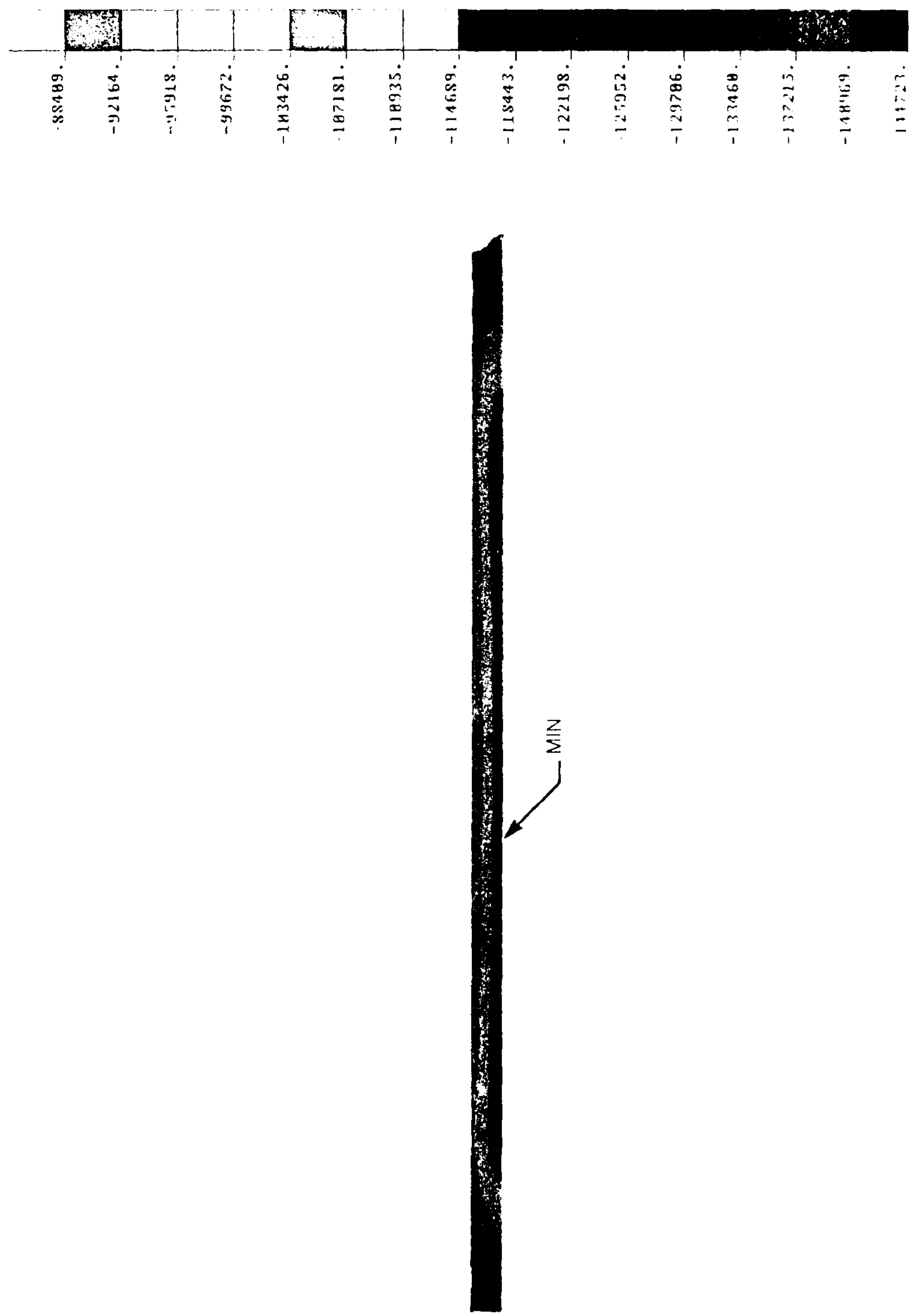

Figure 19. Minimum principal stress plot of cylinder for 26-inch housing.

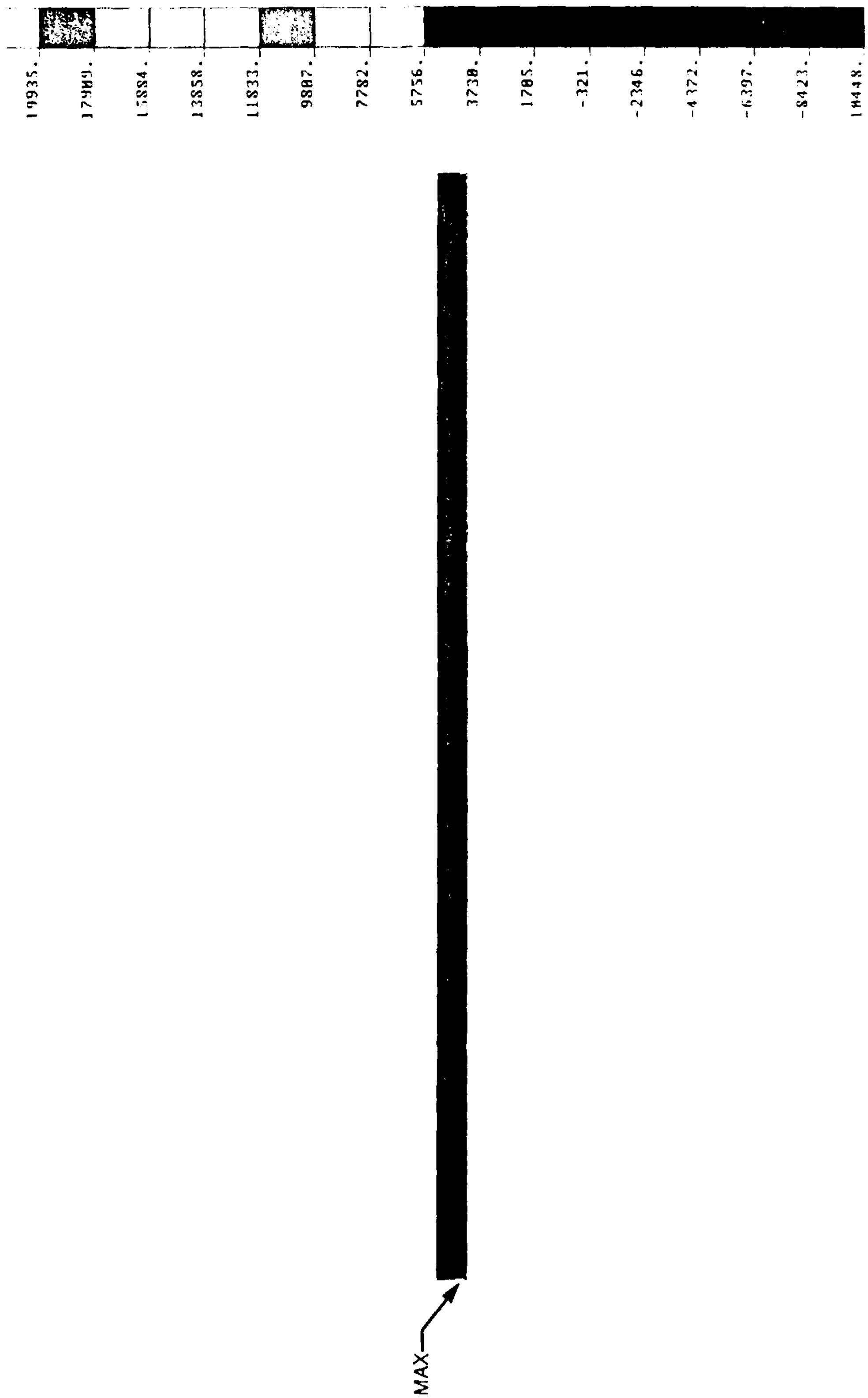

Figure 20. Maximum principal stress plot of cylinder for 26-inch housing.

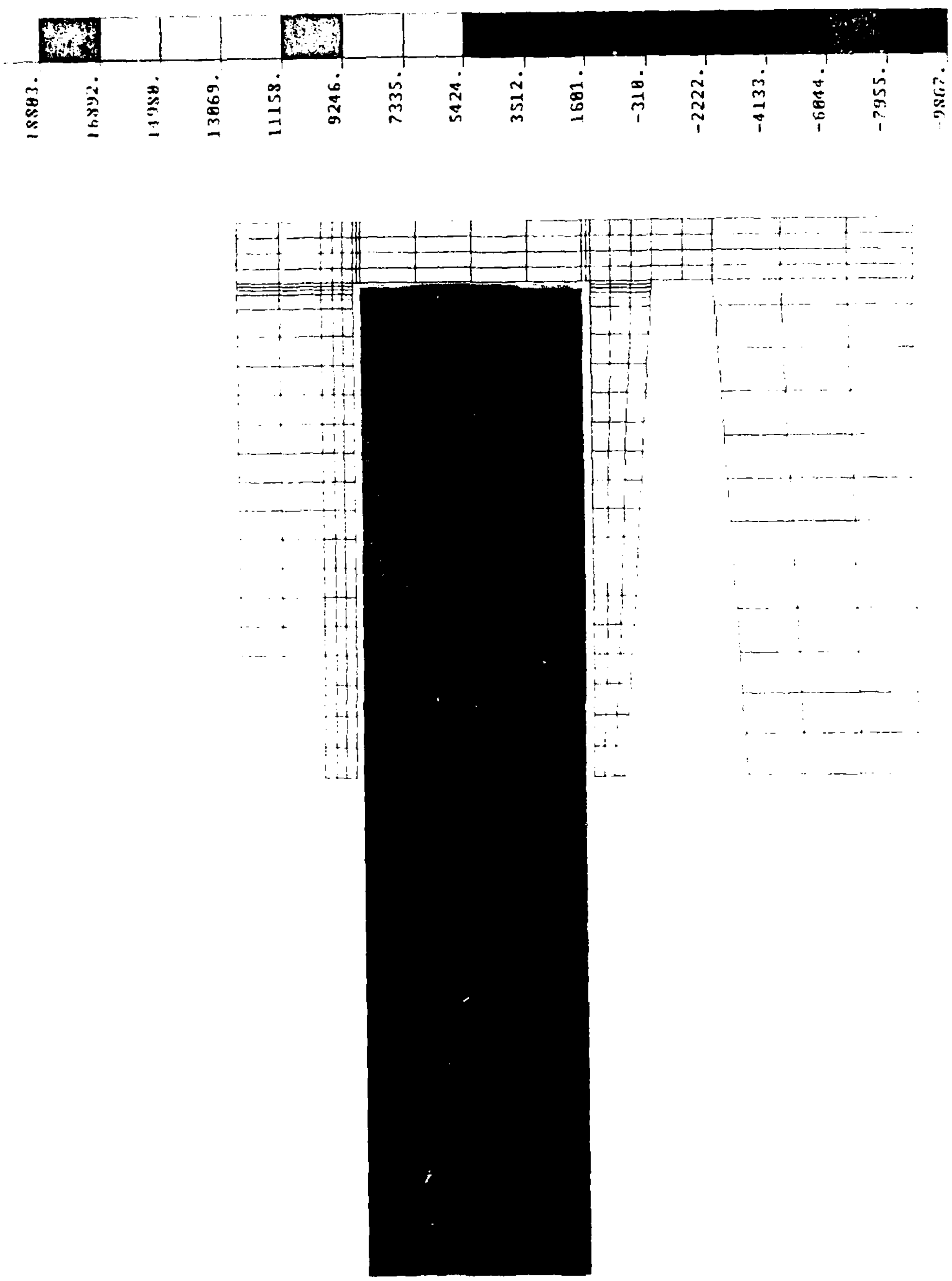

Figure 21. Detail of maximum principal stress plot of *cylinder/central stiffener interface* for 26-inch housing.

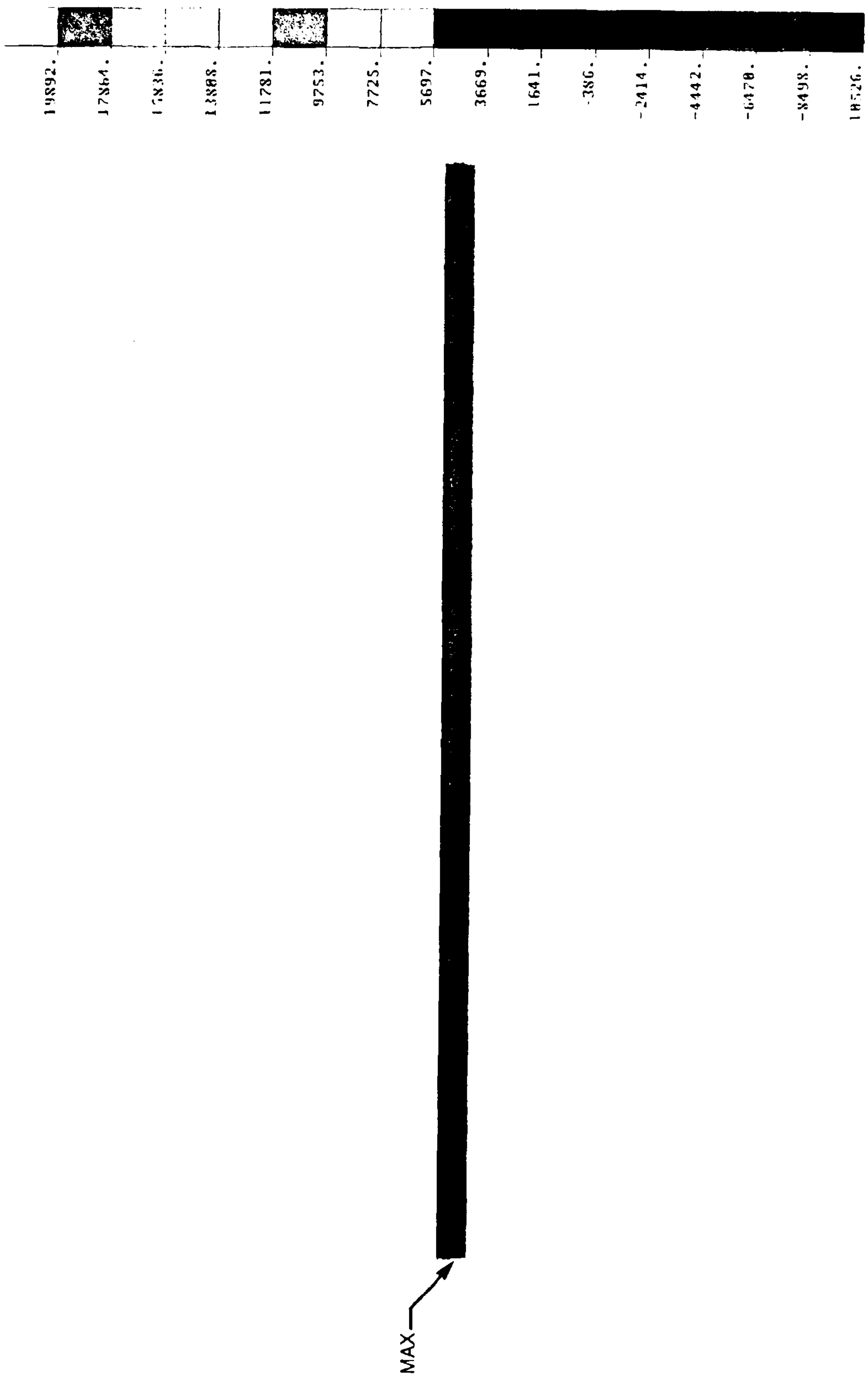

Figure 22. Radial stress plot of cylinder for 26-inch housing.

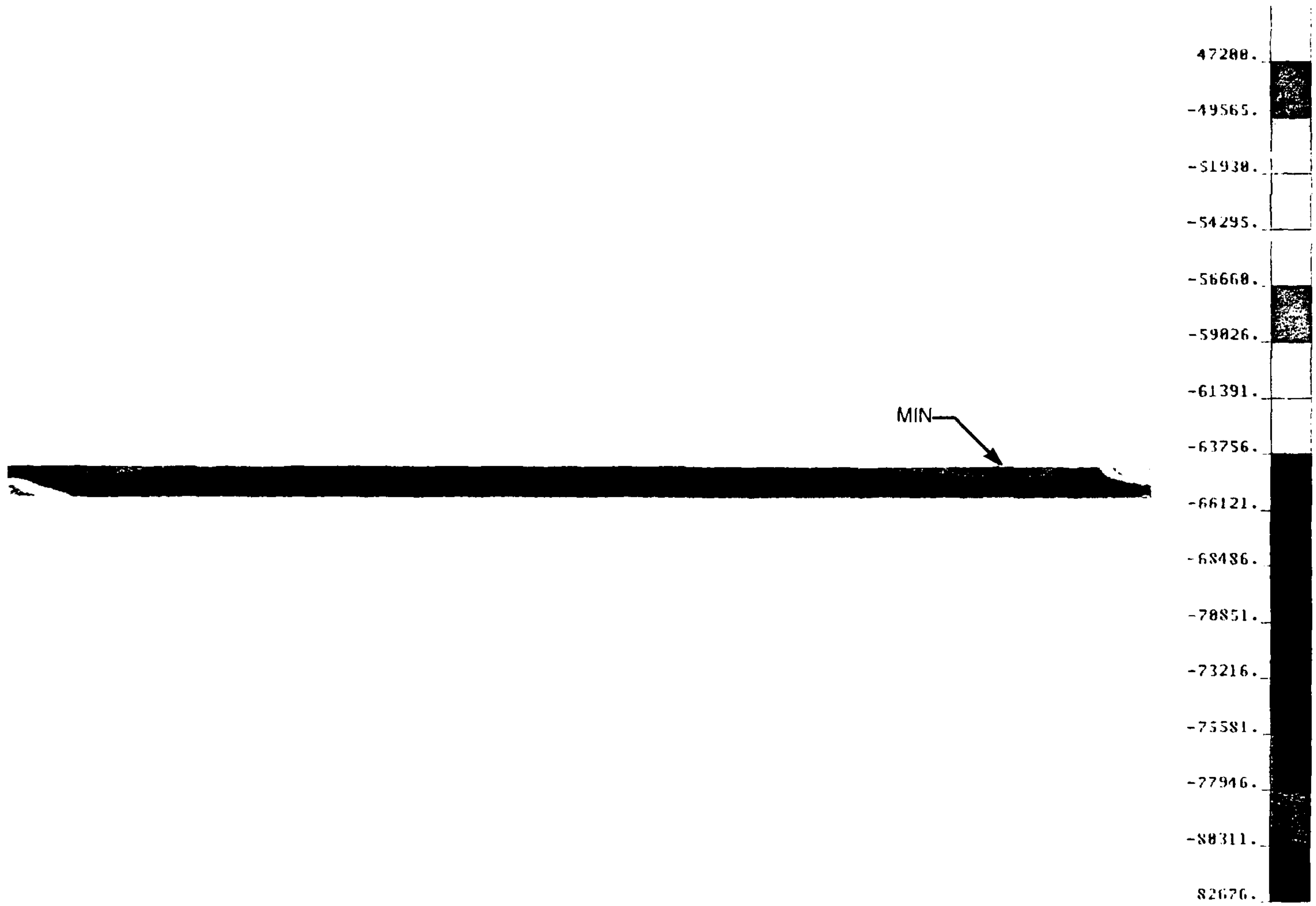

Figure 23. Axial stress plot of cylinder for 26-inch housing.

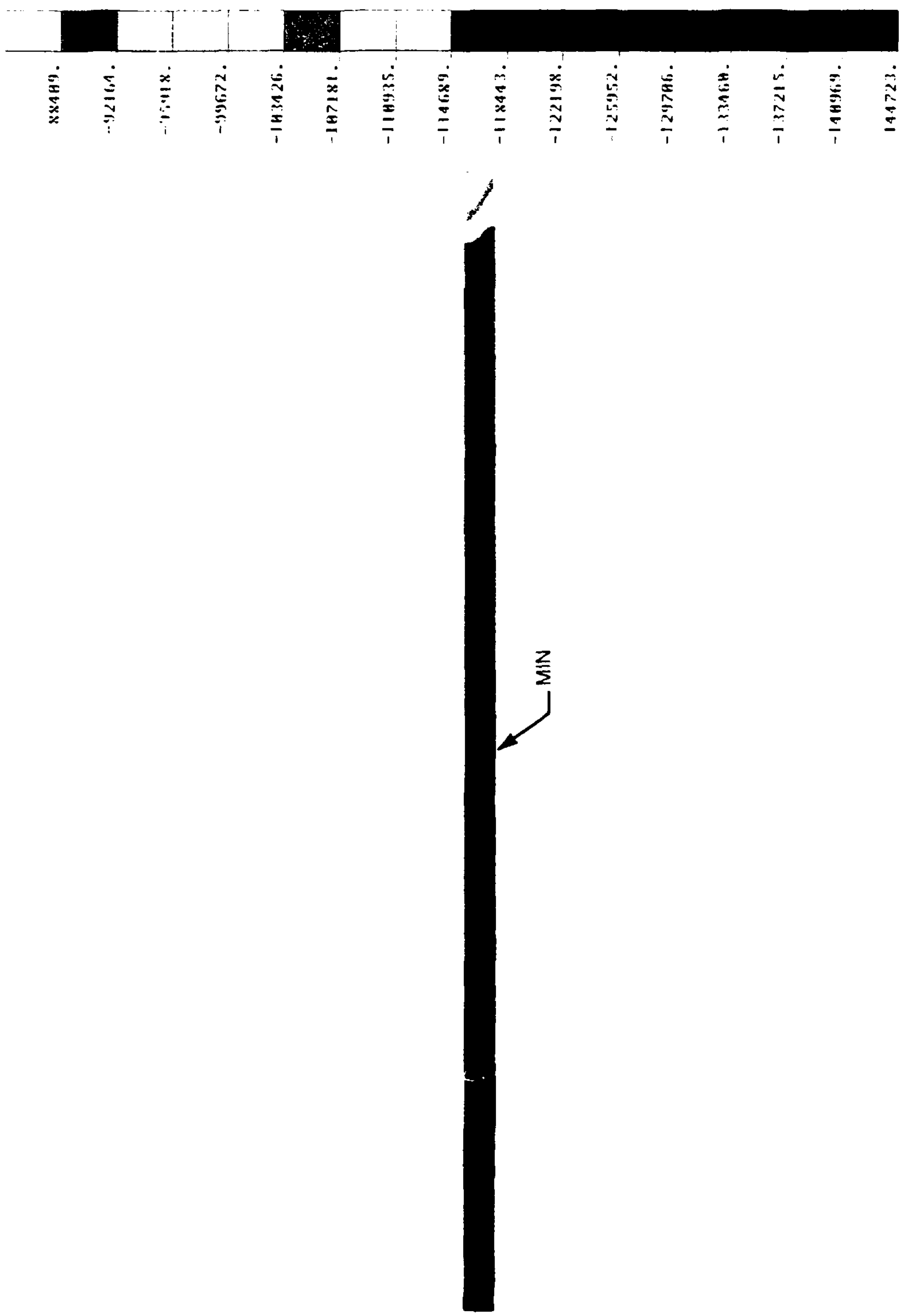

Figure 24. Circumferential stress plot of cylinder for 26-inch housing.

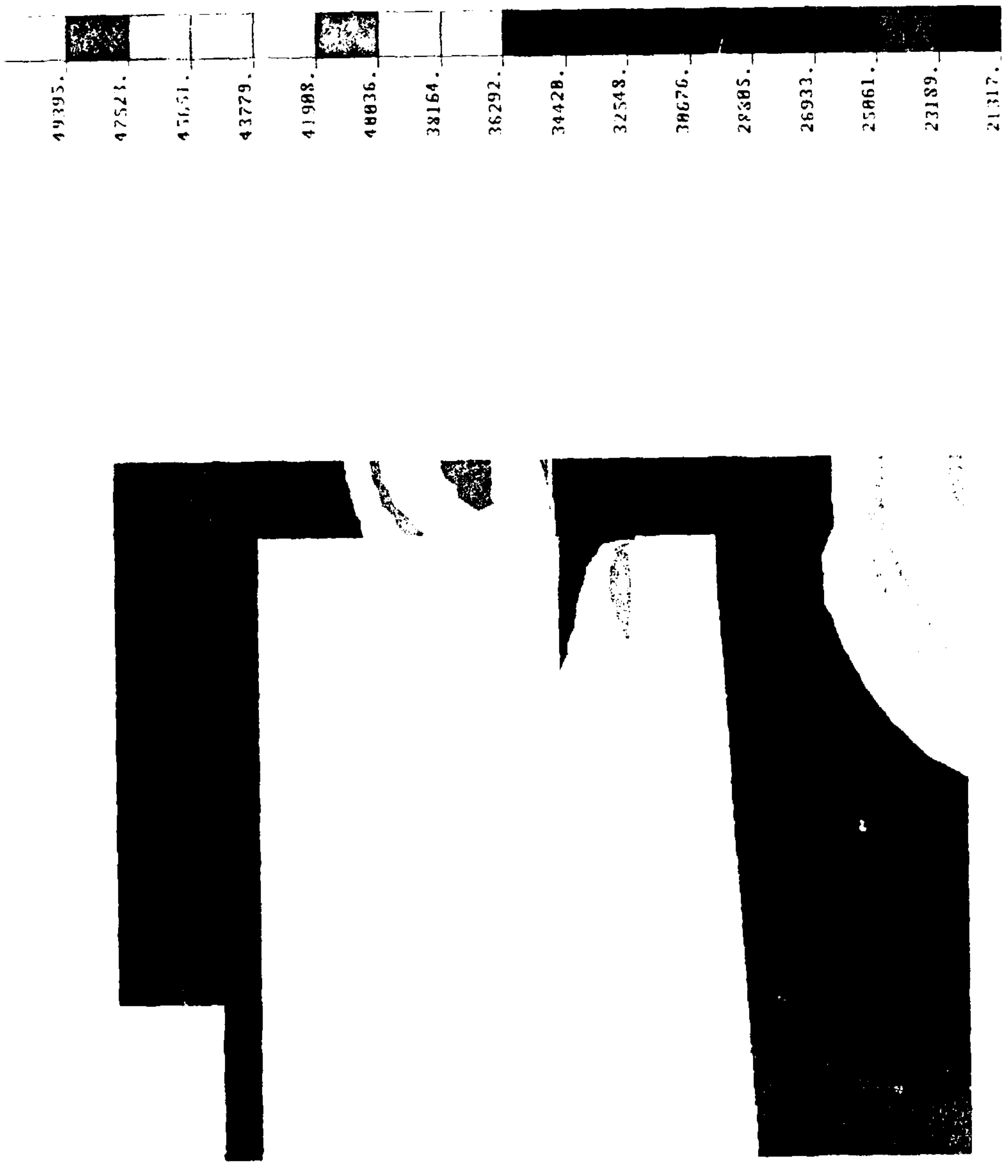

Figure 25. von Mises plot of central stiffener for 26-inch housing.

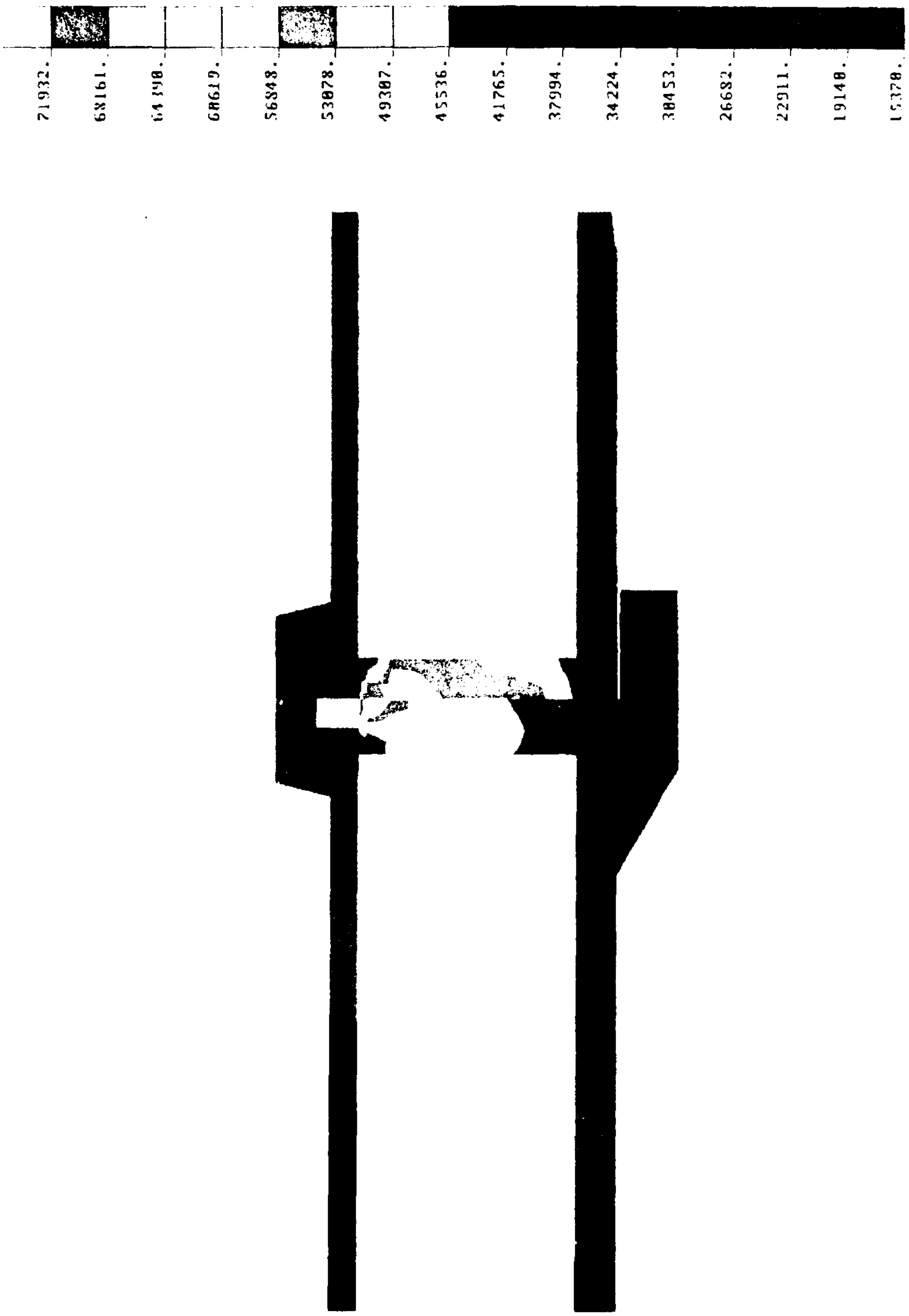

Figure 26. von Mises stress plot of hemisphere and cylinder end cap for 26-inch housing.

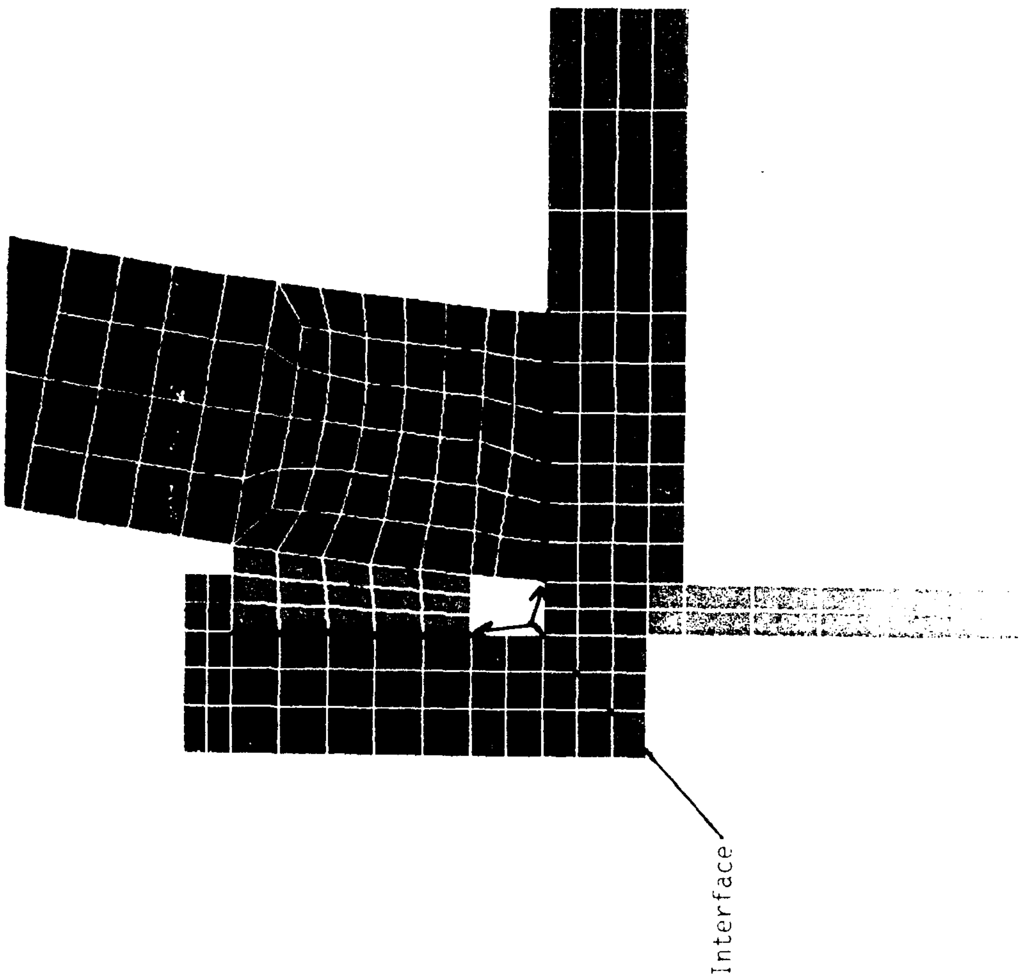

Figure 27. Finite element mesh for modeling electrical feedthrough penetrator for 26-inch housing.

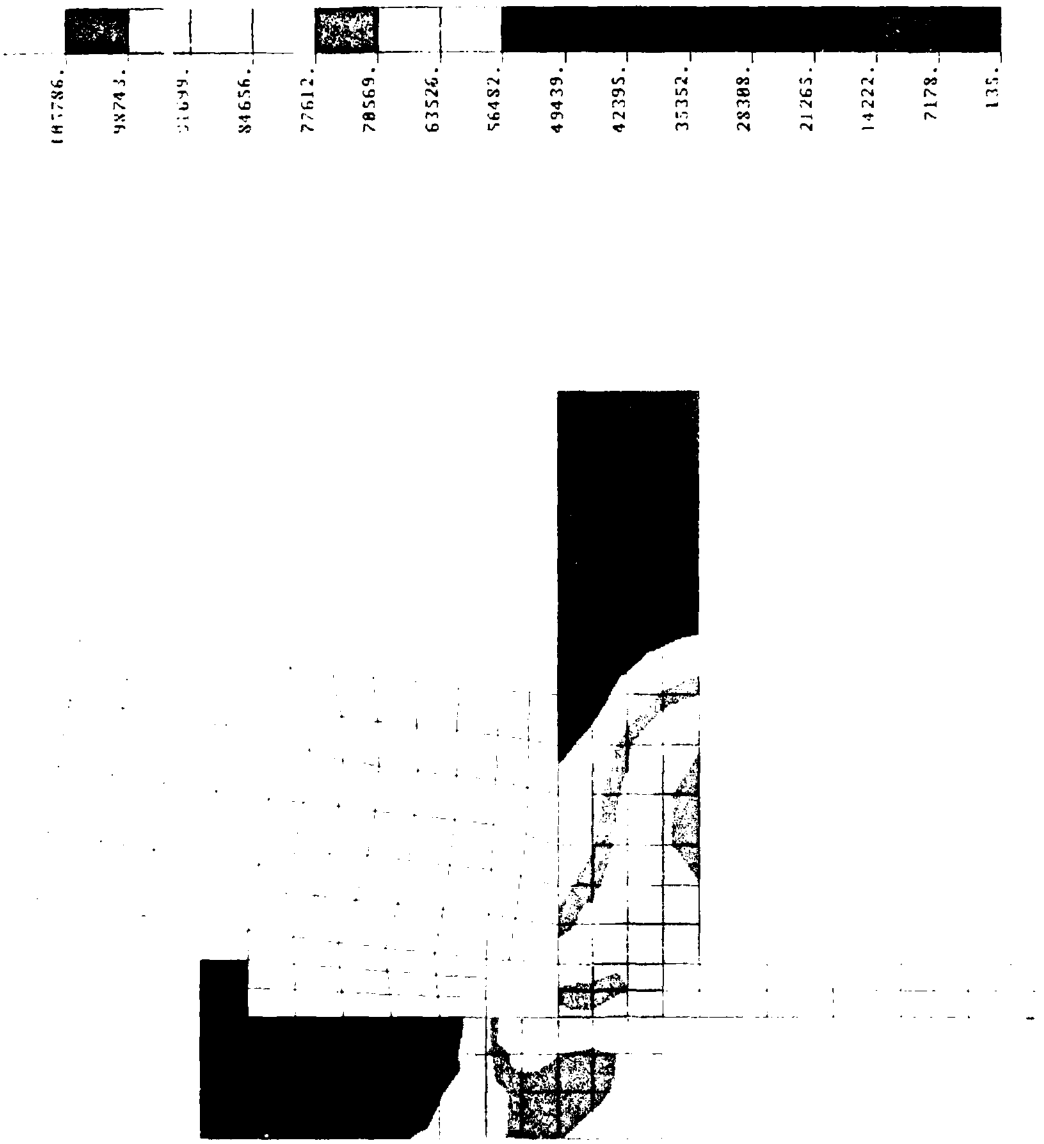

Figure 28. von Mises stress plot of electrical feedthrough penetrator for 26-inch housing.

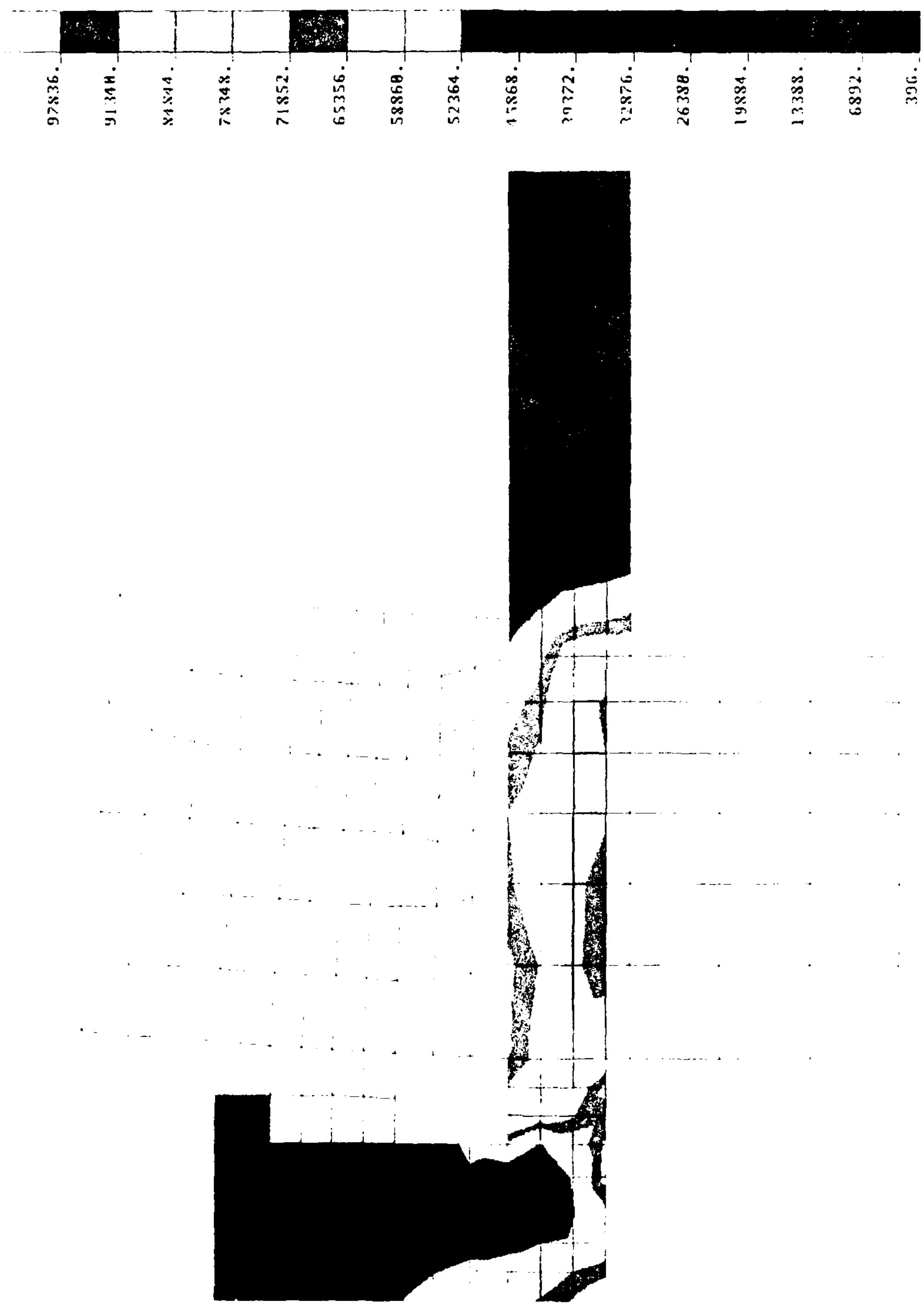

Figure 29. von Mises stress plot of pressure relief valve penetrator for 26-inch housing.

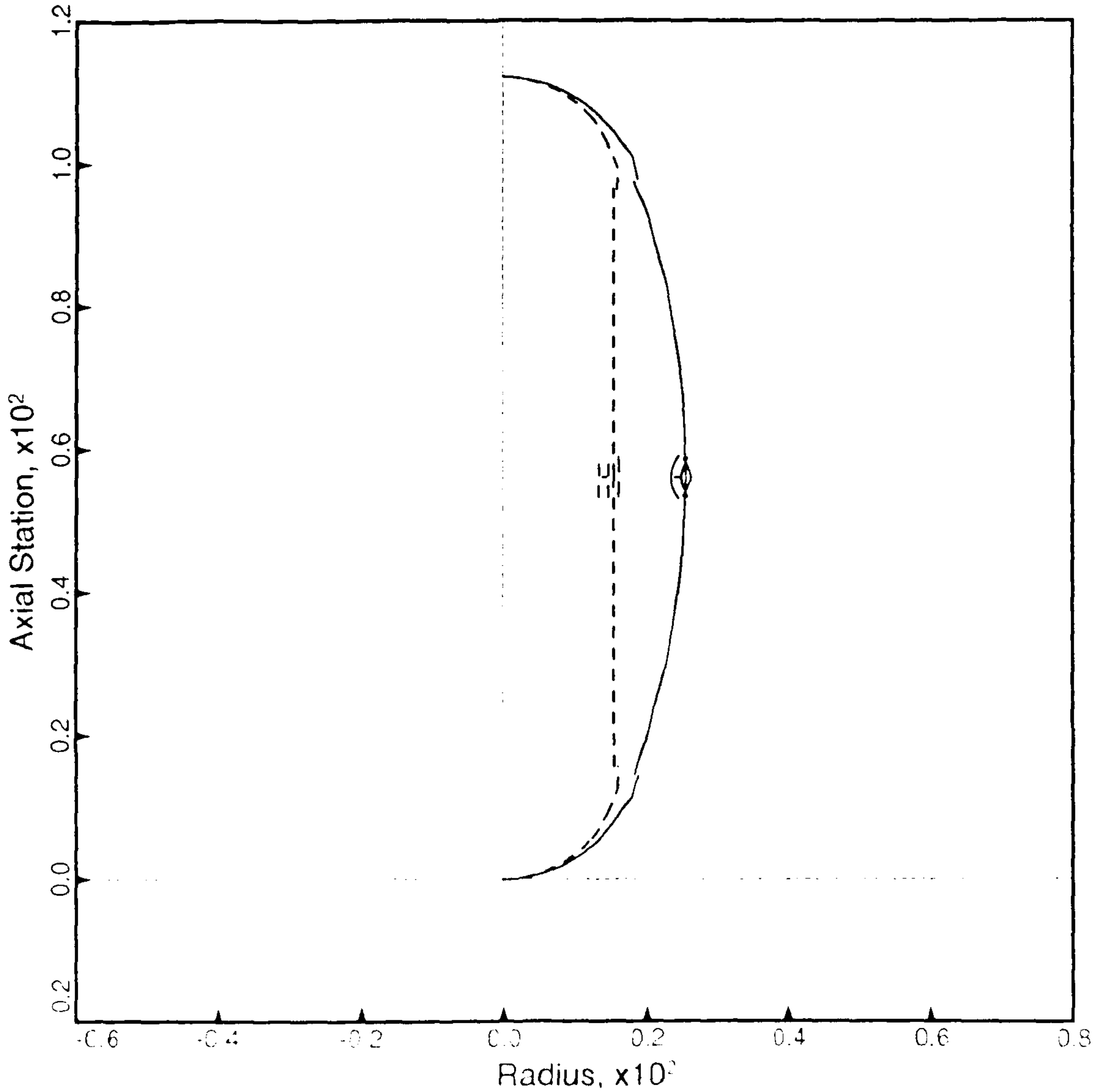

Figure 30. N=2 buckled configuration for 33-inch housing under external hydrostatic pressure.

Figure 31. Comparison of undeformed and deformed shapes of 33-inch housing.

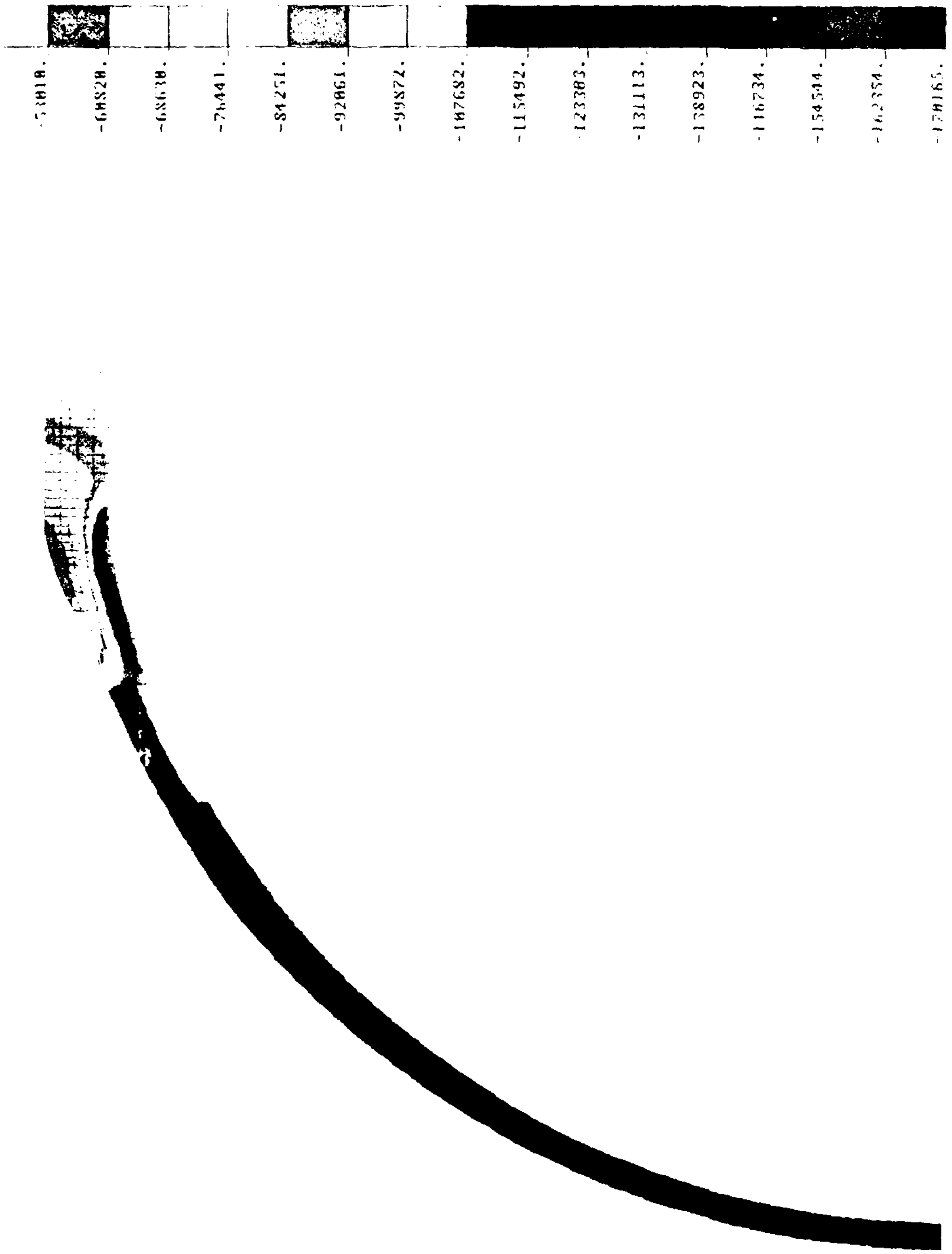

Figure 32. Minimum principal stress plot of Type 4 hemisphere for 33-inch housing.

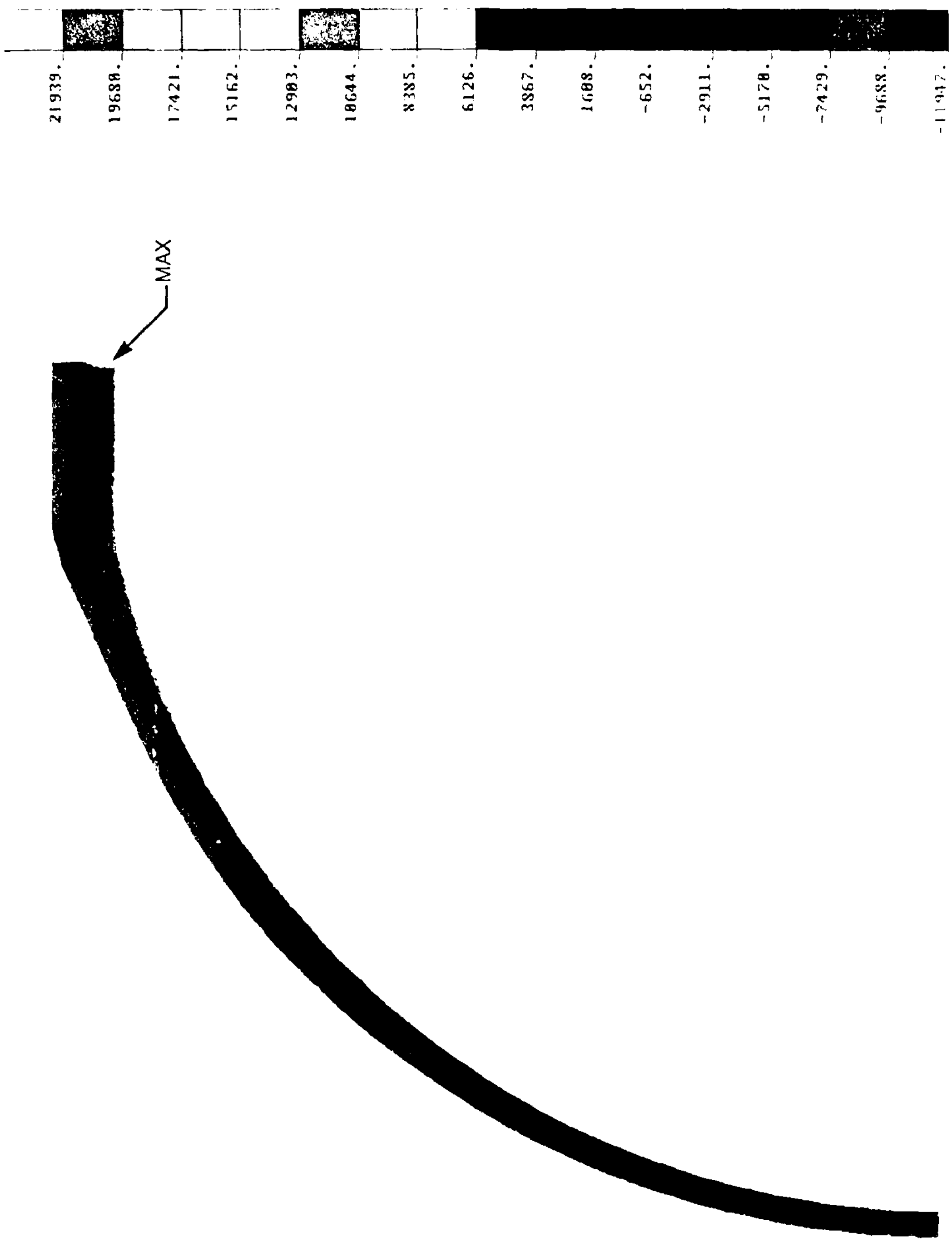

Figure 33. Maximum principal stress plot of Type 4 hemisphere for 33-inch housing.

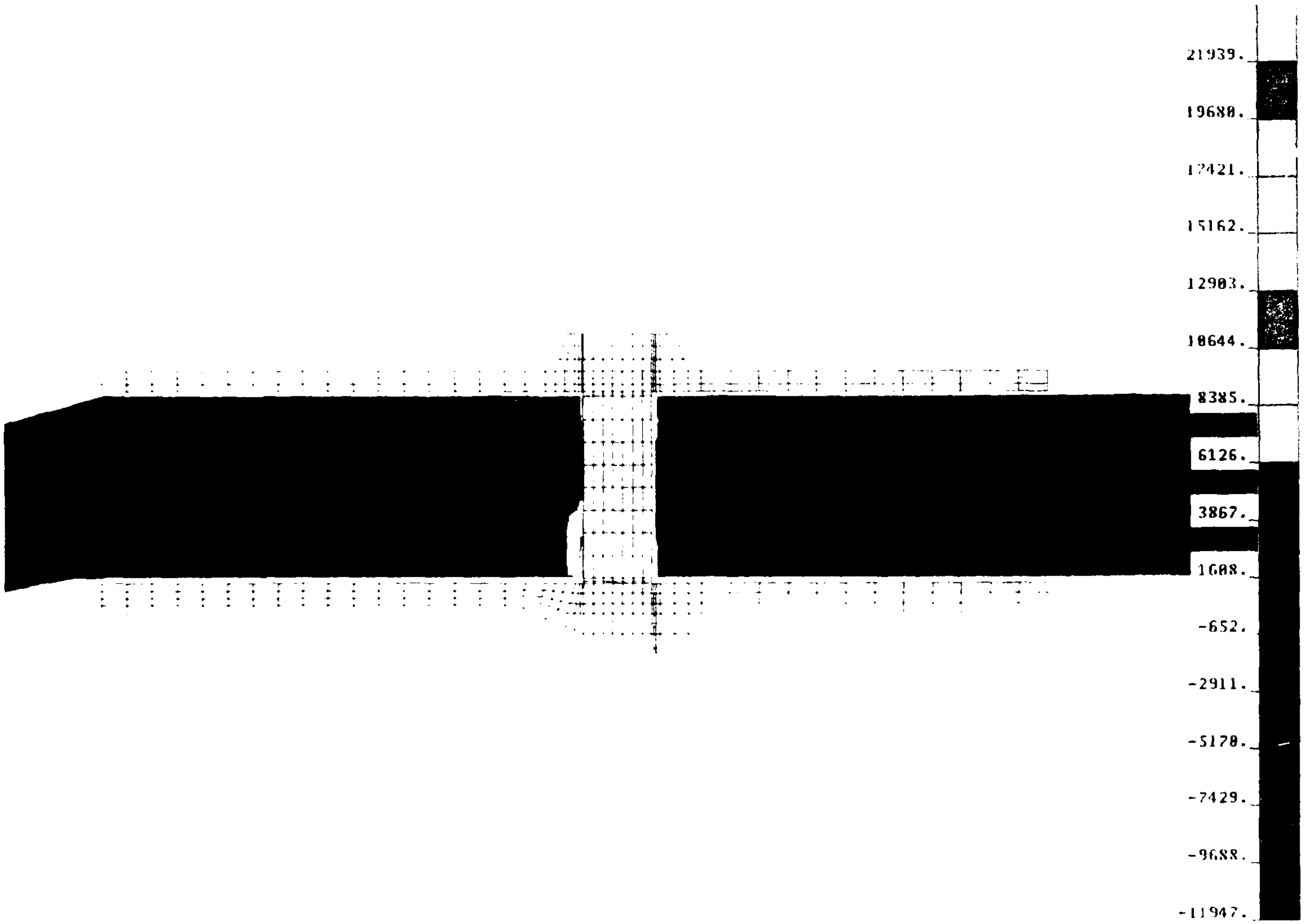

Figure 34 Detail of maximum principal stress plot of Type 4 hemisphere/cylinder interface for 33-inch housing.

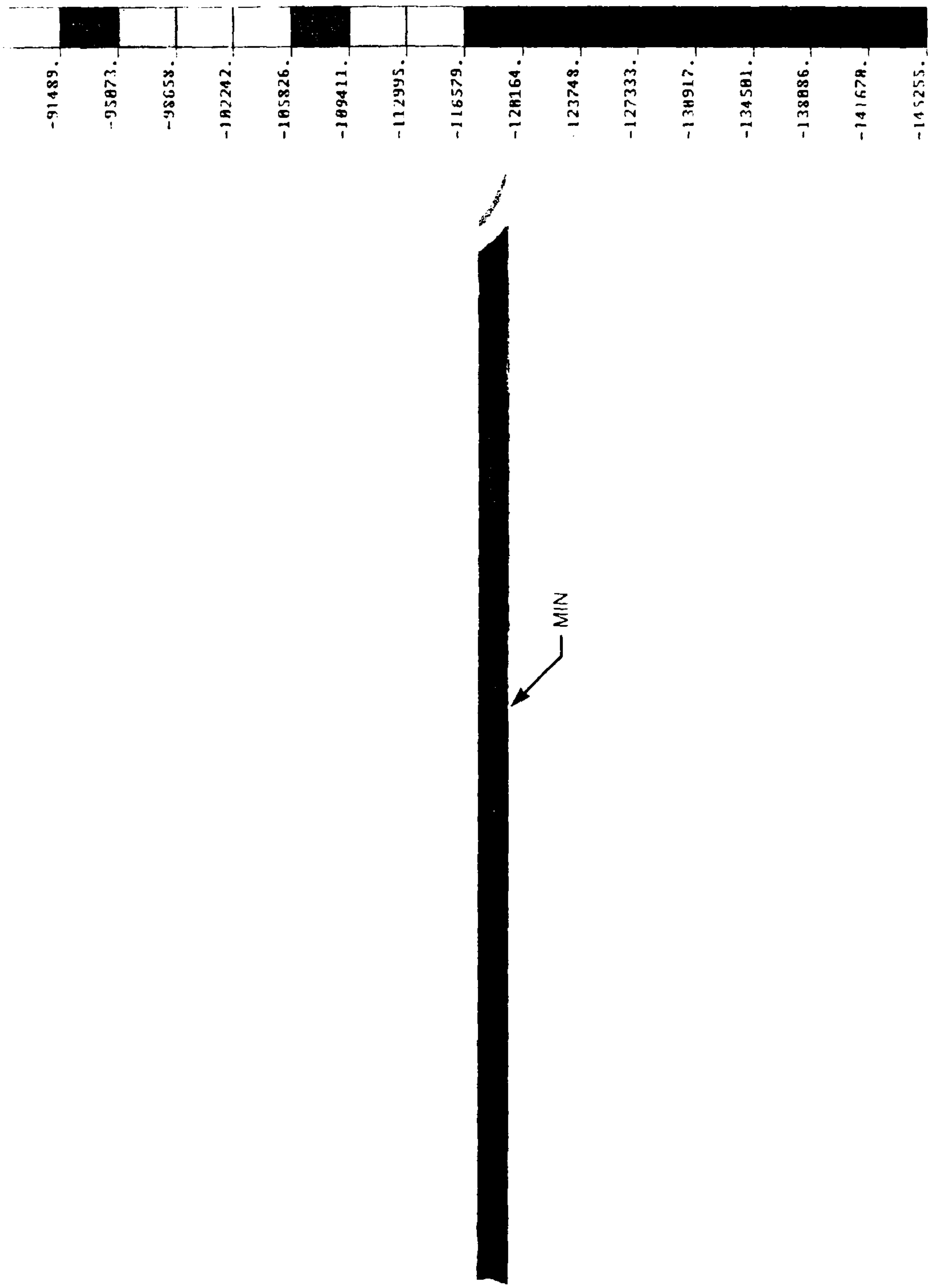

Figure 35. Minimum principal stress plot of cylinder for 33-inch housing.

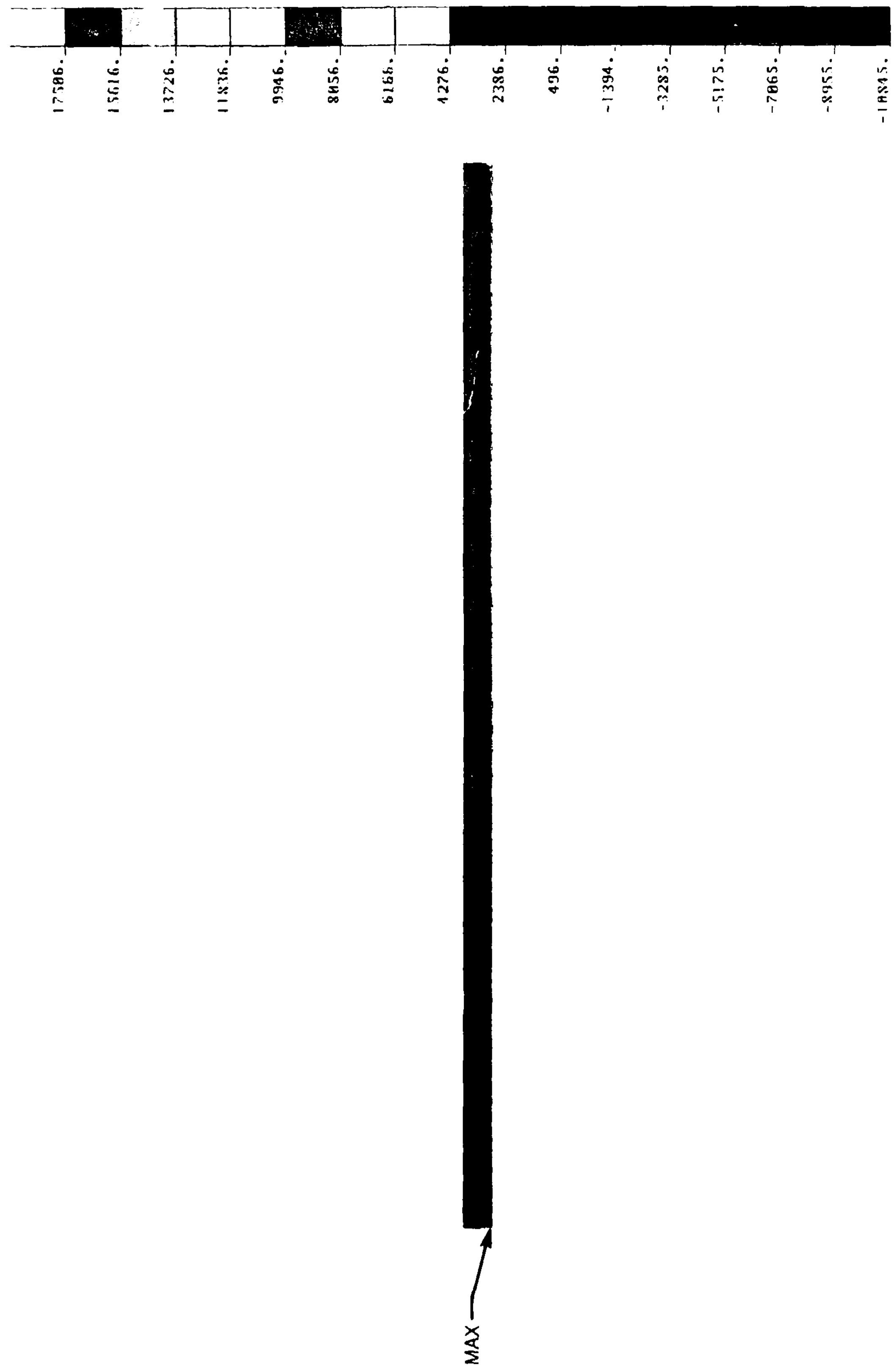

Figure 36. Maximum principal stress plot of cylinder for 33-inch housing.

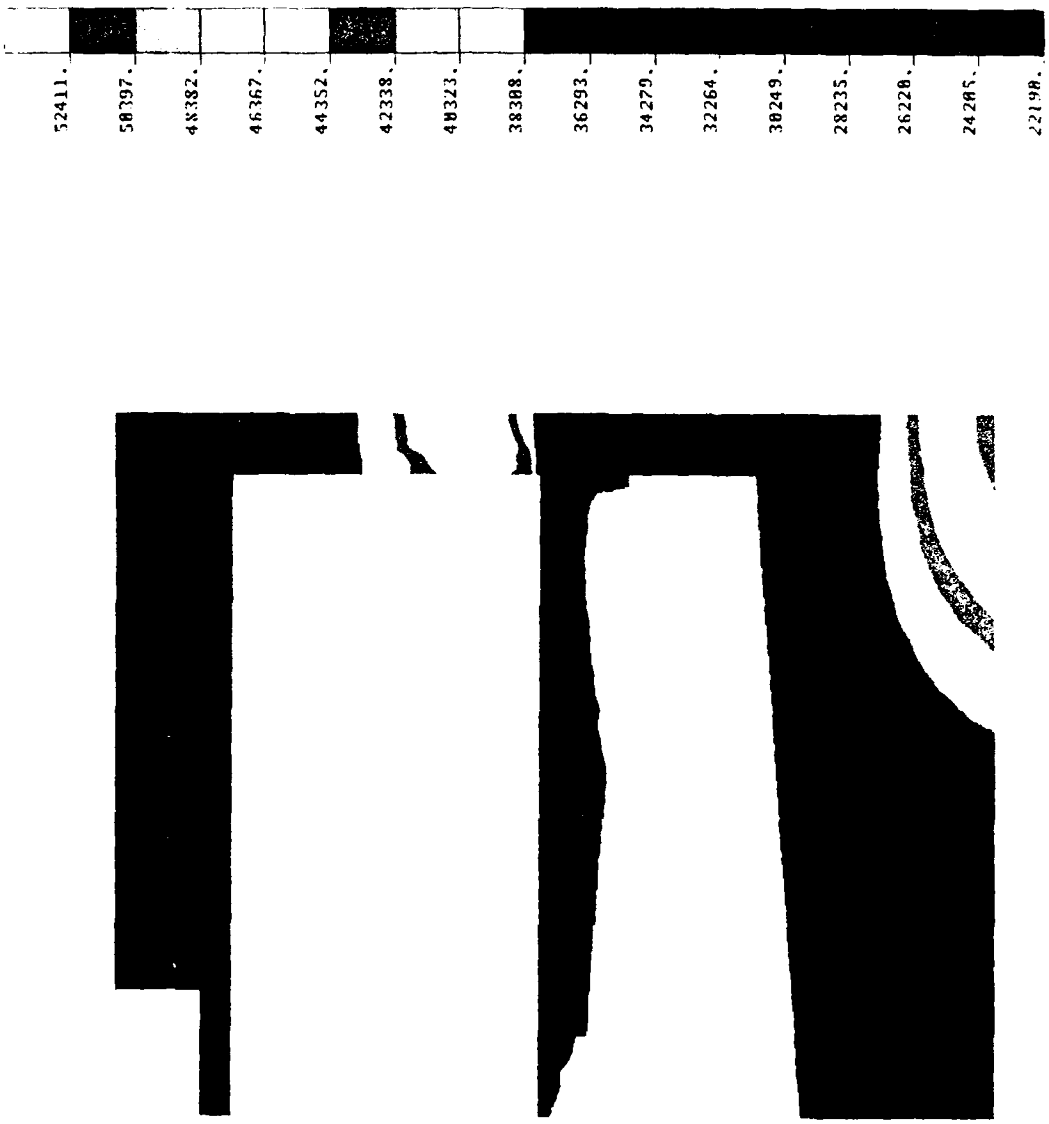

Figure 37. von Mises stress plot of central stiffener for 33-inch housing.

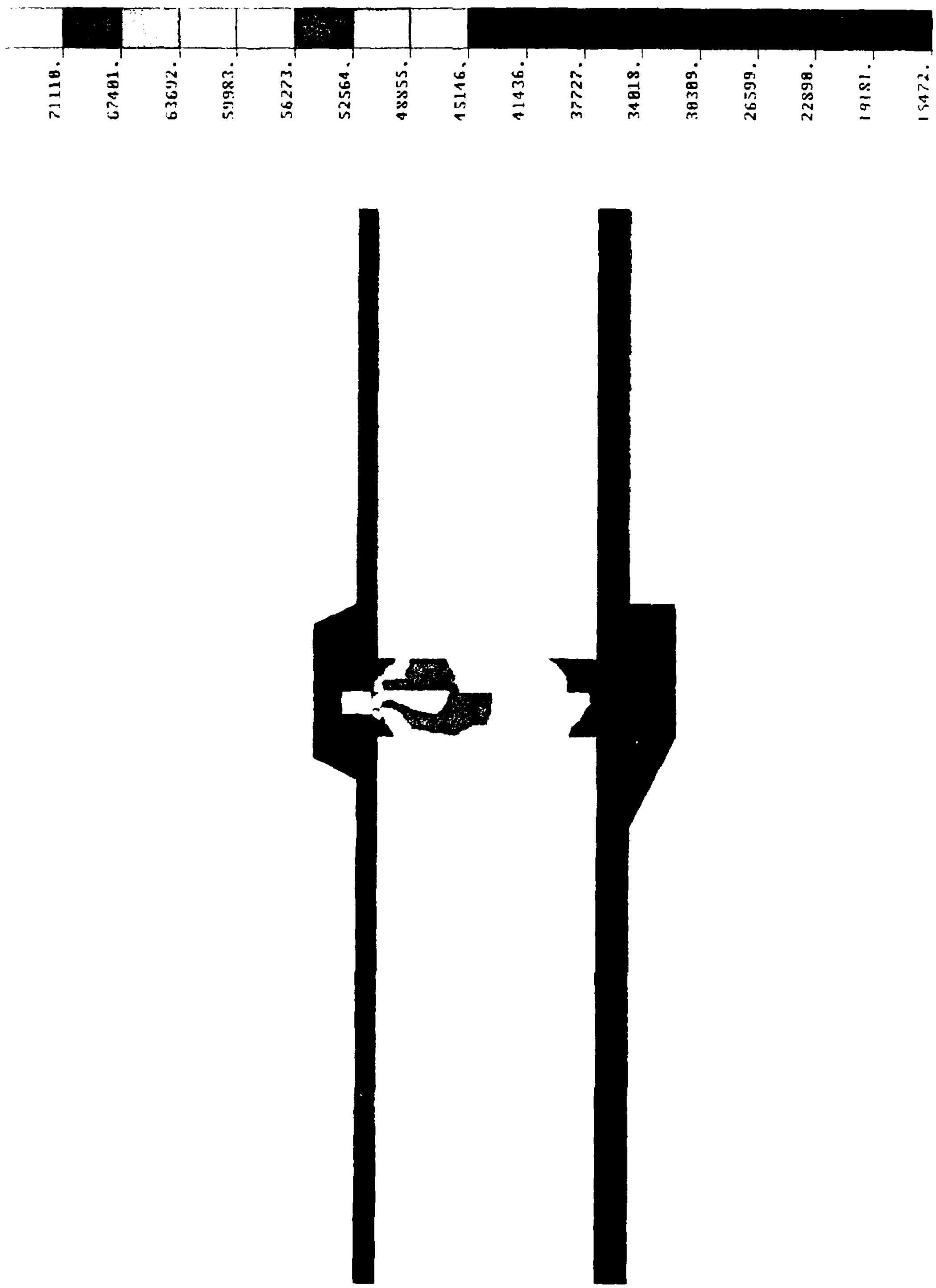

Figure 38. von Mises stress plot of hemisphere/cylinder end cap interface for 33-inch housing.

Table 1. Typical materials for construction of deep submergence pressure housings.

Material	Weight (lb/in_3)	Modulus of Elasticity (Mpsi)	Elasticity Weight	Compressive Strength (kpsi)	Strength Weight
Steel (HY 80)	0.283	30	106	80	280
Steel (HY 130)	0.283	30	106	130	460
Aluminum (7075-T6)	0.100	10	100	73	730
Titanium (6Al-4V)	0.160	16	100	125	780
Glass (Pyrex)	0.080	9	112	100	1250
Glass Composite	0.075	3.5	47	100	1330
Graphite Composite	0.057	16	280	100	1750
Beryllia Ceramic 99%	0.104	51	490	300	2885
Alumina Ceramic 94%	0.130	44	338	300	2310
Glass Ceramic (Pyroceram 9606)	0.093	17.5	188	350	3760
Silicon Carbide	0.114	59	517	450	3947
Boron Carbide	0.089	63	707	400	4494
Alumina/SiC Composite (Lanxide 90-X-089	0.124	43	346	300	2419
B_4C/Al Composite (Dow Chemical)	0.093	45	483	350	3763
Silicon Nitride	0.119	44	370	400	3361

Table 2. Design allowables for structural analysis of 26-inch and 33-inch housings at 9,030 psi external hydrostatic pressure.

Material	Strength	Stress Component	Safety Factor
Ceramic	Compressive strength (300 Kpsi)	Minimum principal membrane stress	2.00
Ceramic	Compressive strength (300 Kpsi)	Minimum principal stress at localized stress concentration	1.50
Ceramic	Flexural strength (53 Kpsi)	Maximum principal stress at localized stress concentration	3.00
Titanium	Proportional limit (90 Kpsi)	von Mises stress	1.33
Titanium	Proportional limit (90 Kpsi)	von Mises stress at localized stress concentration	1.00

Safety factor for bifurcation buckling of housings shall be 1.25 at proof load for 10,000 psi external hydrostatic pressure. (Corresponds to a safety factor of 1.38 at operating pressure of 9,030 psi.)

Table 3. Stress analysis results for 26-inch and 33-inch housings at 9,030 psi external hydrostatic pressure.

25-INCH HOUSING			
Component	Stress Component	Maximum Value (psi)	Safety Factor
Ceramic hemi, Type 6	Minimum principal stress	-146,820	2.04
Ceramic hemi, Type 6, at through hole	Minimum principal stress	-204,400	1.47
Ceramic hemi, Type 4	Minimum principal stress	-155,700	1.93
Ceramic cylinder	Minimum principal stress	-130,680	2.30
Ceramic hemi, Type 6	Maximum principal stress	17,065	3.11
Ceramic hemi, Type 4	Maximum principal stress	16,710	3.17
Ceramic cylinder	Maximum principal stress	18,000	2.94
Hemi end cap/cylinder end cap	von Mises	64,925	1.39
Central stiffener	von Mises	44,600	2.02
2-inch penetrator	von Mises	95,525	0.94
1-inch penetrator	von Mises	88,345	1.02
33-INCH HOUSING			
Component	Stress Component	Maximum Value (psi)	Safety Factor
Ceramic hemi, Type 4	Minimum principal stress	-153,660	1.95
Ceramic cylinder	Minimum principal stress	-131,165	2.29
Ceramic hemi, Type 4	Maximum principal stress	19,810	2.68
Ceramic cylinder	Maximum principal stress	15,810	3.35
Hemi/cylinder end cap	von Mises	64,210	1.40
Central stiffener	von Mises	47,330	1.90

APPENDIX A: ENGINEERING DRAWINGS OF 26-INCH OD AND 33-INCH OD CERAMIC PRESSURE HOUSINGS

FIGURES

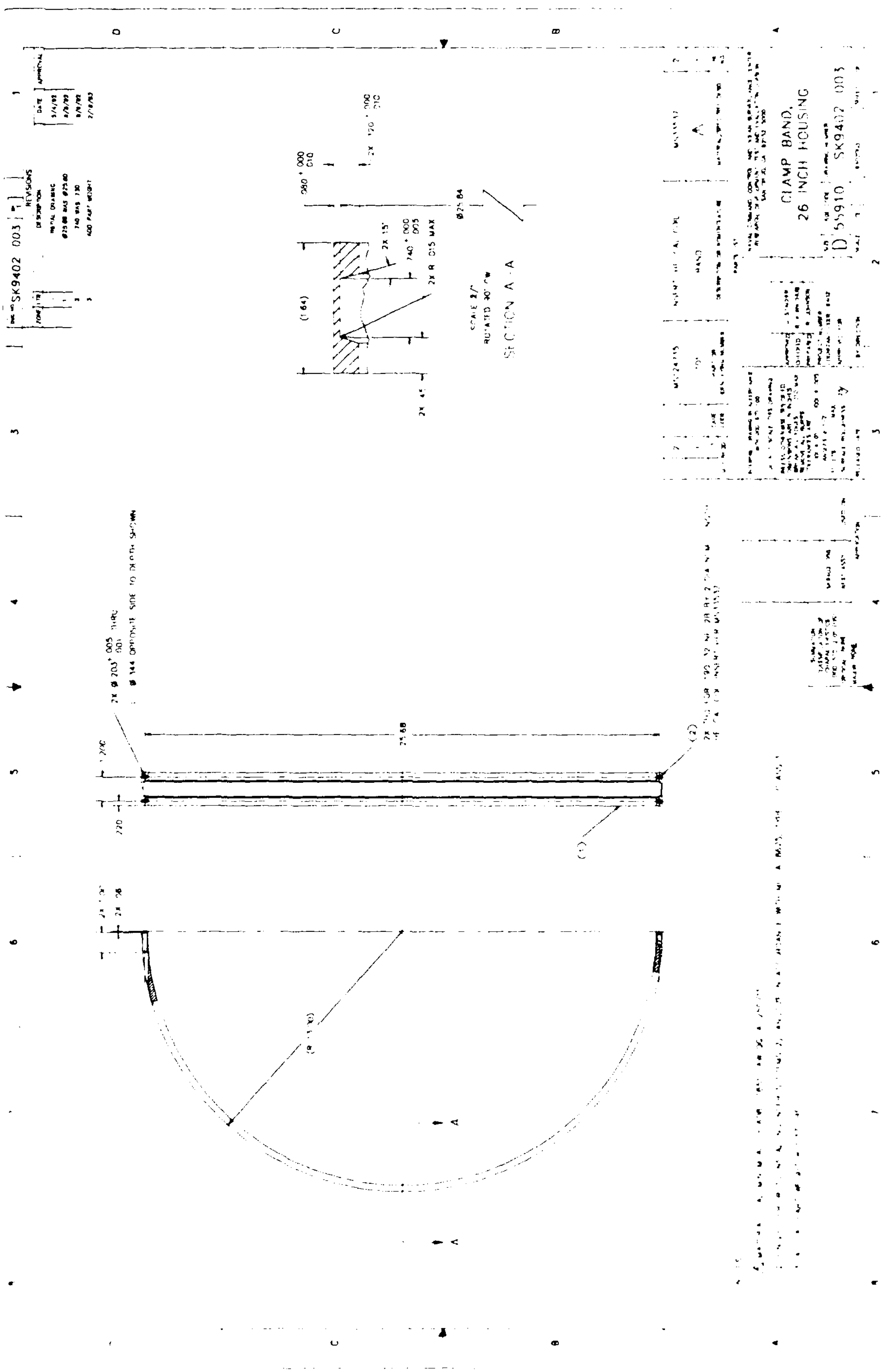

Figure A-1. 26-inch housing clamp band.

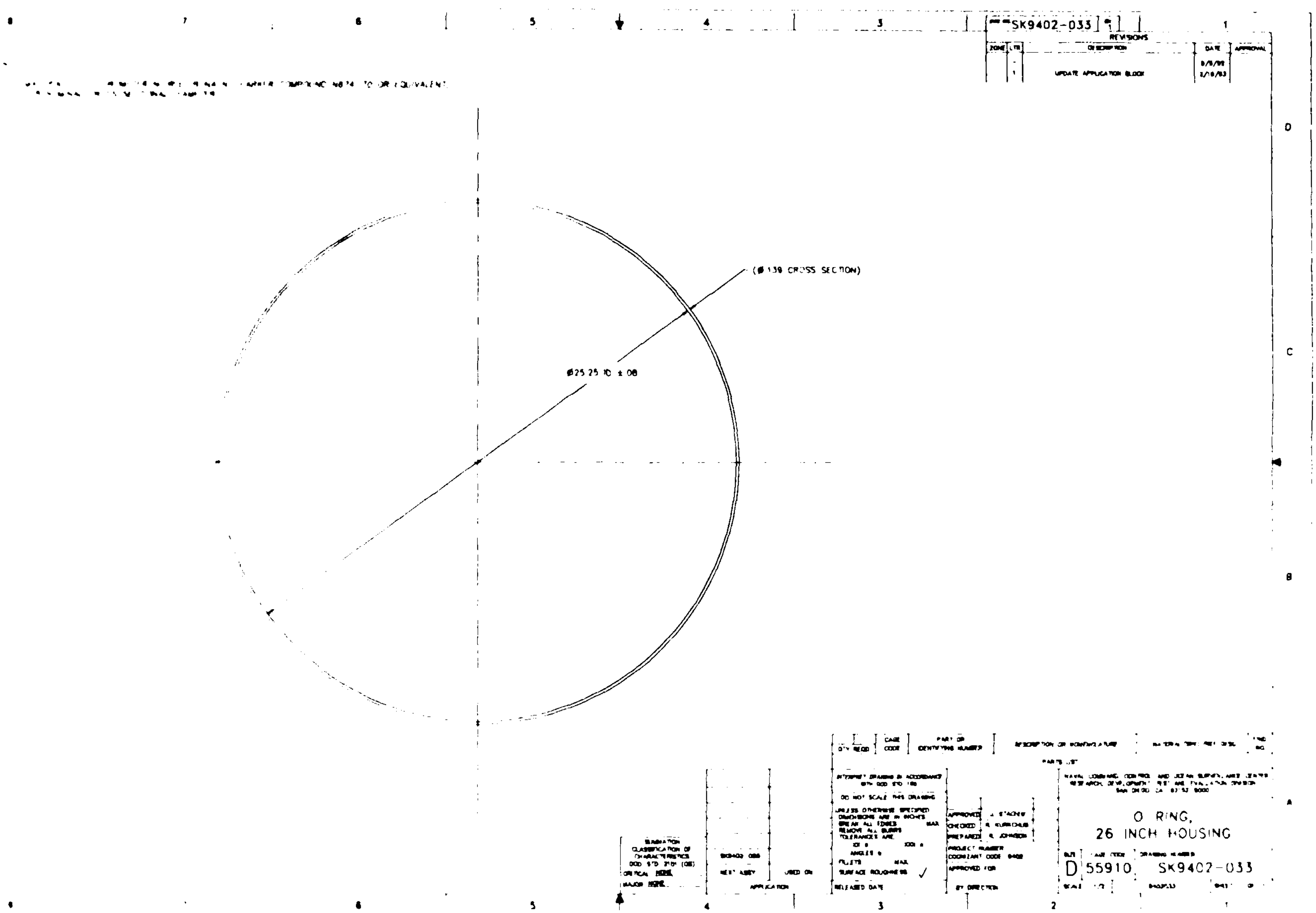

Figure A-2. 26-inch housing O-ring.

SK9402-052

ZONE	LTR	REVISIONS DESCRIPTION	DATE	APPROVAL
			6/29/82	
	1	REMOVE ITEM 14	2/22/83	

QTY REQD	CAGE CODE	PART OR IDENTIFYING NUMBER	DESCRIPTION OR NOMENCLATURE	MATERIAL/SPEC REF DESG	FIND NO
AR			SILICONE COMPOUND	MIL S 8660	24
AR			EPOXY		23
AR			ADHESIVE		22
4		MS18066-15	SCREW, CAP, SOCKET HD HEX, CRES, 190 32UNF 3A X 1.25 L		21
12		MS51959 77	SCREW, FLT CSK HD, 82°, CRES, 250-20UNC 2A X 375 L		20
4		2 226	O-RING	⚠	19
2		2 214	O-RING	⚠	18
1	55910	SK9402 82-003-01	FAIRING, HEMI 26 INCH HOUS		17
2	55910	SK9402-051	CLAMP, FAIRING, 26 INCH HOUS		16
1	55910	SK9402 049-1	GASKET, FAIRING 26 INCH HOUS		15
					14
4	55910	SK9402 031-4	WASHER, PENETRATION, ELEC FEED		13
4	55910	SK9402-031-3	SPACER, PENETRATION, ELEC FEED		12
4	55910	SK9402 031-2	NUT, PENETRATION, ELEC FEED		11
4	55910	SK9402 031-1	PENETRATION, ELEC FEEDTHRU		10
2	55910	SK9402 030-4	WASHER, PENETRATION, PRES REL		9
2	55910	SK9402 030-3	SPACER, PENETRATION, PRES REL		8
2	55910	SK9402 030-2	NUT, PENETRATION PRES RELIEF		7
2	55910	SK9402 030-1	PENETRATION PRESSURE RELIEF		6
2	55910	SK9402 028	LIFT PAD FAIRING		5
1	55910	SK9402 027	LIFT LUG, FAIRING		4
1	55910	0128603	GASKET, 26 INCH HOUSING		3
1	55910	SK9402 001	HEMI ENDCAP 26 INCH HOUSING		2
1	55910	012275	CERAMIC HEMI, TYPE 8 26 INCH HOUS		1

PARTS LIST

INTERPRET DRAWING IN ACCORDANCE WITH DOD STD 100

DO NOT SCALE THIS DRAWING

UNLESS OTHERWISE SPECIFIED DIMENSIONS ARE IN INCHES

APPROVED J. STACHIW

CHECKED R. KURKCHUB

PREPARED R. JOHNSON

PROJECT NUMBER

COGNIZANT CODE 9402

NAVAL COMMAND, CONTROL, AND OCEAN SURVEILLANCE CENTER
RESEARCH, DEVELOPMENT, TEST AND EVALUATION DIVISION
SAN DIEGO, CA 92152 5000

ASSY., FORWARD HEAD,
26 INCH HOUSING

SIZE D | CAGE CODE 55910 | DRAWING NUMBER SK9402-052

SCALE 1/2 | SHEET 1 OF 3

NEXT ASSY SK9402 055 | USED ON | APPLICATION

ELIMINATION CLASSIFICATION OF CHARACTERISTICS DOD STD 2101 (OS)
CRITICAL NONE
MAJOR NONE

Figure A-3. 26-inch housing forward head assembly, Sheet 1.

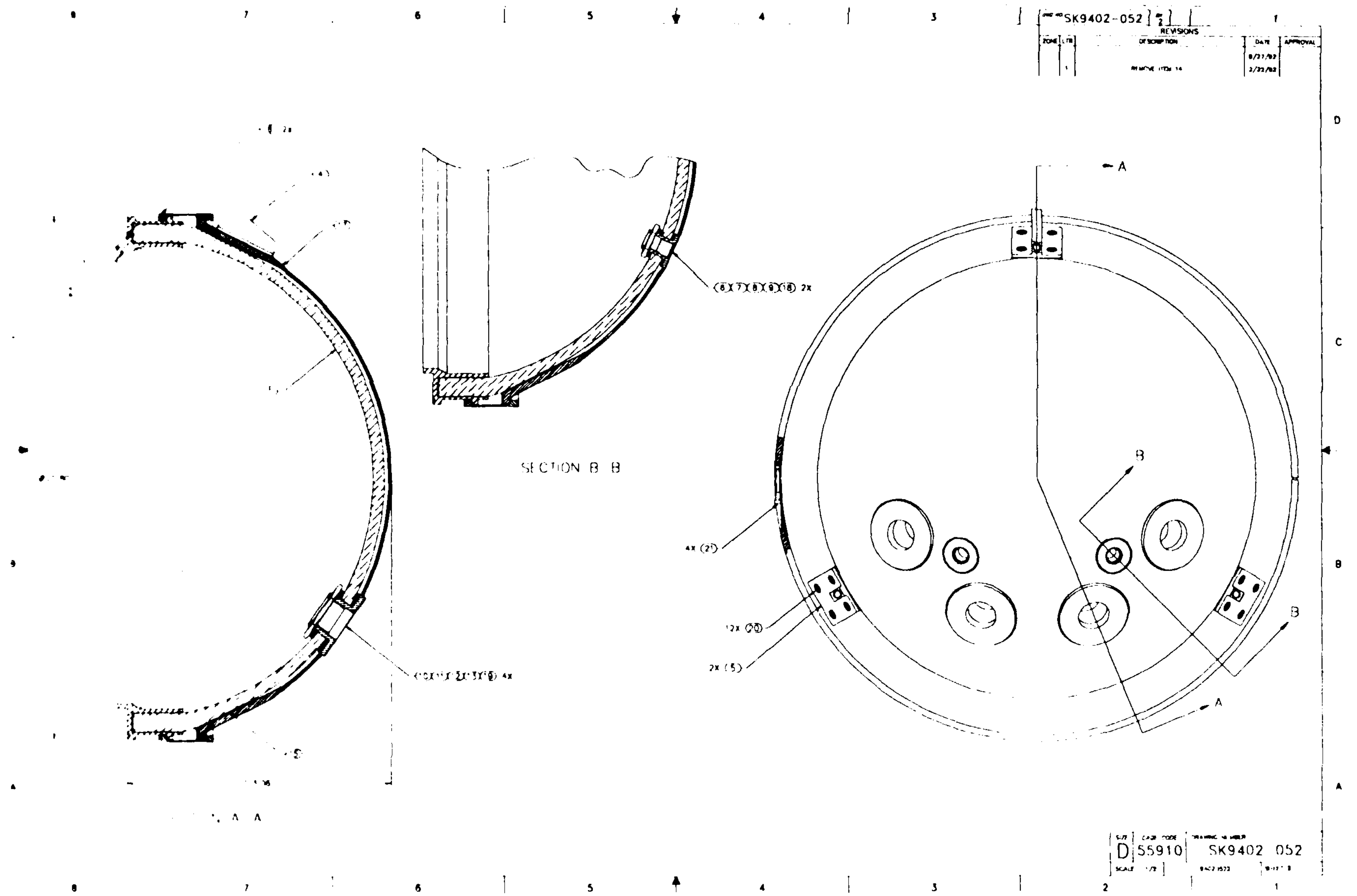

Figure A-3. 26-inch housing forward head assembly, Sheet 2.

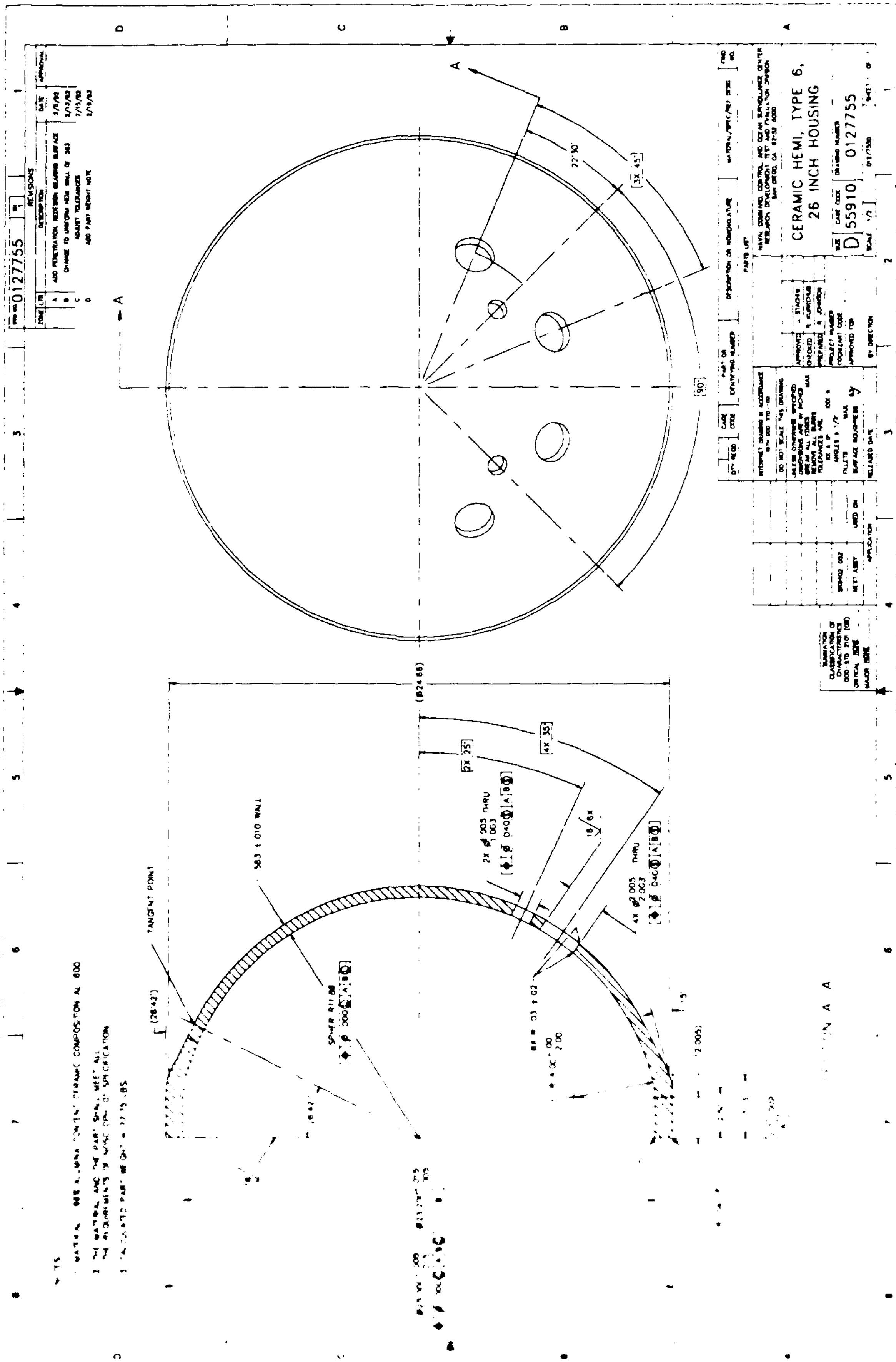

Figure A-4. 26-inch housing Type 6 ceramic hemisphere.

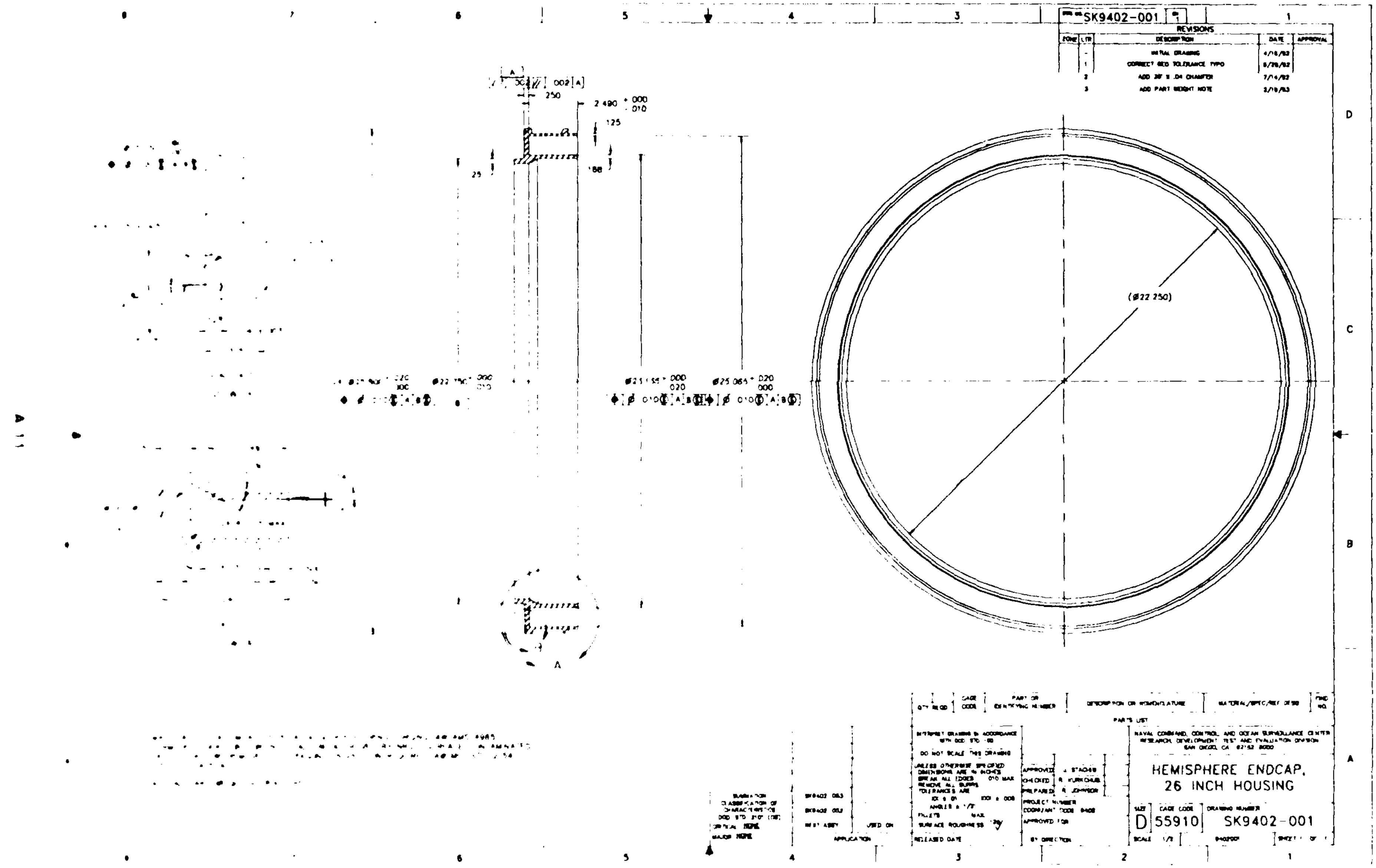

Figure A-5   26-inch housing hemisphere end cap.

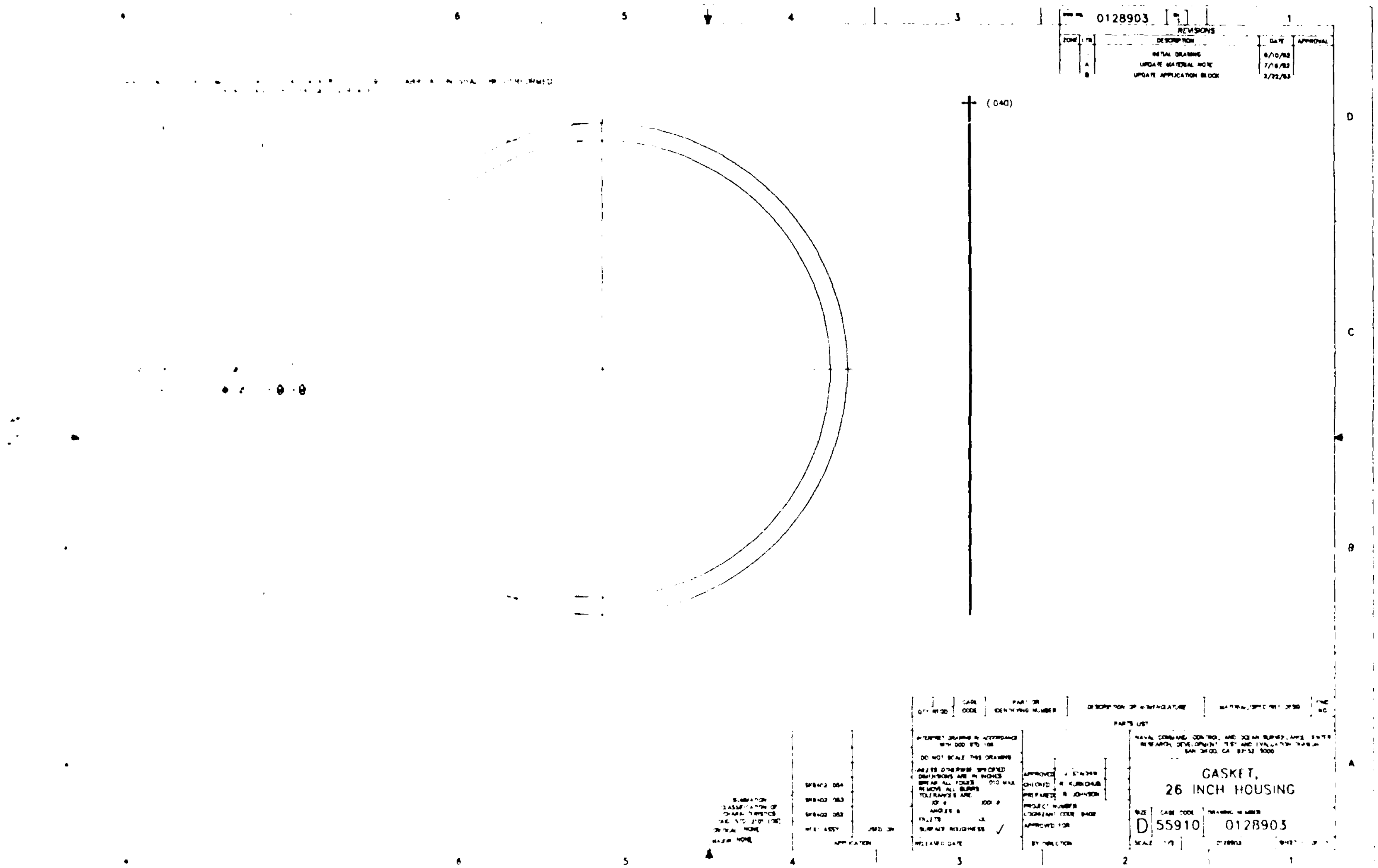

Figure A-6. 26 inch housing gasket.

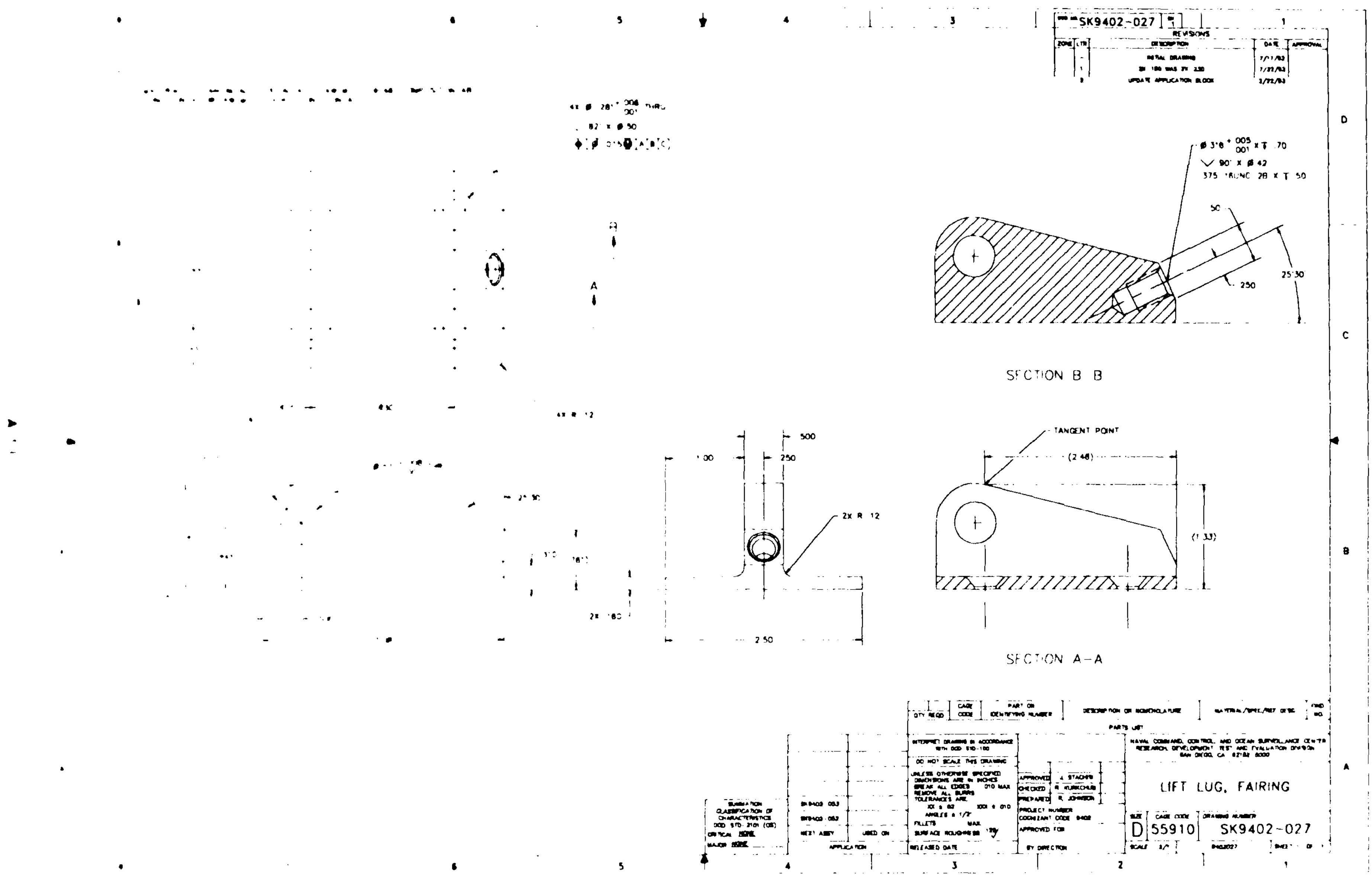

Figure A-7. Fairing lift lug.

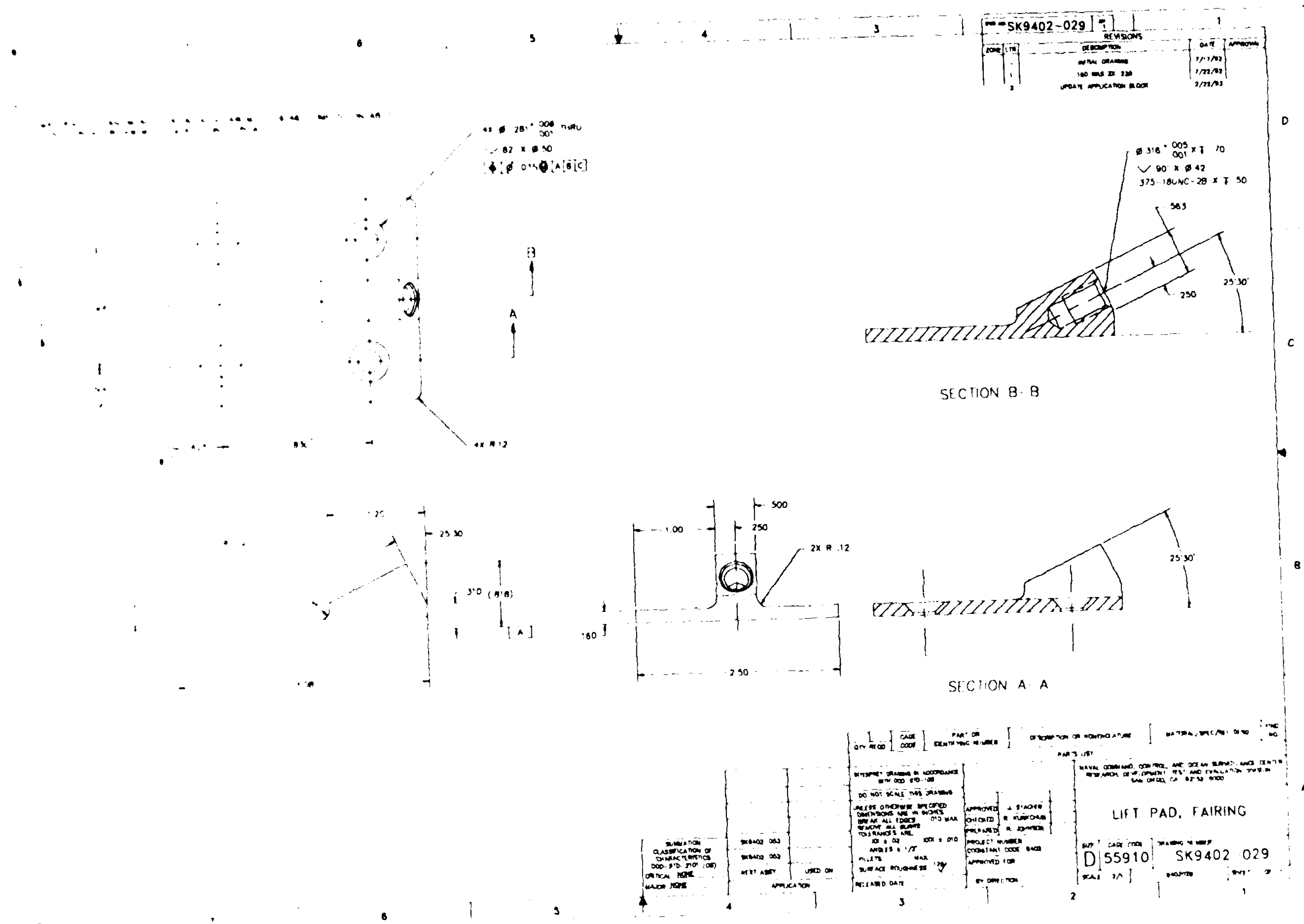

Figure A-8. Fairing lift pad.

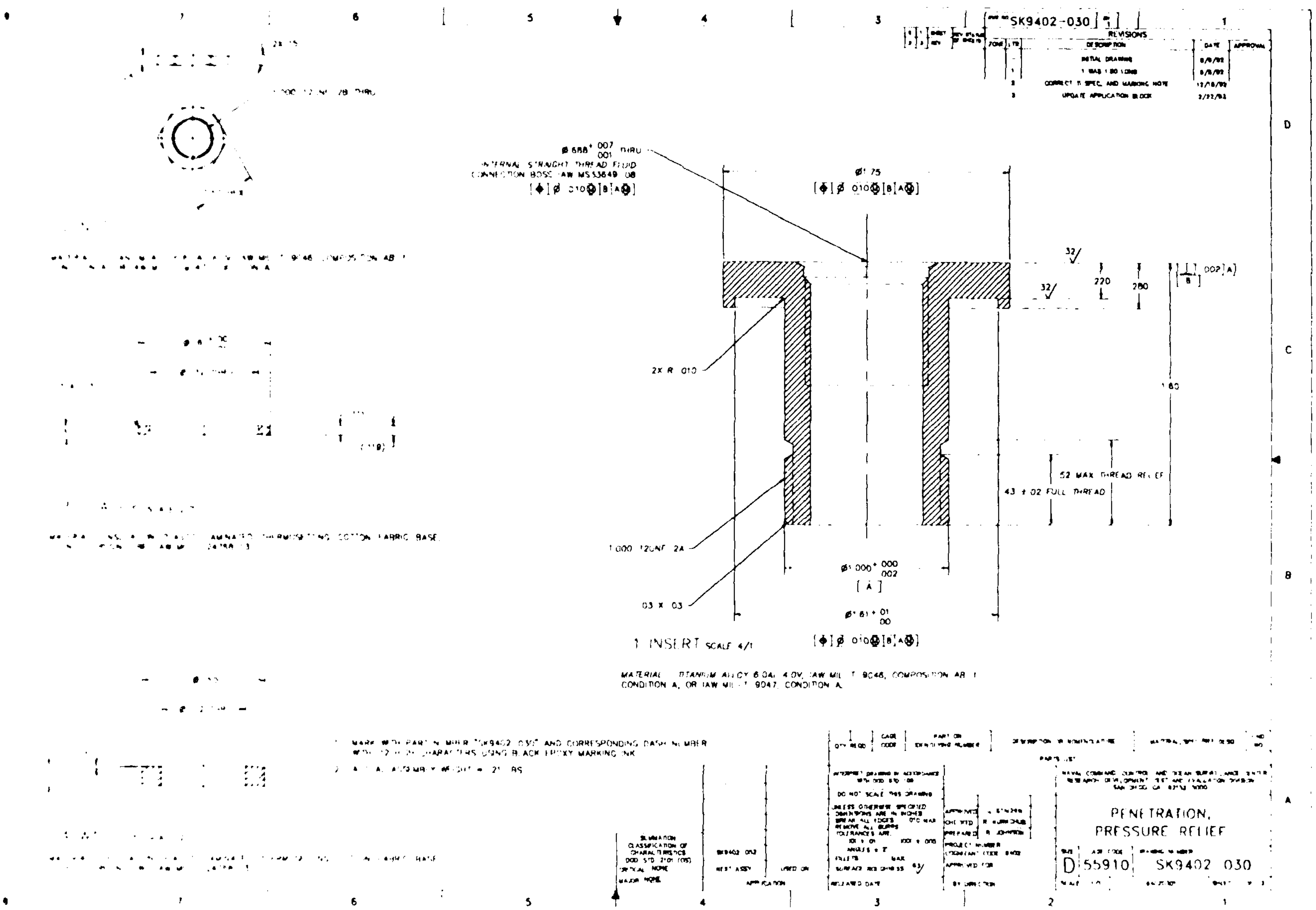

Figure A-9. Pressure relief penetration, Sheet 1.

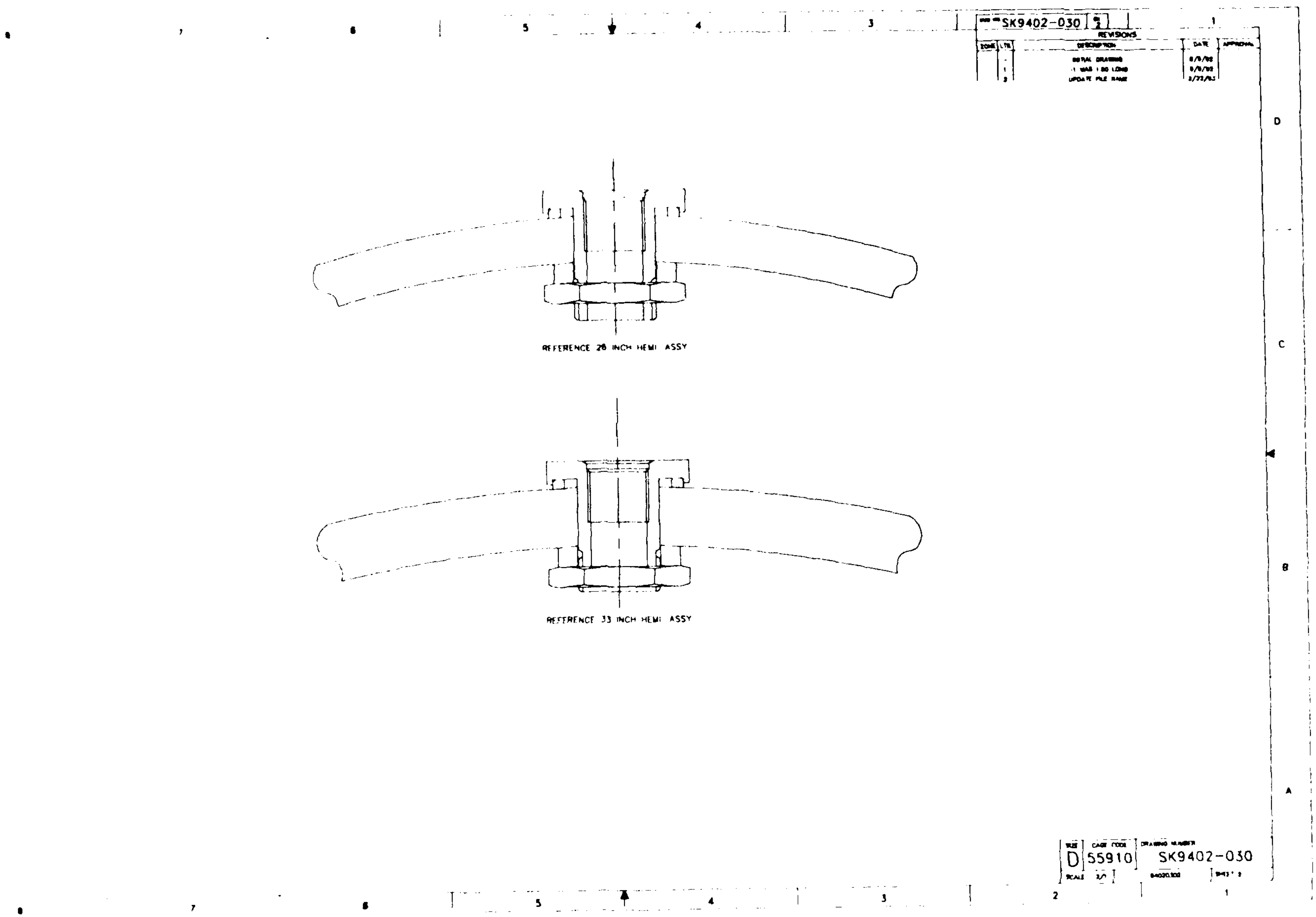

Figure A-9. Pressure relief penetration, Sheet 2.

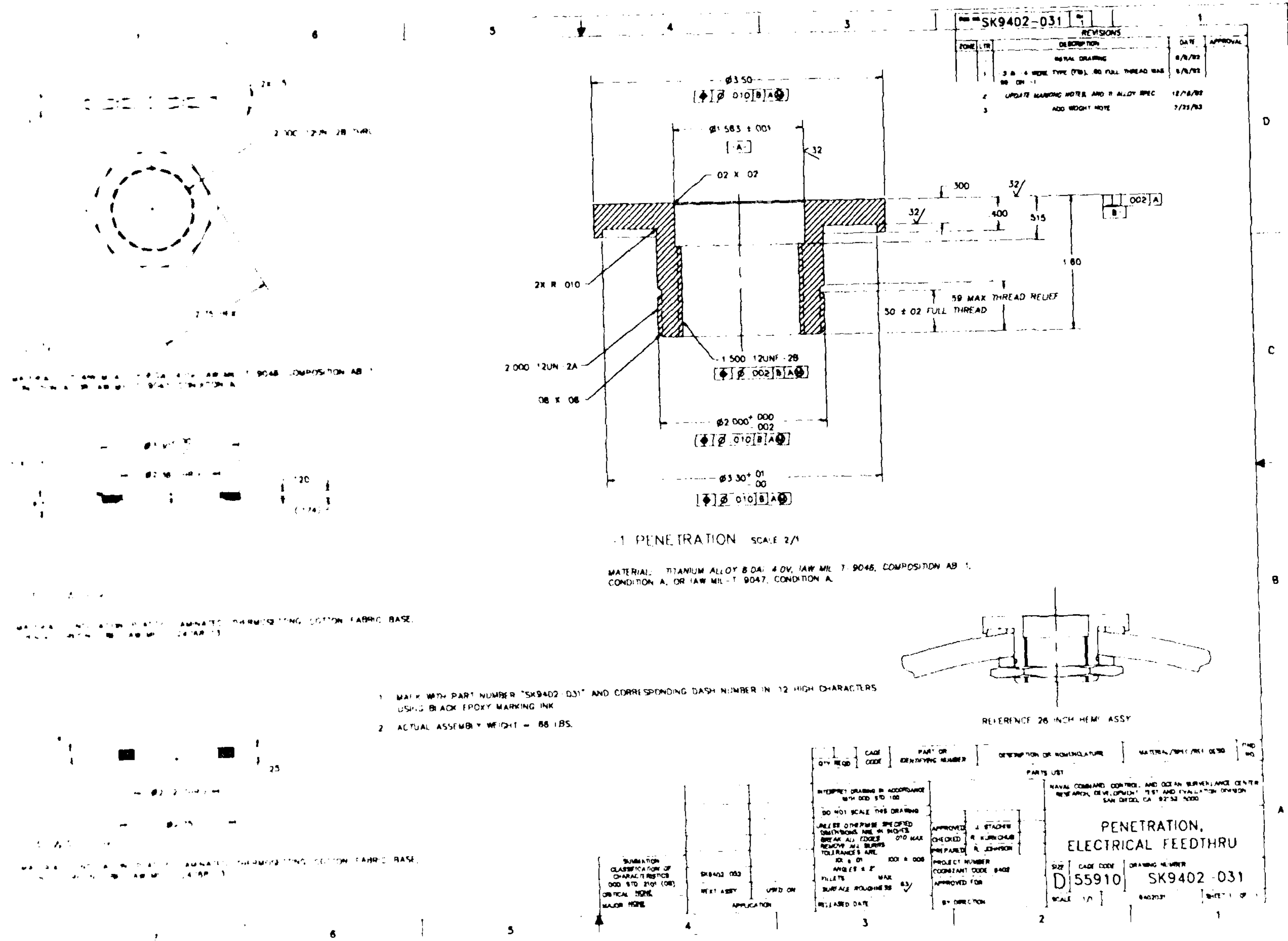

Figure A-10. Electrical feedthrough penetration.

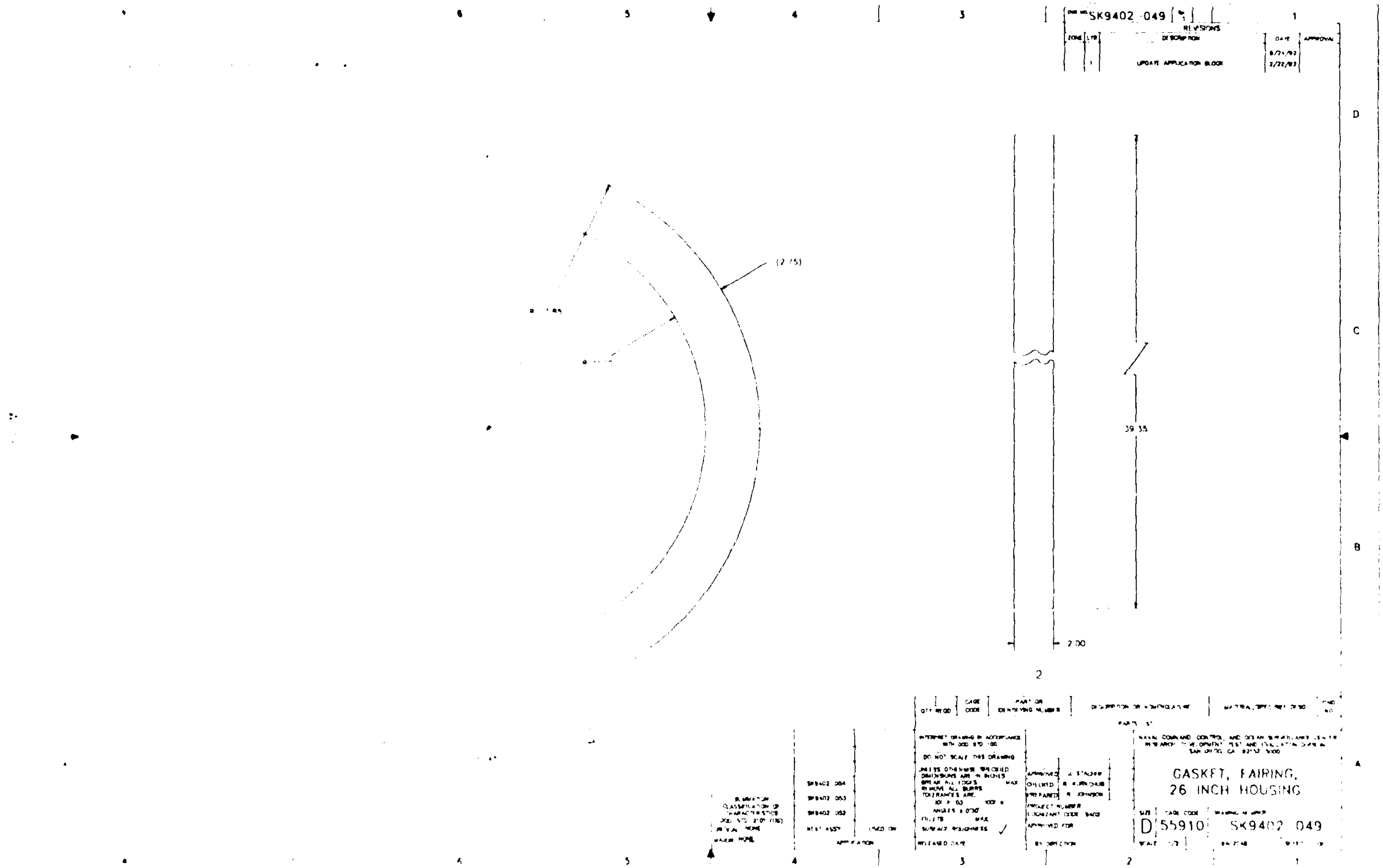

Figure A-11   26 inch housing fairing gasket.

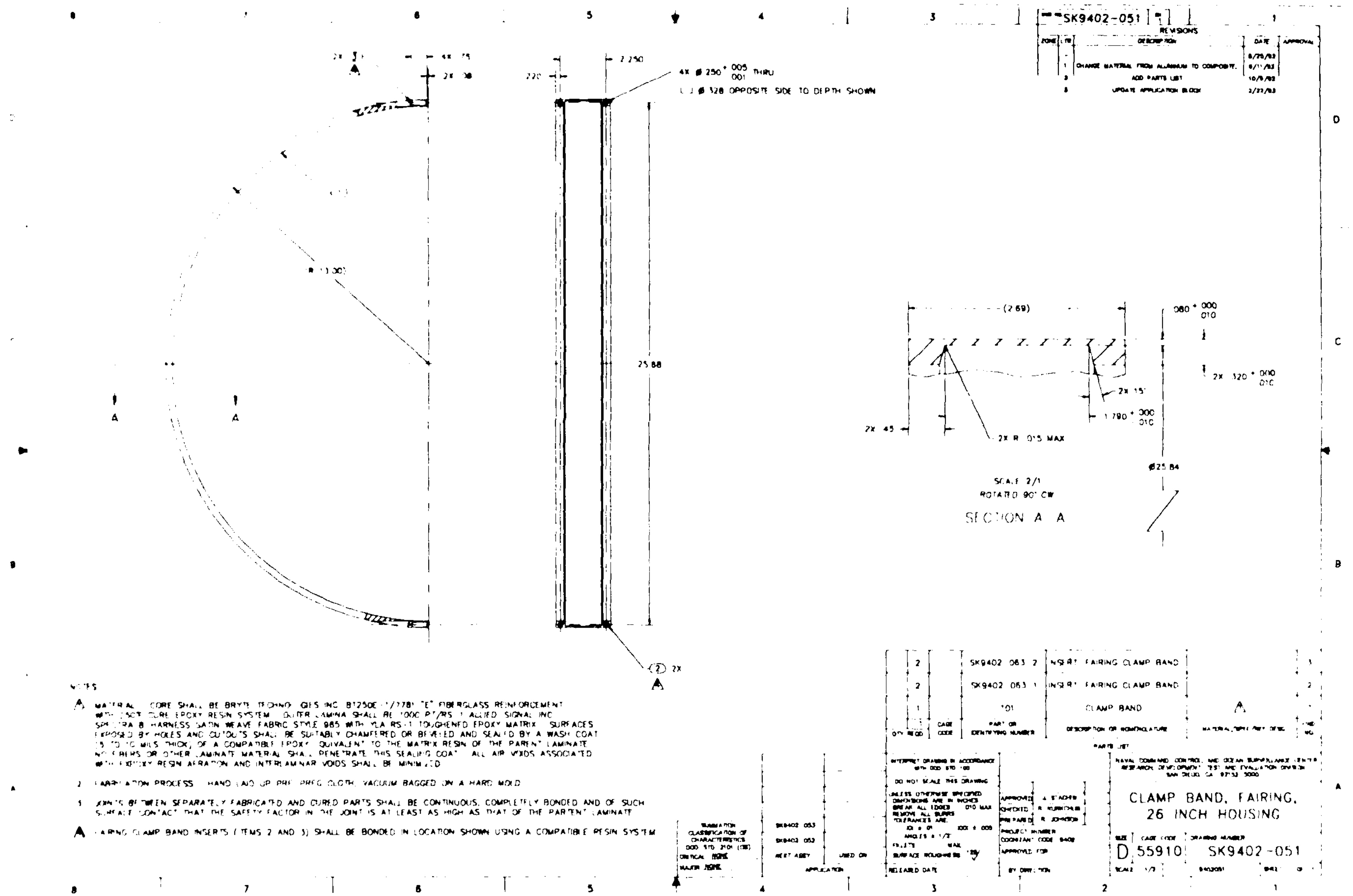

Figure A-12. 26-inch housing fairing clamp band.

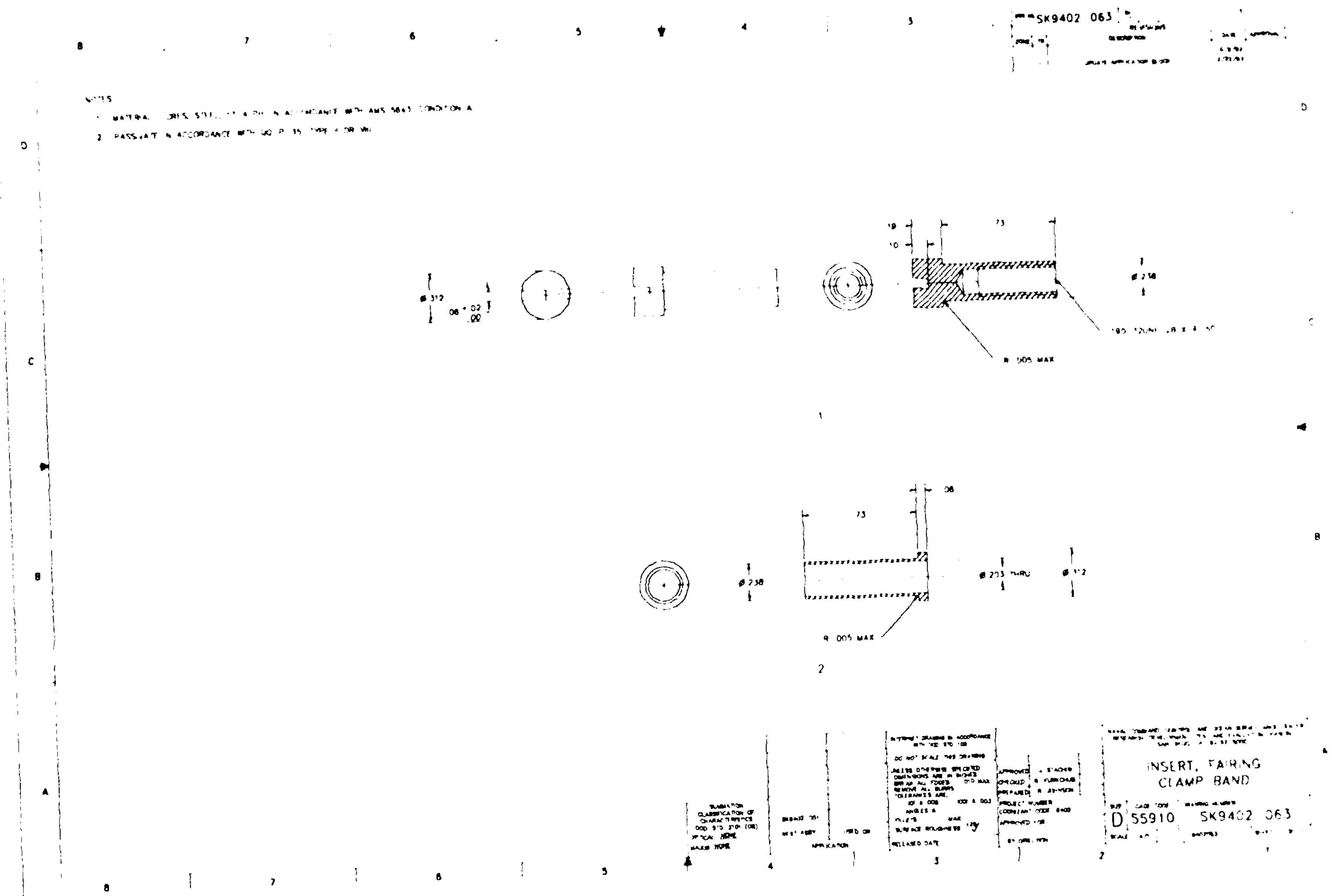

Figure A-13. Fairing clamp band insert.

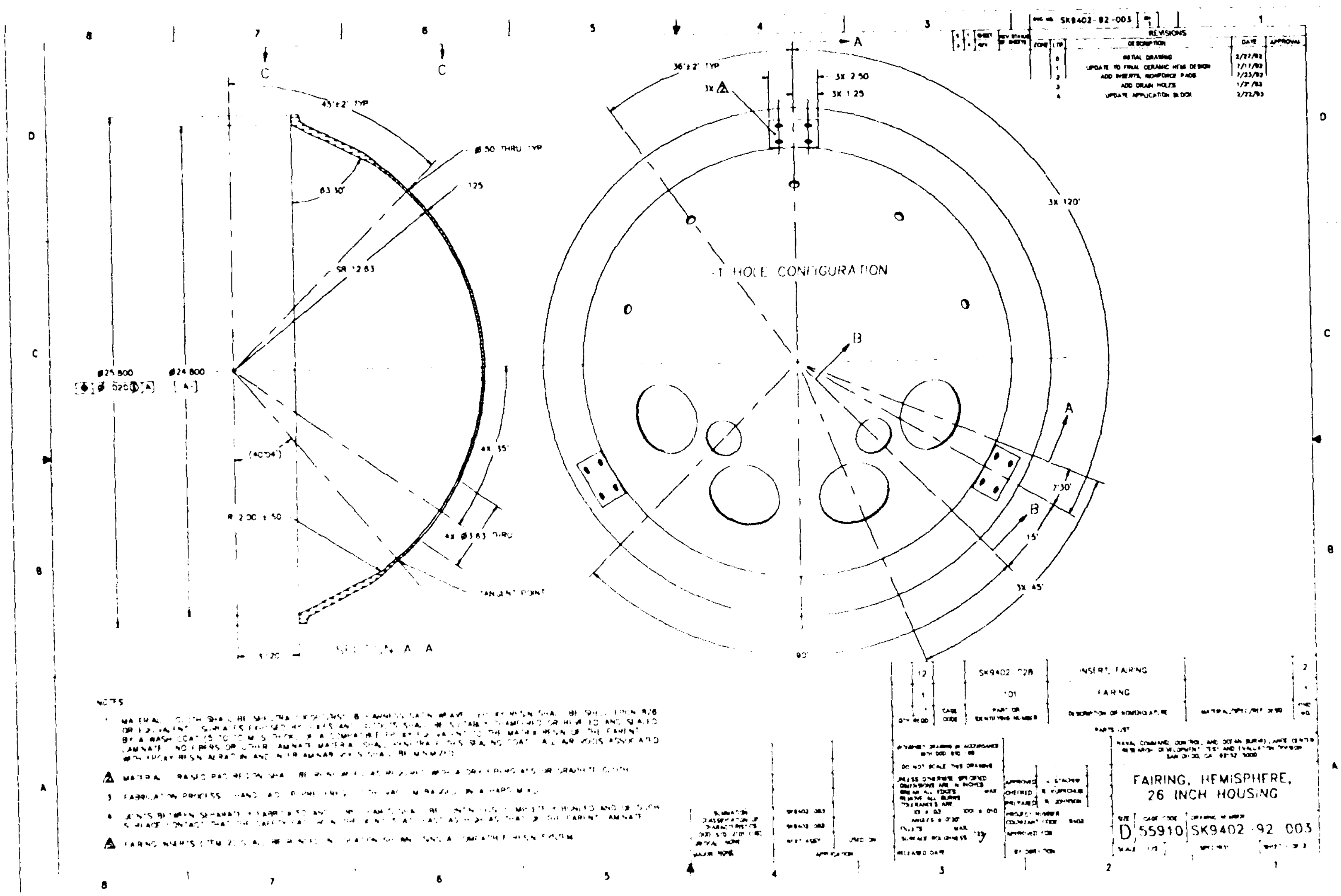

Figure A-14. 26-inch hemisphere fairing, Sheet 1.

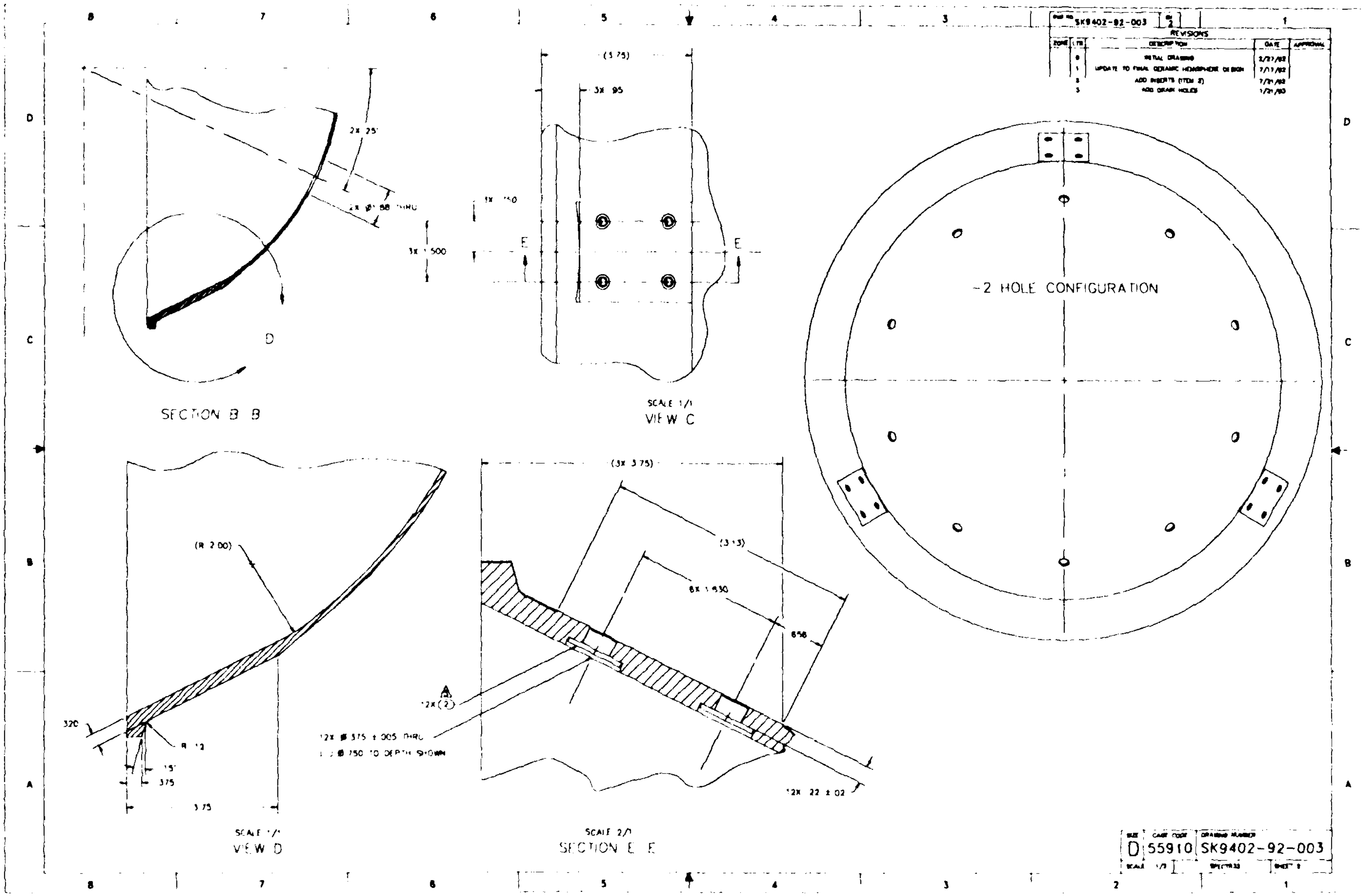

Figure A-14. 26-inch hemisphere fairing, Sheet 2.

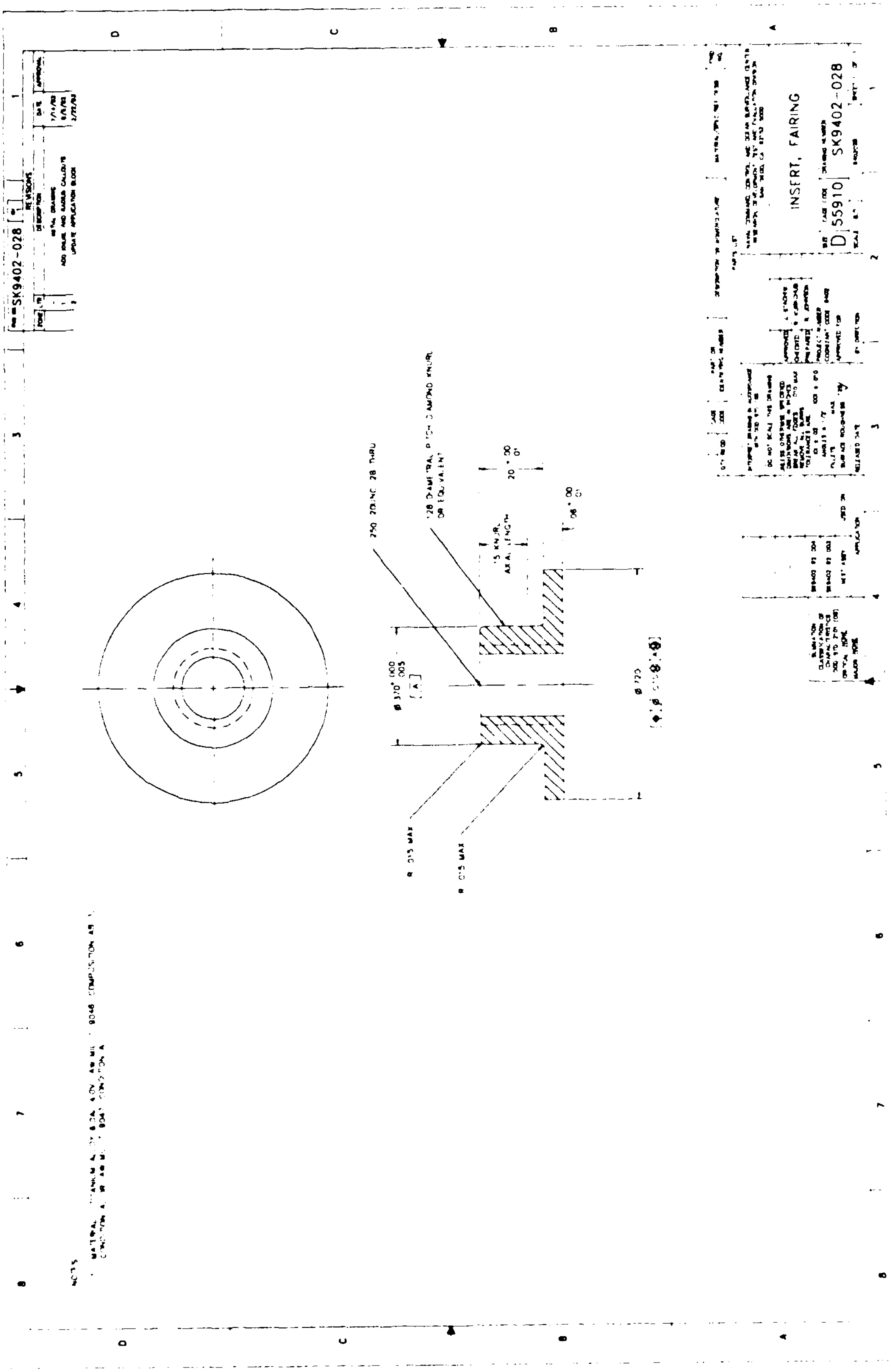

Figure A-15. Fairing insert.

SK9402-053

REVISIONS

ZONE	LTR	DESCRIPTION	DATE	APPROVAL
			6/27/82	
	1	UPDATE APPLICATION BLOCK	3/23/83	

QTY REQD	CAGE CODE	PART OR IDENTIFYING NUMBER	DESCRIPTION OR NOMENCLATURE	MATERIAL/SPECIFICATION	FIND NO.
					15
					14
AR			EPOXY		13
AR			ADHESIVE		12
4		MS16996-15	SCREW, CAP, SOCKET HD, HEX, CRES, .190-32UNF-3A X 1.25 L		11
12		MS51958-77	SCREW, FLT CSK HD 82°, CRES, .250-20UNC-2A X .375 L		10
1	55910	SK9402-82-003-01	FAIRING, HEM., 26 INCH HOUS.		9
2	55910	SK9402-051	CLAMP, FAIRING, 26 INCH HOUS.		8
1	55910	SK9402-049-1	GASKET, FAIRING, 26 INCH HOUS.		7
					6
2	55910	SK9402-028	LIFT PAD, FAIRING		5
1	55910	SK9402-027	LIFT LUG, FAIRING		4
1	55910	0129903	GASKET, 26 INCH HOUSING		3
1	55910	SK9402-001	HEM. ENDCAP, 26 INCH HOUSING		2
1	55910	0127848	CERAMIC HEM., TYPE 4, 26 INCH HOUS.		1

PARTS LIST

INTERPRET DRAWING IN ACCORDANCE WITH DOD-STD-100

DO NOT SCALE THIS DRAWING

APPROVED: J. STACHIW
CHECKED: R. KURKCHUB
PREPARED: R. JOHNSON

NAVAL COMMAND, CONTROL AND OCEAN SURVEILLANCE CENTER
RESEARCH, DEVELOPMENT, TEST AND EVALUATION DIVISION
SAN DIEGO, CA 92152-5000

ASSY., AFT HEAD,
26 INCH HOUSING

SIZE	CAGE CODE	DRAWING NUMBER
D	55910	SK9402-053

Figure A-16. 26-inch housing aft head assembly, Sheet 1.

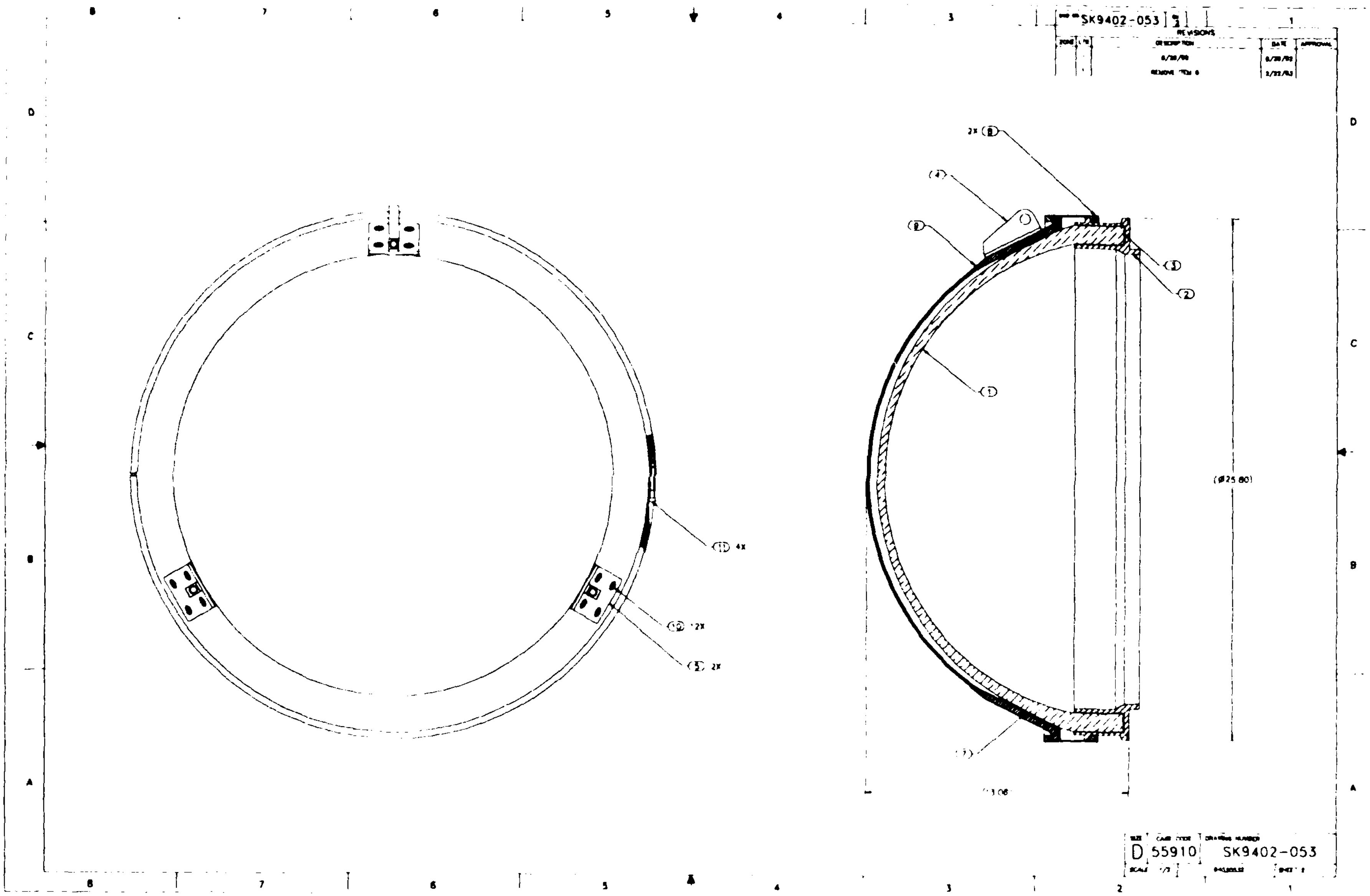

Figure A-16. 26-inch housing aft head assembly, Sheet 2

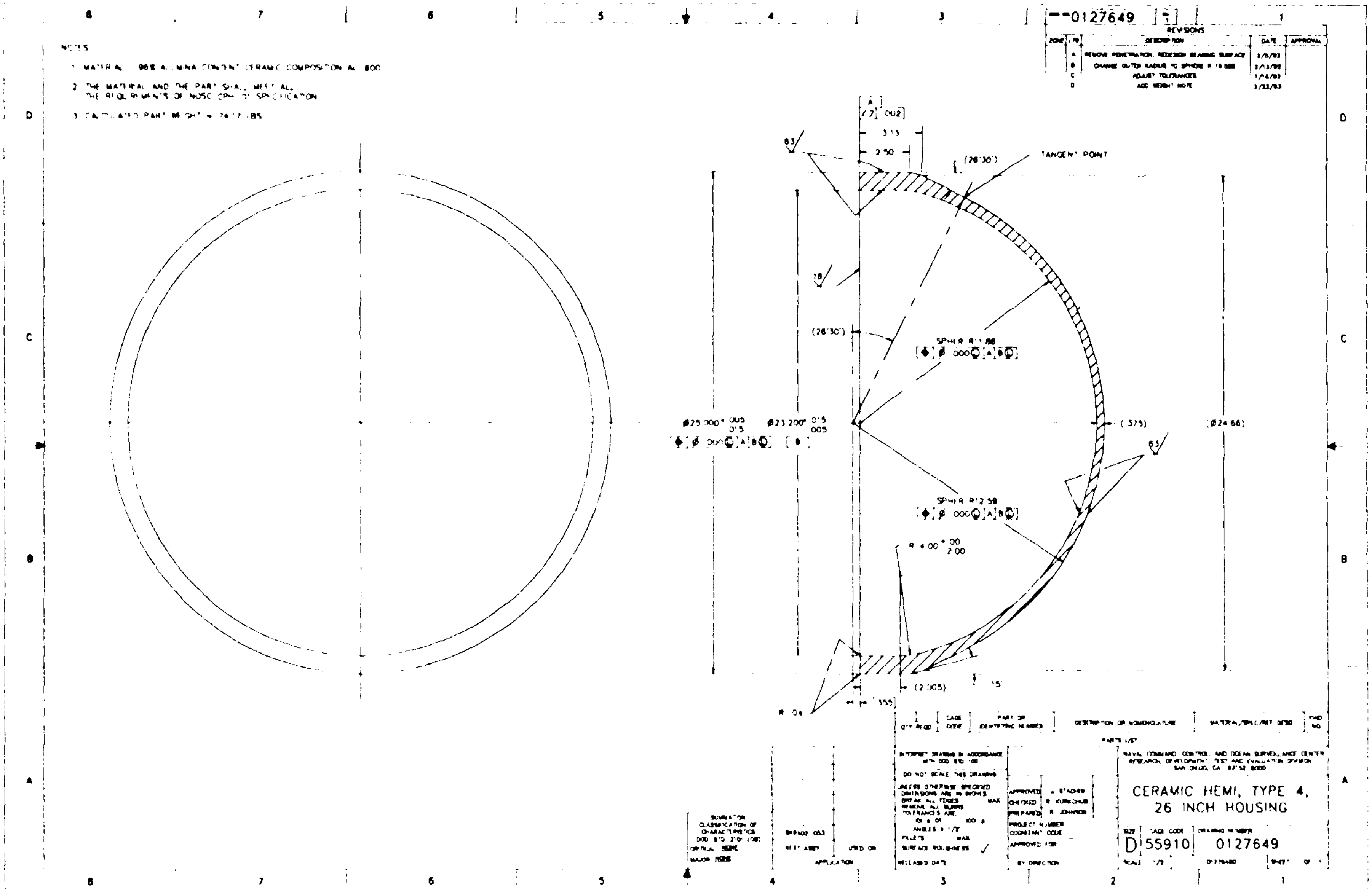

Figure A-17. 26-inch housing Type 4 ceramic hemisphere.

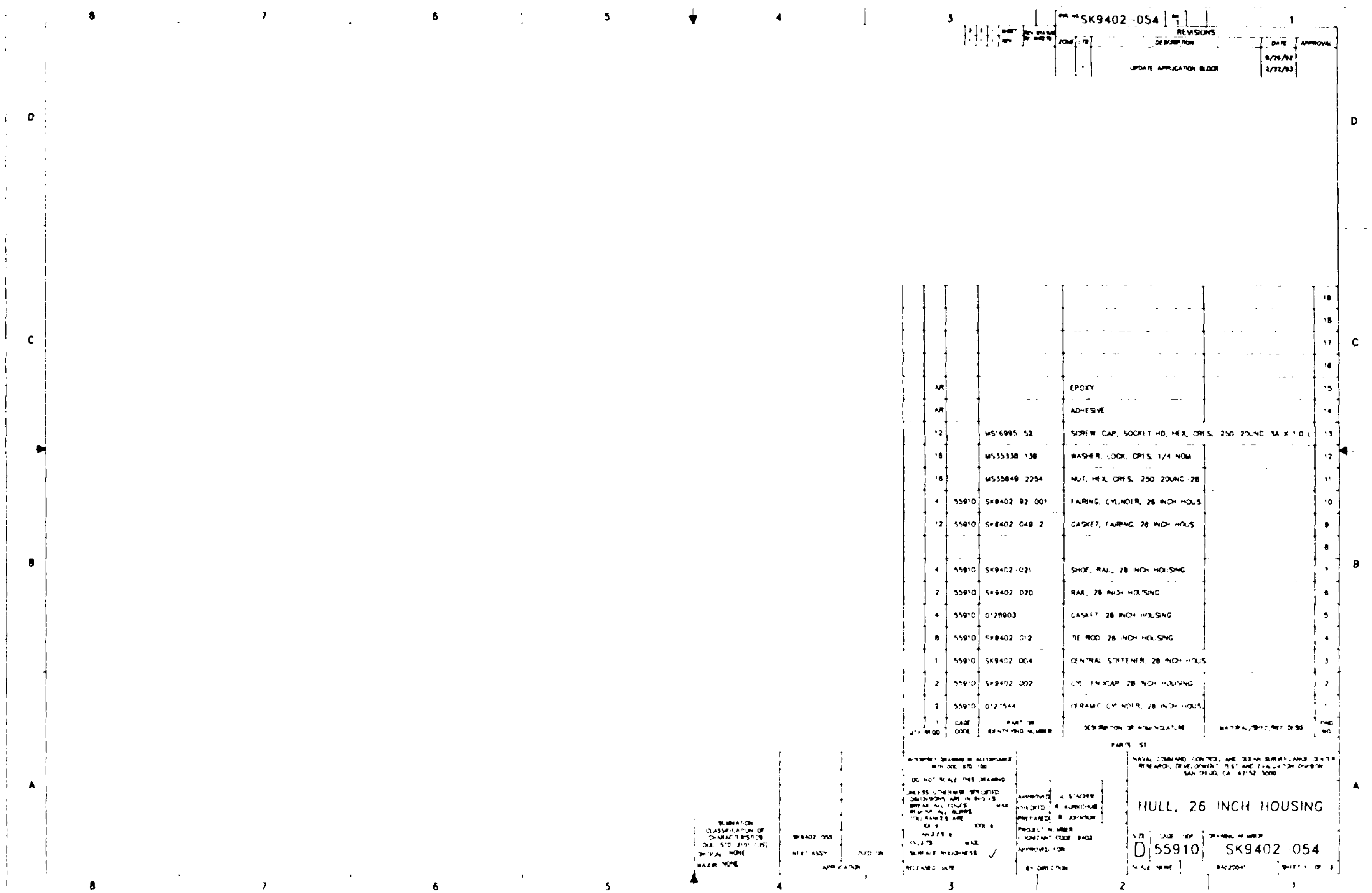

Figure A-18. 26-inch housing hull, Sheet 1.

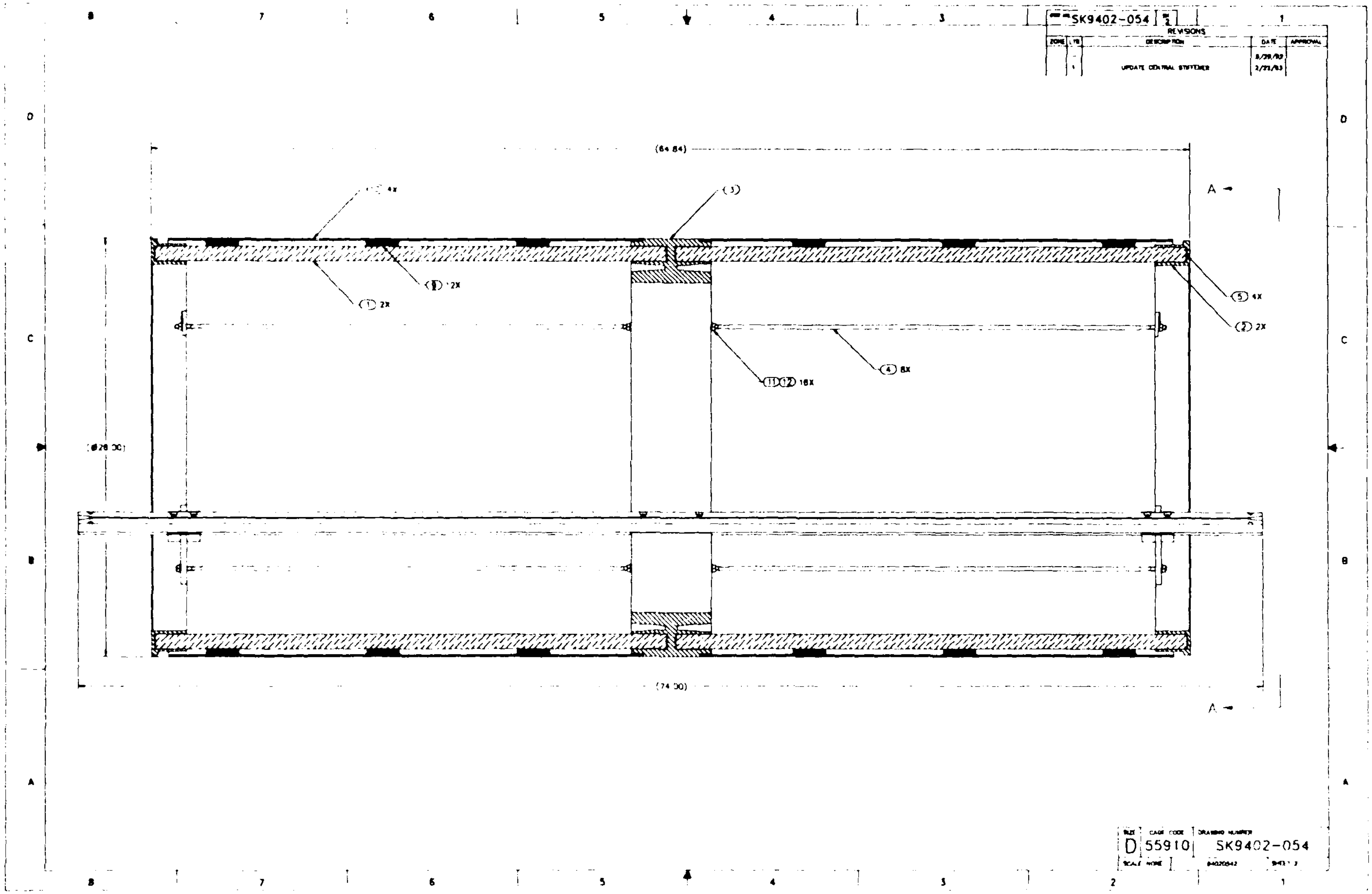

Figure A-18. 26-inch housing hull, Sheet 2.

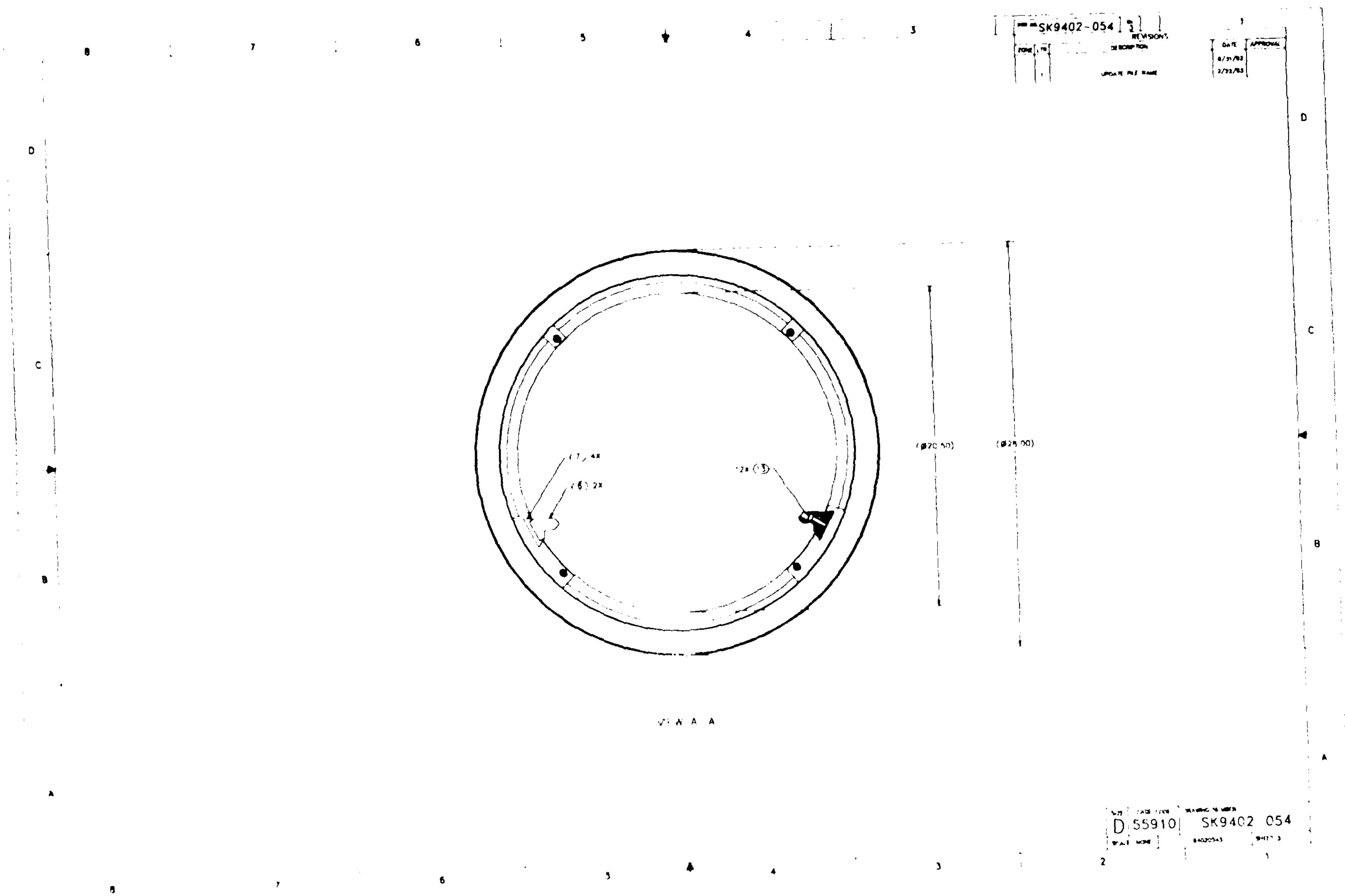

Figure A-18. 26-inch housing hull, Sheet 3.

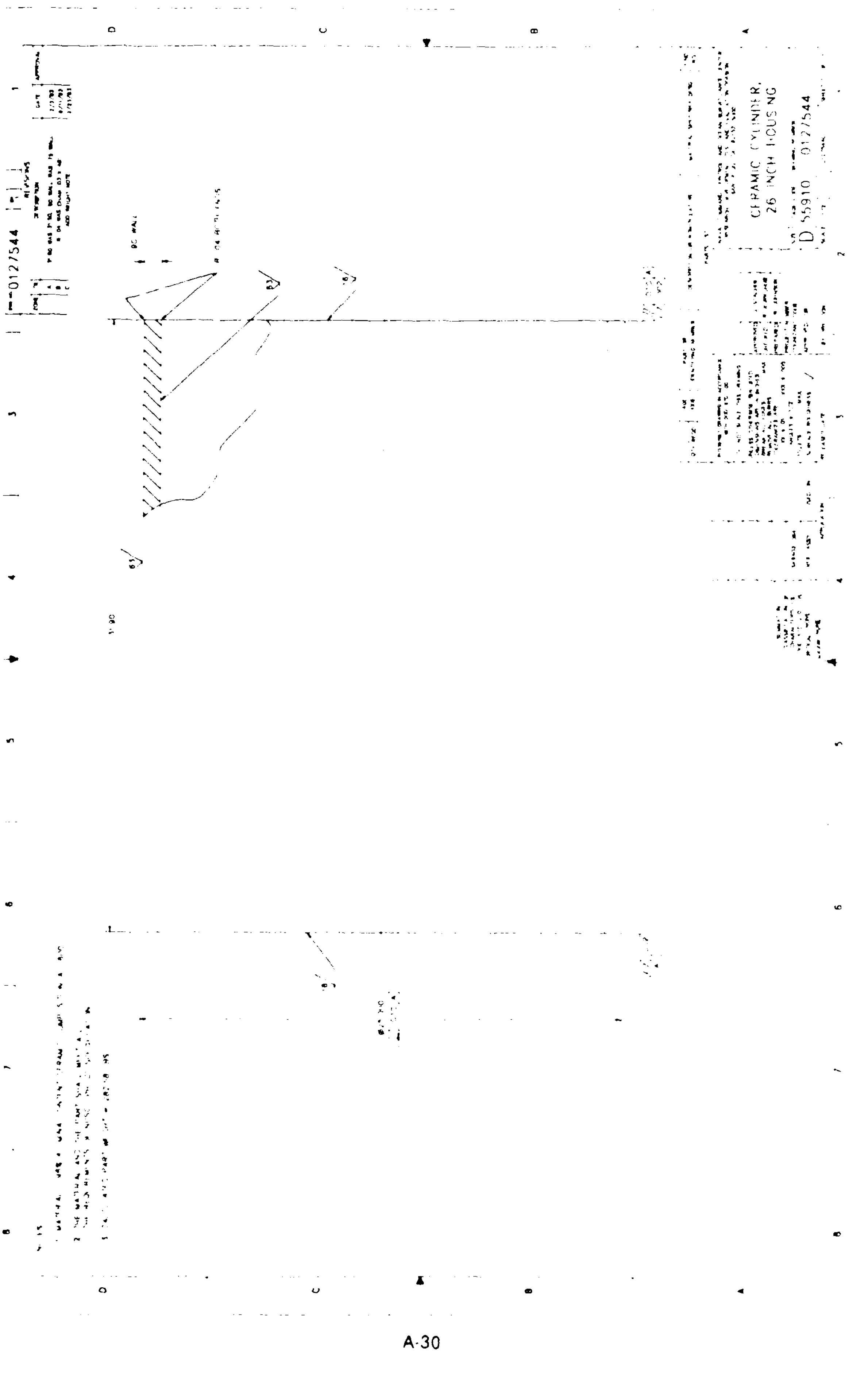

Figure A-19 26 inch housing ceramic cylinder.

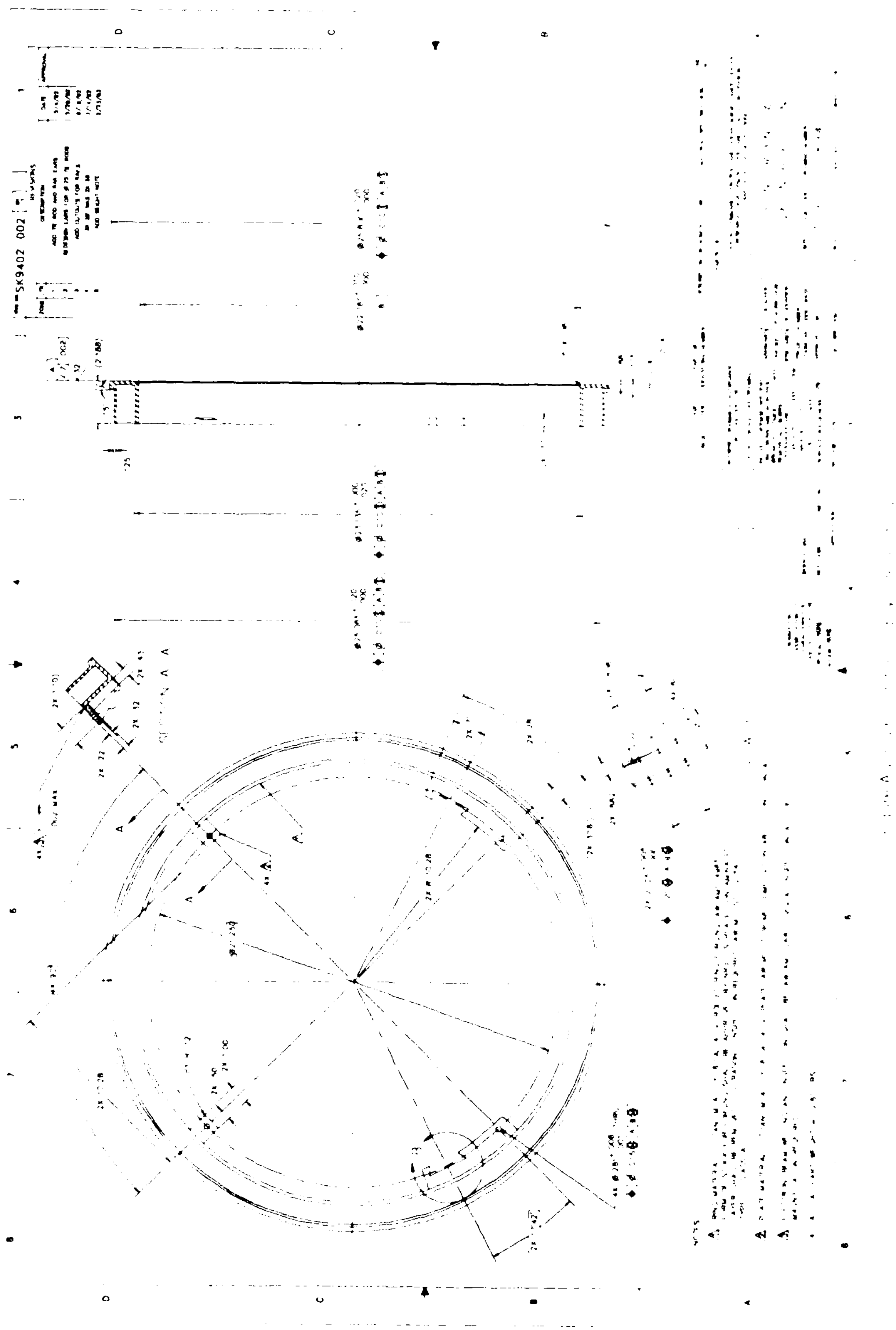
SK9402 002

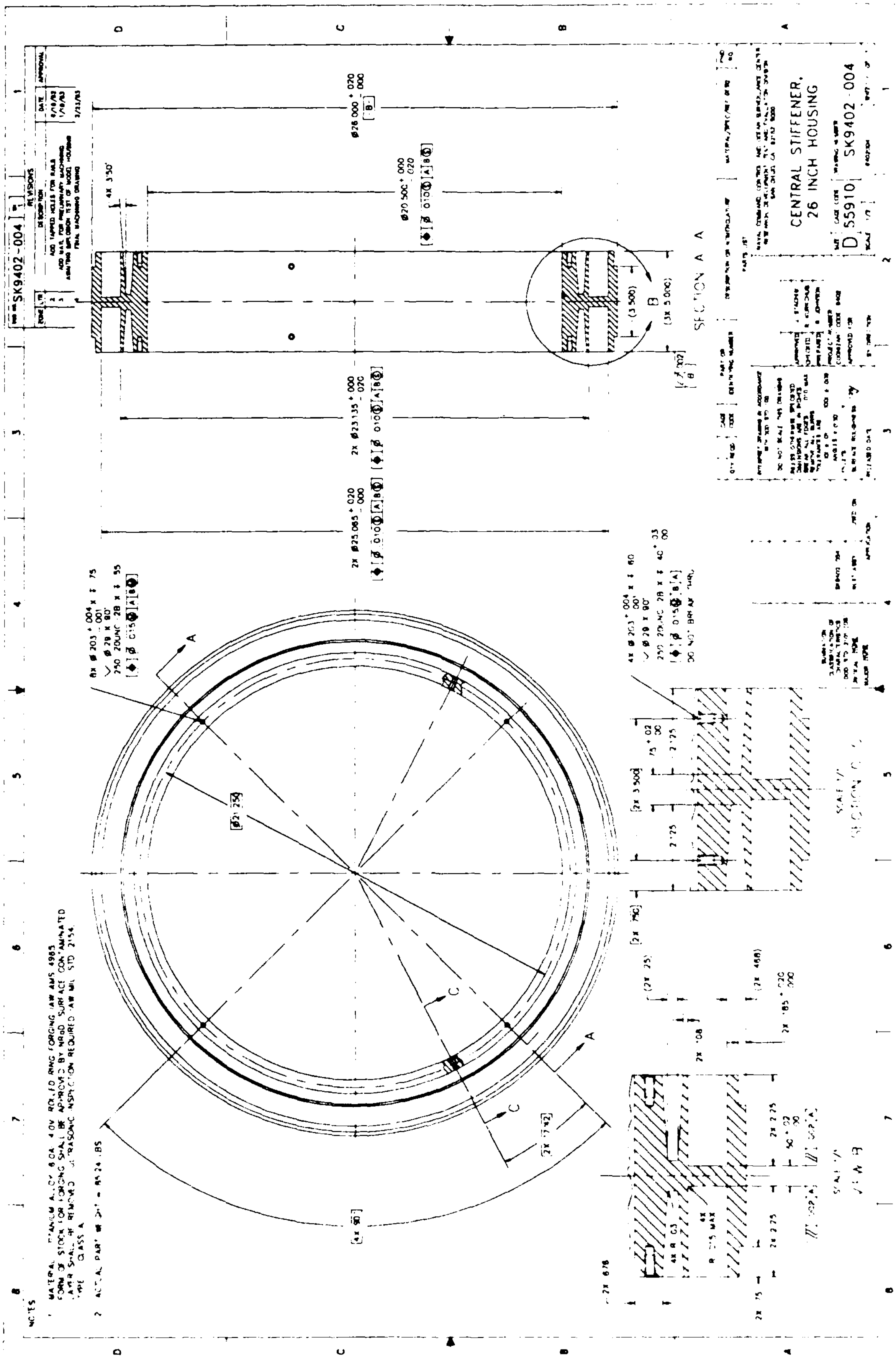

Figure A-21. 26-inch housing central stiffener.

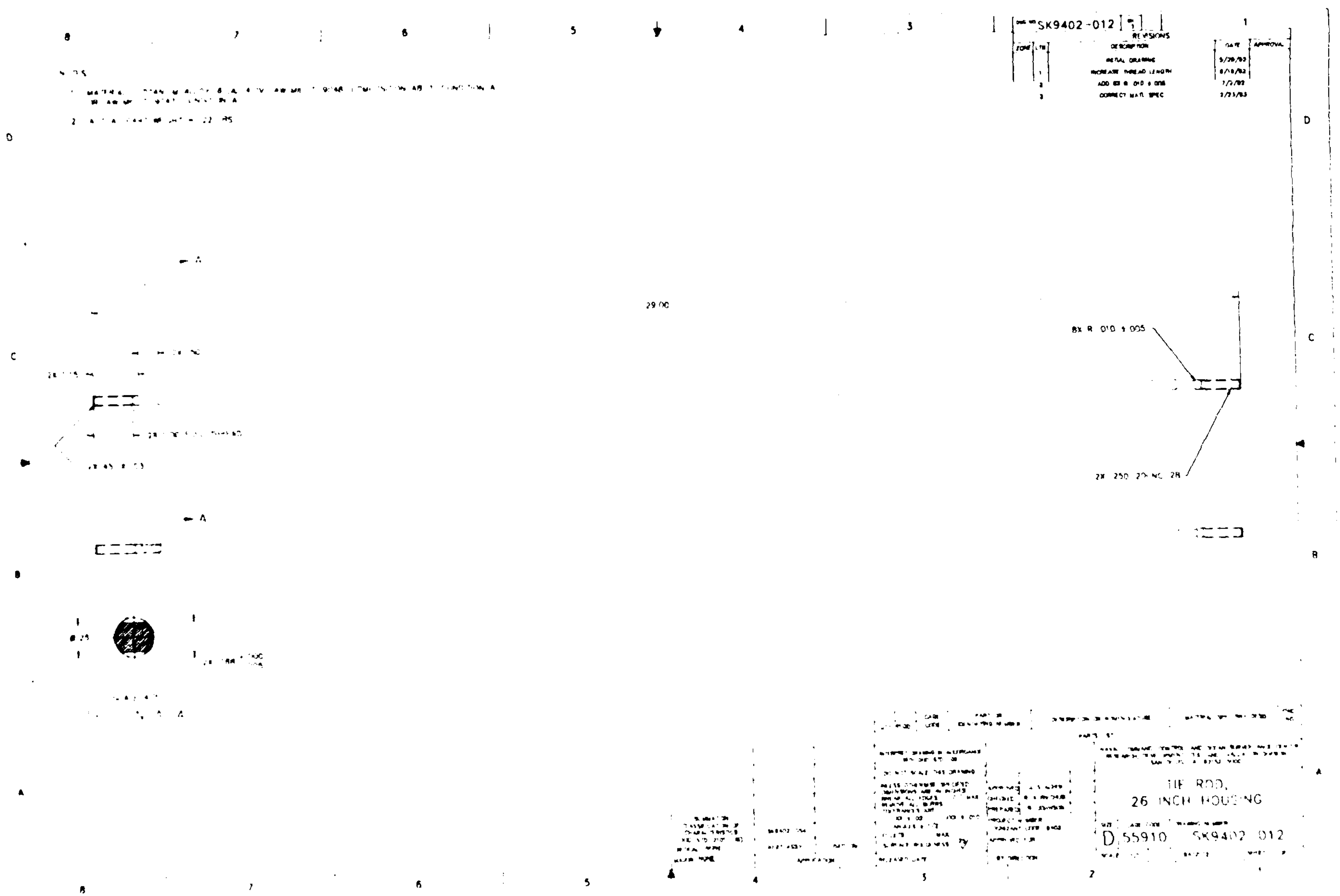

Figure A-22. 26-inch housing tie rod.

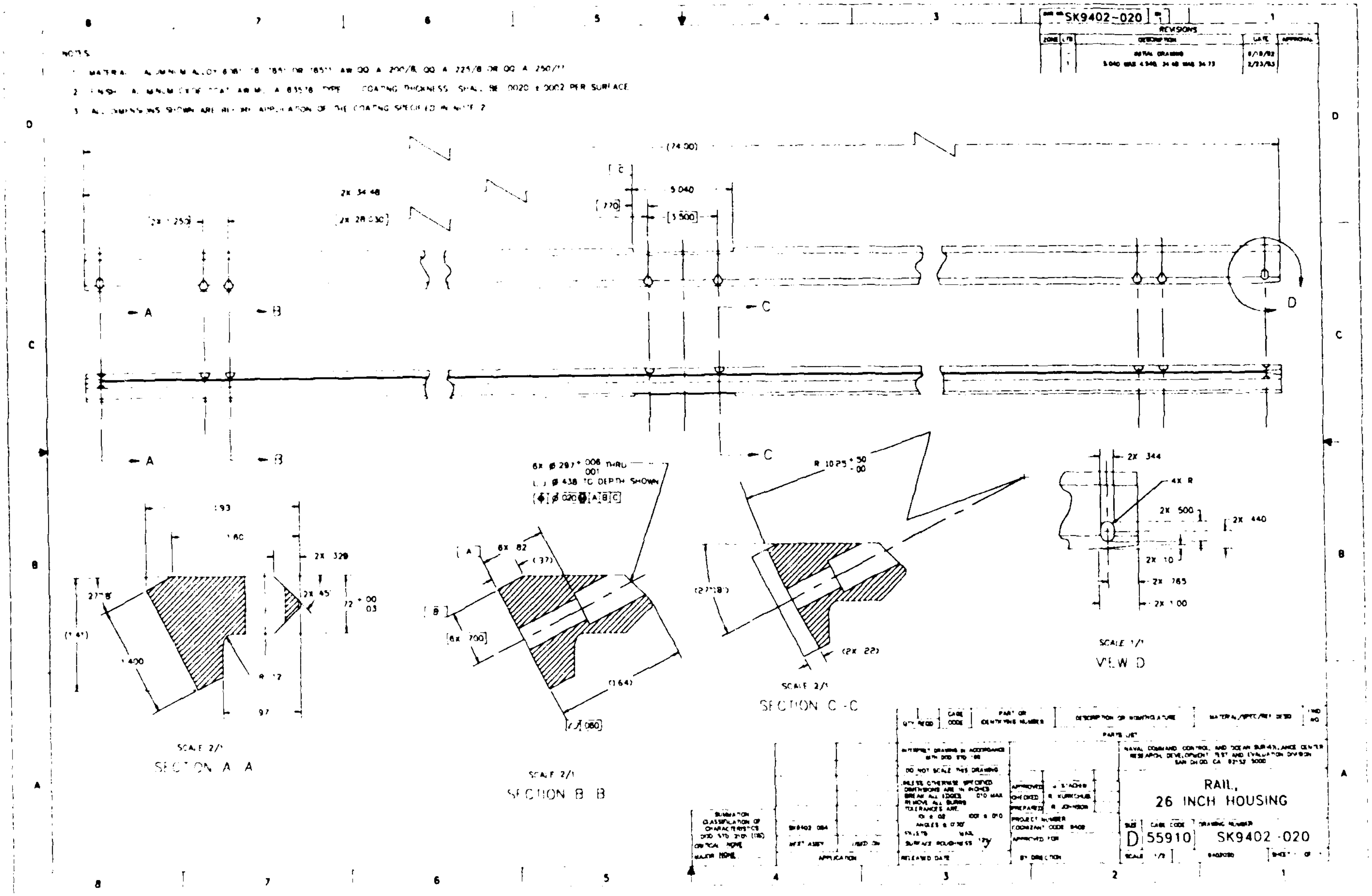

Figure A-23. 26-inch housing rail.

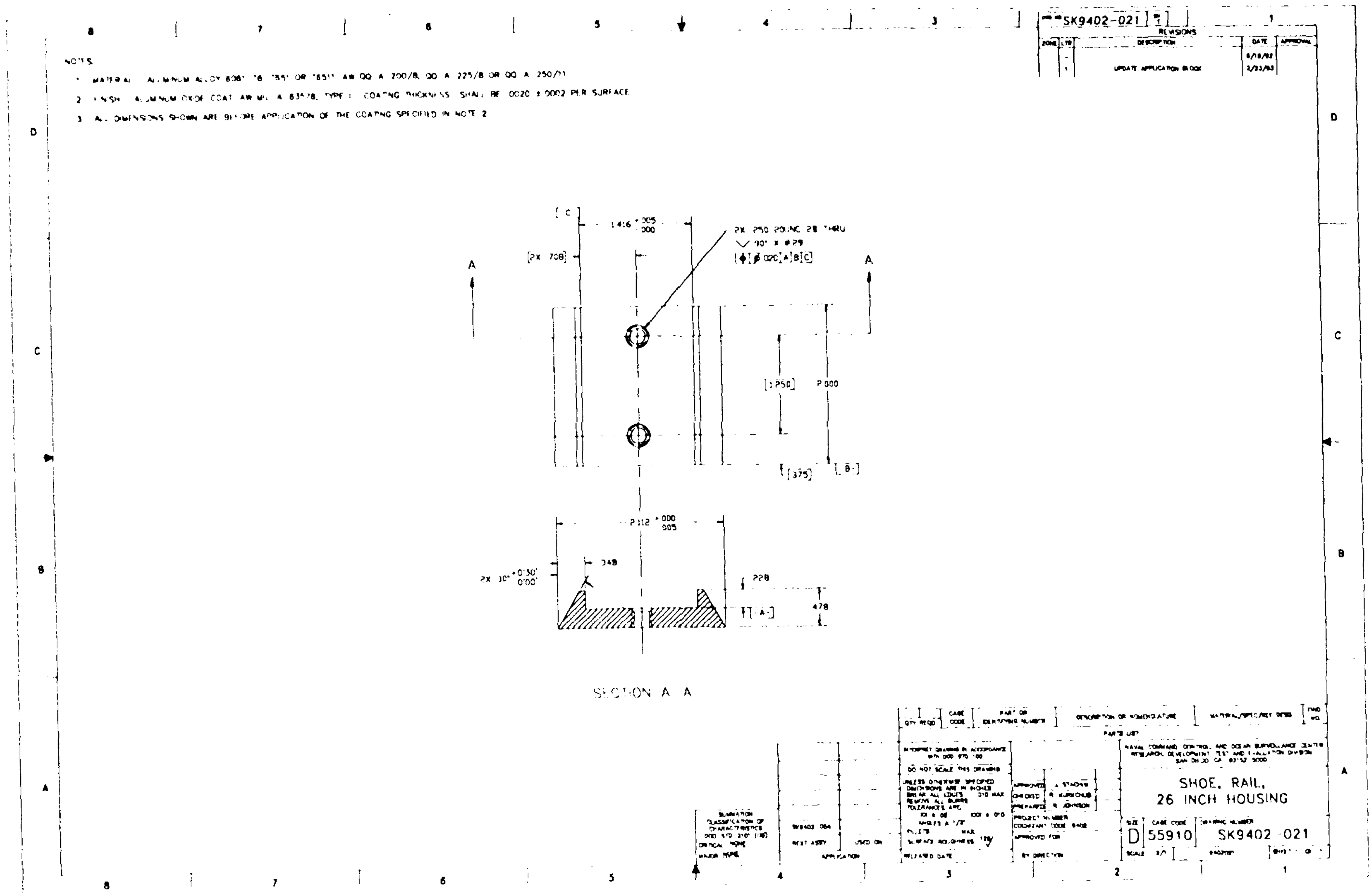

Figure A-24. 26-inch housing rail shoe.

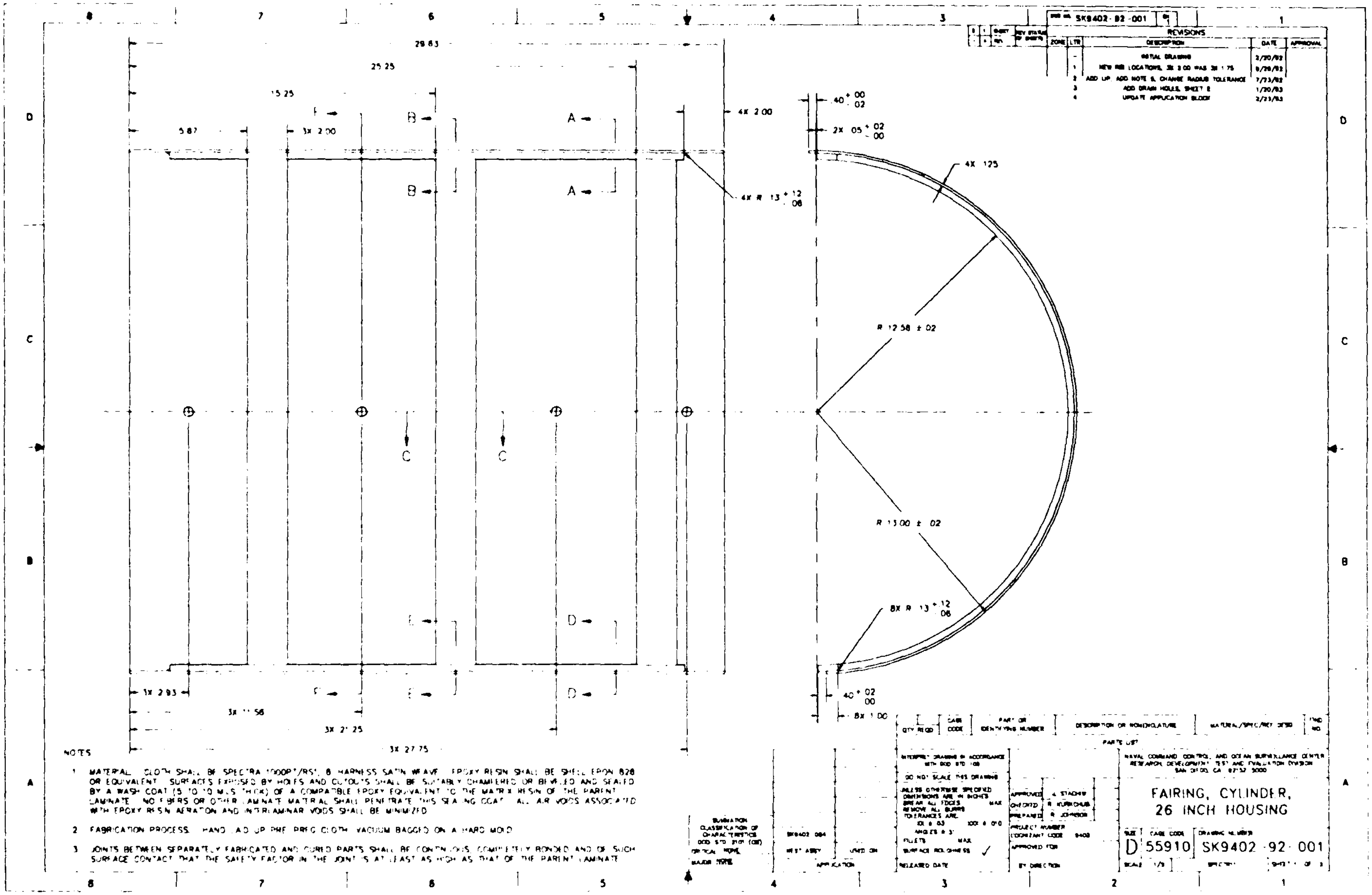

Figure A-25. 26-inch housing cylinder fairing, Sheet 1.

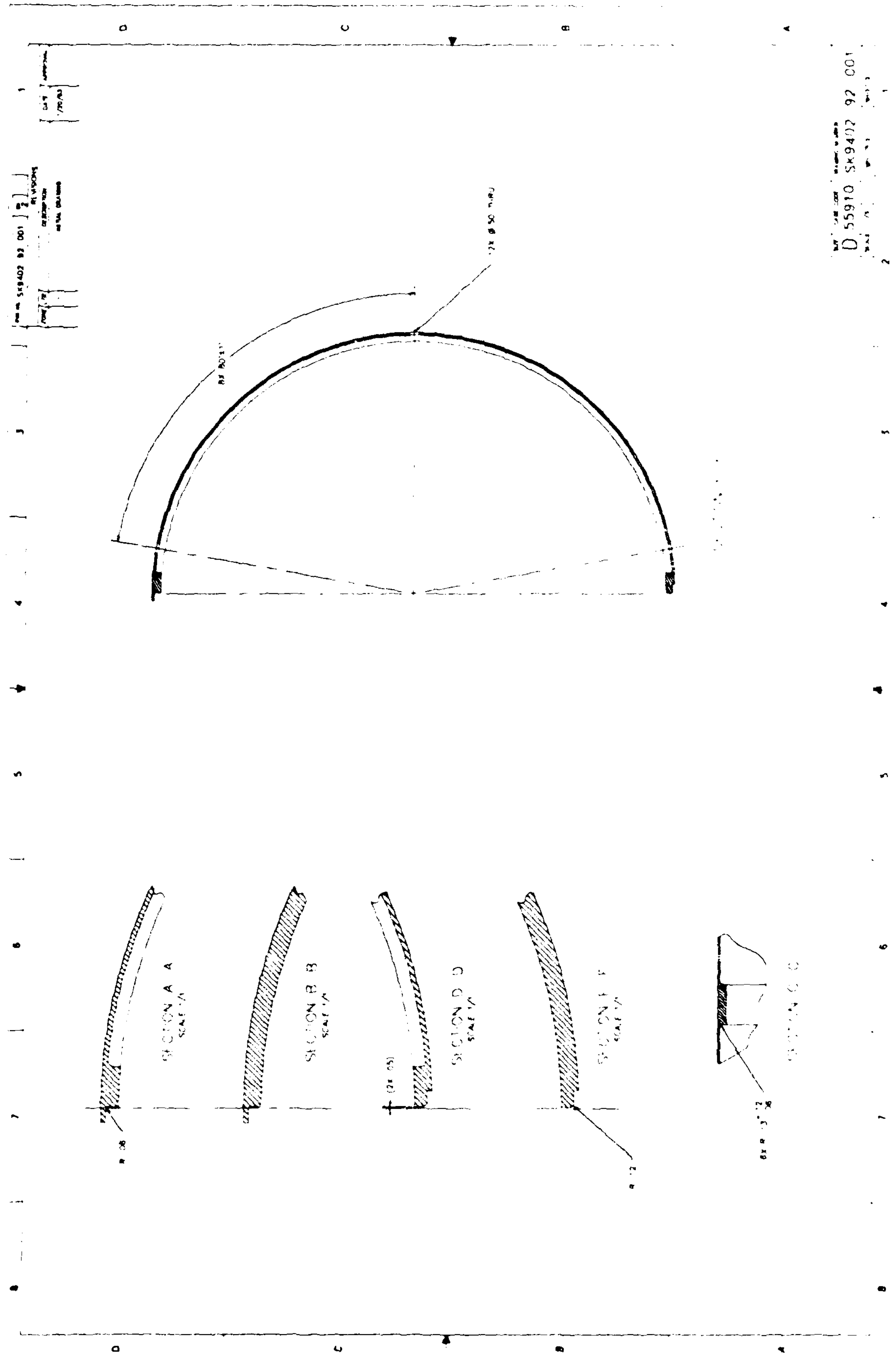

Figure A-25. 26-inch housing cylinder fairing, Sheet 2

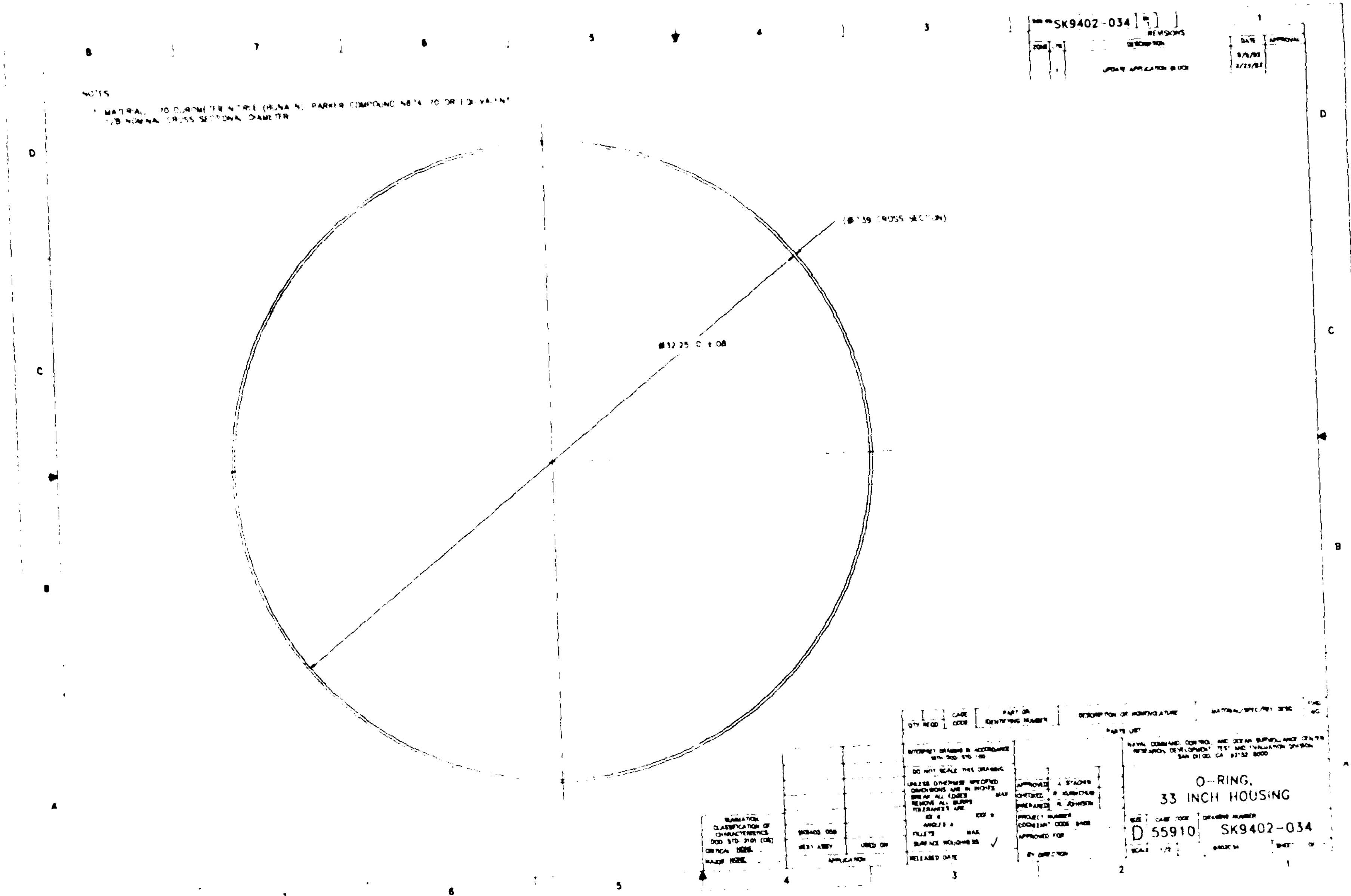

Figure A-26. 33-inch housing O-ring.

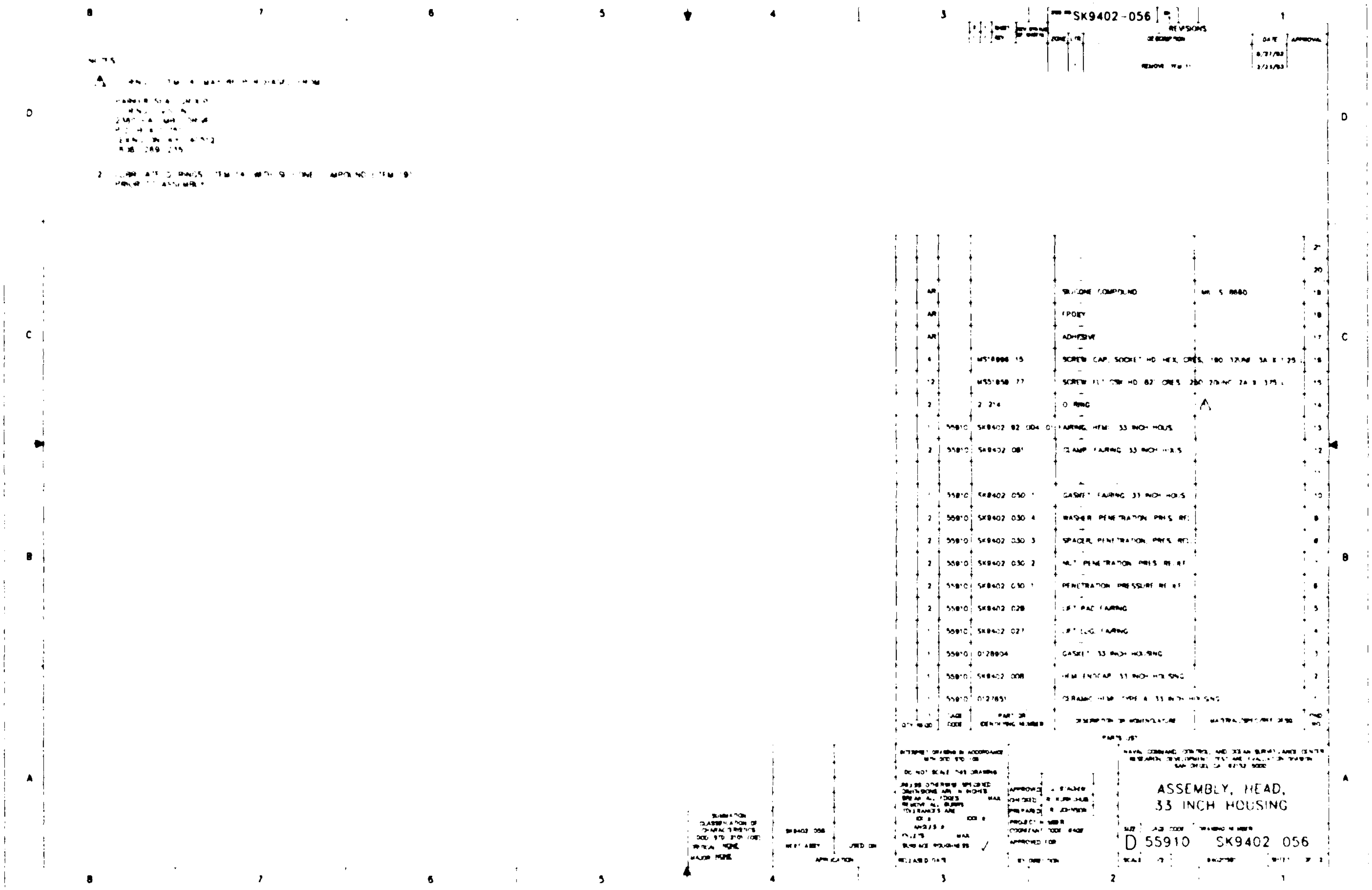

Figure A-27. 33-inch housing assembly, Sheet 1.

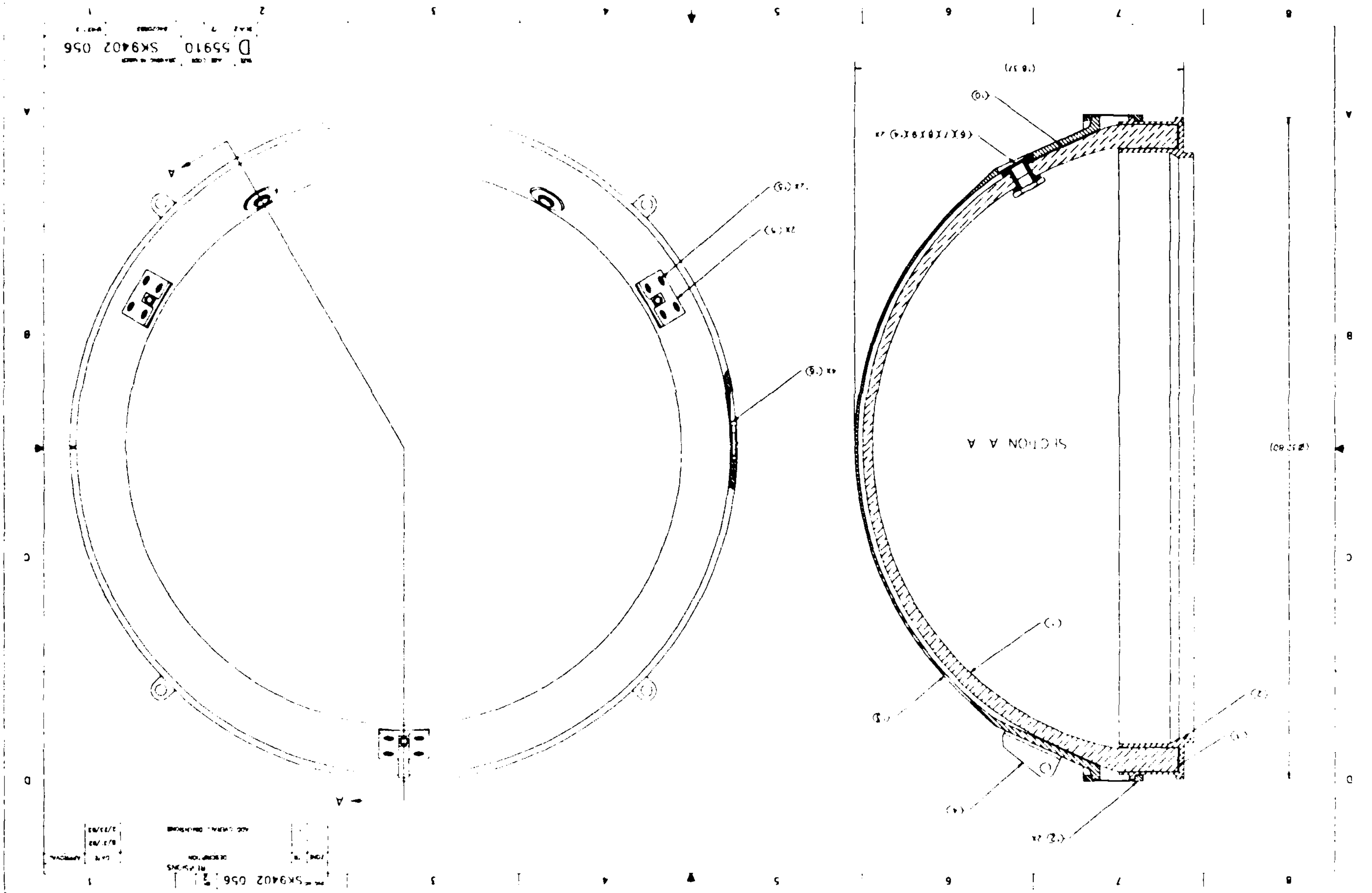

Figure A-27. 33-inch housing assembly, Sheet 2.

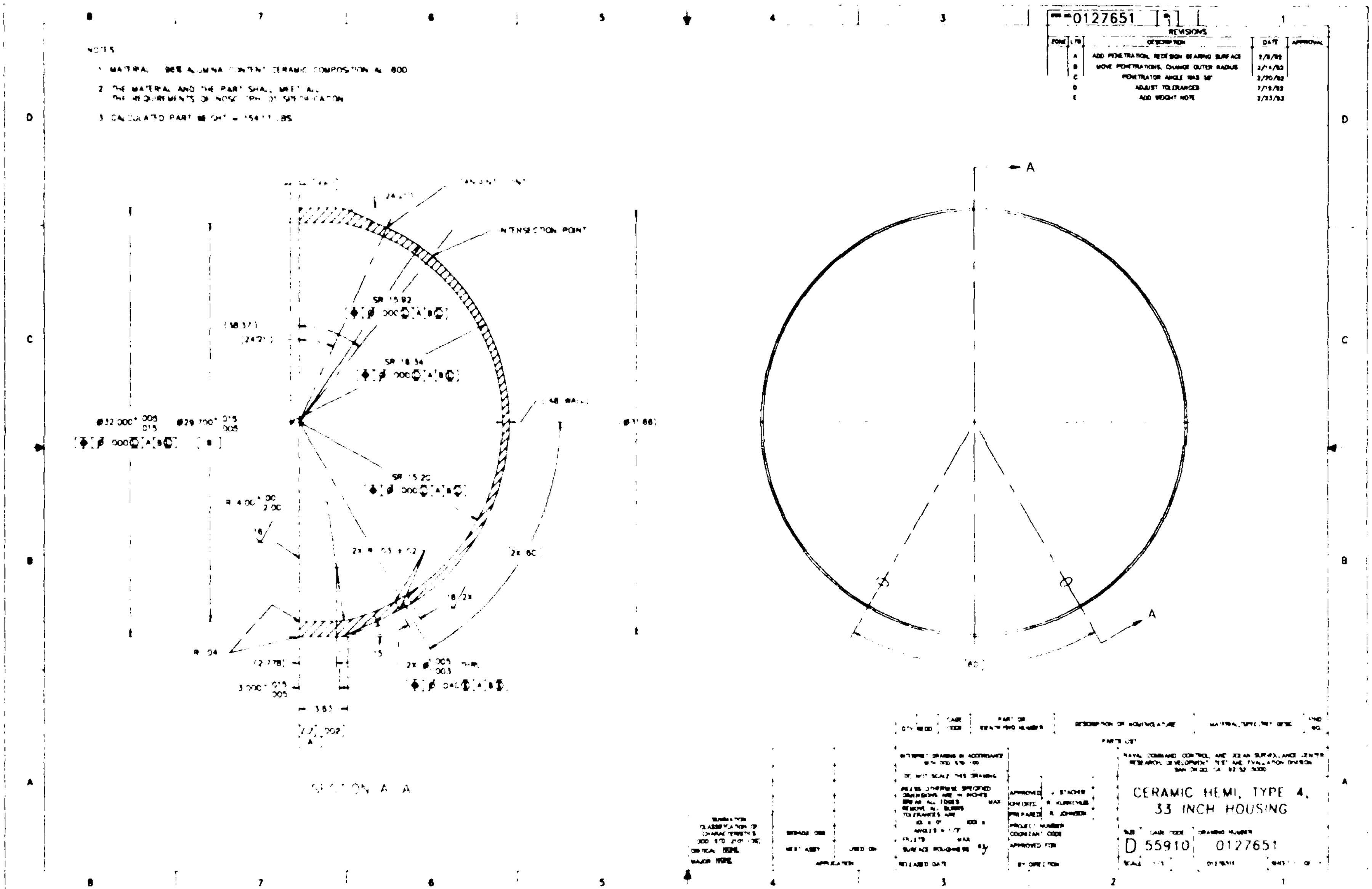

Figure A-28. 33-inch housing Type 4 ceramic hemisphere

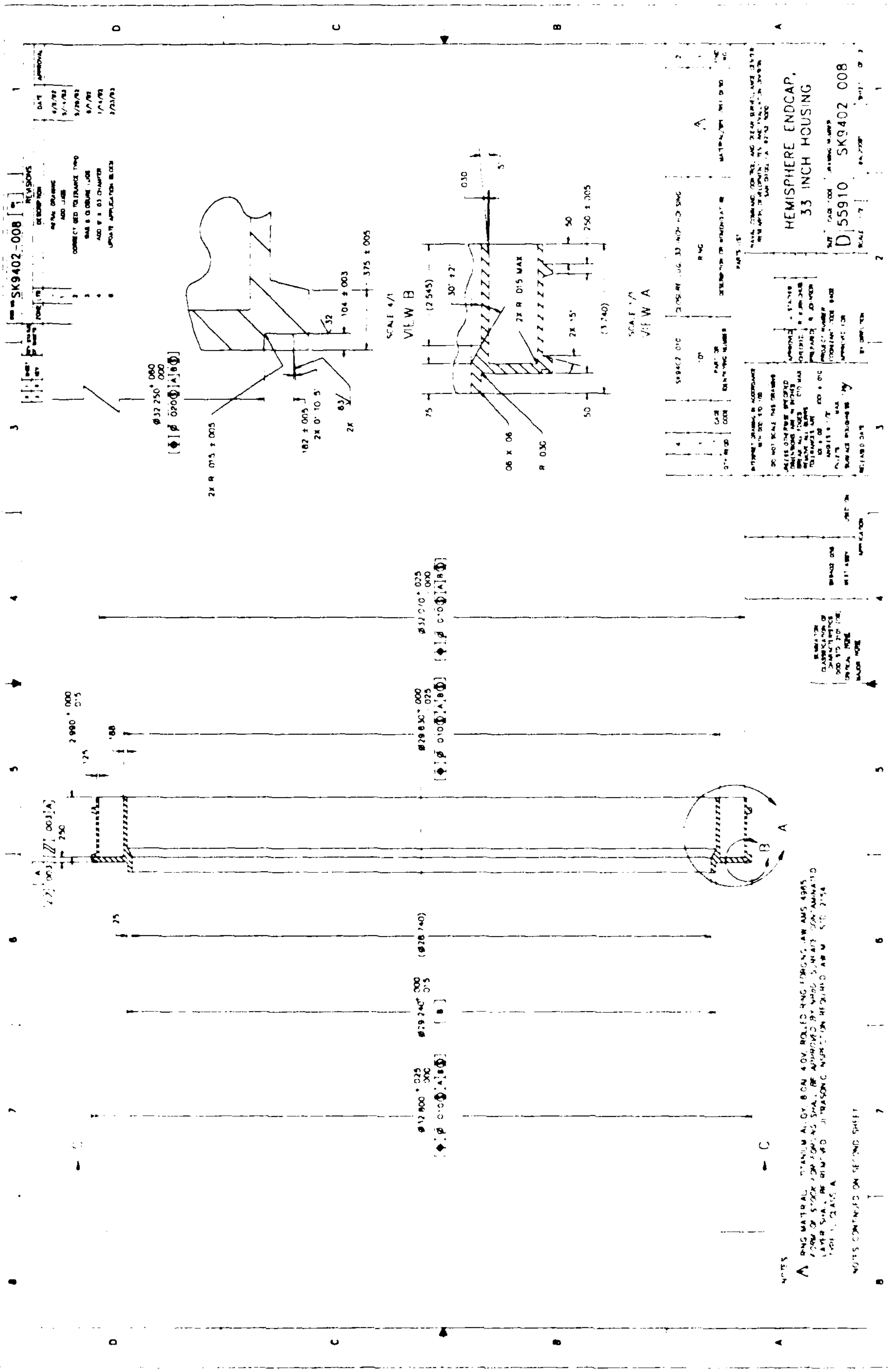

Figure A-29. 33-inch housing hemisphere end cap, Sheet 1.

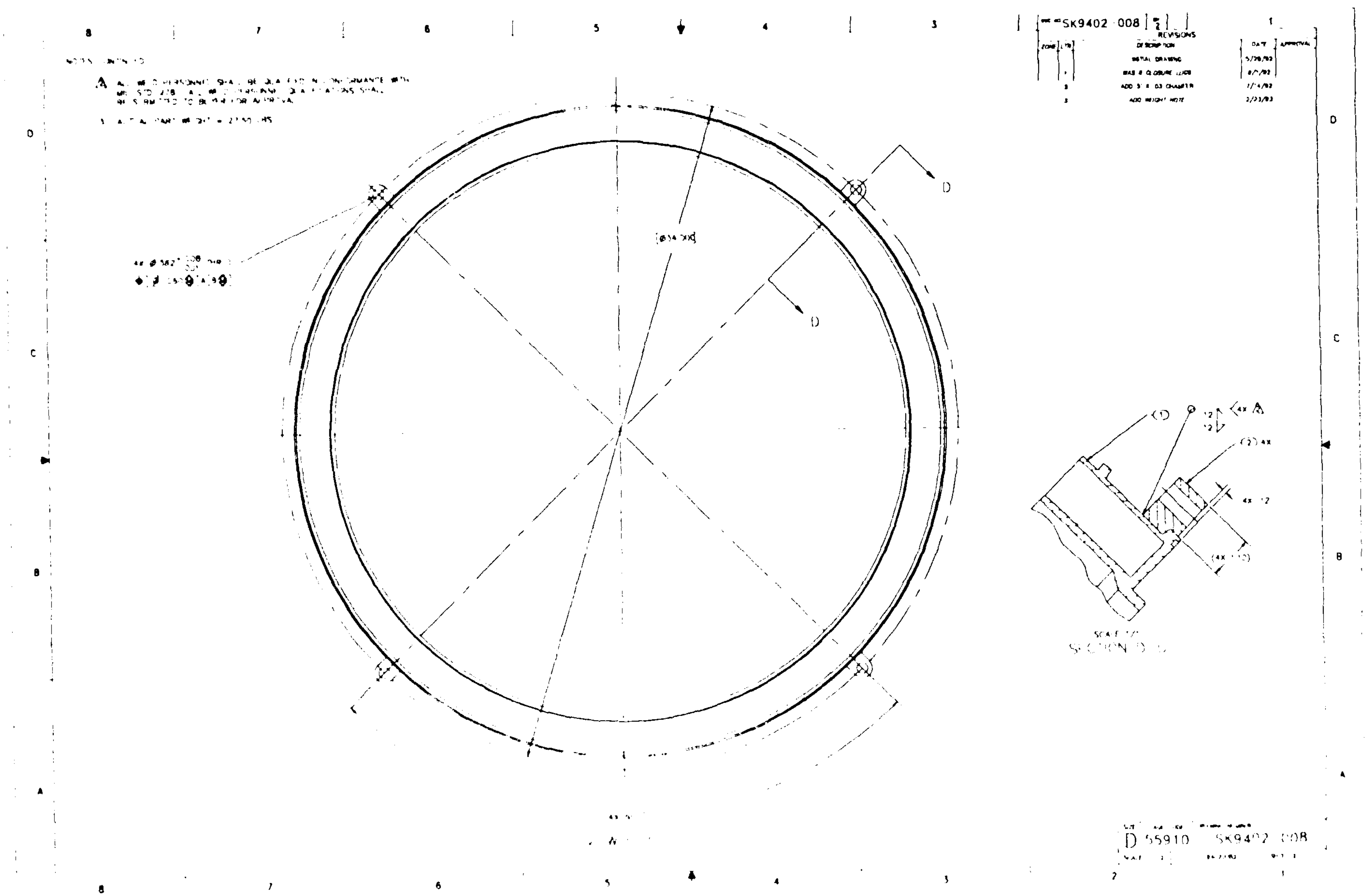

Figure A 29 33-inch housing hemisphere end cap. Sheet 2.

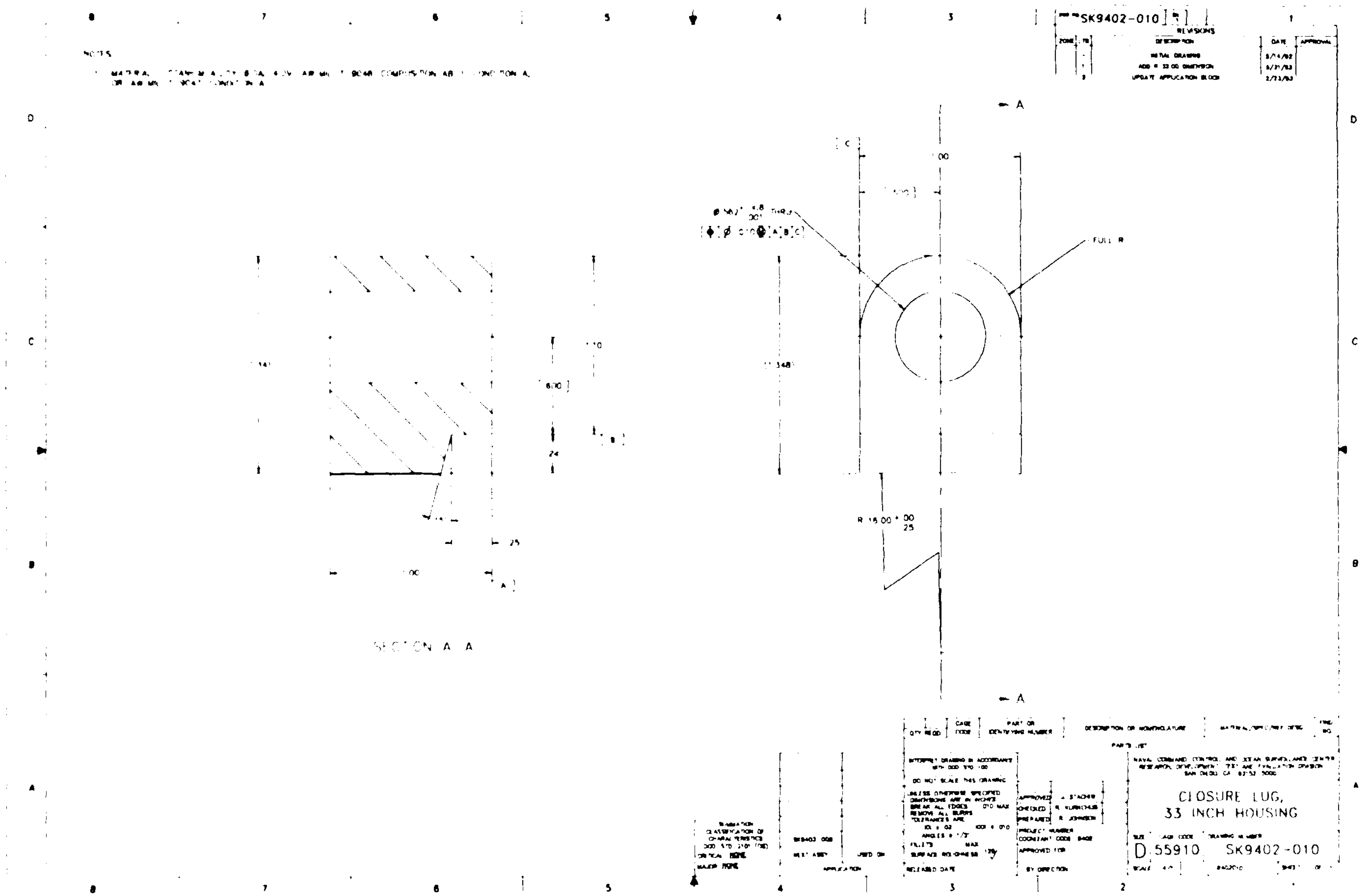

Figure A-30. 33-inch housing closure lug.

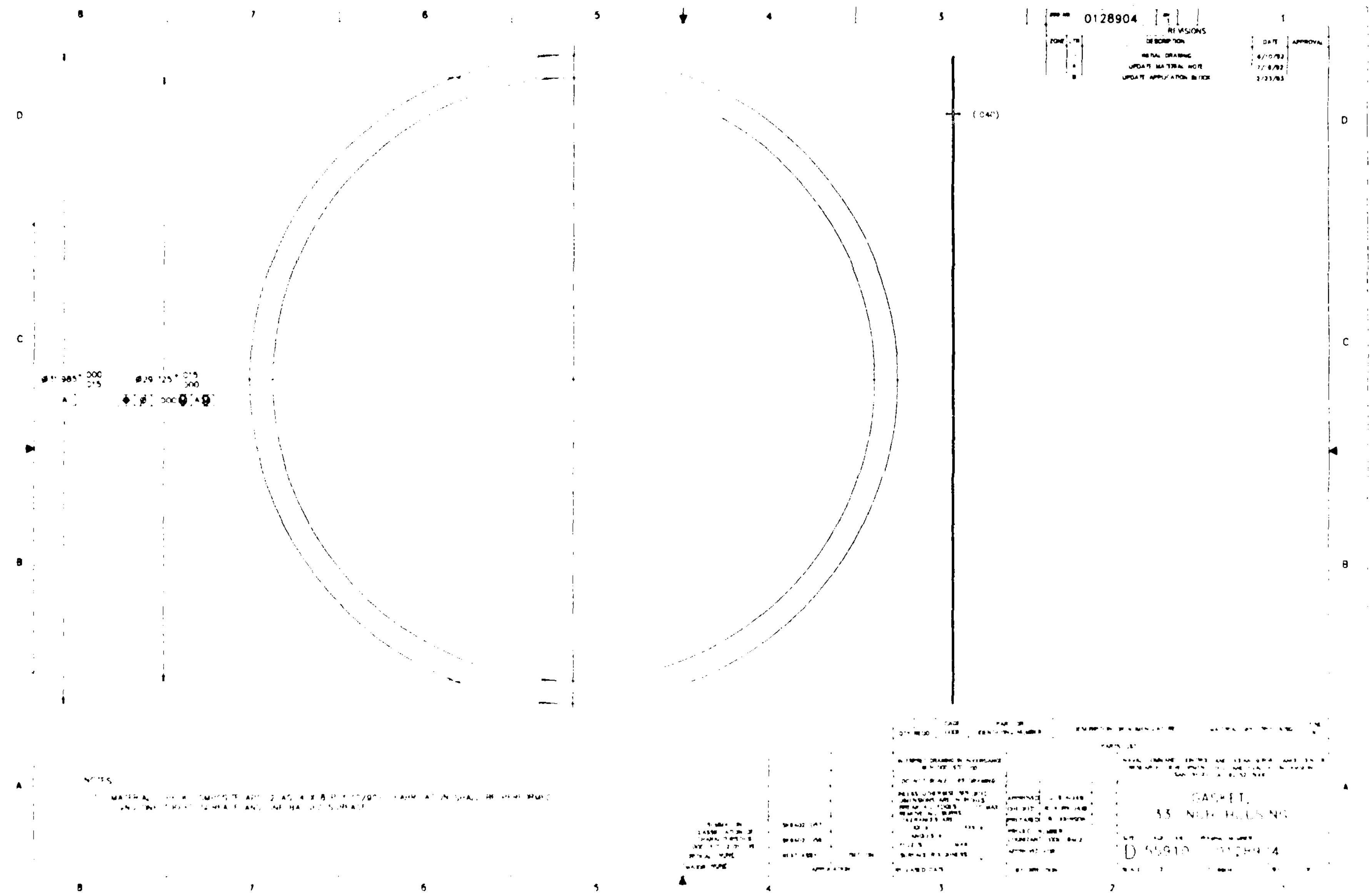

Figure A-31 33 inch housing gasket

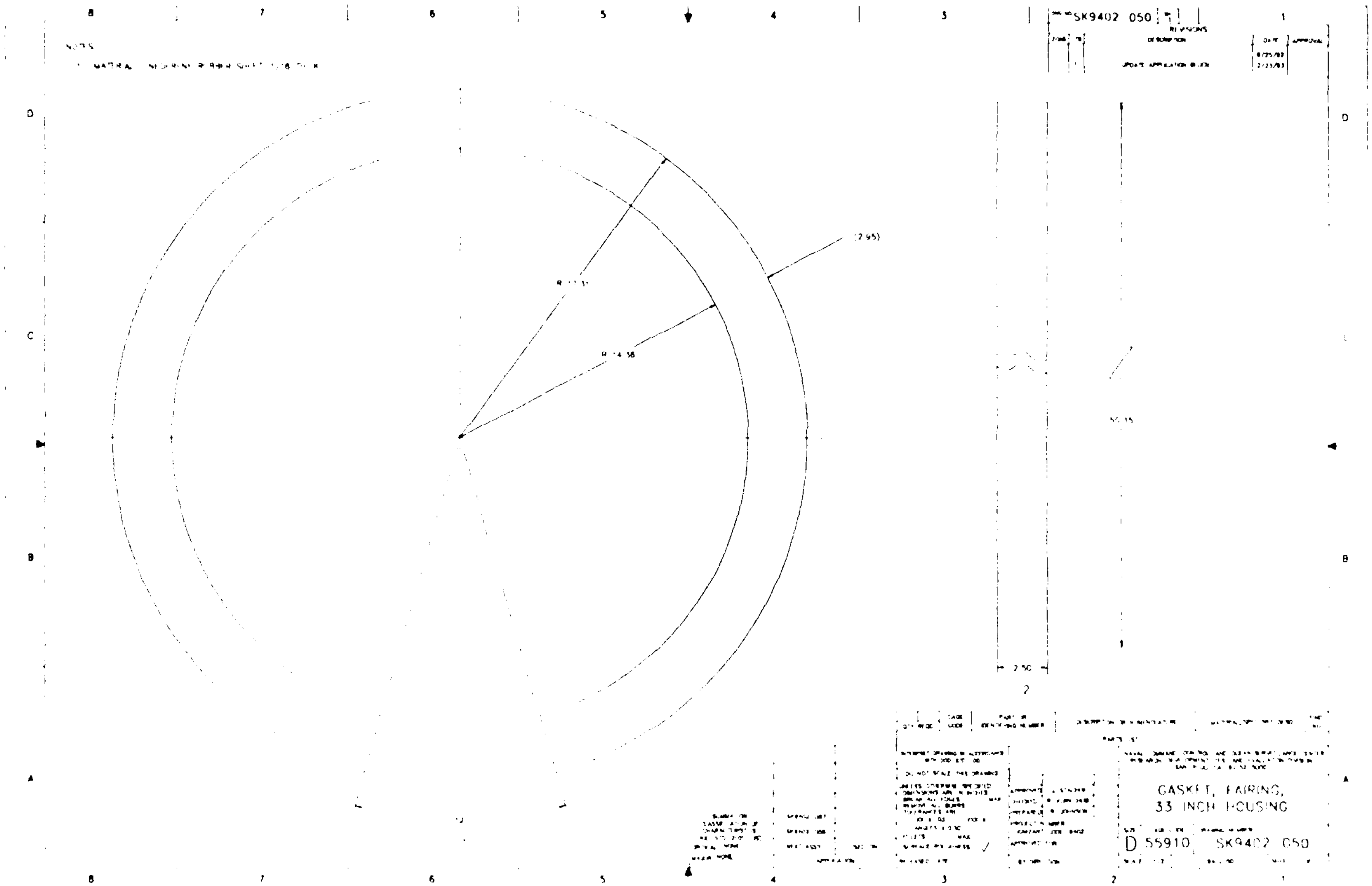

Figure A-32 33-inch housing fairing gasket.

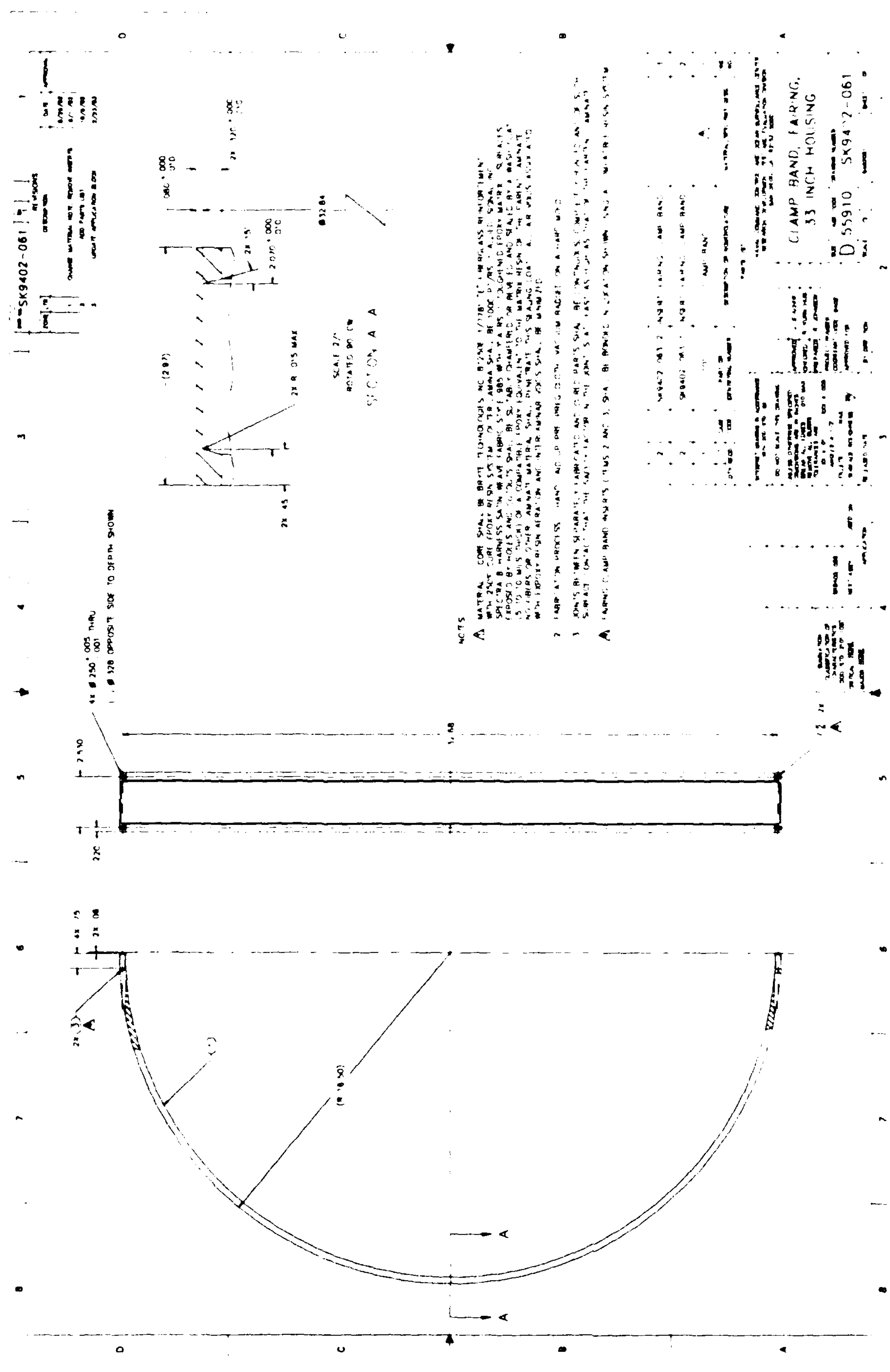

Figure A-33 33-inch housing fairing clamp band.

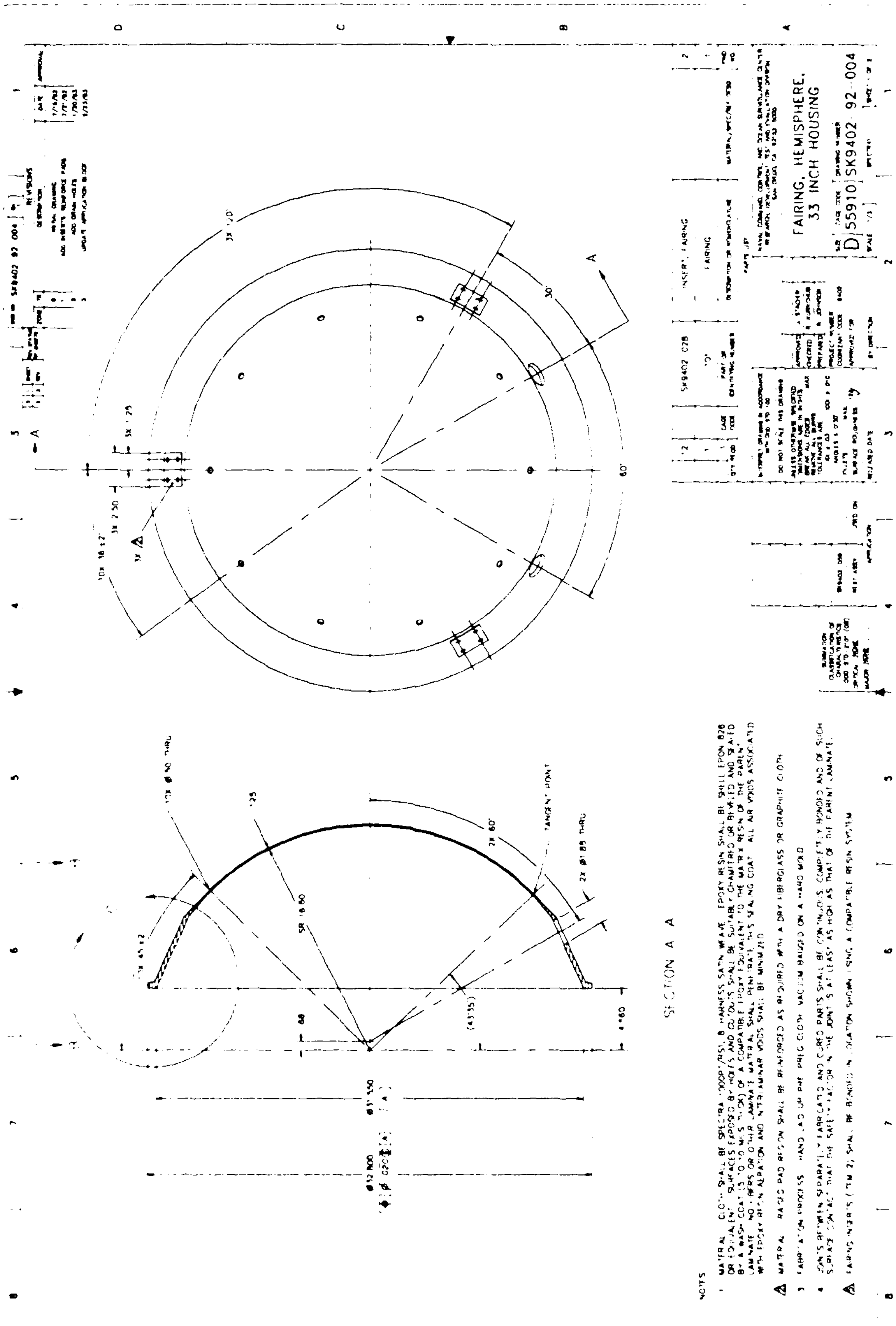

Figure A-34. 33-inch housing hemisphere fairing, Sheet 1.

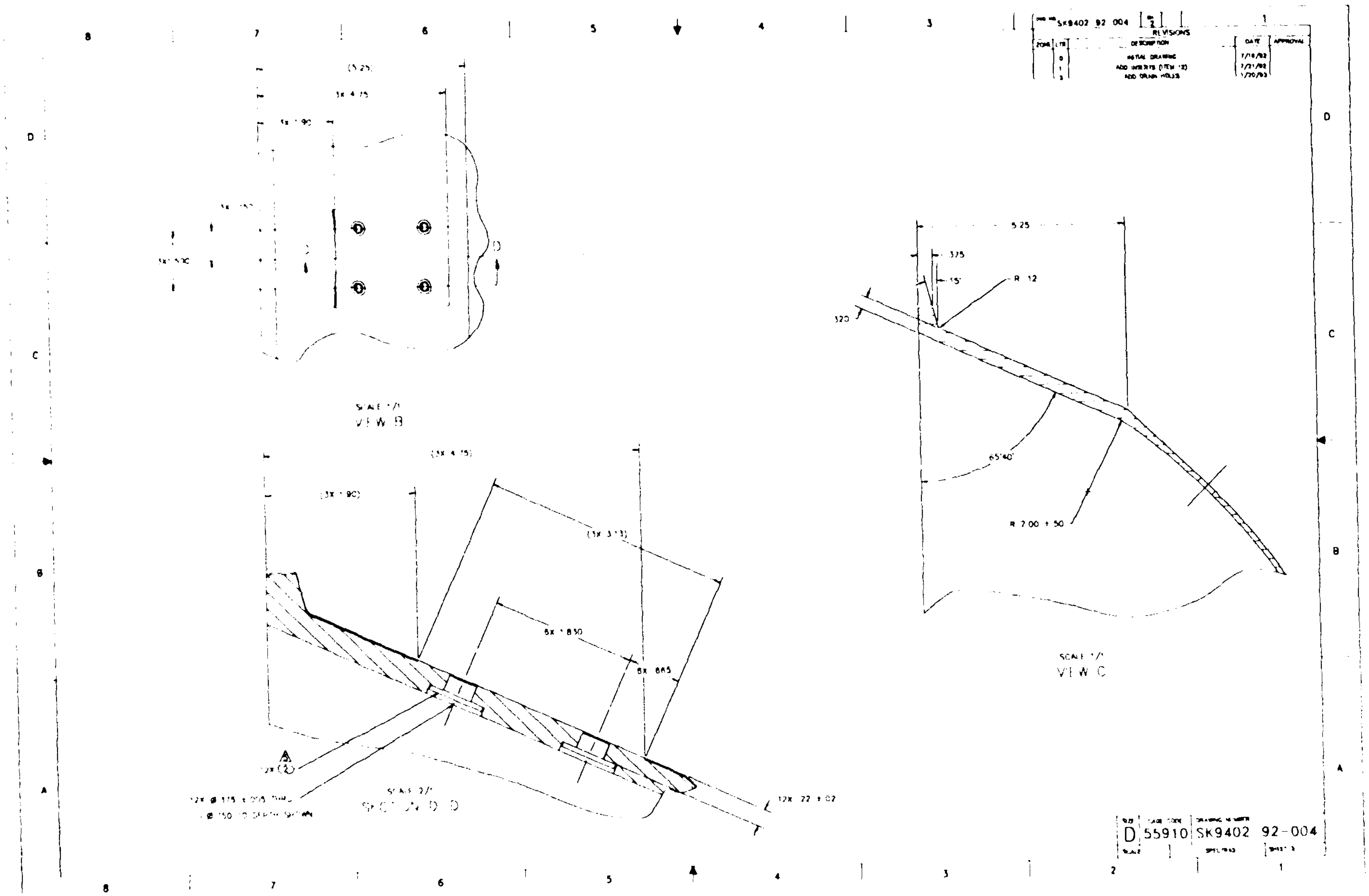

Figure A-34. 33-inch housing hemisphere fairing, Sheet 2.

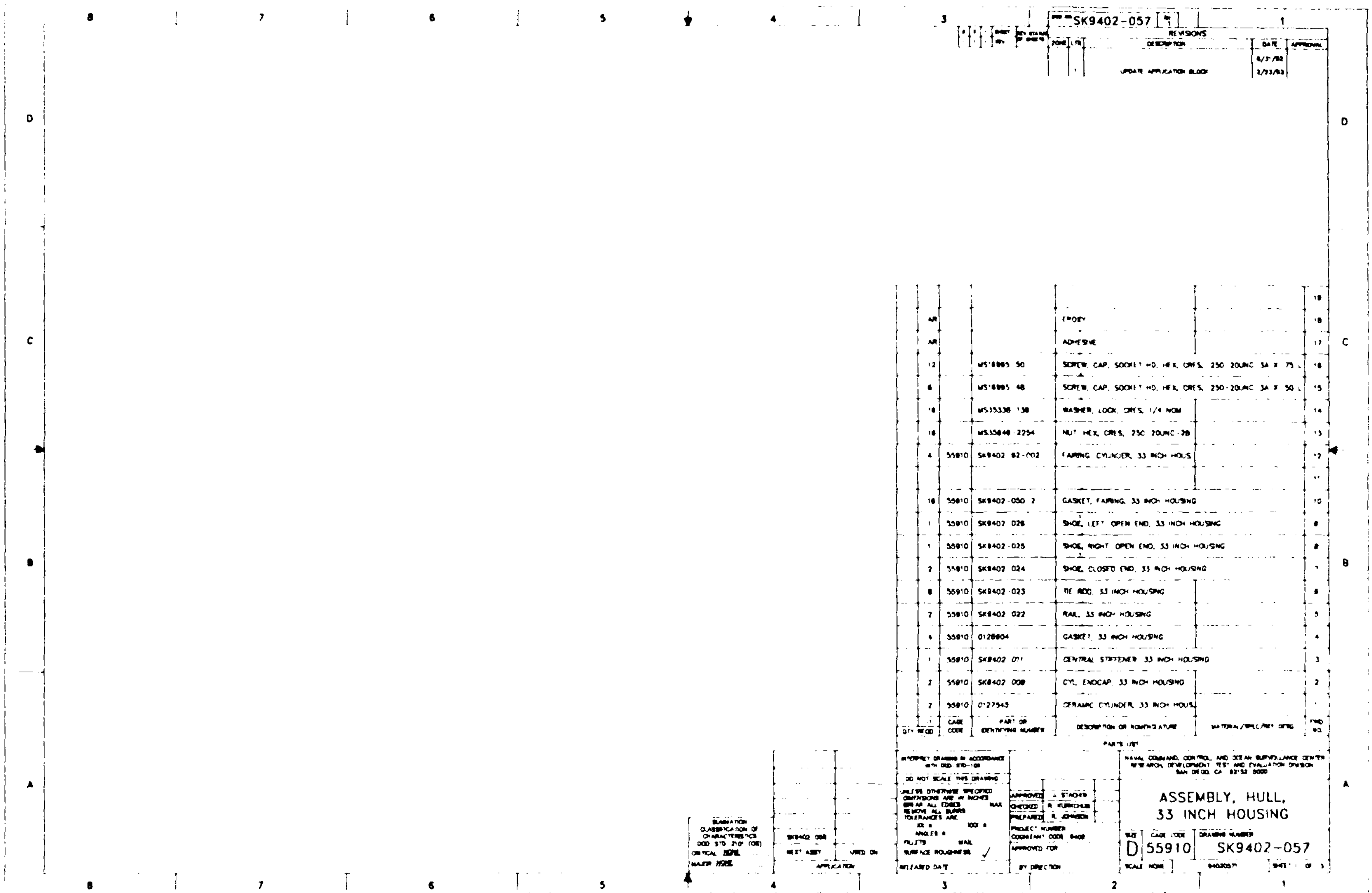

Figure A-35. 33-inch housing hull assembly, Sheet 1.

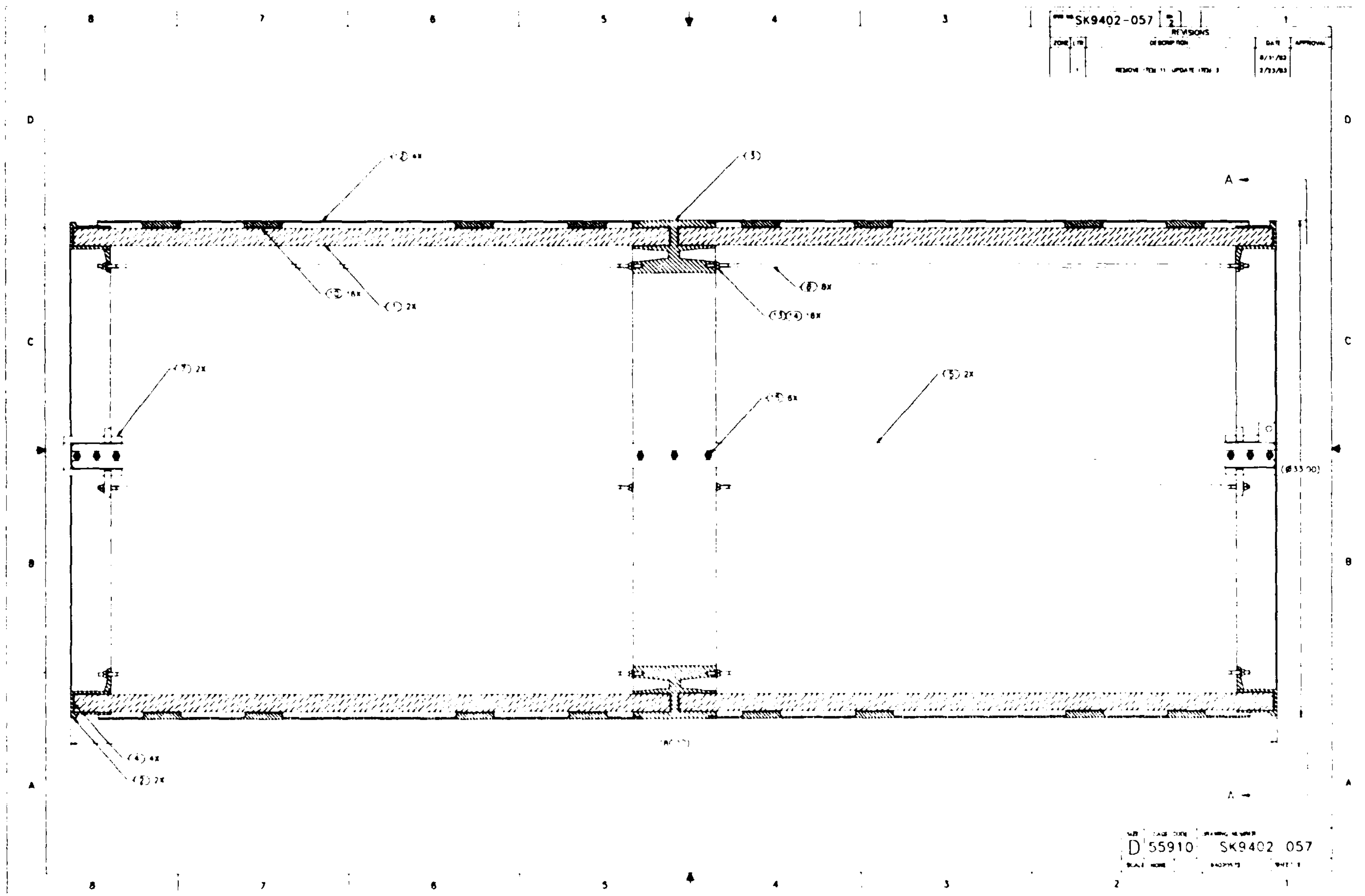

Figure A-35. 33-inch housing hull assembly, Sheet 2

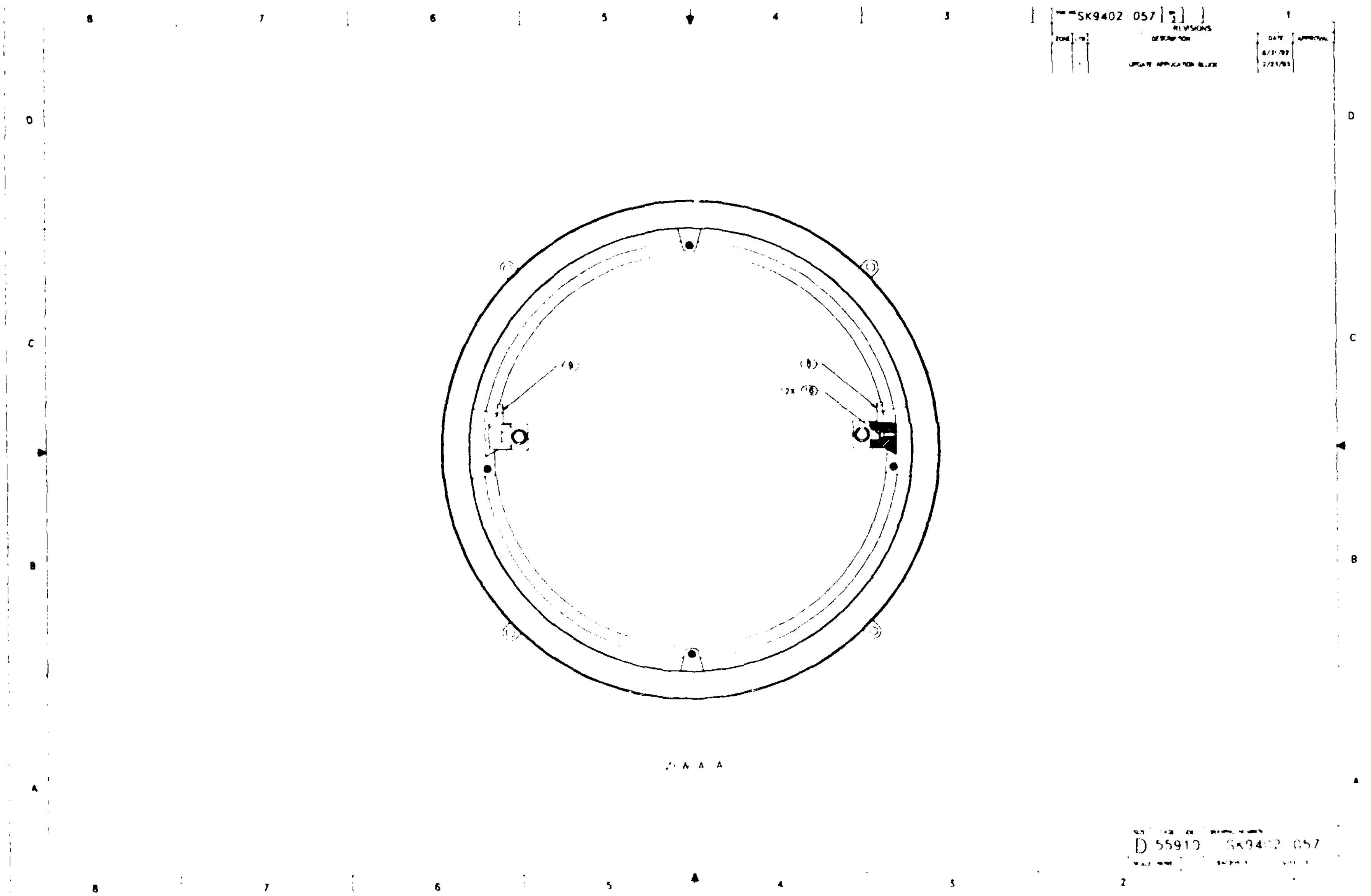

Figure A-35. 33-inch housing hull assembly, Sheet 3

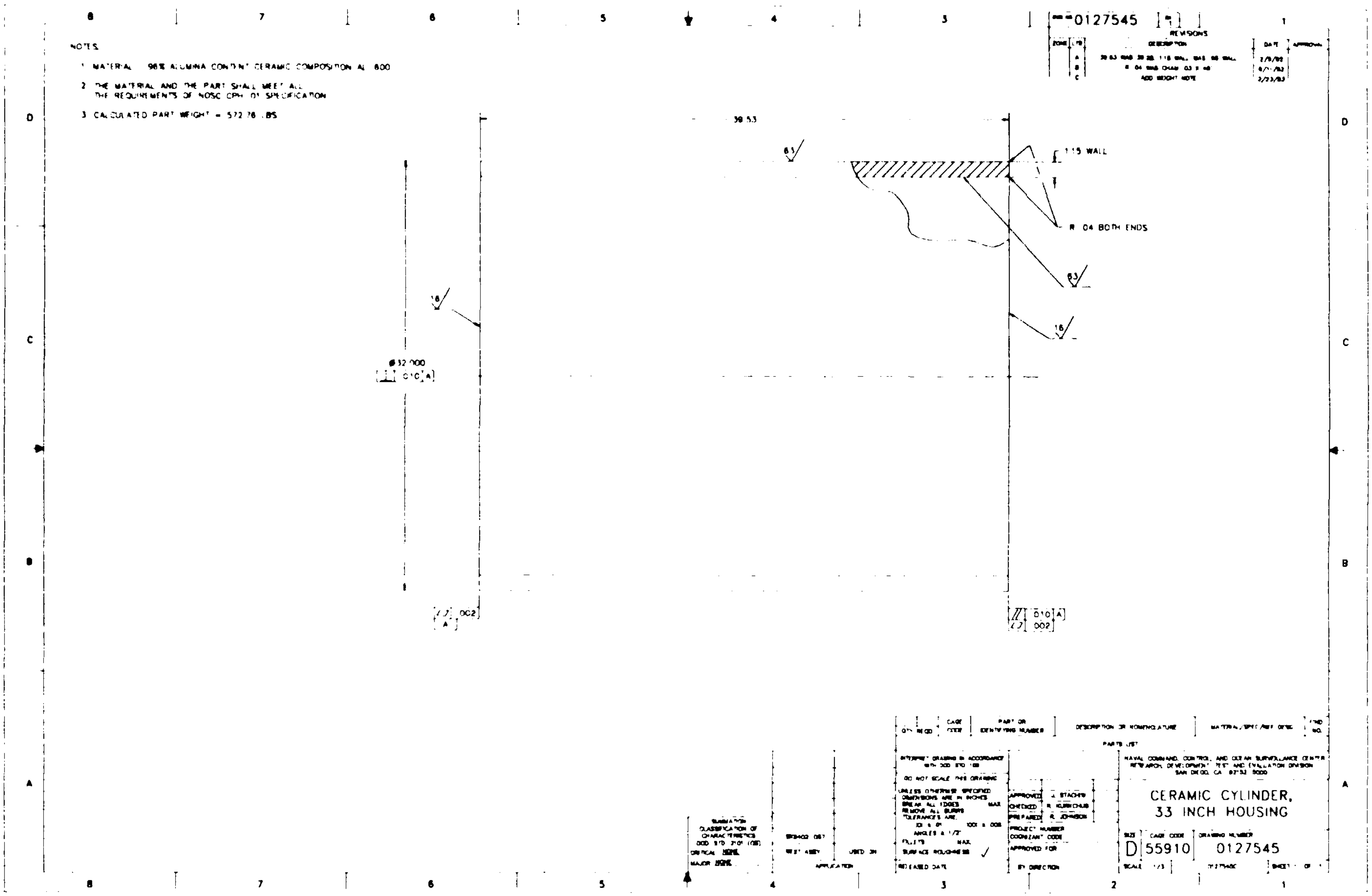

Figure A-36. 33-inch housing ceramic cylinder.

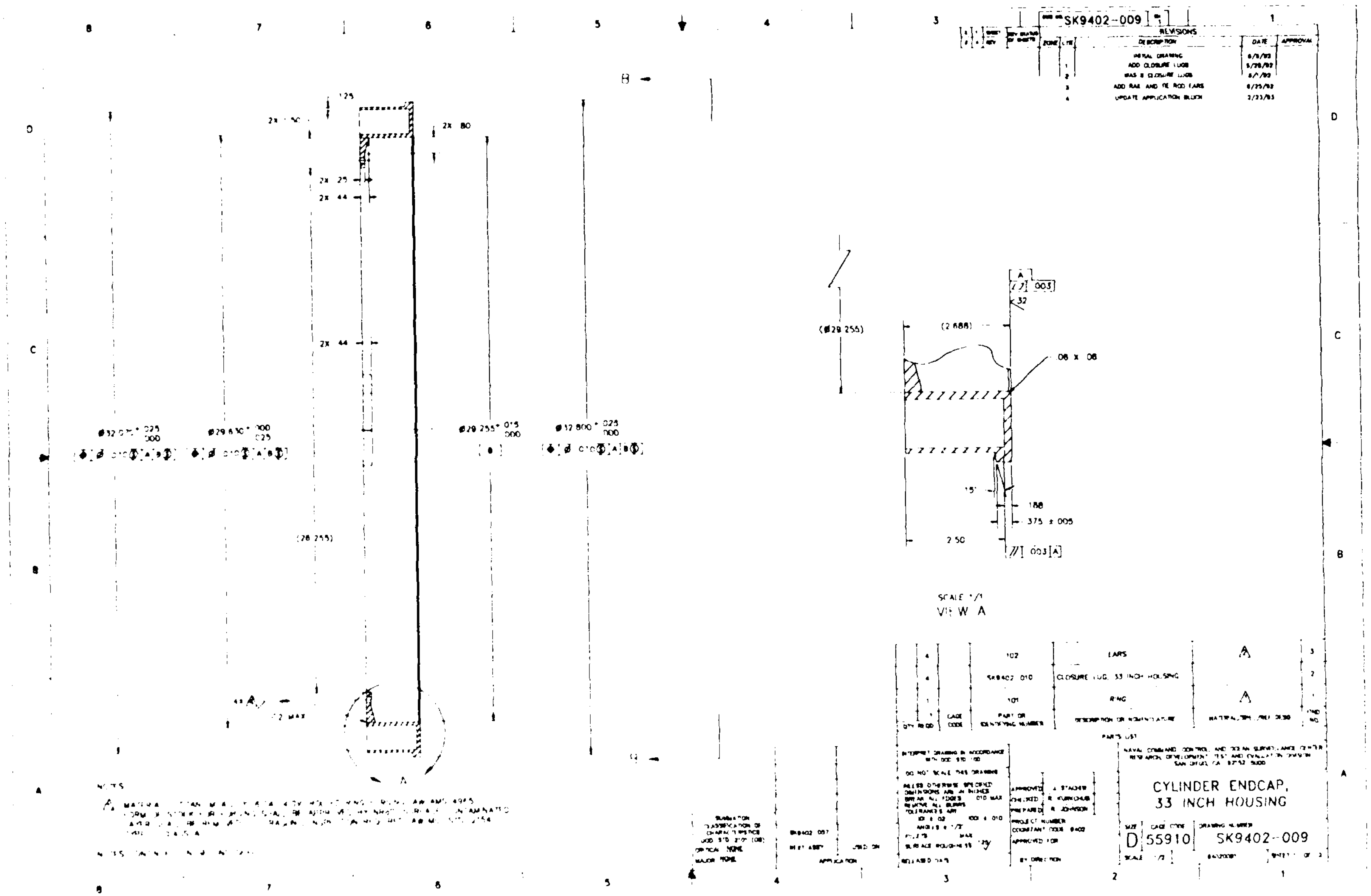

Figure A-37. 33 inch housing cylinder end cap, Sheet 1.

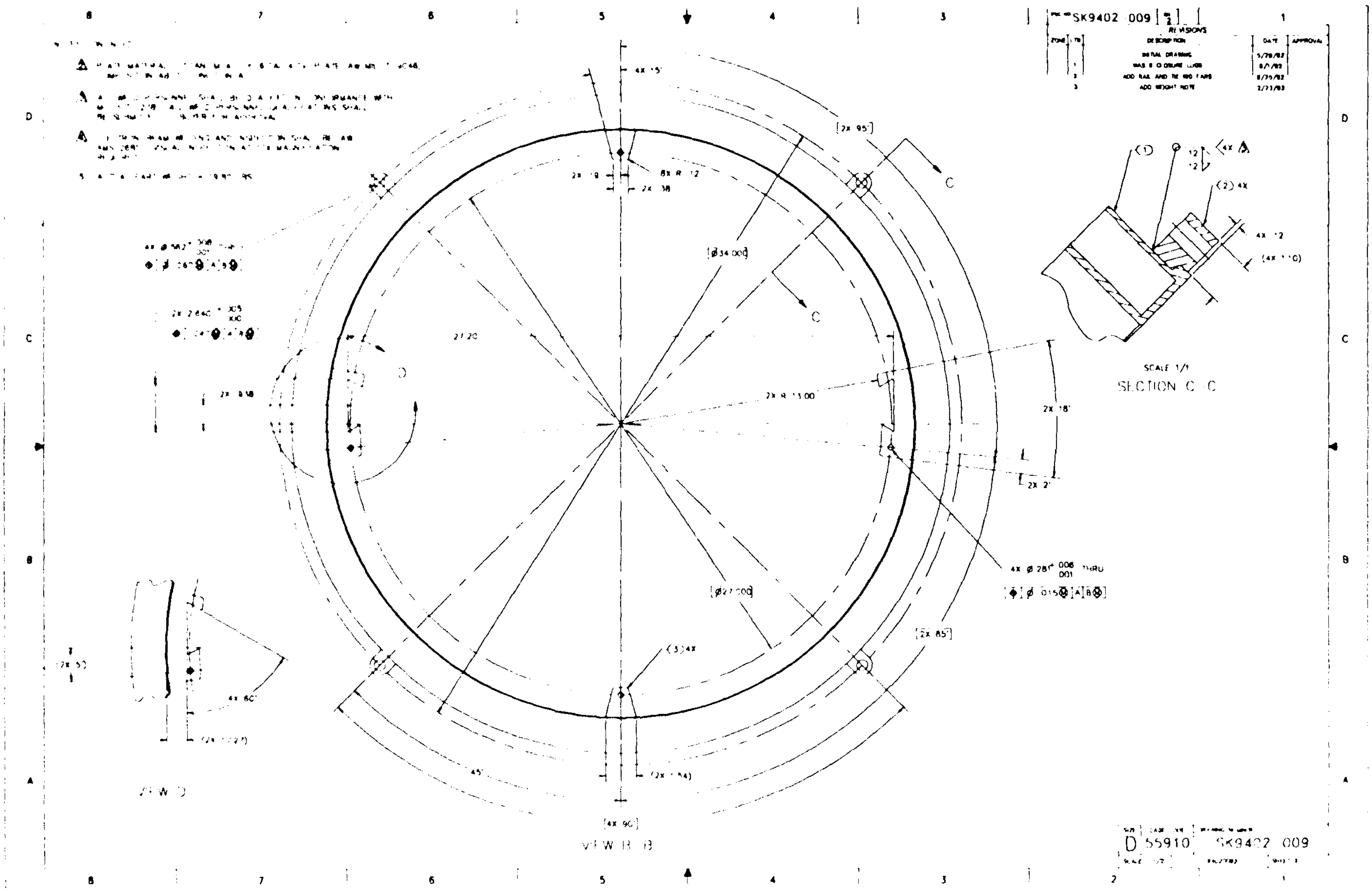

Figure A-37. 33-inch housing cylinder end cap, Sheet 2.

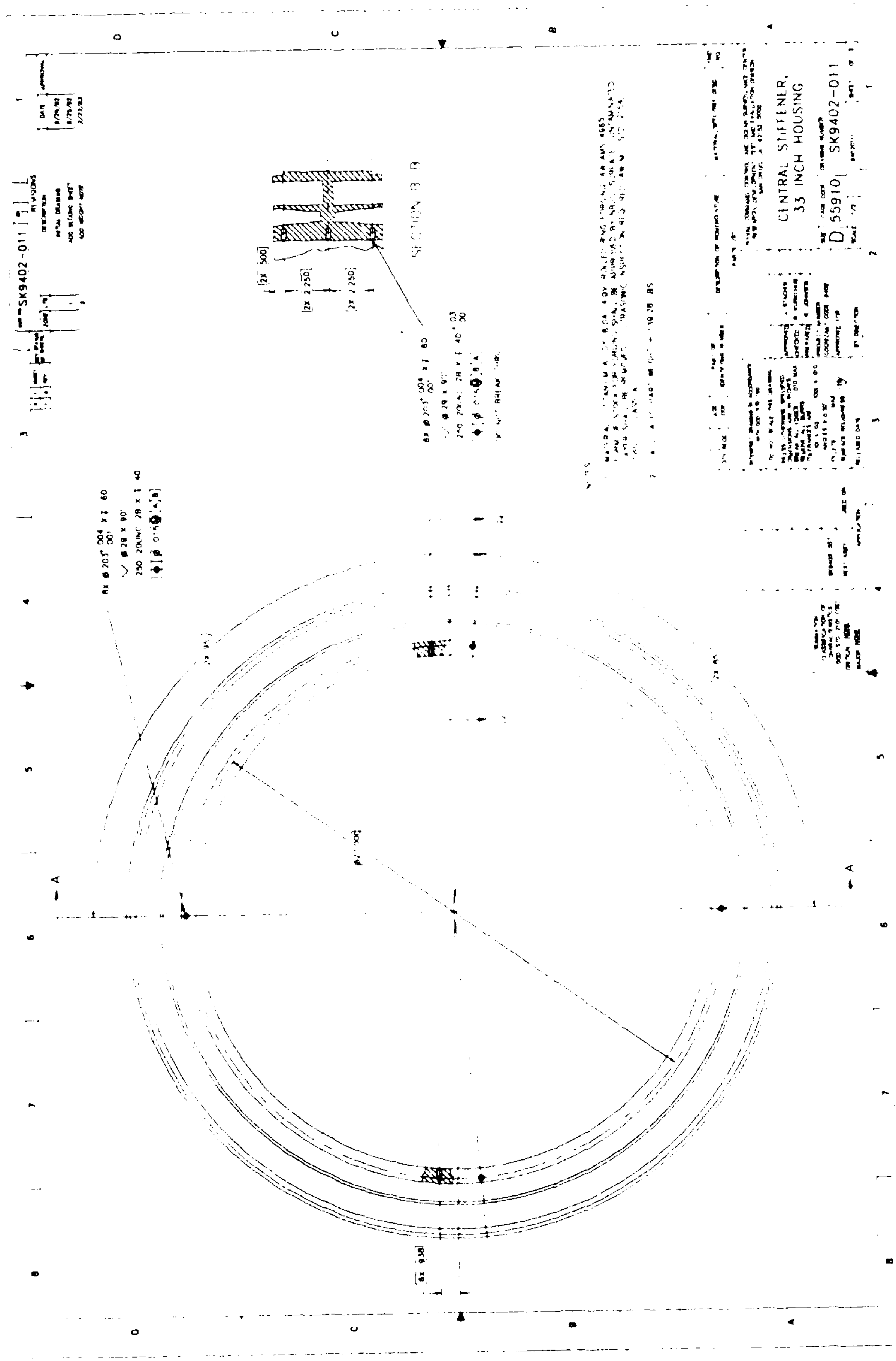

Figure A-38. 33-inch housing central stiffener, Sheet 1

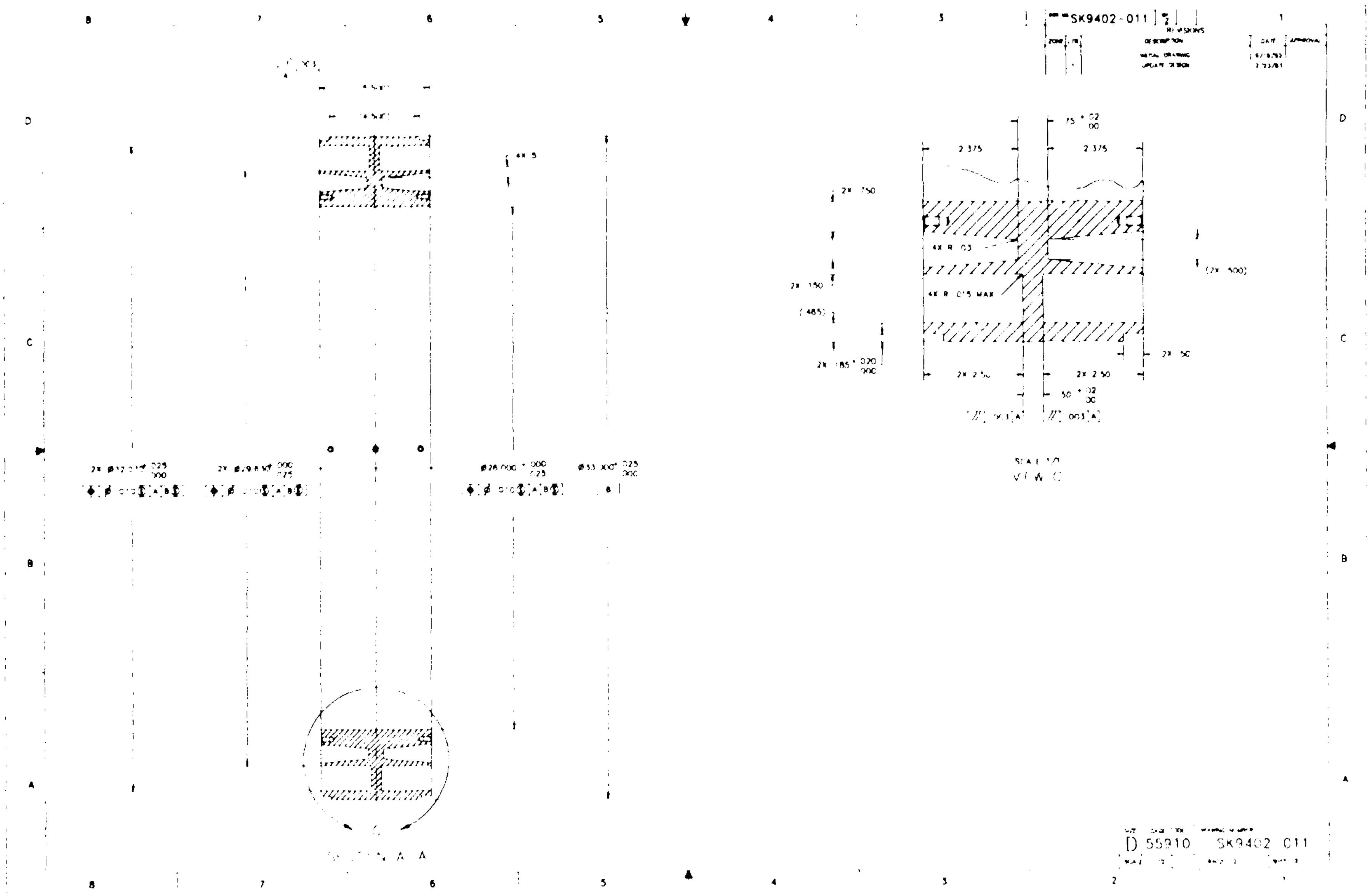

Figure A-38 33-inch housing central stiffener, Sheet 2.

Figure A.39 .33 inch housing rail

Figure A-40 33 inch housing tie rod

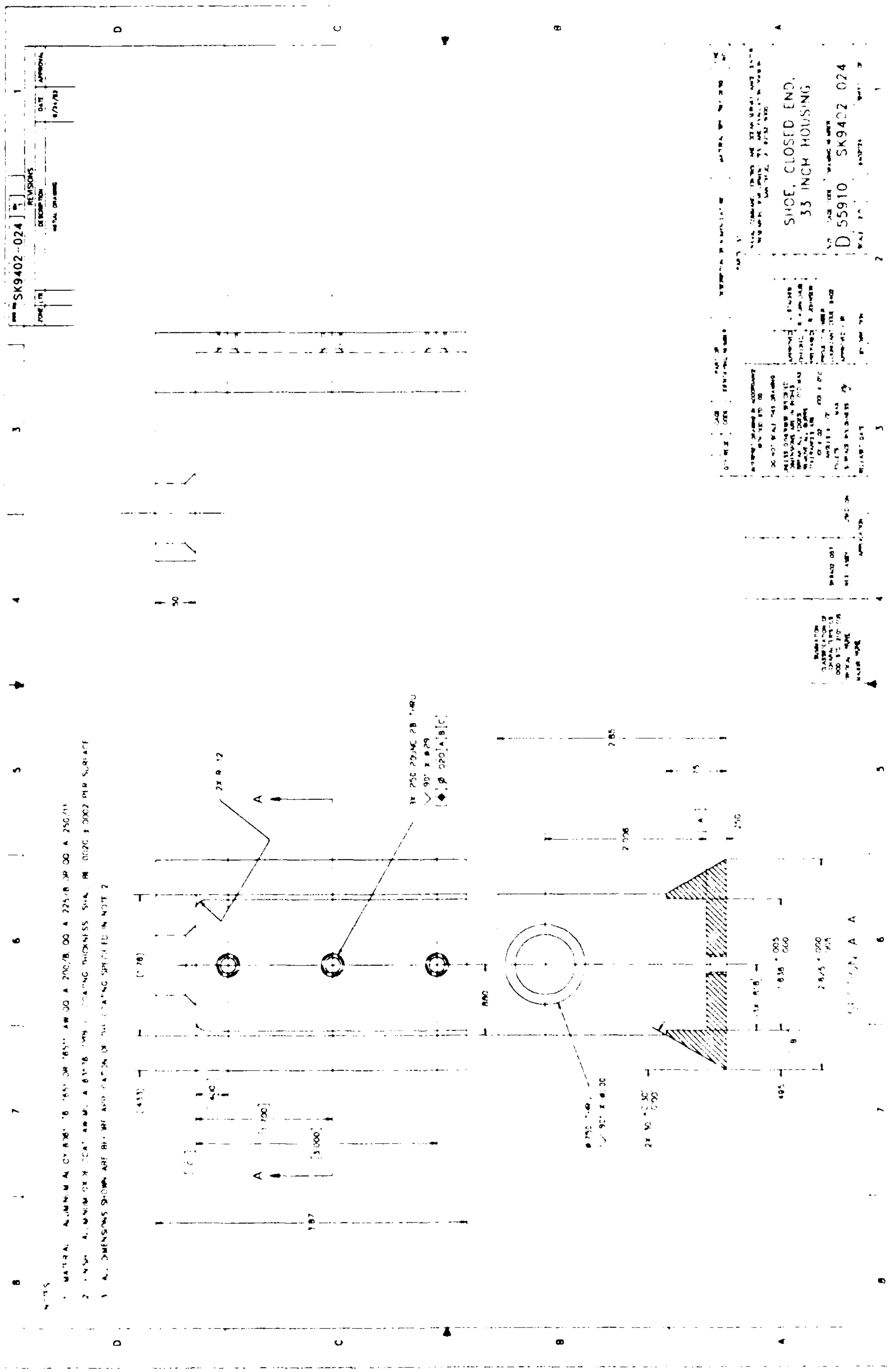

Figure A-41. 33-inch housing closed end shoe.

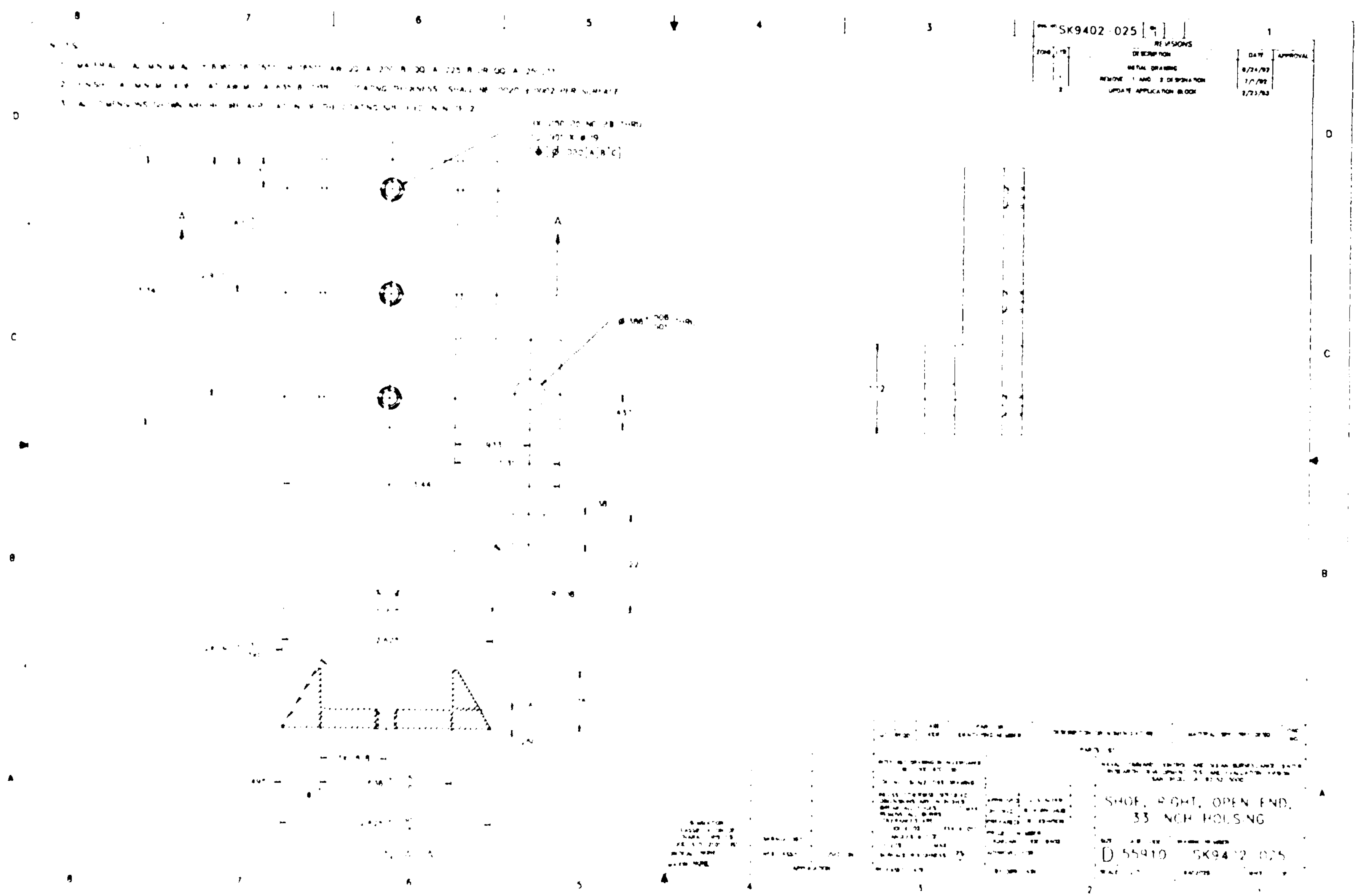

Figure A-42. 33-inch housing open end right shoe

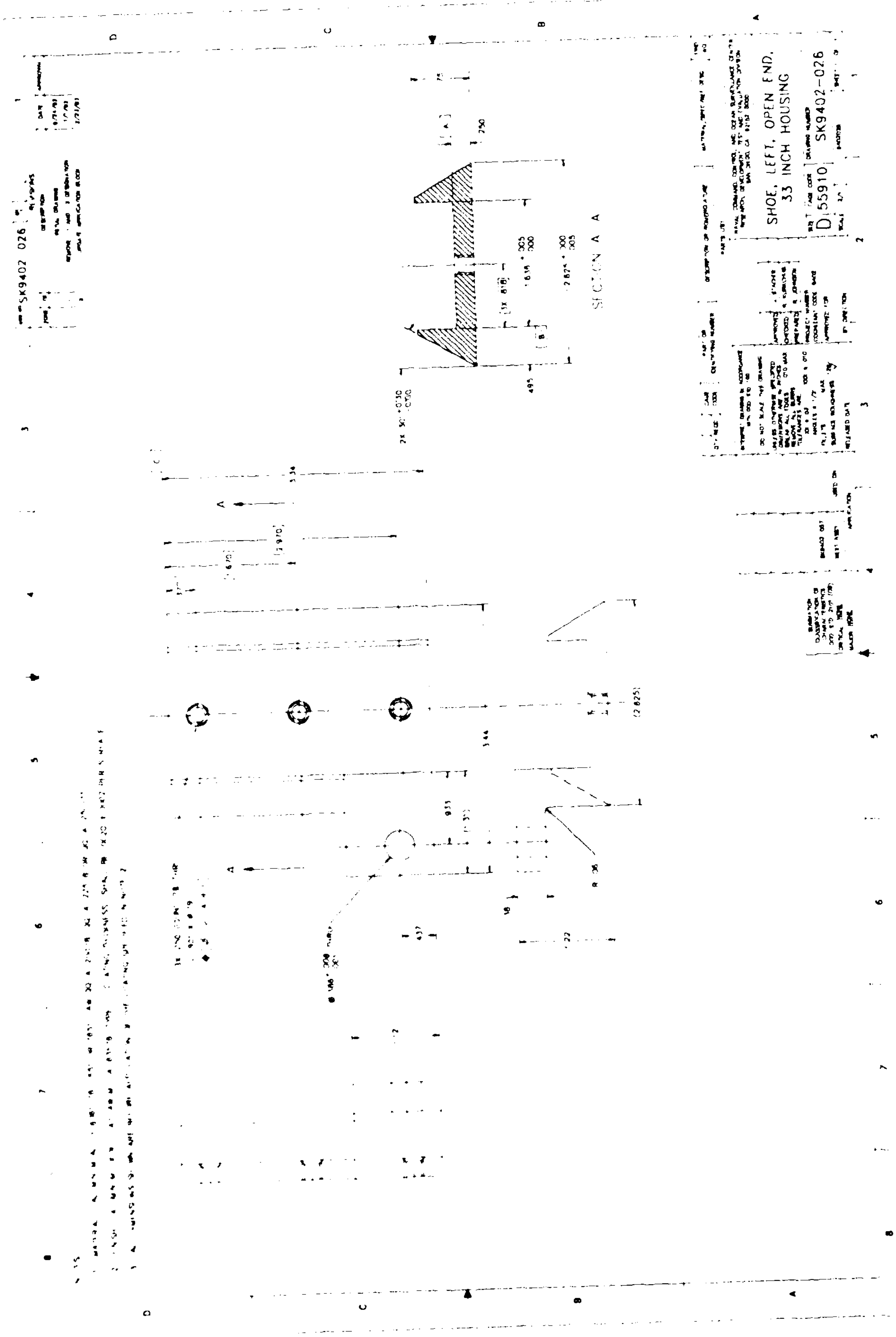

Figure A-43. 33-inch housing open end left shoe.

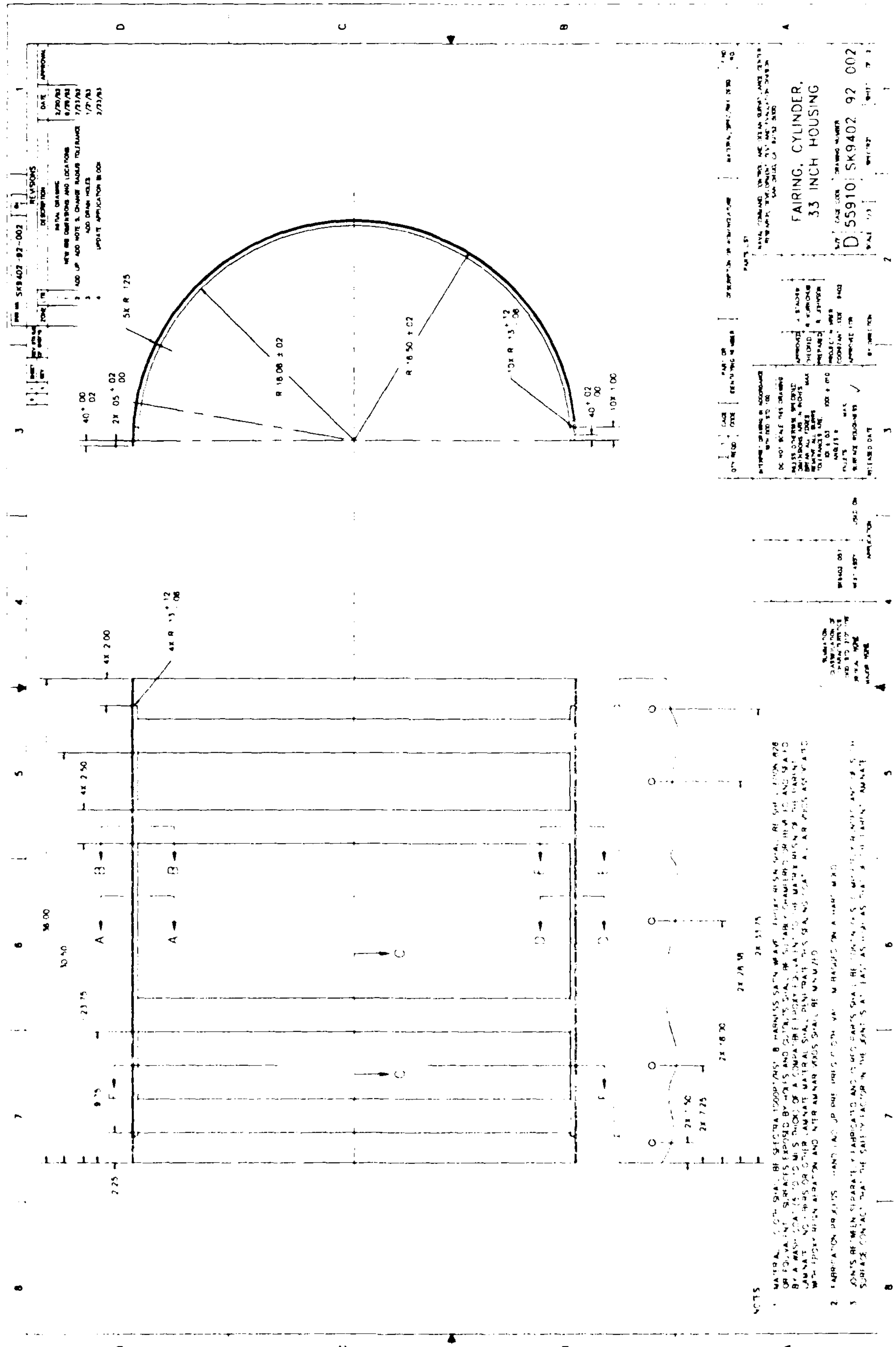

Figure A-44. 33-inch housing cylinder fairing, Sheet 1.

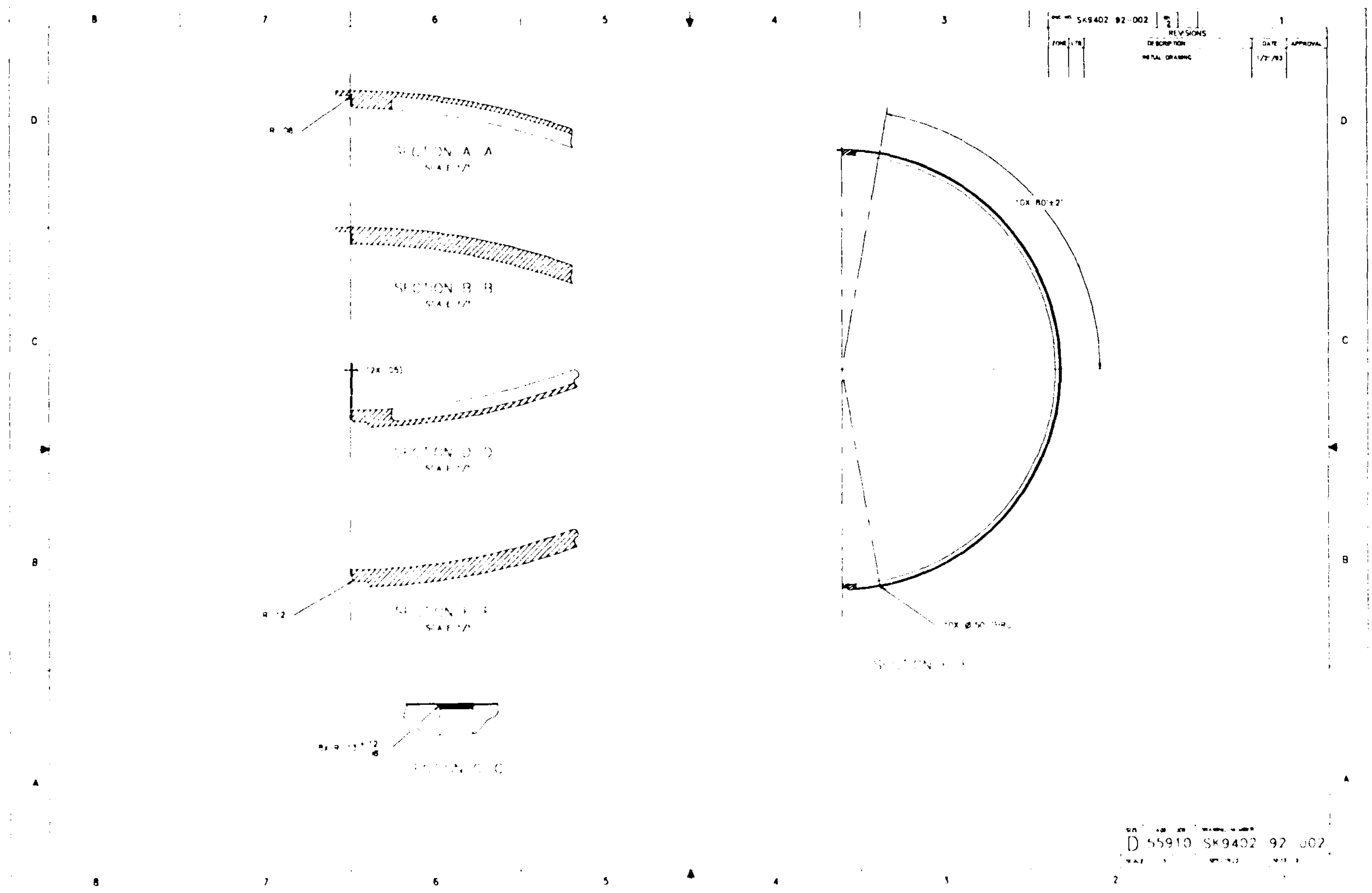

Figure A-44. 33-inch housing cylinder fairing, Sheet 2

REPORT DOCUMENTATION PAGE

Form Approved
OMB No. 0704-0188

1. AGENCY USE ONLY (Leave blank)	2. REPORT DATE March 1993	3. REPORT TYPE AND DATES COVERED Final

4. TITLE AND SUBTITLE

DESIGN AND STRUCTURAL ANALYSIS OF ALUMINA-CERAMIC HOUSINGS FOR DEEP SUBMERGENCE SERVICE
Fifth Generation Housings

5. FUNDING NUMBERS

PE: 0603713N
PROJ: S0397
ACC: DN302232

6. AUTHOR(S)

R. P. Johnson, R. R. Kurkchubasche, and J. D. Stachiw

7. PERFORMING ORGANIZATION NAME(S) AND ADDRESS(ES)

Naval Command, Control and Ocean Surveillance Center (NCCOSC)
RDT&E Division
San Diego, CA 92152-5000

8. PERFORMING ORGANIZATION REPORT NUMBER

TR 1583

9. SPONSORING/MONITORING AGENCY NAME(S) AND ADDRESS(ES)

Naval Sea Systems Command
Washington, DC 20362

10. SPONSORING/MONITORING AGENCY REPORT NUMBER

11. SUPPLEMENTARY NOTES

12a. DISTRIBUTION/AVAILABILITY STATEMENT

Approved for public release; distribution is unlimited.

12b. DISTRIBUTION CODE

13. ABSTRACT (Maximum 200 words)

Two alumina-ceramic pressure housings for deep-submergence application were designed and structurally analyzed as part of a research program whose goal is to determine the structural performance of large alumina-ceramic housings. The high specific strength and modulus of alumina ceramic allows the designer to obtain lower weight-to-displacement (W/D) ratios than would be obtainable with more traditional materials such as titanium. The two large housings use a number of advanced design features such as skirted hemispheres, an epoxy-bonded central joint stiffener, a minimum clear-bore diameter requirement, GFR PEEK composite gaskets protecting the ceramic bearing surfaces, and an almost neutrally buoyant spectra fairing for impact protection. The smaller of the two housings has a 26.0-inch diameter (OD), 90.96-inch overall length, and has a calculated W/D ratio of 0.585, while the larger housing has a 33.0-inch OD, 112.84-inch overall length, and a calculated W/D ratio of 0.556. Both housings were designed for a 20,000-foot service depth (9,030 psi external pressure). They are scheduled to be assembled, proof tested, and cyclically tested during the summer of 1993.

14. SUBJECT TERMS ceramics external pressure housing ocean engineering	15. NUMBER OF PAGES 141 16. PRICE CODE

17. SECURITY CLASSIFICATION OF REPORT	18. SECURITY CLASSIFICATION OF THIS PAGE	19. SECURITY CLASSIFICATION OF ABSTRACT	20. LIMITATION OF ABSTRACT
UNCLASSIFIED	UNCLASSIFIED	UNCLASSIFIED	SAME AS REPORT

UNCLASSIFIED

21a. NAME OF RESPONSIBLE INDIVIDUAL	21b. TELEPHONE (include Area Code)	21c. OFFICE SYMBOL
R. P. Johnson	(619) 553-1935	Code 9402

NSN 7540-01-280-5500

Standard form 298 (BACK)

UNCLASSIFIED

THE AUTHORS

RICHARD P. JOHNSON is an Engineer for the Ocean Engineering Division. He has held this position since 1987. Before that, he was a Laboratory Technician for the Ocean Engineering Laboratory, University of California at Santa Barbara from 1985–1986, and Design Engineer in the Energy Projects Division of SAIC from 1986–1987. His education includes a B.S. in Mechanical Engineering from the University of California at Santa Barbara in 1986, and an M.S. in Structural Engineering from the University of California, San Diego, in 1991. He has published "Stress Analysis Considerations for Deep Submergence Ceramic Pressure Housings," *Intervention '92*, Marine Technology Society. He is a member of the Marine Technology Society.

RAMON R. KURKCHUBASCHE is a Research Engineer for the Ocean Engineering Division and has worked since November 1990 in the field of deep submergence pressure housings fabricated from ceramic materials. His education includes a B.S. in Structural Engineering from the University of California at San Diego, 1989; and an M.S. in Aeronautical/Astronautical Engineering from Stanford University in 1990. His experience includes conceptual design, procurement, assembly, testing, and documentation of ceramic housings. Other experience includes buoyancy concepts utilizing ceramic, nondestructive evaluation of ceramic components. He is a member of the Marine Technology Society, and has published "Elastic Stability Considerations for Deep Submergence Ceramic Pressure Housings," *Intervention '92*, Marine Technology Society.

DR. JERRY STACHIW is Staff Scientist for Marine Materials in the Ocean Engineering Division. He received his undergraduate engineering degree from Oklahoma State University in 1955 and graduate degree from Pennsylvania State University in 1961.

Since that time he has devoted his efforts at various U.S. Navy Laboratories to the solution of challenges posed by exploration, exploitation, and surveillance of hydrospace. The primary focus of his work has been the design and fabrication of pressure resistant structural components of diving systems for the whole range of ocean depths. Because of his numerous achievements in the field of ocean engineering, he is considered to be the leading expert in the structural application of plastics and brittle materials to external pressure housings.

Dr. Stachiw is the author of over 100 technical reports, articles, and papers on design and fabrication of pressure resistant viewports of acrylic plastic, glass, germanium, and zinc sulphide, as well as pressure housings made of wood, concrete, glass, acrylic plastic, and ceramics. His book on "Acrylic Plastic Viewports" is the standard reference on that subject.

For the contributions to the Navy's ocean engineering programs, the Navy honored him with the Military Oceanographer Award and the NCCOSC's RDT&E Division honored him with the Lauritsen-Bennett Award. The American Society of Mechanical Engineers recognized his contributions to the engineering profession by election to the grade of Life-Fellow, as well as the presentation of Centennial Medal, Dedicated Service Award and Pressure Technology Codes Outstanding Performance Certificate.

Dr. Stachiw is past-chairman of ASME Ocean Engineering Division and ASME Committee on Safety Standards for Pressure Vessels for Human Occupancy. He is a member of the Marine Technology Society, New York Academy of Science, Sigma Xi and Phi Kappa Honorary Society.